

Transparent Ductility

Reinforcing a structural glass girder

Martien Rademakers

June 2009

Master Thesis report

Faculty of Civil Engineering and Geosciences

Delft University of Technology

In cooperation with:

Glass and Transparency research group, Department of Building Technology, Faculty of Architecture, TU Delft

And:

Veromco B.V., Saint Gobain Glass, Amersfoort

Graduation committee:

Prof.Ir. L.A.G. Wagemans (TUDelft, Faculty of Civil Engineering & Geosciences - Chairman)

Prof.Dipl.-Ing. J.N.J.A. Vamberský (TUDelft, Faculty of Civil Engineering & Geosciences)

Ir. P.C. Louter (TUDelft, Faculty of Architecture)

Student:

J.M.Rademakers

Waalstraat 14

2515 XL Den Haag

Tel.: 06-41433324

E-mail: Martienr@yahoo.com

Student nr: 1071440

The logo for TU Delft, featuring a stylized flame icon above the text 'TU Delft'.

Delft University of Technology

The logo for Saint-Gobain Glass, featuring a stylized building icon above the text 'SAINT-GOBAIN GLASS'.




Preface

Glass is an almost magical material that catches the eye by being invisible. It is known for its transparency and notorious for its brittleness. Due to this characteristic it has afforded itself a special role in the building industry. Glass is traditionally used as separating element and the only loadings it had to withstand were its own weight, weather and direct loadings. A much less recognized fact is that glass is a stiff and potentially very strong material. For example; glass fiber can be counted among the strongest fibers on the market.

Still the structural use of glass has been something of the last decades. As it will be clear in this thesis, the design of a safe, completely transparent structural glass element is not something that is done easily and the odds on designing it in this thesis were unfavorable. But Babylon was not built in one day either and it has been inspiring to try to contribute a small piece to the science of structural glass, however trivial it might have turned out to be.

My gratitude goes to the members of my graduation committee for their efforts and ideas, Liesbeth for helping me in the laboratory, Jeroen for providing me with prototype elements, my parents and Calvin for reading my report (twice) and Anneloes for the helping me with the layouts.

Measurements in mm
Scale: undefined

-  Adhesive
-  Glass
-  Reinforcement

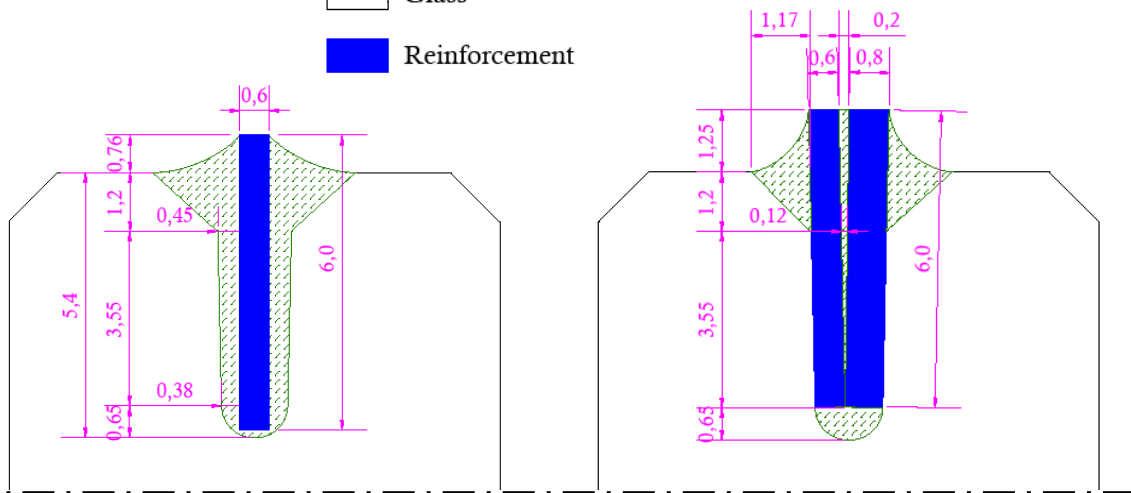


Figure 1, Close-up of cross-section of glass pane with SGG Plug-in groove and reinforcement. Left: geometry 1, right: geometry 2.

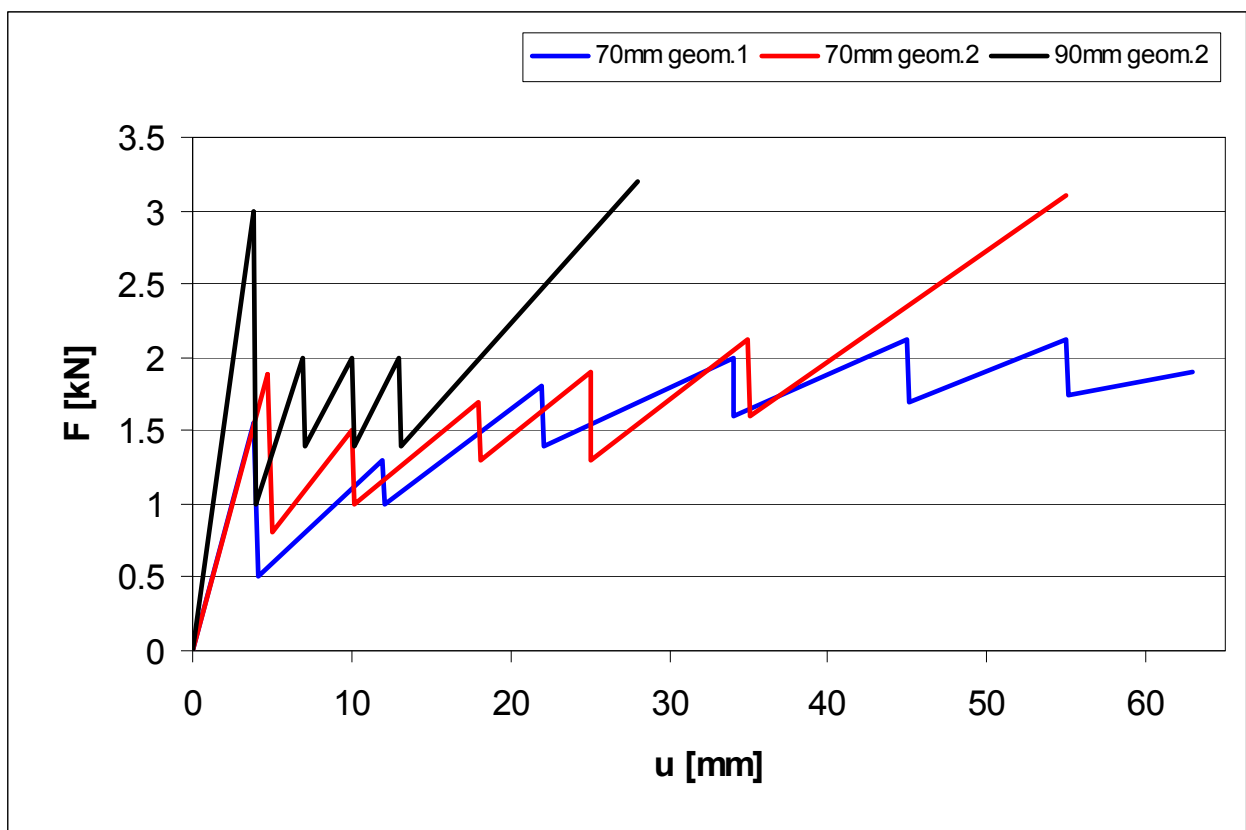


Figure 2, Typical force-displacement curves for three different girder types that are designed for this thesis.

Abstract

Transparency and light are hot items in building design and massive structural elements often form an unwelcome necessity for architects. The structural use of glass could be an ideal solution to this problem, but as yet it has not been widely applied. The problem is that although glass is a transparent, strong and stiff material, it is feared by structural engineers for its brittle and unpredictable failure behavior.

Many studies have proven that the introduction of reinforcing elements can provide a safe failure behavior for glass girders, but none of them seem transparent enough. This study focused on developing a new and more transparent solution to reinforce a structural glass girder.

An exploratory study into the subject has resulted in a selection of appropriate reinforcing materials and adhesive systems. This resulted in three possible concepts for reinforcing methods:

1. Laminated glass girder with reinforcements in the laminate.
2. Adhesively bonded reinforcement in the SGG Plug-in groove under in the girder.
3. Pre-stressed element in the SGG Plug-in groove and reinforcement adhesively bonded under the girder.

Concept 2 was deemed the most suitable and chosen to be worked out further.

Stainless steel, glass fiber and carbon fiber were selected as potentially suitable materials for reinforcing elements. They were tested for strength, stiffness and ductility. Carbon fiber turned out to be the strongest and sufficiently stiff and was chosen as reinforcement material for this research.

Apart from that, efforts were made to develop a stronger and more transparent glass fiber bar.

The adhesives DELO Rapid 03 Thix, Huntsman Araldite 2011, 2013 and 2020 were tested in several different adhesive layer thicknesses. Araldite 2011 was chosen as best suitable in this application.

The strength of the adhesive joint between the glass pane and the reinforcement in the groove was determined before the girder was dimensioned. Tensile pull-out tests were done on small reinforced glass specimens with a length of 150mm and 2 different reinforcement geometries (see *Figure 1*):

1. Thin reinforcement, thick adhesive layer
2. Thick reinforcement, thin adhesive layer.

The strength of the joint was comparable for both geometries. Geometry 2 was stiffer than geometry 1, but geometry 1 seemed to ensure the best ductility for the girder.

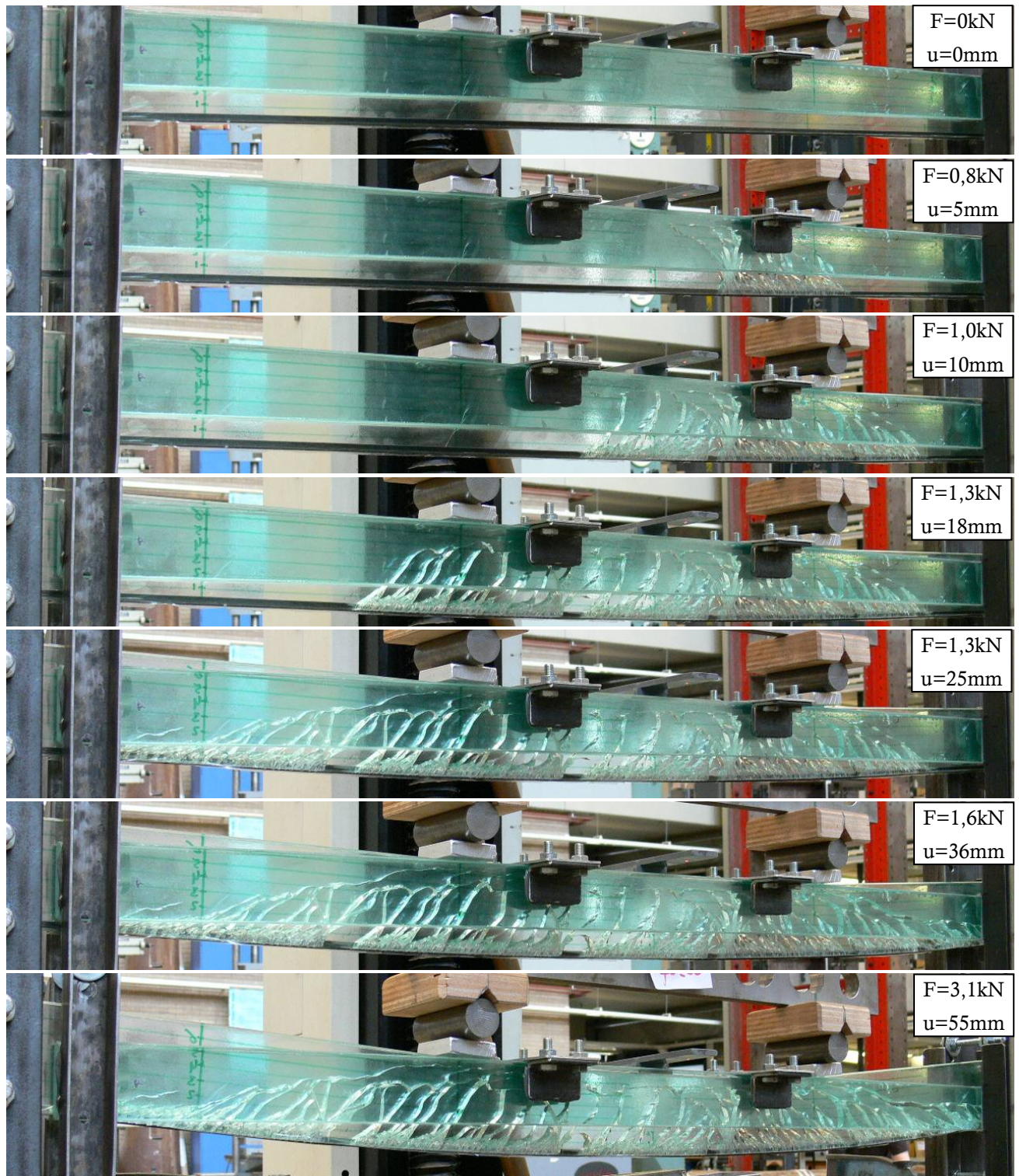


Figure 3, Specimen 70-06 at different moments during the four point bending test. Specimen dimensions are $l*w*h=1500x10x70$ mm. The photos are taken directly after each new crack occurred, corresponding to the fallbacks in force that are displayed in the red curve in Figure 2.

Both geometries were applied in two girder prototypes with dimensions 1500x70x10mm. 3 specimens of each geometry were tested up to total failure in a displacement controlled four point bending test. Both showed good residual load bearing capacity accompanied with large deformations (see *Figure 2* and *Figure 3*).

The governing factor for ultimate failure of both geometries was the bending moment. The reinforcement was pulled out of the glass pane by tensile force.

Geometry 2 was applied in slightly larger girders, with a height of 90mm. Again good residual load bearing capacity was obtained, with slightly smaller deformations.

This time not bending moment, but shear force was governing for ultimate failure: the reinforcement was torn out of the glass perpendicular to the direction of the reinforcement.

Further conclusions were that the strength of the glass was not severely affected by the milling of the SGG Plug-in groove and small production imperfections do not have a large influence on the structural behavior of the girder.

The goal of this master thesis; to develop a reinforced structural glass girder with safe failure behavior where reinforcing elements are invisible or at least hardly noticeable, has been partly reached.

The developed girder with carbon fiber reinforcement shows ductile failure behavior with sufficient residual deformation and load bearing capacity. However the black reinforcement is clearly visible in the bottom of the girder.

A similar girder reinforced with specially developed transparent glass fiber meets the demand for transparency much better. However in the developed geometry it does not show a safe ductile failure behavior.

This research has proven that the SGG Plug-in groove is suitable for adhesively bonding carbon fiber reinforcement in a small span structural glass girder.

Apart from that, the research has lead to the development of a transparent glass fiber element with a very high tensile strength that can be applied as reinforcement in glass elements.

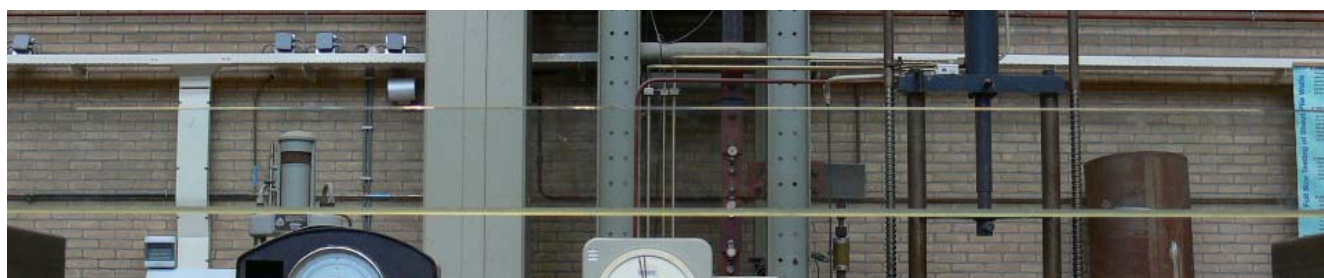


Figure 4, 90mm high glass girder mounted with glass fiber reinforcement in SGG Plug-in groove in bottom of girder.

Key to symbols

Table 1, Key to symbols

Symbol	Unit	Entity
l	[mm]	Length
h	[mm]	Height
d	[mm]	Width
E	[N/mm ²]	Young's modulus
A	[mm ²]	Surface area
ϵ	[mm/mm]	Strain
θ	[°] / [rad]	Angle of rotation
u	[mm]	Deflection/sag/displacement
γ	[%]	Angle of deformation of adhesive joint
ρ	[g/cm ³]	Density
\varnothing	[mm]	Diameter
k	[N/mm]	Spring stiffness
$\sigma_{i.gl.}$	[N/mm ²]	Stress in glass pane at initial failure
$\sigma_{i.re.}$	[N/mm ²]	Stress in reinforcement at initial failure
$\sigma_{max.re.}$	[N/mm ²]	Stress in the reinforcement at ultimate failure
M_i	[Nmm]	Bending moment at initial failure
$M_{i.gl.}$	[Nmm]	Bending moment, taken by the glass at initial failure
$M_{i.re.}$	[Nmm]	Bending moment, taken by the reinforcement at initial failure
M_{max}	[Nmm]	Bending moment at ultimate failure
F_i	[N]	Applied force by the pressure bench at initial failure
F_{max}	[N]	Applied force by the pressure bench at ultimate failure
q	[N/mm]	Divided load
N	[N]	Normal force
N_v	[N]	Vertical component of normal force
N_h	[N]	Horizontal component of normal force
$I_{re.}$	[mm ⁴]	Moment of inertia of reinforcement
$I_{gl.}$	[mm ⁴]	Moment of inertia of glass pane
$I_{re.geom.1}$	[mm ⁴]	Moment of inertia of reinforcement geometry 1
$I_{re.geom.2}$	[mm ⁴]	Moment of inertia of reinforcement geometry 2

Table of Contents

Preface	3
Abstract.....	5
Key to symbols	8
Table of Contents	9
1. Introduction.....	11
2. Problem analysis	15
3. Literature Study	17
3.1 Glass	17
3.2 Laminating systems	29
3.3 Reinforcements	41
4. Reinforcing concepts.....	57
4.1 Introduction.....	57
4.2 Requirements.....	59
4.3 Glass fiber reinforcements in the laminate.....	61
4.4 Reinforcement in the glass pane.....	65
4.5 Pre-stress in the glass pane, reinforcement under the girder	69
4.6 Conclusions and recommendations.....	73
5. Tests.....	75
5.1 Introduction.....	75
5.2 Material tests	77
5.3 Aluminum pull-out tests.....	83
5.4 Glass pull-out tests	97
5.5 Preliminary beam tests	115
6. Beam tests	127
6.1 Introduction.....	127
6.2 Method.....	129
6.3 Results.....	130
6.4 Discussion	161
6.5 Conclusions and Recommendations	171
7. Discussion	172
8. Conclusions	174
9. Recommendations	175
11. References	176

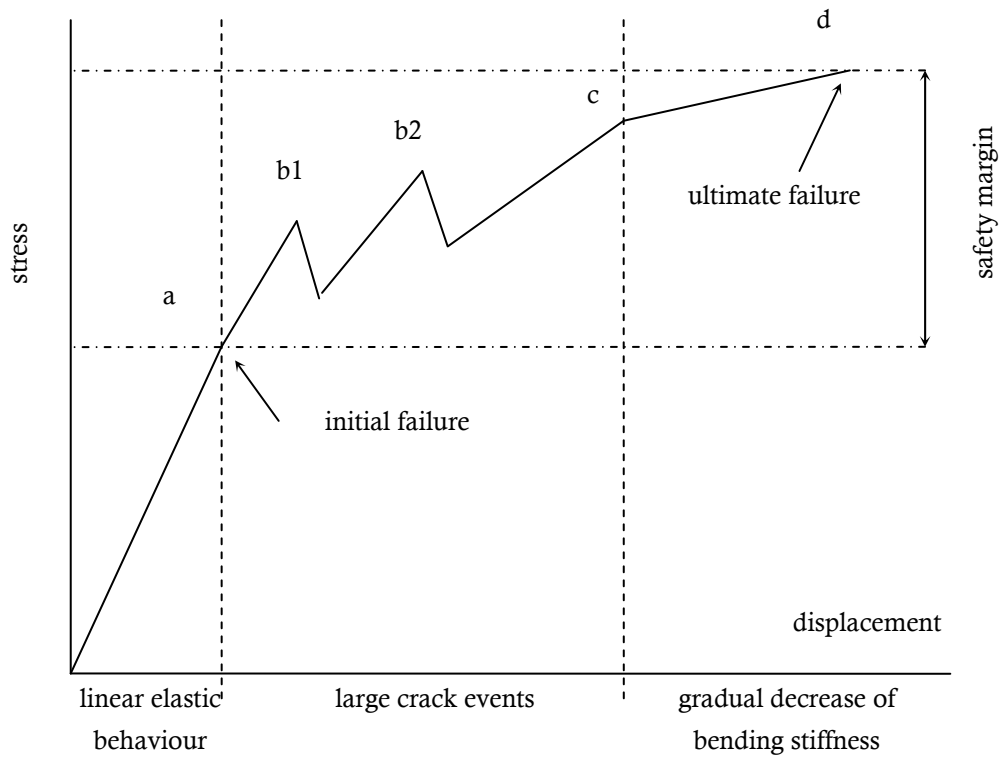


Figure 5, Desired stress-displacement diagram of bending tests of a structural glass beam.[12]

- a) Initial failure, the first crack occurs in the bottom of the beam.
- b) Every peak resembles another crack, the cracks grow further and further as the load is increased.
- c) The beam is cracked all over, it is clear that it will collapse soon.
- d) Ultimate failure, the beam collapses completely.

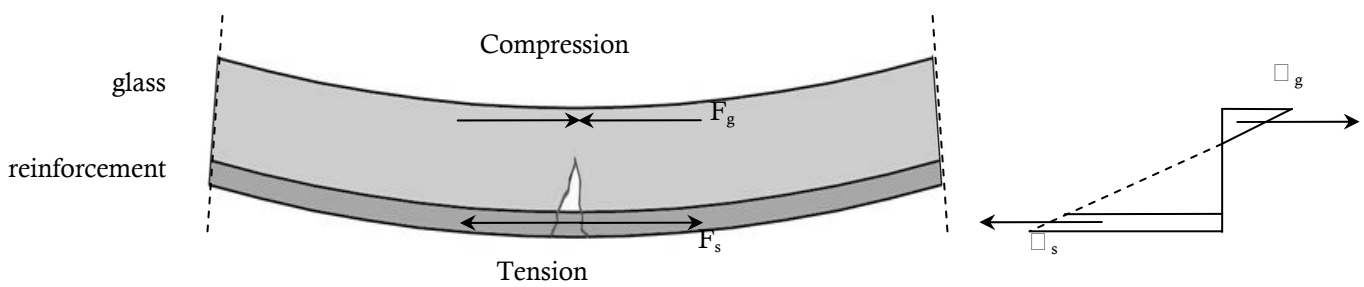


Figure 6, Distribution of forces after initial glass failure. [12]

1. Introduction

Transparency and light are hot items in building design and massive load bearing elements often form an unwelcome necessity for architects. The structural use of glass could be an ideal solution for this problem.

Glass has fascinated mankind for over five millennia. It is known for its transparency and strength, but also for its brittle failure behavior. Where it was first used merely for decorations and art objects, the applications have expanded over the centuries. Structural glass however, is a relatively new concept.

An important aspect of a structure is that it ‘warns’ before failure. Warning means obvious change in structural behavior indicating imminent failure, without the loss of structural function. This is visualized by a stress-displacement diagram like presented in *Figure 5*. Important aspects are a decrease in bending stiffness accompanied with large deformations and a sufficient residual load bearing capacity.

A material with roughly similar structural properties to glass is concrete. Since the Egyptian era, men have used concrete as building material. The problem was that it could hardly withstand tensile forces and it was very sensitive to brittle failure. Structural use of concrete took a leap in 1867 when Josef Monier patented the use of steel reinforcements in planters. Reinforced concrete opened up a whole new range of possibilities in building engineering, resulting into a revolution in architectural design. Nowadays it is one of the main construction materials.

Glass also has a very high compressive strength compared to its practical tensile strength. Unlike concrete however, is the absence of plastic deformation ability. Because of this, large stress peaks arise at small flaws in the surface that result in capricious and brittle fracturing. In the design of a glass girder it is evident that the height of those stress peaks is controlled and

that measures are taken to allow residual load-bearing capacity after initial failure.

There are two ways of ensuring the safe application of glass as structural material.

The first is over-dimensioning the element so that the occurring stress will never exceed the strength of the material. This method is widely applied in structural glass design nowadays and results in large and heavy structures.

With such a glass beam the stress-displacement curve in *Figure 5* would still end at point a: it would deform linearly up to the point of brittle failure where it collapses without any warning.

A much more subtle way of ensuring safety is to introduce a warning capacity in the girder, like reinforcements did for concrete. This involves measures to ensure the rest of the curve in *Figure 5*; the ability to deform plastically in the ultimate limit state.

The introduction of reinforcing elements in a glass girder seems a logical step. Various studies have shown that reinforcements can ensure a safe failure behavior, but the problem remains that they often form a clearly visible and therefore disturbing element. It seems that the universal law on ‘retention of misery’ still applies. The perfect structural glass girder (transparent *and* stiff *and* strong *and* ductile) has not been manufactured yet.

Reinforcements in a glass girder will neither enhance the strength nor the stiffness of the element in the serviceability state, but merely provide safety after the initial failure.

This master thesis will focus on the development of a new, more transparent reinforcing method for a structural glass girder and the guarantee of its safety by practical research.

Chapter 3 describes the theoretical study that is done to reveal the possibilities and bottlenecks in this subject. The material glass and its known applications are reviewed, existing methods for reinforcing are mapped, a range of possible materials for reinforcing elements is generated and a study into the principles of adhesive bonding is done.

Chapter 4 concerns several reinforcing concepts. It begins with creating a framework by setting a list of requirements. This is followed by the description of three different concept reinforcing methods. Although all three are interesting, one concept is chosen to be worked out further.

The structural behavior of the chosen reinforcing method is based on extensive practical research. The tests that were done to validate the behavior of the girder are described in chapter 5:

Paragraph 5.1 contains the selection of three possible reinforcement materials from the range that is reviewed in chapter 3. They are tested for tensile strength and stiffness and eventually one is chosen for further use in this thesis. A small exploring test is done to gain insight in the affects of adhesive layer thickness to the strength of the connection. This is presented in 3.2.

Before the girder is dimensioned, the strength of the connection of the reinforcement to the glass pane has to be specified. Paragraph 5.4 describes tests where this is done: small-scale glass specimens are reinforced in different geometries. The reinforcement is then pulled out and the force and displacement are measured. In paragraph 5.5 preliminary beam tests with three specimens are described that are done to refine a satisfactory test setup and to gain insight in the behavior of the intended reinforcing method.

The information that is gained from the tests in Chapter 5 is used in the dimensioning of several prototypes for the girder. These prototypes are tested in for failure behavior and structural safety which is presented in chapter 6.

The report is finalized with a reflection on this thesis from which conclusions are drawn and recommendations are made for further research.

2. Problem analysis

Problem statement

There are several proven methods to reinforce structural glass girders, but most of them still have clearly visible disturbing reinforcing elements.

The 'market' desires a structural glass element where the reinforcement is not visible, or at least hardly noticeable.

Goal

The goal of this master thesis is to find an alternative method for reinforcing a structural glass girder where optimal structural behavior is combined with maximum transparency.

Design Brief

The problem is tackled by investigating possibilities and generating several concepts for reinforcing a glass girder. One concept is chosen to be worked out and subjected to practical tests to ensure its safety in failure.

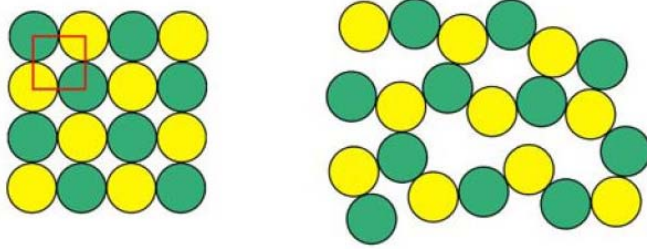


Figure 7, Crystalline structure on the left. Amorphous on the right.[3]



Figure 8, Rock-crystal [18]

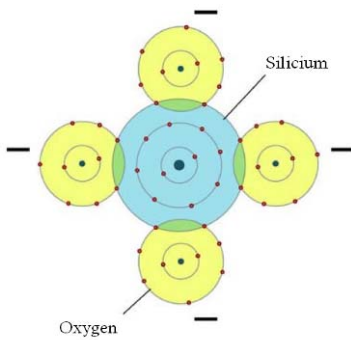


Figure 9, Silicium atom, bonded by four oxygen atoms that still demand 1 extra electron to be in electrically stable state [3]

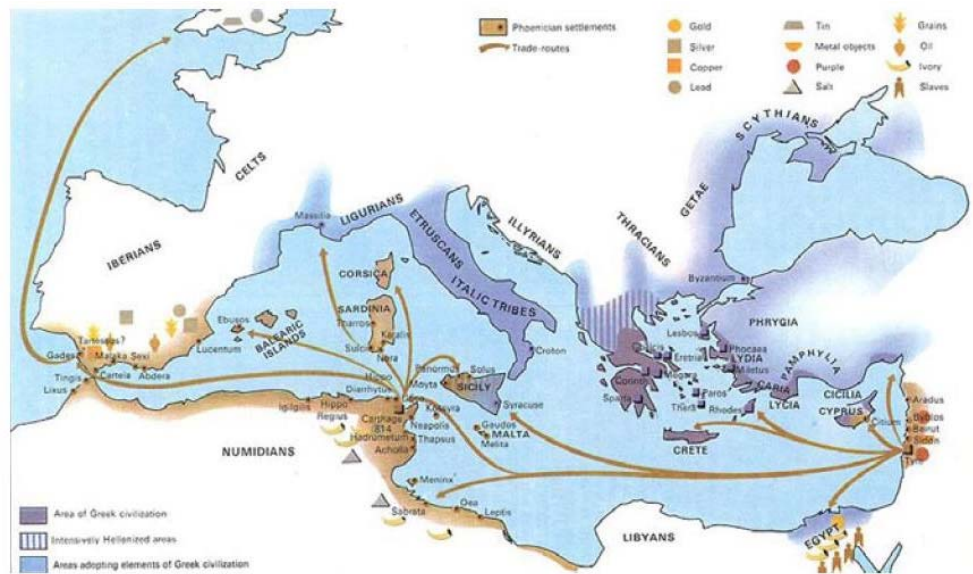


Figure 10, Phoenician trading area [3]

Table 2, Properties of different glass types [1]

Type	SiO ₂ amount	Additives	Melting temperature (°C)	Characteristics
Quartz glass	99,5%	-	1750	Very high melting point, low thermal expansion coefficient
Float glass	70%	NaO ₂ (15%), CaO (10%)	700	Low melting point, high thermal expansion coefficient
Crystal glass	70%	PbO (10%), NaO ₂ (15%)	700	Low melting point, high density, relatively soft and therefore easy to polish
Aluminumsilica glass	70%	Al ₂ O ₃	800	Good thermal shock resistance
Borosilica glass	70%	B ₂ O ₃	1000	High melting temperature, very low thermal expansion coefficient, good resistance against chemicals

3. Literature Study

3.1 Glass

History

Before 3000 B.C. the only glass known to man was rock-crystal, found in mountain caves (see *Figure 8*). In those days it was an almost magical material that looked like ice, but did not melt. The invention of glass-making was done by accident. It is told by an almost mythical tale of Phoenician traders, described by the Roman writer 'Plinius the Elder' in his magnum opus "Historia Naturalis":

"The river Belus (in nowadays Lebanon, see *Figure 10*) is muddy but deep, only revealing its sands when the tide retreats. The sand does not glisten until it has been tossed about by the waves and its impurities removed. Then and only then, when the sand is thought to have been cleansed by the scouring action of the sea, it is ready for use. The beach extends for not more than half a mile, but for many years this area was the dole producer of glass.

The story goes that one day a Phoenician ship belonging to traders in soda called there and spread out along the shore to make a meal. There were no stones on the beach to support their cooking-pots, so they placed lumps of soda from their ship under them. When these became hot and fused with the sand on the beach, streams of an unknown translucent liquid material flowed and this was the origin of glass." [1]

Accidentally the traders heated the right ingredients to the right temperature: sand, soda and chalk. The sand contained siliciumdioxide, the soda contained sodium carbonate and the seashells on the beach contained chalk, or calcium carbonate.

In the fire they were melted together into 'siliciumquatrooxide', which is the basic molecule of glass (see *Figure 9*).

Chemical properties

Glass is a special material. It is transparent, hard and breakable, but when heated it flows like water. In some ways, glass is comparable to water, or more like ice. Chemically glass is inorganic and amorphous.

Amorphous means that glass is neither solid nor liquid, but somewhere in between; in 'glassy' state. Theoretically glass still flows at room temperature, be it very slowly. Some wrongly say that this is known by the fact that old windows are thicker at the bottom than at the top. Actually this is the result of the ancient production process (see *Figure 12*, Crown glass) and not of the viscosity of the glass. It has never changed noticeably over the centuries. At room temperature the viscosity is so high that it would take more than 20.000 years to even sense the slightest change in shape.

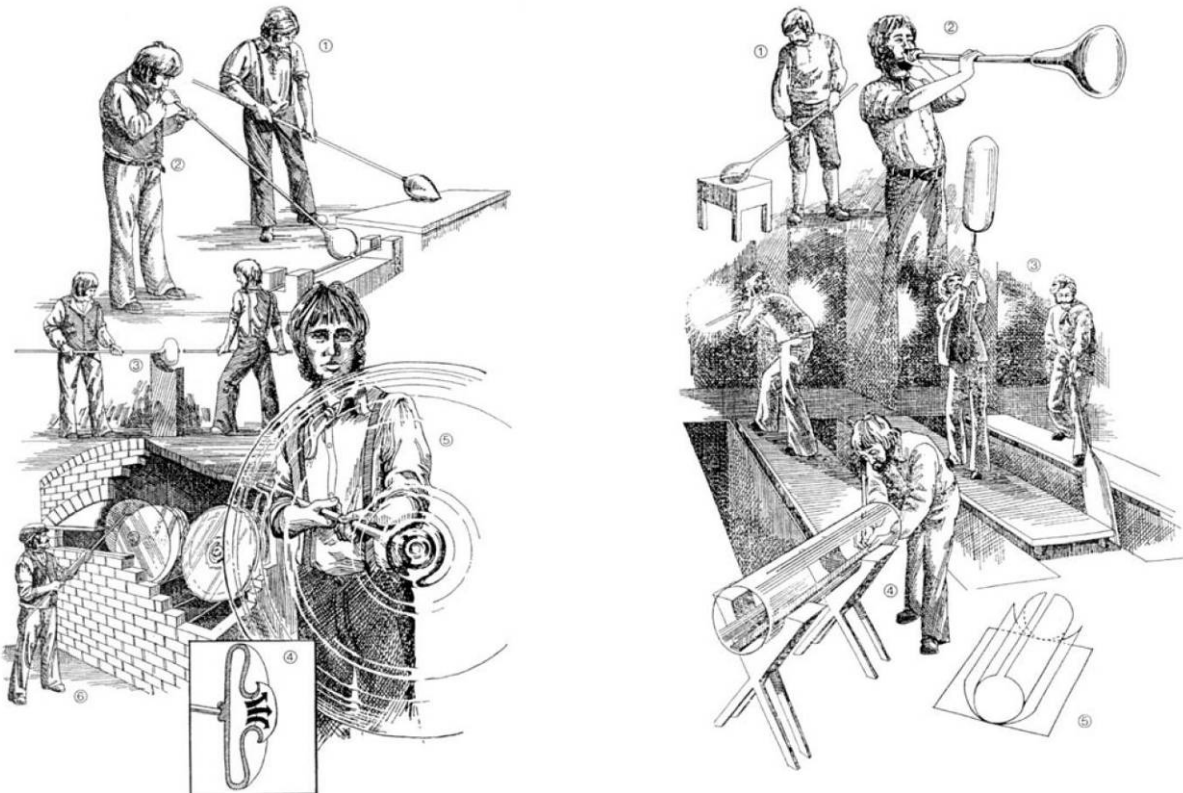


Figure 12, left: production of Crown glass, right: production of cylinder glass

- | | |
|--|---|
| <ol style="list-style-type: none"> 1) The melted glass taken out of the oven with a blowpipe and shaped into a pear-shape on a table. 2) Heating, blowing and spinning into a balloon-shape. 3) When the balloon is big enough, the blowpipe is removed and replaced by a iron bar on the other side. 4) The glass ball is reheated and spinned at high speed. The edge where the blowpipe used to be is pressed to the outside by the centrifugal force, shaping the glass into a pancake. 5) The pancake during spinning. 6) The glass discs are reheated in an oven to remove the residual stresses in the material and cooled down slowly. | <ol style="list-style-type: none"> 1) The molten glass is taken out of the oven by a blowpipe and reshaped. 2) The glass is shaped into a balloon with a flat bottom. 3) After reheating the balloon is shaped into a cylinder. 4) The cylinder is cut open. 5) The open cylinder is heated again, stretched out and cooled down slowly. |
|--|---|

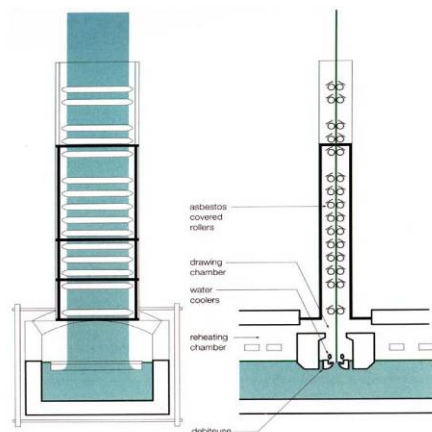
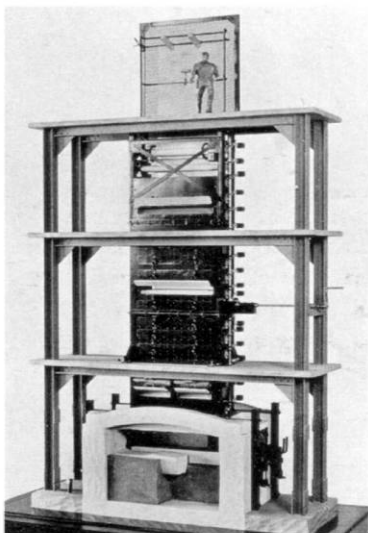


Figure 11, Pulling-glass method.

There are several different types of glass. All of them have silicium (SiO_2) as main component. By adding supplementary materials to the mixture, the characteristics can be changed. The main types of glass and briefly their characteristics are given in *Table 2*.

Production process over the centuries

Over the centuries many ways of shaping glass have evolved. The most widely known is with the blowpipe and was invented in Syria in the first century. 'Glass blowing' created the possibility of making all kinds of objects like bowls, glasses and vases.

With this method, several ways of producing glass sheets were developed to use glass in window panes.

The Romans came up with the first one: liquid glass was poured over a flat stone where it solidified. Then it was polished on both sides until it was transparent enough to look through. This was of course very time consuming and expensive (see *Figure 13*).

Later on the Romans came up with a new method: a blown sphere was pricked open at the opposite side from the blowpipe and then rotated very quickly until a large pancake shaped circle was formed. From this circle, rectangular or diamond shaped parts were cut that could be used. The maximum possible size of these was about 400 x 300 mm (see *Figure 12*).

Another method was developed in the 14th century around the city Strasbourg. A blown sphere was stretched into a cylinder. This cylinder was cut open and spread out, resulting in a thin flat sheet. In the 18th century, glass planes of 1000 x 800 mm could be created (see *Figure 11*).

The next step was made in Belgium around 1900 with the method of 'pulling glass'. A steel bar is lowered in a bath of molten glass. It is then pulled upwards, dragging a thin sheet along with it which is cooled and solidified by the air. This way wide and long sheets can be produced.

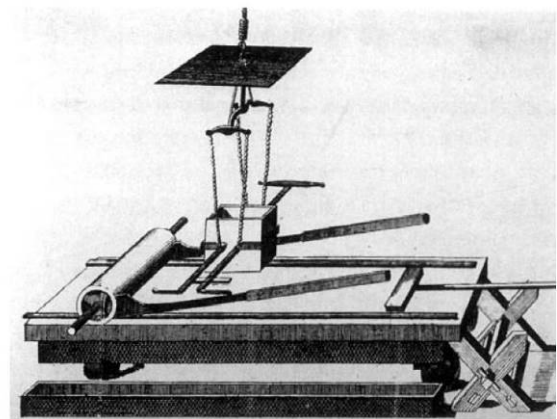


Figure 13, Table pouring method.

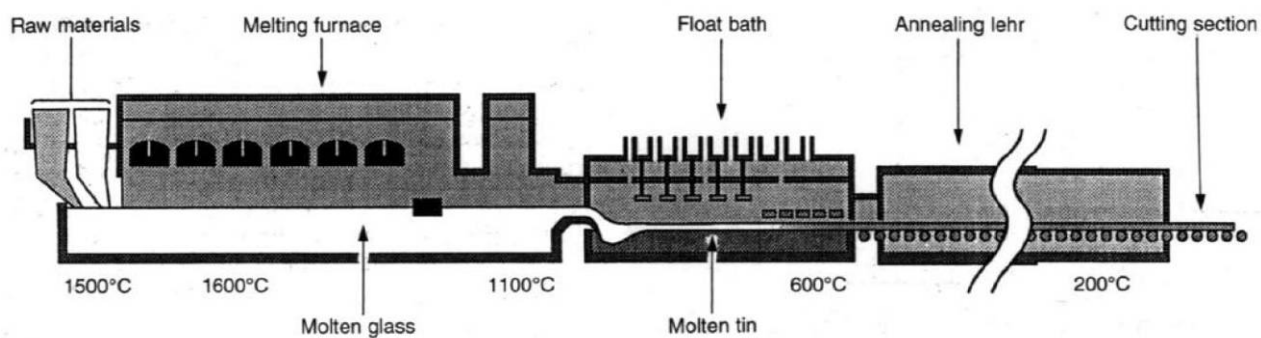


Figure 14, Float glass production process.

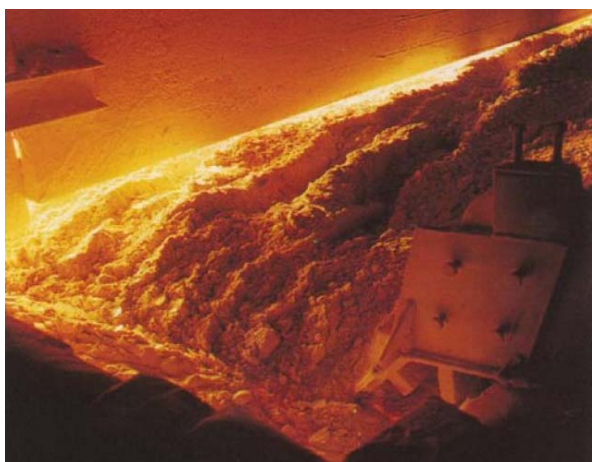


Figure 16, Raw material mixed in the right quantities.



Figure 15, glass heated in the furnace.

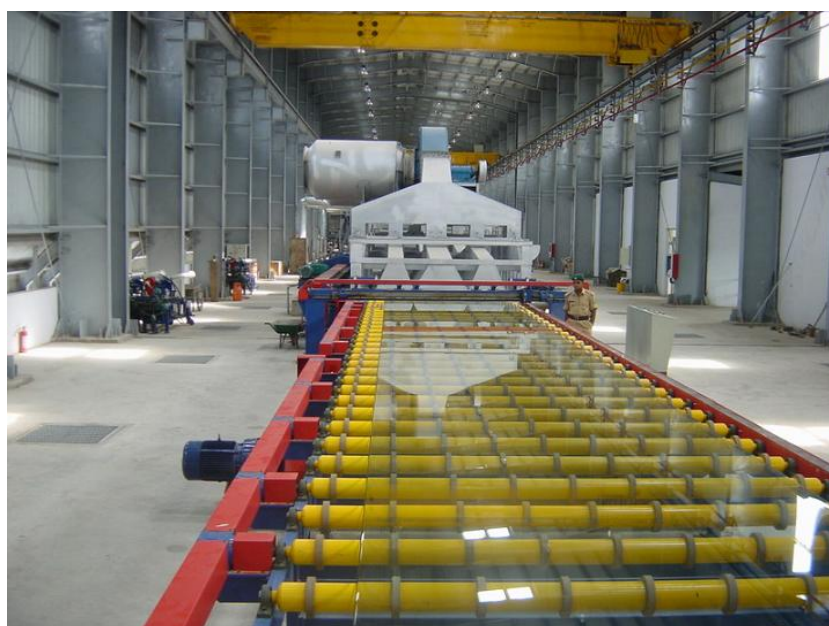


Figure 17, Float glass production line.

Modern glass production

Almost all modern glass panes are produced by the 'float-glass' principle. This method of glass production is invented by the Pilkington brothers in 1959 in England. The production is done in several stages:

The commodities, mainly sand, soda, chalk and dolomite, are mixed in exact quantities. Together with recycled glass gravel they are poured into the oven where they are heated to 1350 °C. To remove impurities, the liquid glass is kept at this temperature for several hours.

The glass is then smoothly poured into the beginning of a 500m long bath of liquid tin. Because of the difference in specific weight, the molten glass floats on the tin bath. This results in a perfectly smooth, flat layer of glass that constantly floats to the end of the bath. The temperature gradually drops from 1100 °C to 600 °C at the end where it is in plastic, but solid state.

The glass pane that continuously floats out of the tin bath is then supported by rollers. By adjusting the speed of the rollers, the glass can be stretched into different thicknesses.

It is guided through several facilities where coatings or texture in the surface can be applied.

Further cooling of the glass is done little by little to prevent unequal shrinkage that result in internal stress, this process is called 'annealing'. When the glass is cooled to room temperature, it is cut into pieces of 3200 x 6000 mm for transportation purposes.

Float glass can be ordered in thicknesses from 2 to 25mm (see *Table 3*). Although technically any thickness is possible, for production reasons the choice is limited. Every time a factory changes the speed of the rollers

and thus the thickness of the glass ribbon, a certain length is not equally flat, making it worthless for sale. Swapping thickness is expensive and therefore most facilities produce the same ribbon, continuously, for years in a row.

To gain the required structural width for a girder thicker than 12 mm the glass has to be laminated. This means that multiple layers of glass are stacked on to each other with layers in between that bond to both surfaces.

Another argument for laminating is that the outer layers can function as safety buffer for incoming objects. These outer layers are referred to as 'sacrificial' panels.

Table 3, Standard float glass thicknesses and their tolerance [1].

Float glass is available in the following thicknesses	
Glass thickness	Tolerance
2, 3, 4, 5, 6 mm	± 0,2 mm
8, 10, 12 mm	± 0,3 mm
15 mm	± 0,5 mm
19, 25 mm	± 1,0 mm

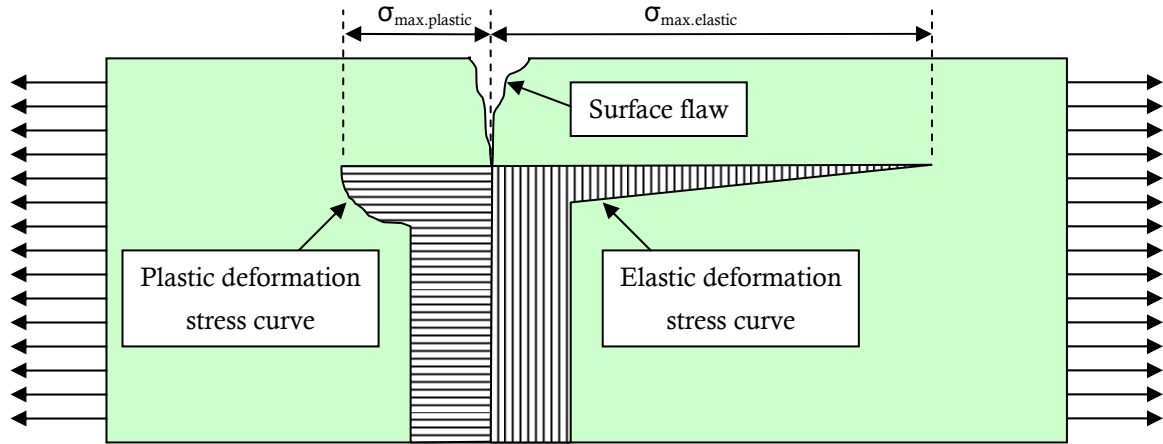


Figure 20, Plastic and elastic stress concentration curve at a surface flaw in a glass surface (at the right) loaded under tensile stress. Based on [4].

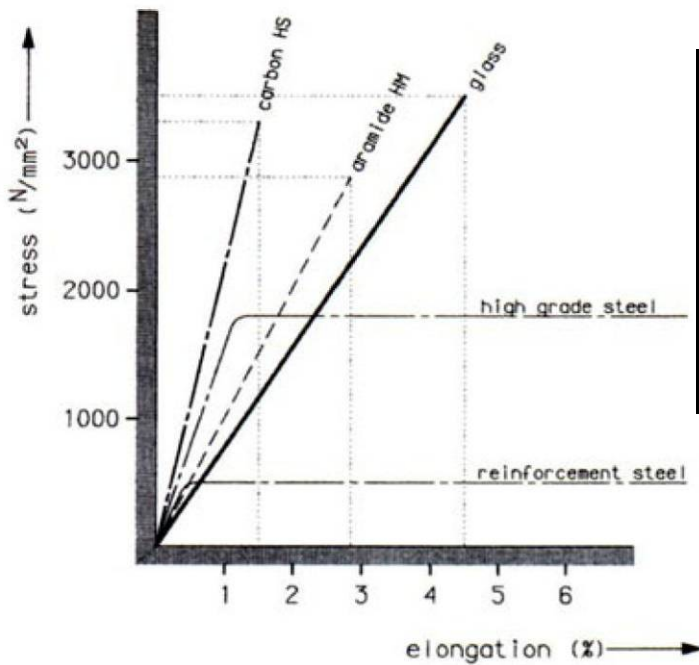


Table 4, Float glass properties [1]

Float glass properties		
Density	25	[kN/m ³]
Young's modulus	70-75	[GPa]
Shear modulus	29	[GPa]
Tensile bending strength	30-90	[N/mm ²]
Compressive bending strength	700-900	[N/mm ²]
Softening temperature	560-580	[°C]
Thermal expansion coefficient	9,0*10 ⁶	1/K

(left) Figure 19, Stress-elongation curve of laboratory produced glass compared to other materials. [2]

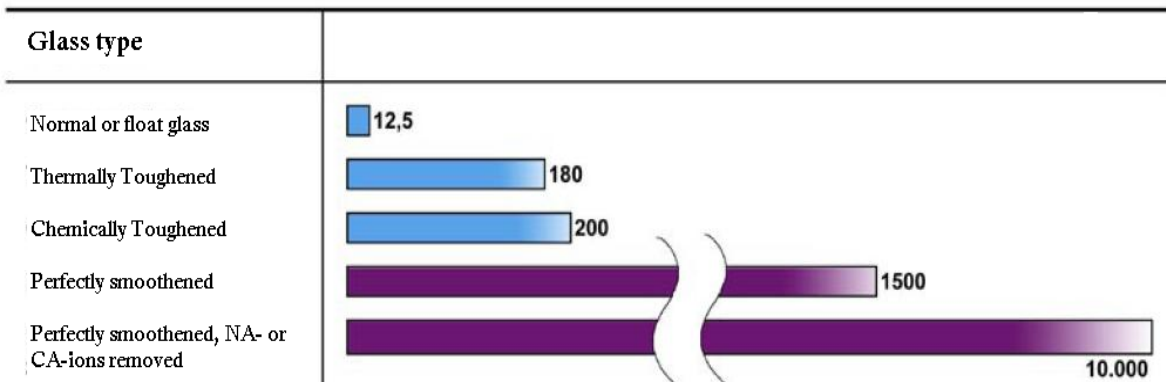
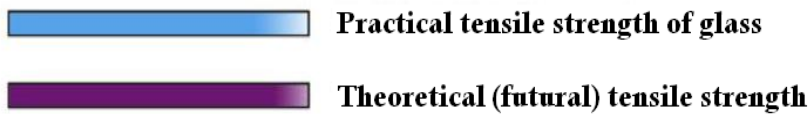


Figure 18, Allowable tensile bending stress under permanent load, as adopted by Rob Nijisse (ABT Bouwtechniek). [3]

Mechanical properties of glass

Theoretically, glass has a very high compressive and tensile strength of 6500 N/mm² which has been reached with laboratory produced glass under perfect circumstances.

In practice, the ultimate tensile strength is much lower: 27 N/mm² to 62 N/mm² is used for calculations, depending on the condition the glass is in. This is because stress peaks arise at the bottom of microscopic cracks, exceeding the ultimate tensile strength (see Figure 20). The stress peak causes the crack to grow, increasing the stress, etc. This causes the sudden brittle breaking, virtually without warning.

In materials that yield before failure, this stress peak is reduced to the yielding strength of the material: the material locally deforms, spreading out the stress over a larger area. Glass behaves completely elastic up to the breaking strength, so the stress is not spread out nor the peak reduced.

The relative height of the stress peak is given by the concentration factor ($K_{\sigma;c}$) [3]:

$$K_{\sigma;c} = \frac{\sigma_{\max}}{\sigma_{\text{average}}}$$

For glass the following is given, where L is the crack length:

$$K_{\sigma;c} = 0,76$$

$$K_{\sigma;c} = \sigma_c \sqrt{\pi L}$$

$$\sigma_c = 0,43 \sqrt{\frac{1}{L}}$$

Because the ultimate compressive strength is much higher than the practical tensile strength, structural glass girders usually do not break due to compressive stress failure.

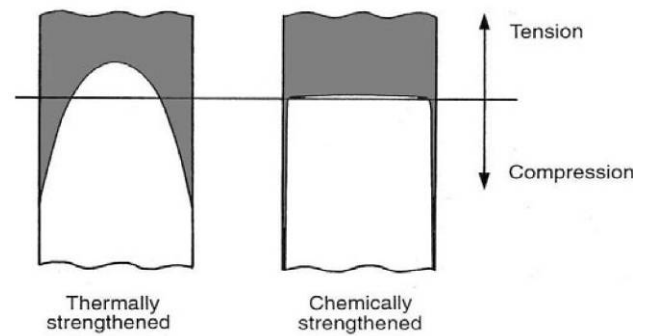


Figure 22, Internal stress distribution in cross-section of tempered glass panes. [1]

Various other mechanical properties can be found in **Table 4**.

Tempered glass

Tempered glass is specially treated glass where the surface is loaded under compression and the core under tension. This allows more tensile forces to be applied to the glass because the cracks are initially loaded under compression.

Additional advantage is that toughened glass is less sensitive to aging, which means that the allowable tensile bending stress under permanent loading is much higher.

Tempering glass is mainly done by thermal treatment: The glass is heated to 650 °C. Then the surface is cooled rapidly by air cannons. This causes the surface to cool quicker than the core, resulting in a parabolic stress distribution over the cross section. Tempering can also be done by chemical treatment, resulting in a different stress curve.

The internal stress contains a lot of energy that is all released at once when a fracture occurs. This makes the glass break into many small pieces all over the pane (see *Figure 21*).

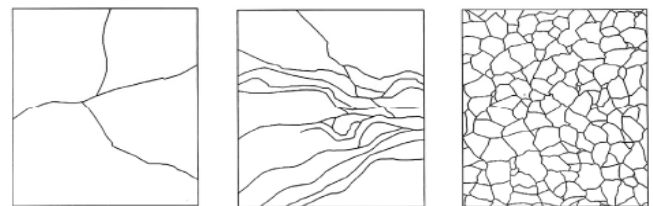
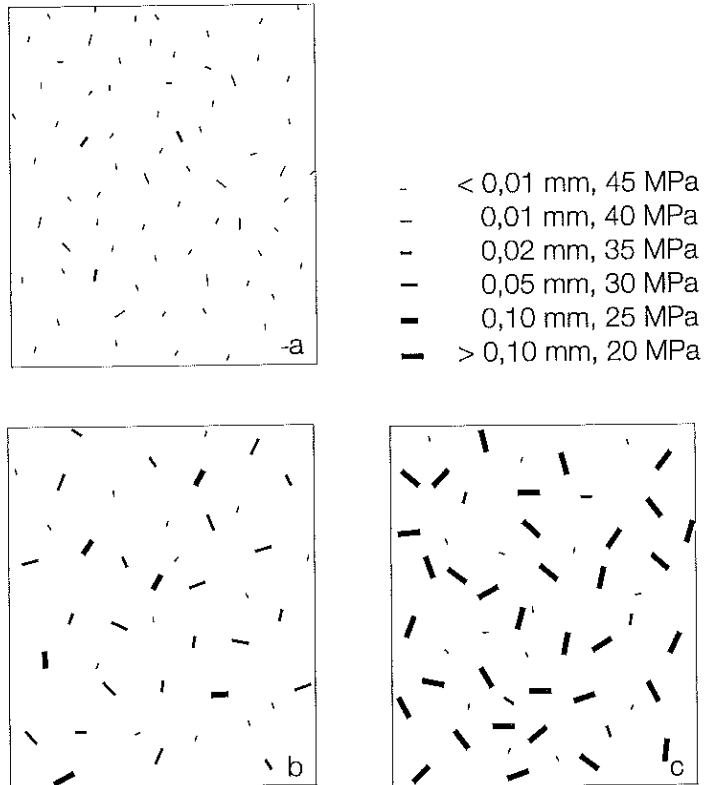


Figure 21. Crack pattern of three types of glass. [1]

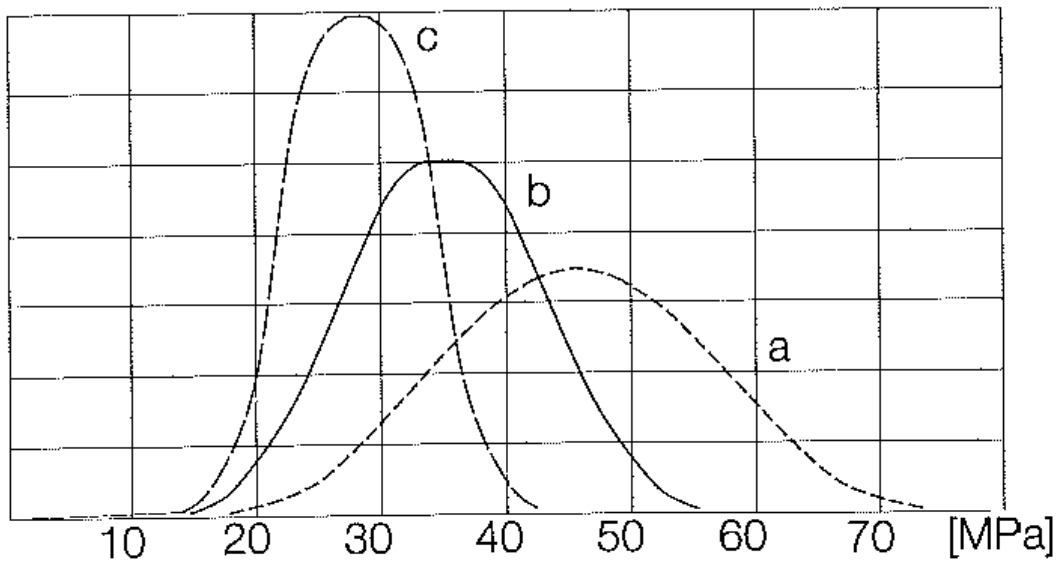
Left: Annealed.

Middle: Heat strengthened.

Right: Fully tempered.



Distribution of surface damage for a) new glass, b) weathered glass, c) glass with inherent damage.



Normal distribution curves for a, b, c

Figure 23. Statistical distribution of glass strength in relation to surface damage. [1]

Edge works

When glass is cut to size, the edges are notorious for their sharpness. Apart from that, irregularities in the surface of glass panes have a great influence on the tensile strength, as it was explained in the previous paragraph. Therefore the edges are finished in a variety of ways.

Edge works can be done by means of grinding and polishing. There are many different cutters on the market creating various shapes.

The simplest one is the 'normal cut', also called arrissed edge (see *Figure 24*). This means that the sharp edges of the glass pane are rounded off by a grinding machine, but the end surface of the glass itself remains untouched.

The glass can also be finished by a ground edge. A grinder grazes off a very small edge of the glass pane, eliminating large irregularities like small cracks and fissures, leaving a rough surface. An edge that is cut exactly to size may leave some blank spots. If some more is grinded off the blank spots are removed as well. A grounded edge can also be finished by a polishing machine, removing all roughness and making it completely transparent.

During the lifespan of a glass element, the surface is exposed to suffer damage from all sorts of sources, like scratching, weather, wind, chemicals etc. This has a negative influence on the strength. *Figure 23* shows the influence of surface damage on the strength of glass. This shows that it is evident to prevent weathering of (structural) glass elements if possible.

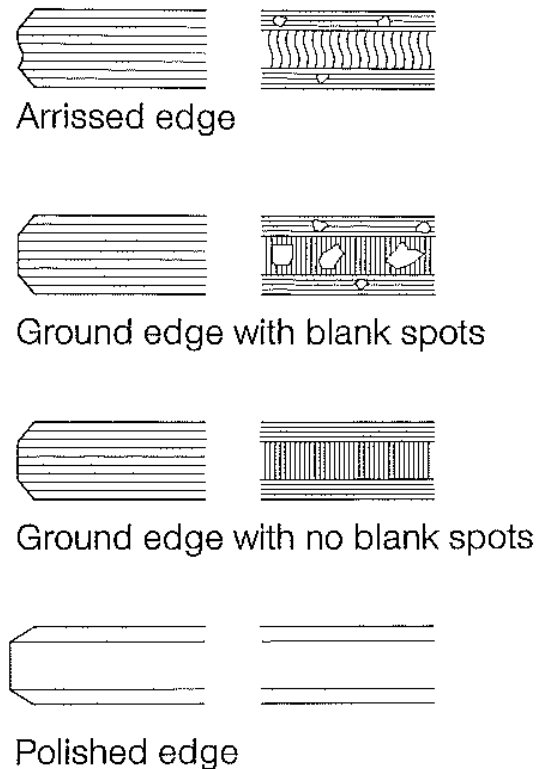


Figure 24, Different ways of finishing glass edges. [1]



Figure 26, Clip-Edge cutting machine. 6 individual cutting blades produce the odd-shaped groove.

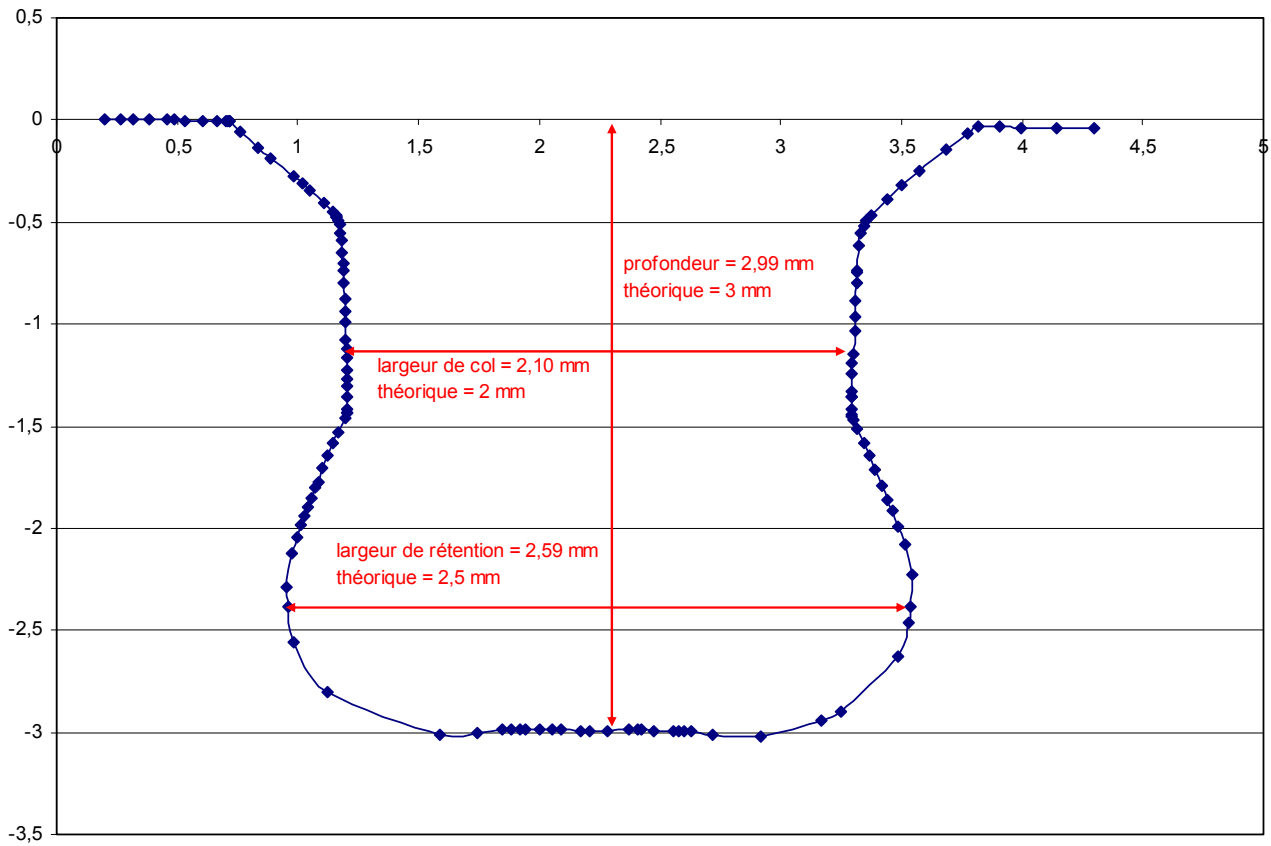


Figure 25, Exact dimensions of the clip-in groove

SGG Clip-in groove

A new cutter by Saint Gobain introduces a small groove into the edge of glass panes under the name 'Clip-In'. The possible glass thickness varies from 8 up to 12 mm. The idea is to attach glass panes at the end grain to each other without elements protruding from the plane. A small plastic barb-profile is 'clipped' into the groove where it is fixated to the glass.

Alternative shapes of the groove can be made with this machine. The maximum possible size that can be produced with the current milling blades is 2mm wide and 6mm deep.

Strength tests of the Clip-Edge groove have been performed on 4-point bending tests in perpendicular direction of the plane, where the groove has proven not to affect the strength of the glass. This test however is not representative of in-plane bending, like in a glass girder.

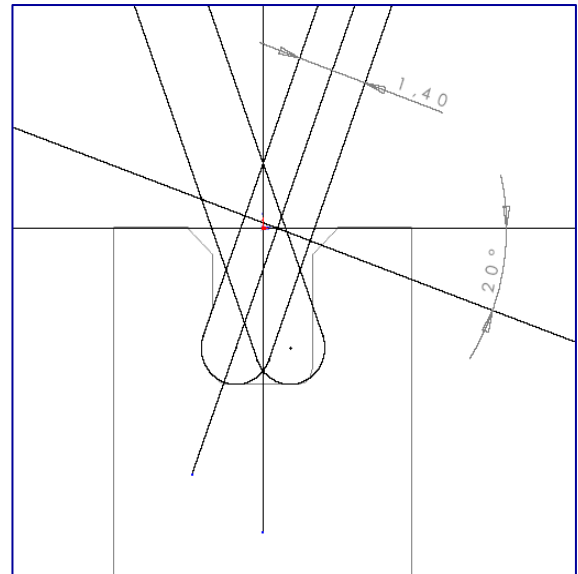


Figure 27, Angles in which the blades are cutting the groove



Figure 28, Close-up of Clip-In groove

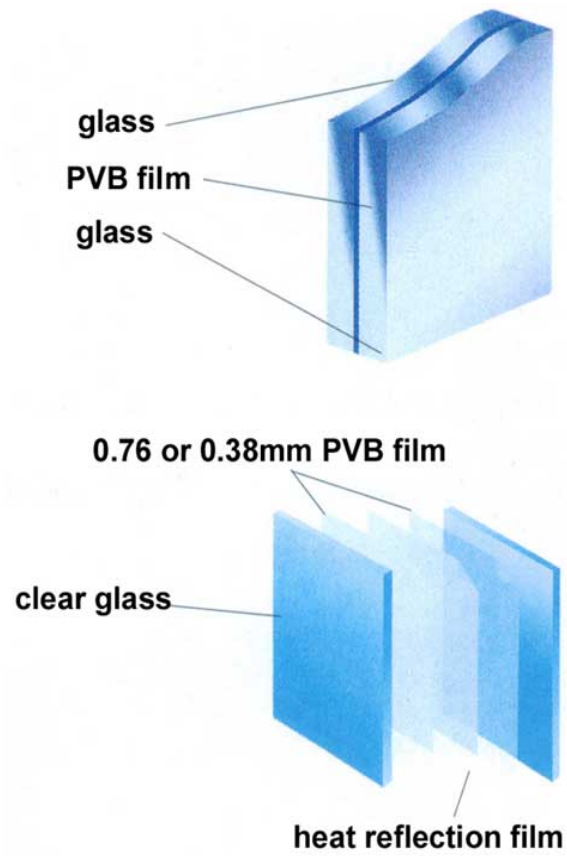


Figure 29, Laminated glass with PVB foil. Also other foils can be integrated in the interlayer



Figure 30, Production PVB film

3.2 Laminating systems

Using a bonding is a technique where two elements are connected with a non-metallurgic extra material that bonds to both surfaces (adhesion) and also has enough strength of its own (cohesion) (see Figure 33).

Advantage of this bonding technique over for example a bolted connection is that the transferred forces are spread out of a large surface. If designed correctly there are no point loads and no stress concentrations in both materials or in the adhesive.

Important in the design of the connection is that static stress levels in the adhesive are controlled. When they exceed certain values, the adhesive will start to creep which will result in loss of strength and eventually in rupture of the joint. The amount of creep in the joint is related to three variables: the stress in the adhesive, the temperature and the time period in which it is loaded.

There are many bonding systems on the market. They can be divided roughly in foils and adhesives. The difference is that a foil is applied in solid state, heated to over a certain softening temperature where it liquefies and bonds to both surfaces. Then it is cooled down again. Adhesive is applied in liquid state and under influence of a certain chemical reaction it is going over to solid state, bonding to both surfaces.

The most suitable systems for application in this thesis are presented in this chapter.

Foils

Two foils are widely used in glass lamination: Poly Vinyl Butyral (PVB) and Sentry Glass Plus (SGP).

Poly Vinyl Butyral (PVB)

This foil is initially developed for use in windscreens of cars. It is known as a soft interlayer with high elasticity, but poor creep performance, looking a bit like PE foil. The foil can be ordered in thicknesses of a multiple of 0,38 mm.

The softening temperature of 55 °C is (just) inside the normal temperature use range. This makes it less applicable for structural use in glass girders.

The laminating process goes as follows:

1. The foil is placed on one layer
2. The element is heated in a furnace to about 250°C and pressed together by rolls.
3. The laminate is cooled down

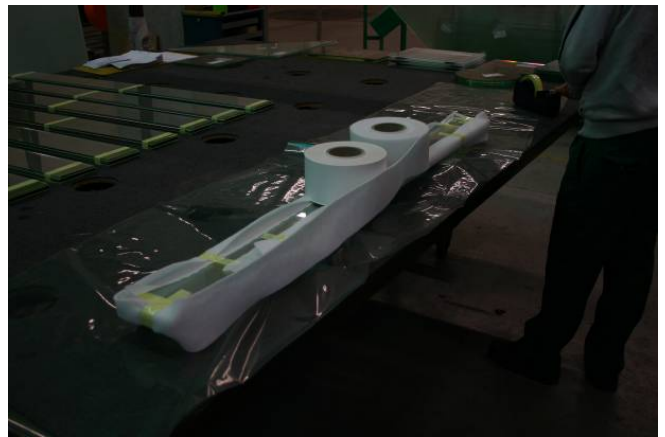
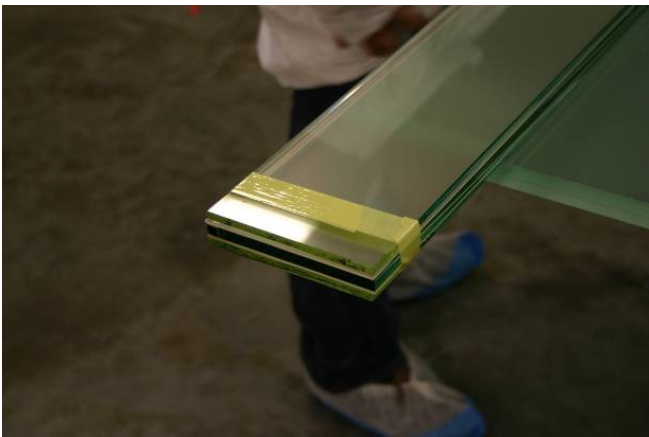


Figure 31, Laminating process with SGP film, from right to left, top to bottom:

- 1) The SGP-foil is being cut to size
- 2) The glass and foil are put on each other
- 3) The laminate is temporarily fixed
- 4) Sharp edges are covered by non-compressible, air-permeable foam.
- 5) The element is covered by foil and sealed
- 6) The air is sucked out of the package until it is in vacuum.
- 7) The element is put on a grid and heated in the autoclave under a pressure of 2 bar and a temperature of 140°C for 120 minutes, excluding the heating and cooling periods of one hour each.

Sentry Glass Plus (SGP)

SGP is produced by DuPont and originally created for security glazing and hurricane windows. It is a much stiffer and stronger interlayer than PVB with excellent clarity. This is also available in thicknesses of 0,38mm.

The laminating process is described in Figure 31.

It is possible to bond this foil to other materials than glass. Prototypes are made where a stainless steel rectangular tube is incorporated in the element. Problem with this technique is that manufacturers are worried that fabrication errors like encapsulations of air in the laminate might occur, resulting in delamination and loss of residual load bearing capacity of the element after a couple of years.

Adhesive systems

The adhesives that are reviewed in this thesis are so called epoxy resins.

The name epoxy is the general classification for a very broad range of products that all have an 'epoxy ring' consisting of two carbon atoms that both are single bonded to the same oxygen atom (see Figure 32). They are all in the family of the 'liquid reaction adhesives'. This means that initially they consist of monomers, pre-polymers and in some cases additives that enable the initiation of the curing. When hardening the monomers bond into high-polymers increasing the molecular weight of the atoms making the substance go over into solid state.

There are three types of fundamentally different polymer formation reactions.

Poly-addition implies the reaction of two reactants without the decomposing of water or other low-molecular connections.

Poly-condensation also implies the reaction of two different monomers, however these form low-molecular decomposition products for example acetic acids that have no further use in the structure.

Poly-merization describes the rest. A typical reaction is the breaking of C=C double bonds allowing two chains of C-C monomers to bond to each other.

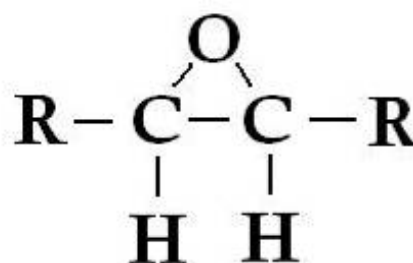


Figure 32, Chemical schematic structure of epoxy ring. [28]

Table 5, Material properties of Sentry Glass Plus. [3]

Property	Units Metric (English)	Value	ASTM Test
Young's Modulus	MPa (kpsi)	300 (43.5)	D5026
Tensile Strength	MPa (kpsi)	34.5 (5.0)	D638
Elongation	%	400	D638
Density	g/cm ³ (lb/in ³)	0.95 (0.0343)	D792
Flex Modulus 23°C (78°F)	MPa (kpsi)	345 (50)	D790
Heat Deflection Temperature at 0.46 MPa	°C (°F)	43 (110)	D648
Coefficient of Thermal Expansion (-20°C to 32°C)	—	10–15 x 10 ⁻⁶ /C°	D696



Figure 33 a+b, a (above): 100% adhesive failure where adhesive is stuck on 1 substrate. b (below): 100% cohesive failure, where adhesive is stuck on both substrates.[18]

Adhesive as interlayer

A thin layer of adhesive can be applied between two sheets of glass which results in a very strong element that is much less sensitive to creep. Another advantage of an adhesive is that the element is not bounded by the maximum measurements of an autoclave, which is 2,4 by 6,0 m.

A disadvantage of an adhesive is that it is hard to apply a constant thickness over the whole surface, resulting in thicker and thinner areas of the interlayer and thus an unpredictable structural behavior. Also encapsulation of dirt is done more easily and the laminating process is more sensitive to human mistakes since it involves more craftsmanship of the manufacturer.

Another disadvantage of an adhesive is that it is almost too strong. When one glass layer breaks, the amount of energy that is released at the point of fracture damages the other layers, resulting in a total collapse of the girder. Also when hardening, the resin will shrink to certain extend, introducing unintentional stresses in the glass.

Adhesive as bonding between reinforcement and glass

Adhesives with high-strength mechanical properties are epoxy resins. These cure under influence of a chemical reaction. This reaction can be started in several ways; Light-activated, UV-curing, 1-part heat curing and 2-part cold curing. In the appendix tables can be found where specific properties of different adhesives are stated.

The ingredients that are responsible for the curing are already in the substance with 1-part resin.

Light-activated resins are hard to work with, because as soon as day-light hits them, they start to harden. UV-curing resins are more interesting. They can be applied

to the element and they start to harden under influence of a UV-lamp. This way the moment of hardening can be controlled which makes the manufacturing process easier.

1-part heat curing epoxy resin is liquid when applied at room temperature. After application the element has to be heated, for instance in an autoclave, where the resin hardens.

2-part epoxy resin consists of two separate liquid substances that have to be mixed in a certain proportion. Directly after they come in contact with each other the hardening process begins. Usually a limited time varying from a few minutes to 2 hours is given in which the resin is still liquid and in this time it has to be applied to the element.

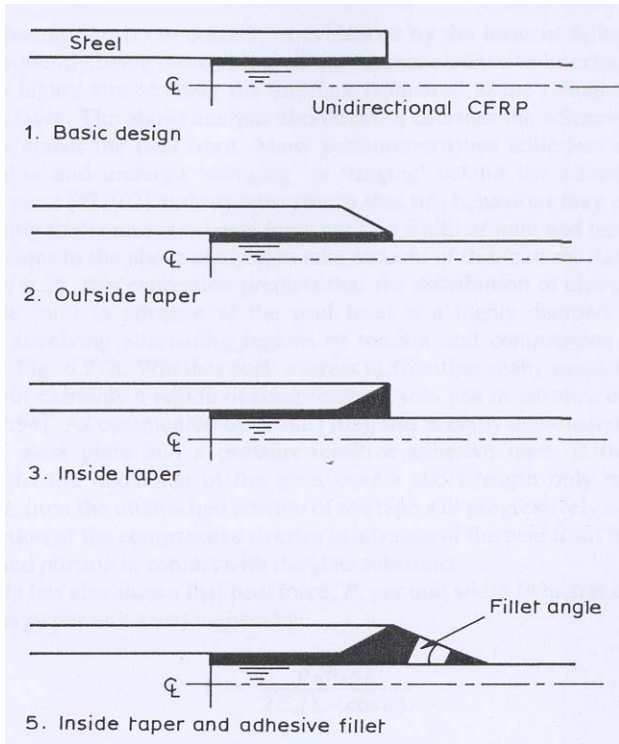


Figure 36 1-4, possible alternative designs to introduce shear stress in the adhesive layer. [6]

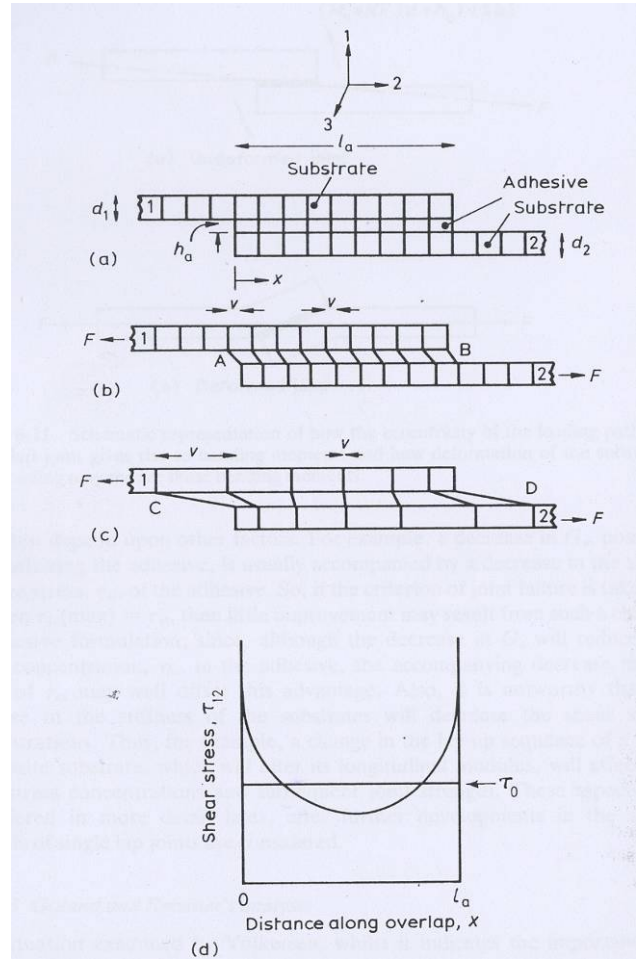


Figure 37 a-d, Schematic representation of single overlap joint. a) unloaded, b) loaded in tension with inextensible substrates, c) - with extensible substrates and d) elastic shear stress distribution in adhesive layer. [6]

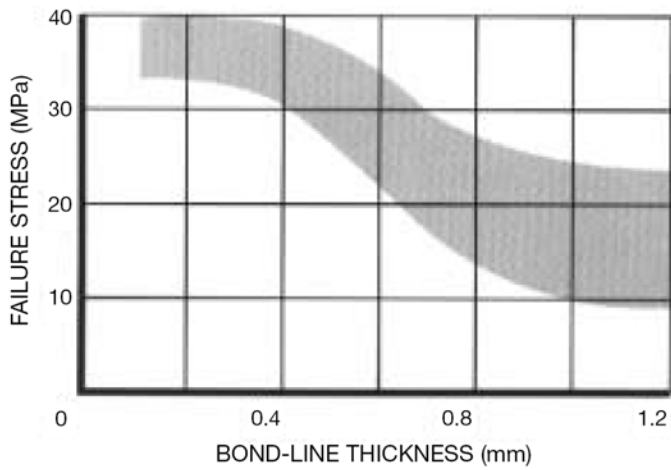


Figure 34, Bond-line thickness vs. Shear strength. [10]

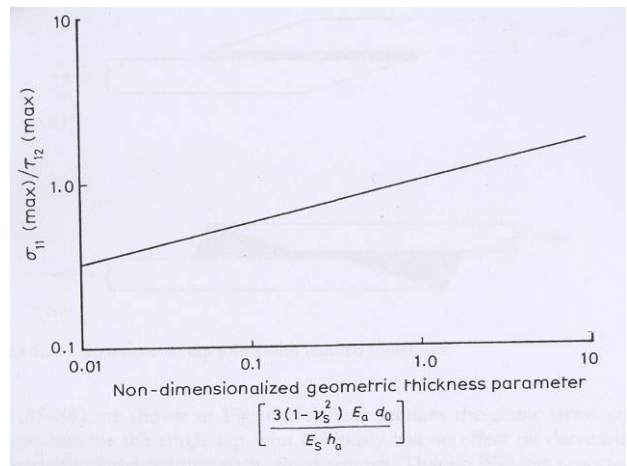


Figure 35, Relative shear/tensile strength of adhesive layer in relation to the thickness of the layer. For every adhesive this curve is different, so the curve can only be interpreted as trendline. [6]

Principles of adhesive bonding mechanics

Stress distribution

In designing adhesively bonded joints it is evident that the stress level in the adhesive is not exceeded.

The first useful stress analysis in adhesive bonded joints was done by Volkersen in 1938. It considers the adhesive to behave as a linear elastic solid substance which deforms only in shear. Note that in adhesive mechanics the displacement due to deformation of the adhesive layer is given in the angle of deformation (see Figure 37b). A thicker layer thus results in larger displacements of the substrates.

Consider a single overlap joint (See Figure 37-a). When the substrates are inextensible materials loaded in tension, they will not deform (see Figure 37-b) and the shear stress in the adhesive will be equally divided over the contact surface of the joint.

When the substrates are extensible materials they will deform because of the shear stress applied by the adhesive (see Figure 37-c). This happens in both substrates, resulting in stress peaks at both ends of the substrates where the adhesive is stretched most (see Figure 37-d). If the stress peaks exceed the ultimate shear strength of the adhesive, the joint will fail.

If the adhesive is a non-plastic material, the stress peak will be high. Various studies have shown that the stress peak is greatly reduced by the plastic-elastic behavior of epoxy adhesives: the adhesive will locally creep, spreading out the stress peak.

The height of the stress peak is related to the E-modulus of the substrates; when the substrates deform a great deal, the stress peak will be high and steep. The less

both substrates deform the lower and more stretched out the stress peak will be.

The stress can also be controlled by (locally) increasing the thickness of the adhesive layer between the substrates (see Figure 36). This cannot be done without consequence however, as it is visible in *Figure 35*. There is an optimum in the strength of the adhesive connection related to the thickness layer, as it is shown in *Figure 34*.

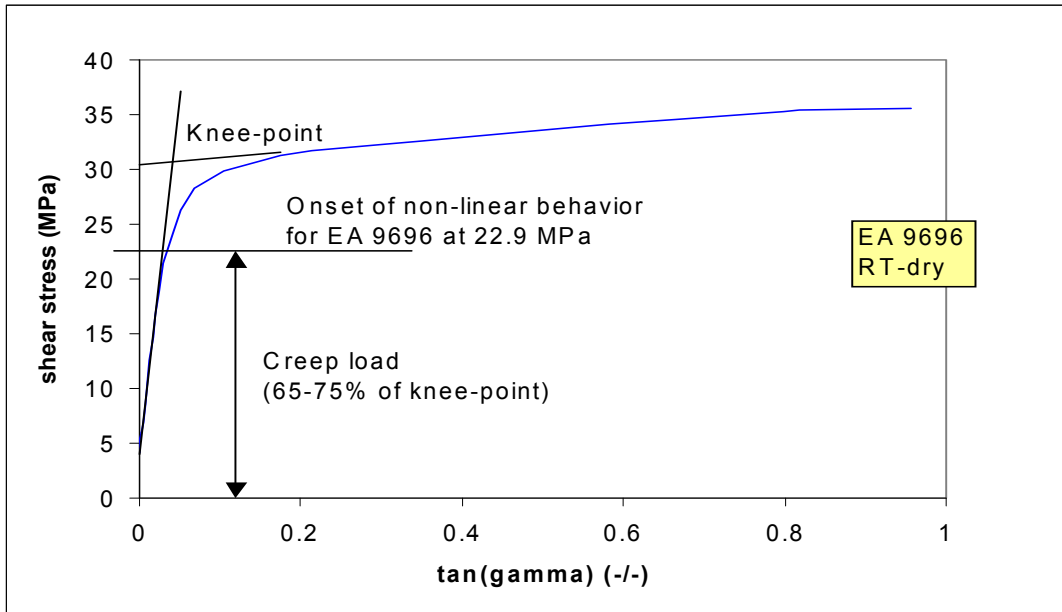


Figure 39, shear stress / $\tan(\gamma)$ diagram where the knee-point is given. [18]

B-D-RT-T-1-4 (Epibond 1590)

Dry / Room temperature / 50% RH

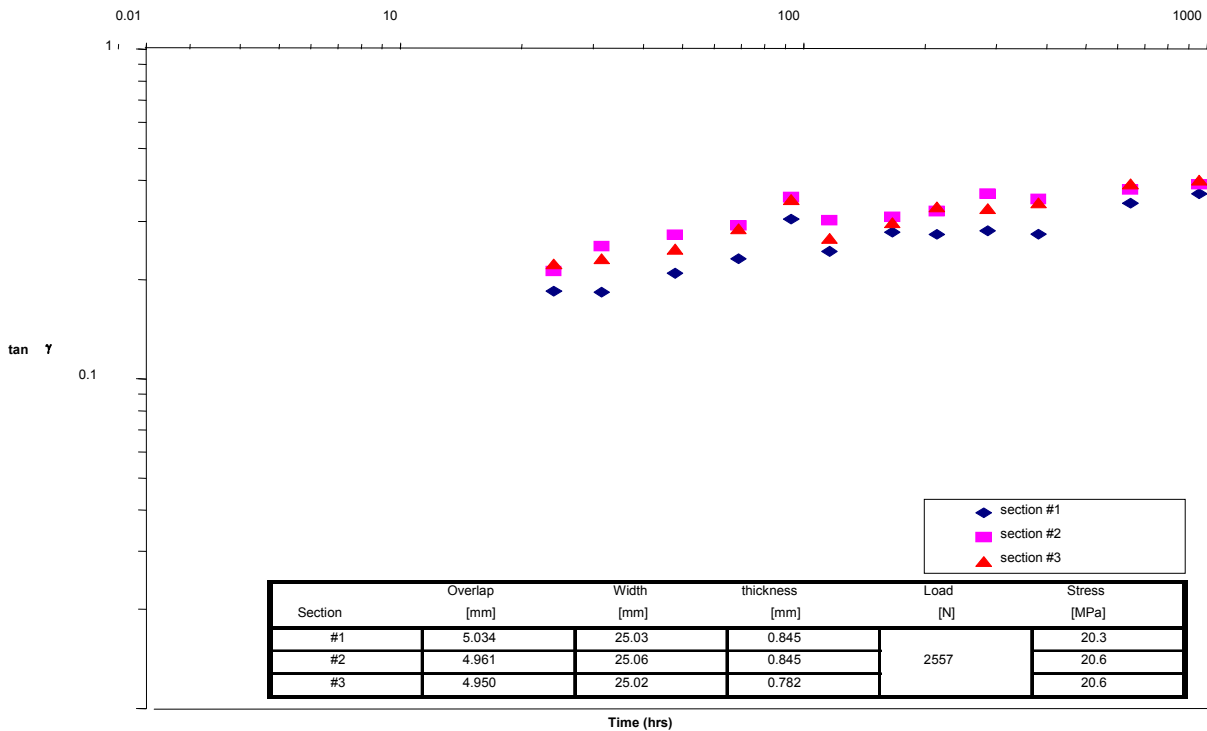


Figure 38, Creep test results. [18]

Creep behavior of adhesive bonding

Little is known about the exact calculation of creep behavior of adhesive systems, because usually in the design all is done to avoid it.

Most important is to avoid stresses in the adhesive above the so called 'knee-point' (see Figure 39). Under the knee-point the adhesive behaves more or less linear. Above that point the creep increases drastically up to the failure point. When the adhesive is loaded well under the knee-point, creep behavior is predictable. The tests from which the results are given in Figure 38 are done at a loading of 65% of the knee-point (see Figure 39).

The displacement/time-curve of creep tests shows a straight line on double logarithmic paper (see Figure 38), meaning that the creep exponentially decreases in time. This line can be extrapolated on various grounds like time or loading. From test results like these, a pretty good estimation can be made of the creep of these adhesives.

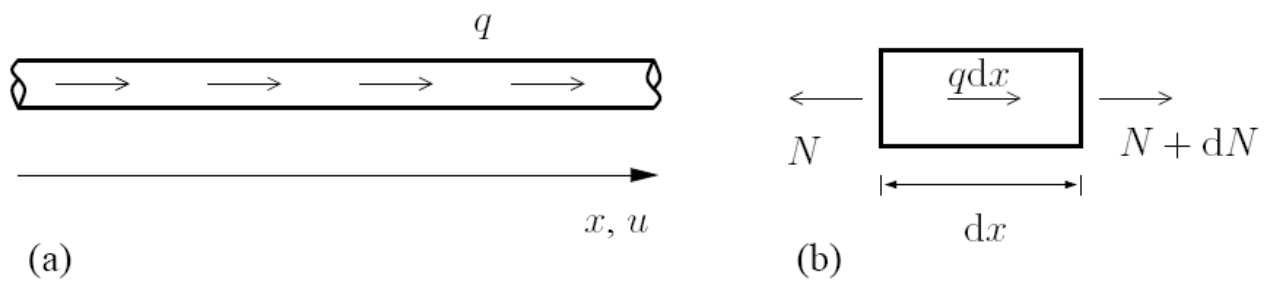


Figure 41 a & b [11]

a) Straight homogeneous bar under distributed axial load.

b) Infinitesimal element of the bar.

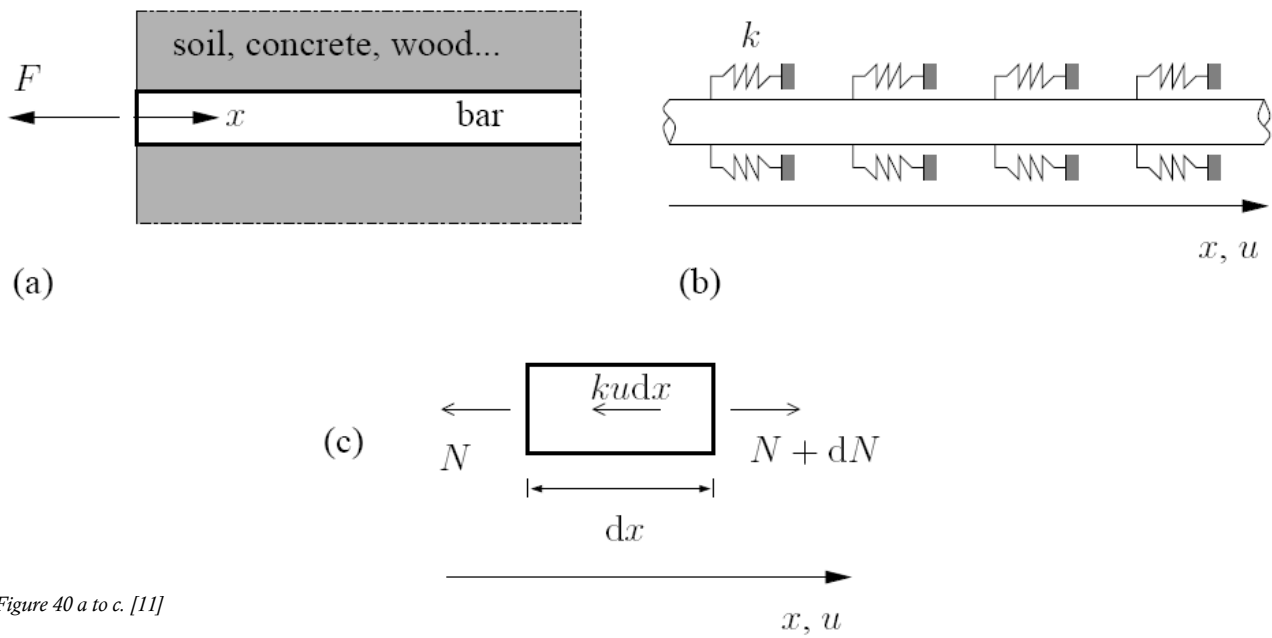


Figure 40 a to c. [11]

Axial deformation of bars and the pull-out problem

To understand the stress distribution over the length of an adhesive joint it is evident to consider the underlying structural principles. To simplify the situation all materials are approached as linear elastic with stiffness E and the elements are considered homogeneous to have homogeneous cross-sections over the length.

Consider **Figure 41a**. The bar undergoes an elongation under the applied load q . A cross-section at x will displace by $u(x)$ and a cross-section at $x+dx$ by $u(x+dx)=u+du$ due to its deformation over length dx . This deformation is measured by the axial strain:

$$\varepsilon = \frac{du}{dx}$$

$$\sigma = E \frac{du}{dx}$$

$$N = EA \frac{du}{dx}$$

From horizontal equilibrium in **Figure 41b** follows:

$$N - (N + dN) - qdx = 0$$

$$-\frac{dN}{dx} = q \rightarrow -\frac{d}{dx} \left(EA \frac{du}{dx} \right) = q$$

$$-EA \frac{d^2u}{dx^2} = q$$

A reinforcing element adhesively connected to- and pulled out of the glass pane could be compared to the situation described in **Figure 40**. The adhesive can be replaced by a set of springs distributed along the length of the reinforcement. This results in a distributed load $p=ku$ with k being the stiffness of the adhesive connection.

The tensile force N in the element at cross-section $x=0$ (F in **Figure 40a**) is resisted by the distributed load p .

Horizontal equilibrium in **Figure 40c** yields:

$$\frac{dN}{dx} = ku \rightarrow \frac{d}{dx} \left(EA \frac{du}{dx} \right) - ku = 0$$

$$EA \frac{d^2u}{dx^2} - ku = 0$$

From this follows:

$$\frac{d^2u}{dx^2} - \alpha^2 u = 0 \text{ with } \alpha^2 = \frac{k}{EA}$$

This is a second order differential equation with a constant coefficient α . The solution can be expressed as:

$$u(x) = C_1 e^{\alpha x} + C_2 e^{-\alpha x}$$

The deflection u at large distance from the applied load is very small and the tensile force at $x=0$ equals F . This implies:

$$u(\infty) \approx 0$$

$$u(\infty) = C_1 e^{\alpha \infty} + C_2 e^{-\alpha \infty} \approx 0 \rightarrow C_1 = 0$$

$$u(x) = C_2 e^{-\alpha x} \rightarrow \frac{du}{dx} = -\alpha C_2 e^{-\alpha x}$$

$$N(0) = EA \frac{du}{dx}(0) = F \rightarrow \frac{du}{dx}(0) = \frac{F}{EA}$$

$$-\alpha C_2 e^{-\alpha 0} = -\alpha C_2 = \frac{F}{EA} \rightarrow C_2 = -\frac{F}{EA\alpha}$$

$$u(x) = -\frac{F}{EA\alpha} * e^{-\alpha x}$$

$$N(x) = F e^{-\alpha x}$$

$$\text{with } \alpha = \sqrt{\frac{k}{EA}}$$

The connection stiffness k is dependent on the E-modulus and thickness of the adhesive layer and on the stiffness of the substrate (in our case the glass pane).

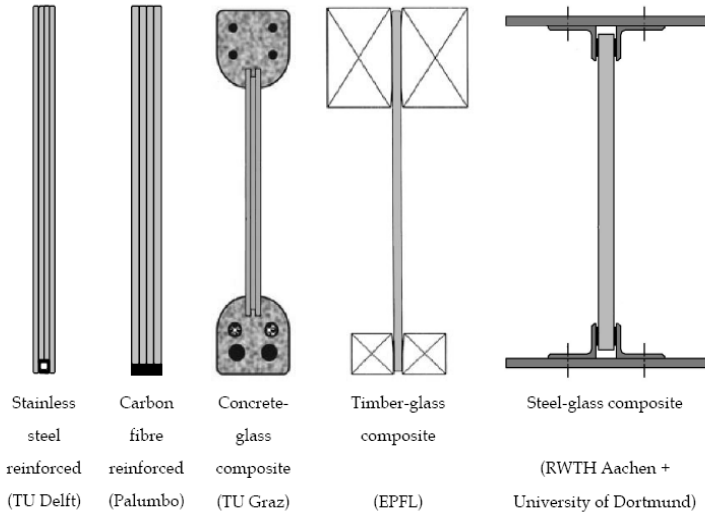


Figure 42, Overview of reinforcing systems [12]



Figure 44, Carbon fiber reinforced structural glass beam by Palumbo[14]

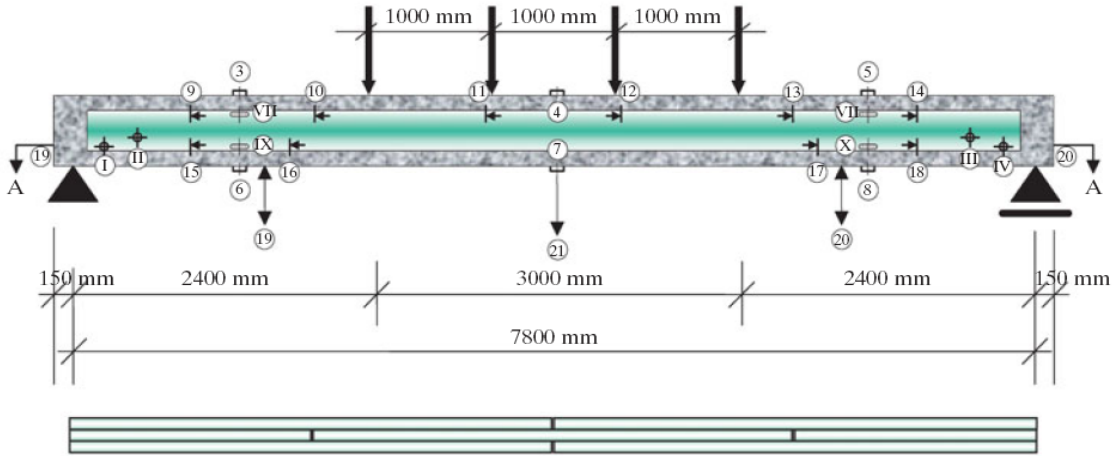


Figure 45, Glass-Concrete composite beam by TU Graz [22]



Figure 43, Timber-Glass composite beam in conference room of Hotel Palafitte in Neuchatel. [24]

3.3 Reinforcements

In the design of a glass girder it is evident that measures are taken to allow residual load-bearing capacity after initial glass failure. Since glass girders usually break due to tensile stresses, it is a logical step to introduce reinforcements that can take over this tensile stress when the glass breaks.

What has been done so far?

Currently there are several methods of reinforcing structural glass girders; some of them even introduce the use of pre-stress. This chapter contains a review of ways of reinforcing glass girders that are done so far (see Figure 42).

Carbon fiber reinforced

Carbon fiber reinforcements in the form of CFRP sheets (Carbon Fiber Reinforced Polymer Sheets) are used in existing wood or concrete structures to provide additional strength or stiffness. This is done for example in reparations when a structure is damaged or proven to be designed insufficient.

In 2005 Palumbo bonded comparable sheets in the tensile zone of a glass girder as post-failure reinforcing element. The concept has been applied for a beam with a span of 6 m in a saddle roof structure (see Figure 44).

Concrete-glass composite

Graz University of Technology [19] developed these composite beams where reinforced ultra-high-performance concrete flanges are joined with a glass web and the steel reinforcements by pouring the concrete in a mould. This method raises questions concerning the limited shear strength, which is mainly transferred via the concrete flanges. Also the long-term stability is not proven to be sufficient because the highly alkaline concrete can corrode the glass [20].

Timber-Glass composite

This beam system has been researched by the Ecole Polytechnique Fédérale de Lausanne [21 & 23]. The flanges are made out of wood and are bonded by adhesives to the web of the beam consisting of one layer of glass. It has been applied in a roof structure spanning 6 m [20].

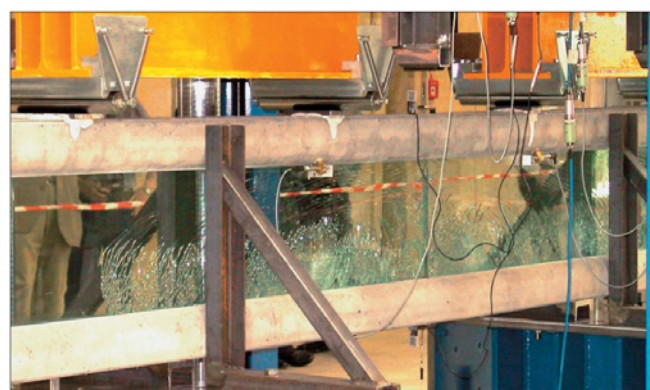


Figure 46, Glass-concrete composite beam by TU Graz. [22]

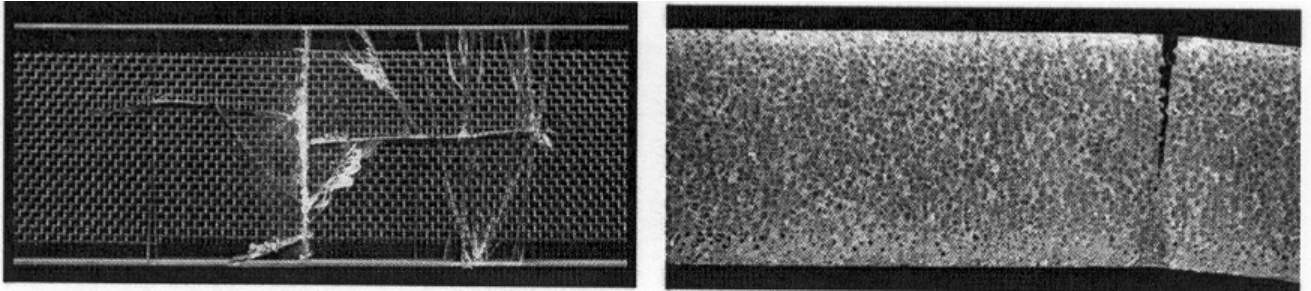
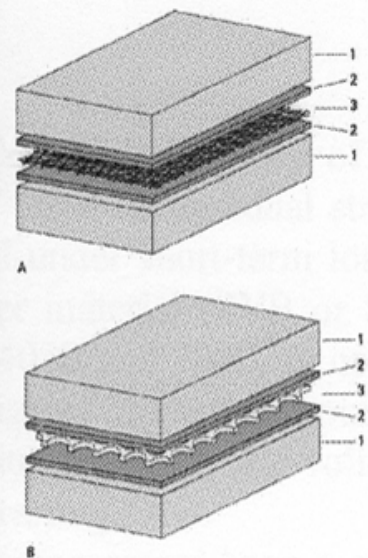
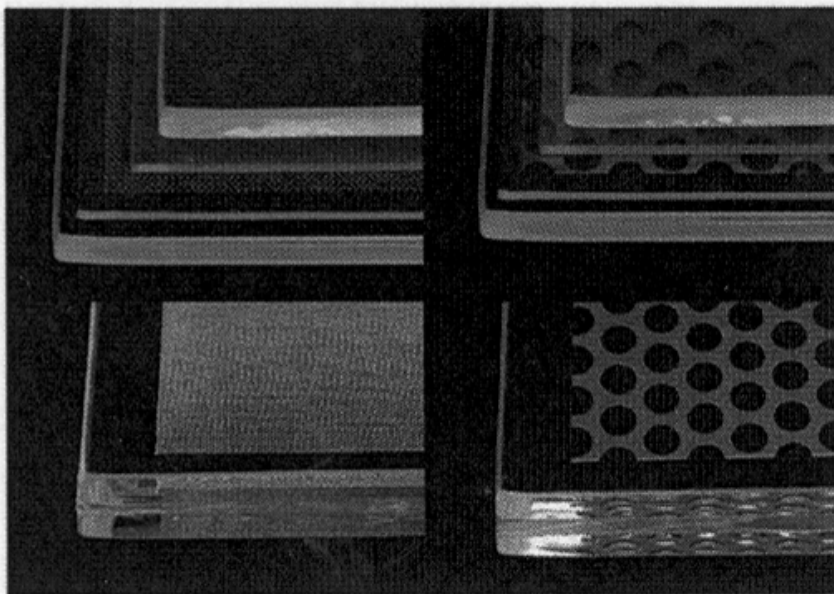


Figure 48, Reinforcement in the laminate after four-point bending test. Left normal floatglass, right heat strengthened. [17]



Assembly of laminated glass (LG): 1. glass; 2. interlayer; 3. reinforcement (steel-wire meshes or thin perforated metal)

Figure 47, Close-up of reinforcement in the laminate. [17]

Steel-glass composite

The Institute of Steel Construction at RWTH Aachen together with the University of Dortmund [25, 26 & 27] designed this composite beam with a laminated glass web and steel flanges (see Figure 49). They are bolted together with steel L-sections. The concept is tested on a beam spanning 12 m with 6 laminated glass panes.

Stainless steel reinforced

This concept is introduced at the faculty of Architecture at Delft University of Technology by Christian Louter. A small stainless steel section is adhesively bonded in the tensile zone of the glass beam acting as reinforcement. A safe failure behavior is obtained; tests have been done for models with a span of up to 7,2 m (see Figure 50).

Reinforcement in the laminate

A stainless steel or carbon fiber net is incorporated in the interlayer (PVB or SGP). The concept is designed and tested for use in laminated glass panes loaded in perpendicular direction to the plane; behavior of this concept in a laminated girder, loaded on bending in the direction of the plane, is unknown.

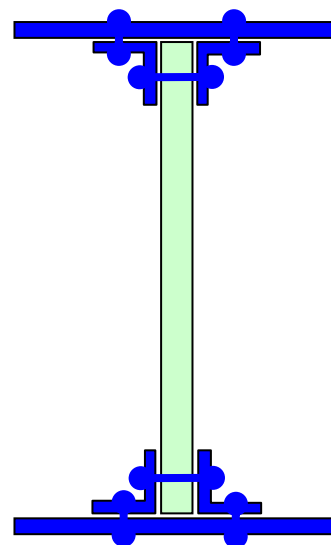


Figure 49, Cross-section of glass-steel composite beam. The flanges are steel (blue), the web is glass (light green).



Figure 50, Proof of residual load bearing strength of stainless steel reinforced glass beam. [12]

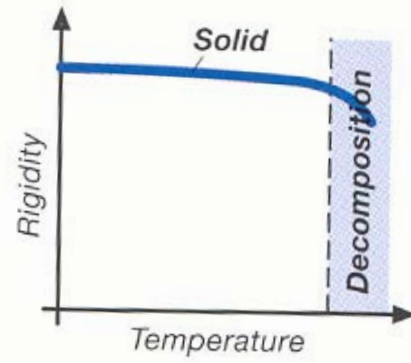
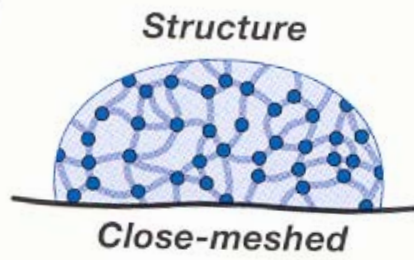


Figure 54, Schematic representation of chemical structure and temperature-rigidity diagram of thermoset material. [3]

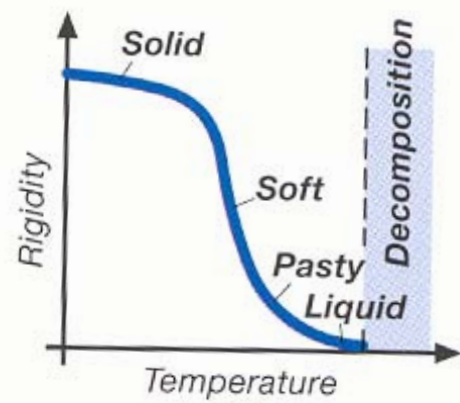
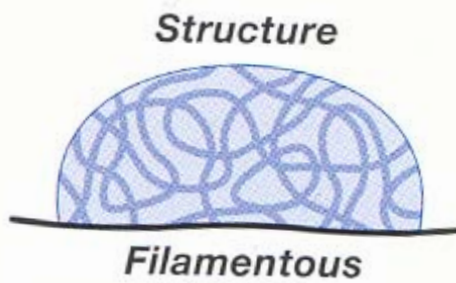


Figure 51, Schematic representation of chemical structure and temperature-rigidity diagram of thermoplast materials. [3]



Figure 53, Nylon is known for its good elongation qualities [28]

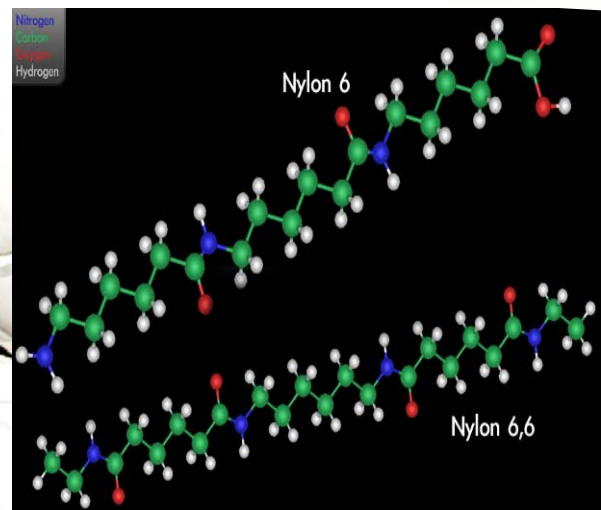


Figure 52, Schematic representation of chemical structure of Nylon [28]

Possible Materials for reinforcements

The reinforcing element has to comply with several demands. A selection has been made of materials with high tensile strengths. The ones that are affordable, possible to obtain, thus appropriate for use can be classified in four categories: polymers, steel, carbon fibers and glass fibers. They are described and reviewed on the following characteristics:

- Yield Strength
- Ultimate Tensile Strength
- Young's Modulus, or modulus of elasticity
- Creep performance
- Manageability, glue ability
- Color/Transparency

First a short study is done into basic chemical properties of polymers. At the end of the paragraph an overview is given of all selected materials.

Polymers

Plastic is a general name for a wide range of synthetic and semi-synthetic polymer products. The majority consists of long chains of carbon and hydrogen atoms bonded to one another, called polymers.

There are many ways to classify polymers; the first classification made here is between thermosets and thermoplastics.

Thermoplastics are transitional plastics: they melt into a liquid when heated and freeze into a brittle glassy state when cooled sufficiently.

Depending on the kind of polymer, the molecules can be bonded by weak Van der Waals forces, stronger dipole-dipole interactions, hydrogen bonding, or

stacking of aromatic rings. These bondings become weaker when the temperature rises. When enough heat is added the bonding force is neutralized and the material becomes liquid.

Thermoset plastics are made up of lines of polymer chains which are bonded by cross-links. They are formed by a chemical reaction where the chains are linked to one another on random places by a strong bond. Prior to the reaction they are usually liquid or knead able. During the reaction they become hard with a rigid three-dimensional structure. Once formed, this structure cannot be reformed again without destroying it.

Some thermosets cure under influence of irradiation (like UV adhesives) or heating (heat curing epoxies), others by addition of a catalytic reformer (like some 2 component epoxy adhesives).

Thermosets transit from solid phase directly into gas phase when sufficient heat is added, skipping the liquid state.

Nylon

Nylon is a polyamide and one of the most common polymers used as a fiber. It is a thermoplastic silky material made of repeating units linked with peptide, or amide bonds.

Nylon fiber has a long elongation, is highly resilient but the tensile strength and E-modulus decrease fast at high temperatures.

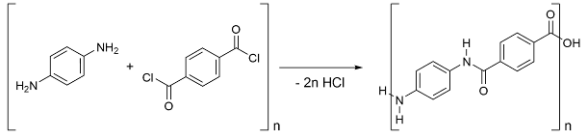


Figure 57, Synthesis of Kevlar [28]

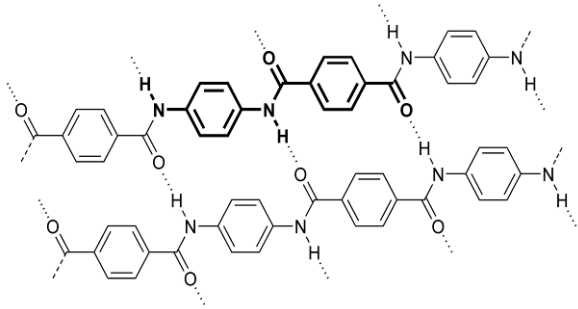


Figure 56, Cross-linking with O-H bonds of polymer chains in Kevlar [28]



Figure 58, Zylon on Spool [28]



Figure 59, Dyneema fiber on spool [28]

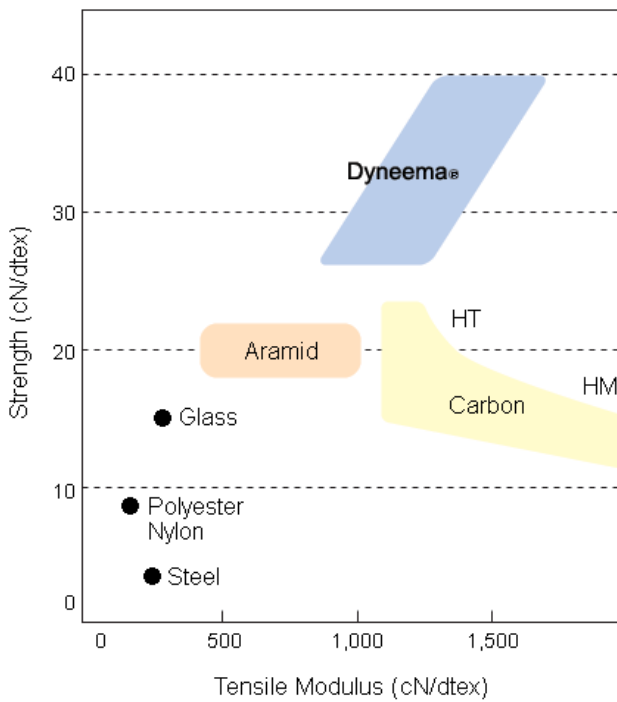


Figure 55, E-modulus - strength diagram of several fibers [28]



Figure 60, Use of Kevlar in bullet-proof vest [28]

Dyneema

Dyneema is a thermoplastic polymer produced by DSM, which is identical in chemical structure to Spectra, produced by Honeywell. The polymer has extremely long chains; therefore it is also called UHMWPE or Ultra High Molecular Weight PolyEthylene. The chains are bonded over the whole range of the extremely long polymer by weak Van der Waals forces. This results in a very tough material, with a high tensile strength and the highest impact strength of any thermoplastic material presently made. Flipside of the medal is that it has a very poor resistance to creep, even at low tensile stress.

The fiber is made through a process called 'gel spinning'. A heated gel of UHMWPE is processed by an extruder. The extrudate is drawn through the air and then cooled down in a water bath. The result is that the polymers in the fiber have more or less the same orientation and therefore exceptional tensile strength and very low friction coefficient.

The product is made for many applications. One of them was a 30 kilometer long space tether in a (failed) satellite project in September 2007. More usual applications are for kite and fishing wire or additive in the coating for skis.

Kevlar

Kevlar was developed by the company Dupont in 1965. In 1978 Akzo started production of a similar fiber under the name Twaron, nowadays manufactured by Teijin.

The polymer is formed from two different monomers into chains of "poly paraphenylene terephthalamide". The chains are cross-linked by O-H bonds of the carbonyl groups and by stacking of the aromatic rings.

This creates a strong thermoset material that sublimates at 450 °C. Kevlar has a good short-time resistance to high temperatures, but when exposed longer its tensile strength reduces.

When Kevlar is spun, the resulting fiber has a great tensile strength of 3100 MPa.

For a polymer the creep resistance is relatively good. When exposed to a tensile stress of 1830 MPa for 1000 days, the creep strain is 13% of the initial elastic strain. After 4000 days this is increased to 14,6%. At 34% of the breaking load, the creep rate β is 0,0015 %/log(t).

Kevlar is used in a variety of products, from bullet-proof vests and fireman gear to tennis rackets and hockey sticks.

Zylon

The thermoset polyurethane synthetic polymer Zylon consists of chains of *p*-phenylene-2,6-benzobisoxazole and is produced by the Toyobo Company. It has a very high Young's modulus (270Gpa) and has a linear elastic behavior up to the breaking point where its elongation is 3,5%.

Zylon has very good creep resistance compared to para-aramid fibers like Kevlar. When a fiber is stressed at 50% of its breaking load for 100 hours, the creep is only 0,03%.

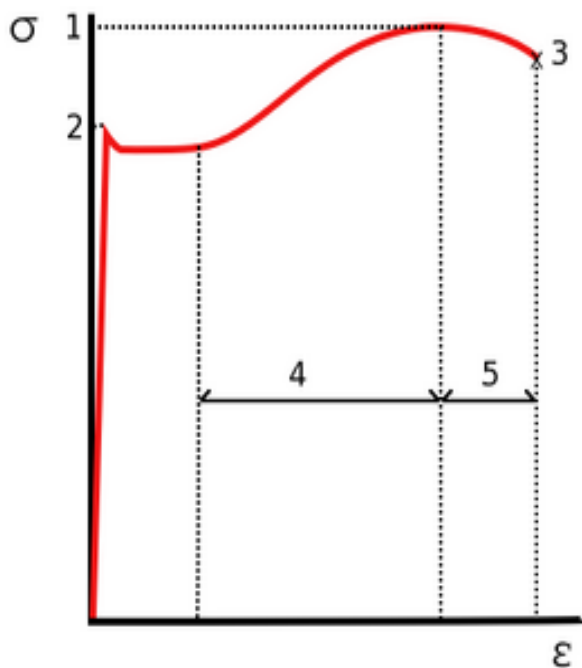


Figure 61, Typical stress/strain curve of structural steel. [28]

1. Ultimate Tensile Strength
2. Yield Strength
3. Rupture
4. Strain Hardening region
5. Necking region



Figure 63, Piano Wire on spool [28]



Figure 62, Strings in Piano [28]

Table 6, Mechanical properties for grades 304 and 316 in the cold worked condition. (C=cold rolled strip)

Designation	Minimum yield strength [N/mm ²]	Minimum tensile strength [N/mm ²]
C700	350	700
C850	530	850
C1000	750	1150
C11150	900	1150
C1300	-	1300

Note: Tensile strengths are given in EN 10088-2 and yield strengths in ENV 1993-1-4.

Metal alloys

Steel

Steel is an alloy consisting mainly of iron, with some carbon content varying between 0,2% and 2%, depending on the grade. Other additives like manganese, chromium, vanadium and tungsten can be added to improve the structural characteristics.

The additives act as a hardening agent, preventing dislocations in the crystal structure of the iron atoms.

In general; the higher the carbon content, the harder and stronger but less ductile the steel.

Reinforcing Steel

Widely used in reinforced concrete, easily available, insensitive to creep at known tensile stresses, high tensile strength and not too expensive. Disadvantage is that the surface of the steel corrodes when exposed to oxygen.

Reinforcing steel is classified by tensile strength and can be obtained in classes up to 1860 N/mm².

Stainless Steel

Stainless steel is obtained when certain additives, like chrome and carbon, are added to the alloy at the right amount.

The stainlessness is based on the fact that the corroded layer at the surface of the metal forms a thin but impermeable skin. The rest of the steel is therefore sheltered from further oxidation. The oxidized layer at the surface of 'normal' steel is porous and therefore lacks this protective quality.

To optimize corrosive and mechanical properties, other elements are added to obtain stainless steel with different characteristics. This results in 5 main groups of stainless steel; austenitic, ferritic, martensitic, duplex and precipitation hardened.

Stainless steel is classified in grades. The higher the grade, the more corrosion resistant the steel is. For grade 304 and 316 the strength figures are given in *Table 6*.

Music Wire

The core of the wire of music instruments like guitars, pianos and violins is a specialized type of wire made from tempered high-carbon steel, also known as 'spring steel' (see Figure 62 and Figure 63). It is a very tough polished wire with extremely high tensile strength, manufactured from steel of a specific composition by cold drawing. It is also used in the fabrication of springs, fishing lures, special effects in the movie industry, for cutting soap and in some hobby applications such as model railroading. There are only a limited number of companies worldwide who are producing this wire: 'Mapes' and 'Newoctave Corporation' in the United States and 'Röslau' in Germany.

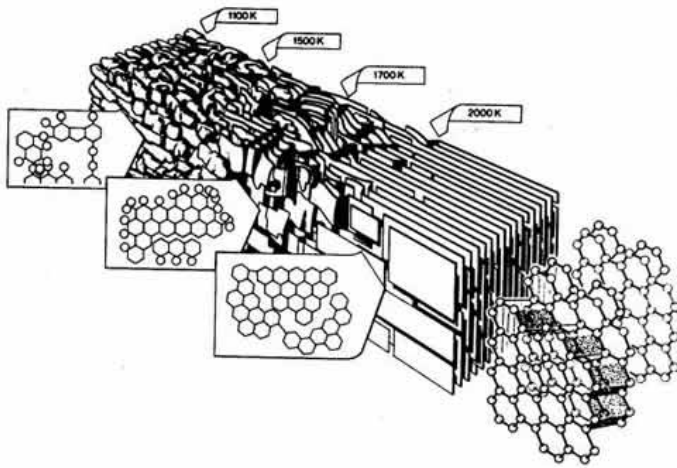


Figure 65, Transition of plain graphite into carbon fiber under heating [28]

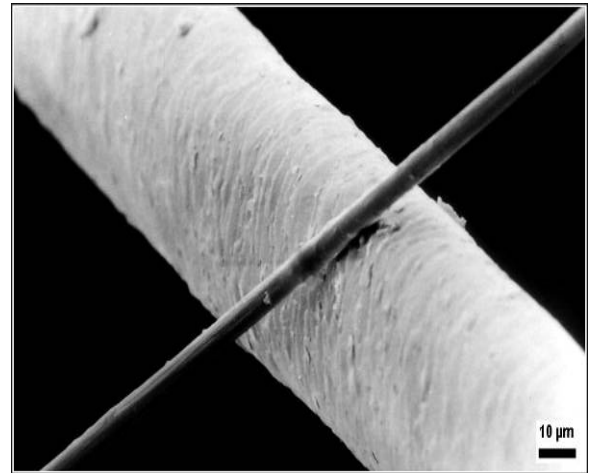


Figure 64, Carbon fiber (dark) in contrast to a human hair (light) [28]

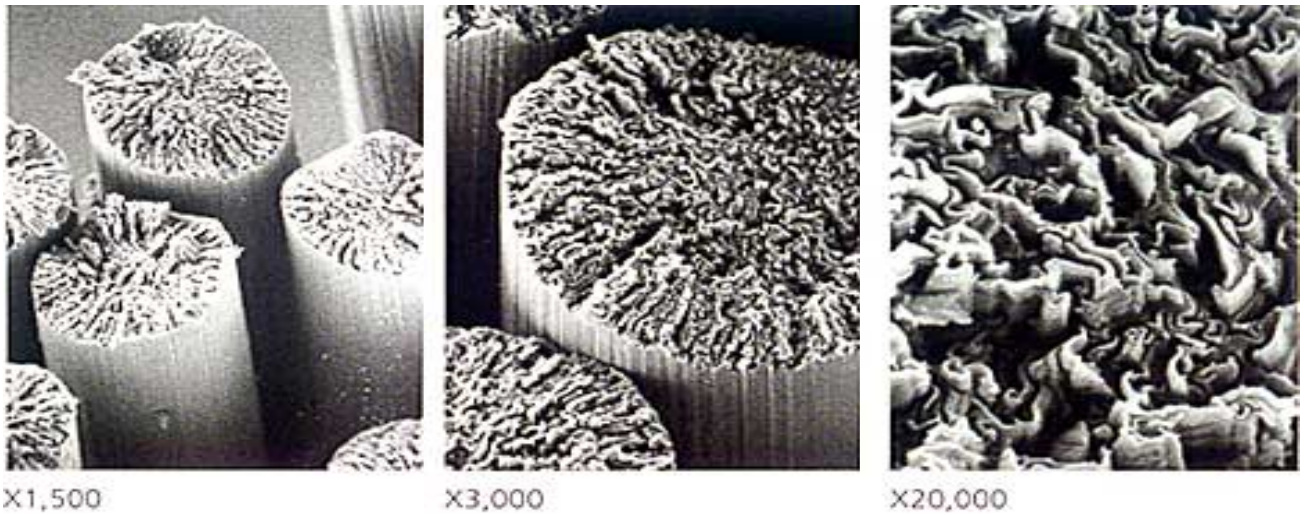


Figure 66, Carbon fiber under microscope in different magnifications [28]

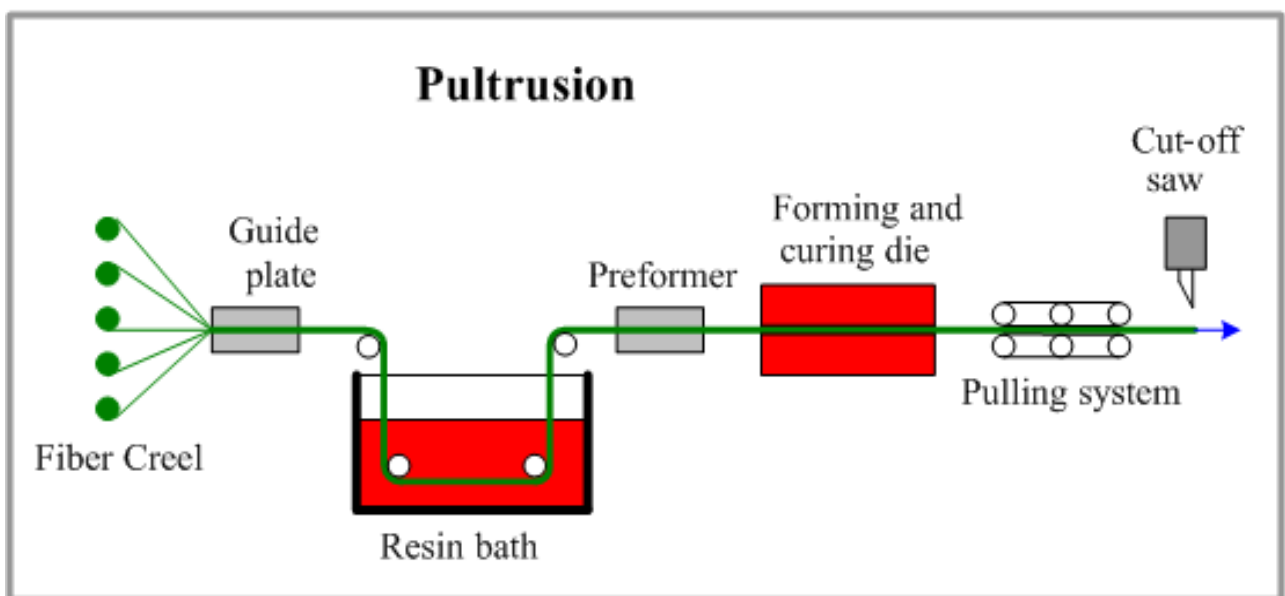


Figure 67, Schematic representation of pultrusion process [28]

Carbon fiber

Carbon fiber is a form of graphite consisting of pure carbon atoms. The carbon atoms in graphite are chaotically arranged. When this is heated to 2200°C the molecular structure reorganizes into multiple sheets of regular hexagonal aromatic rings, a bit like chicken wire (see Figure 65). This results in extremely thin fibers of with diameters ranging from 0,005 mm to 0,010 mm (see Figure 66 and Figure 64).

The fibers are composed mostly of carbon atoms that are more or less aligned to the axis of the fiber, creating a thin filament with extremely high tensile strength. Several thousands carbon fibers are twisted together to form a yarn (see Figure 69).



Figure 69, Carbon fiber yarn on spool [28]

These yarns can be used for itself, woven into a fabric, of bundled unidirectional into a rod by a process that is called pultrusion.

Pultrusion is a process where a large number of small fibers are bundled together by epoxy resin. This results in rods with a constant profile of any shape where the filaments are arranged parallel to the axis of the rod, creating optimal tensile strength. An important factor in calculations with pultruded products is the amount of fibers in the rod. Usually 40%-50% of the surface of the rods consists of fibers, the rest of resin.

The fibers usually consist of carbon fiber or glass fiber.

Carbon fiber rods are used in various applications like model aircrafts and Formula 1 cars.

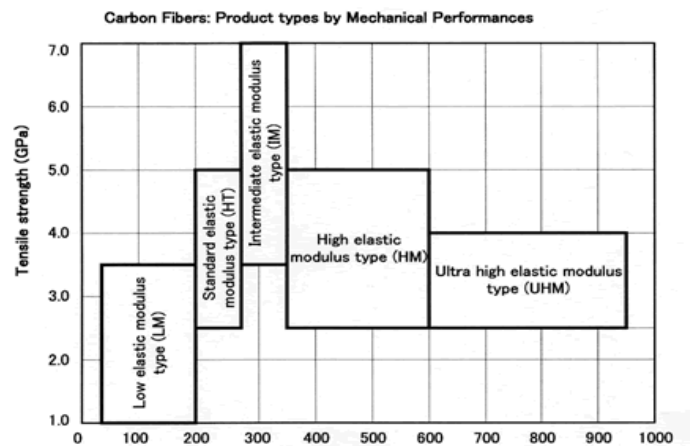


Figure 68, E-modulus / tensile strength diagram of different types of carbon fiber

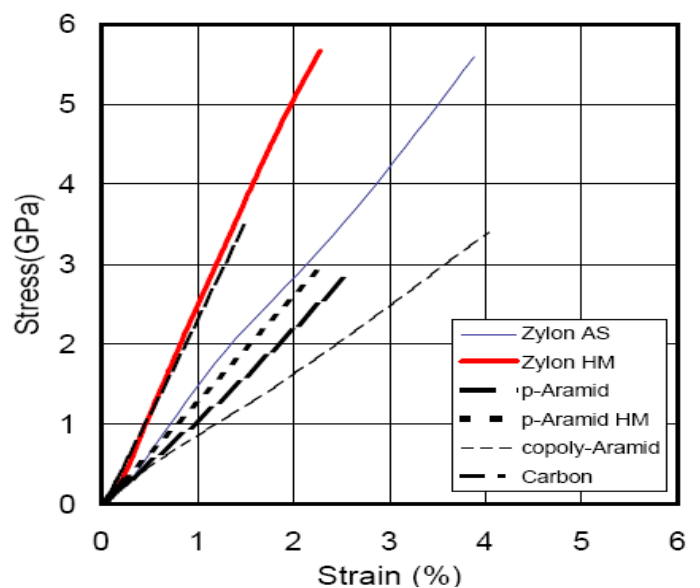


Figure 70, Typical stress / strain curve of the polymer and carbon material



Figure 74, E-Glass fiber, here in use as sound buffer in an exhaust pipe of a car. [28]



Figure 73, Pultruded glass fiber rods. [28]



Figure 71, S-glass fiber fabric. [28]

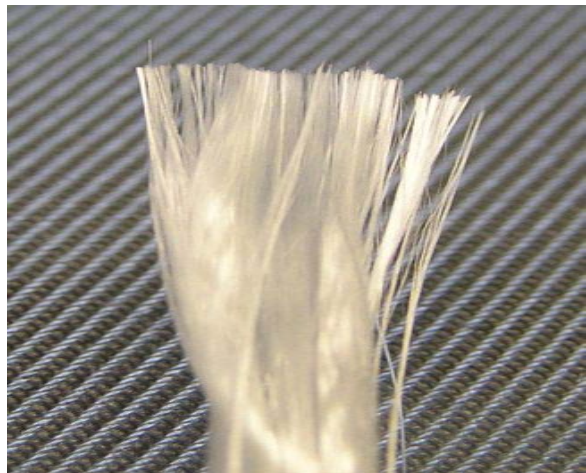


Figure 72, Glass fiber roving. [28]



Figure 75, Canoe reinforced with glass fiber and epoxy. [28]

Glass fiber

There are several types of glass fibers. Two are reviewed: E-Glass and R-glass.

E-glass, or electrical grade glass was originally developed for insulators for electrical wiring. Now it is standard reinforcing element in the material commonly known as fiberglass. It has an ultimate tensile strength of approximately 2000 N/mm² and an E-Modulus of 75 GPa. E-glass has a good heat resistance, is relatively insensitive to moisture and not expensive. Problems are the low fatigue resistance and when not treated correctly its strength reduces over time.

R-glass is comparable to E-glass, but is a bit stiffer and about twice as strong. The E-modulus is 80 GPa and the ultimate tensile strength is 4750 N/mm². It is much harder to obtain and expensive.

Glass fibers are popular for use in combination with epoxy.

It is widely used in boating industry to create strong three dimensional lightweight hulls (see Figure 75).

Other applications are in unidirectional rods (see Figure 73). As stated earlier: the cross-section of a pultruded rod usually consists of more than 50% of epoxy resin which affects the mechanical properties.

Table 7, Summary of material characteristics

	Structural Steel	Stainless Steel
Material	Alloy	Alloy
Yield Strength (MPa)	235-1650	720
Ultimate tensile strength (MPa)	400-1860	860
Young's Modulus (GPa)	210	190-210
Creep performance	No creep up to yield strength	No creep up to yield strength
Fire resistance	Good	Good
Manageability / glueability	Excellent	Excellent
Color	Silver	Silver
Known applications	Structural steel, prestressing strands, etc.	Sailing, structural steel exposed to rough climate, bolts, screws
Important characteristics	Rusts when exposed to Oxygen	
	Piano wire	Carbon Fiber
Material	Alloy	Carbon (graphite)
Yield Strength (MPa)	Elastic behavior up to breaking	Elastic behavior up to breaking
Ultimate tensile strength (MPa)	2300	4000
Young's Modulus (GPa)	200	575
Creep performance	No creep up to yield strength	No Creep
Fire resistance	Good	Excellent
Manageability / glueability	Excellent	Excellent
Color	Silver	Black
Known applications	Musical Instrument	F1 race cars, Sailing boats, airplanes, Space industry.
Important characteristics		
	Nylon	Zylon
Material	Polymer	Polymer
Yield Strength (MPa)	45	Elastic behavior up to breaking
Ultimate tensile strength (MPa)	75	5800
Young's Modulus (GPa)	2,4	270
Creep performance	Poor	Good
Fire resistance	Poor	good
Manageability / glueability	Excellent	Poor
Color	Transparent, White	Silver
Known applications	Stockings, rope, fishing line.	Body armor, Formula 1 cars, rigging for sailing.
Important characteristics	Can be obtained in any shape of fiber, high elongation	Degrades fast when exposed to UV-light

Summary of important characteristics

Table 8, Summary of material characteristics

	Dyneema, Spectra	Kevlar 149
Material	Polymere	Polymere
Yield Strength (MPa)	Elastic behavior up to breaking	Elastic behavior up to breaking
Ultimate tensile strength (MPa)	3400	3100
Young's Modulus (GPa)		179
Creep performance	Poor	Good
Fire resistance	Poor	Good
Manageability / glueability	Excellent	Excellent
Color	White, various coatings	Various
Known applications	Kite wire, mountain sports, sailing .	Body Armor, bicycle tires, racing sails.
Important characteristics		
	E-Glass fiber	R-Glass fiber
Material	Glass Fiber	Glass fiber
Yield Strength (MPa)	Elastic behavior up to breaking	Elastic behavior up to breaking
Ultimate tensile strength (MPa)	2000	3600
Young's Modulus (GPa)	80	85
Creep performance	Zero creep	Zero creep
Fire resistance	Good	Good
Manageability / glueability	Excellent	Excellent
Color	Transparant / white	Transparant / white
Known applications	Reinforcements in composite structures	Reinforcements in composite structures
Important characteristics		

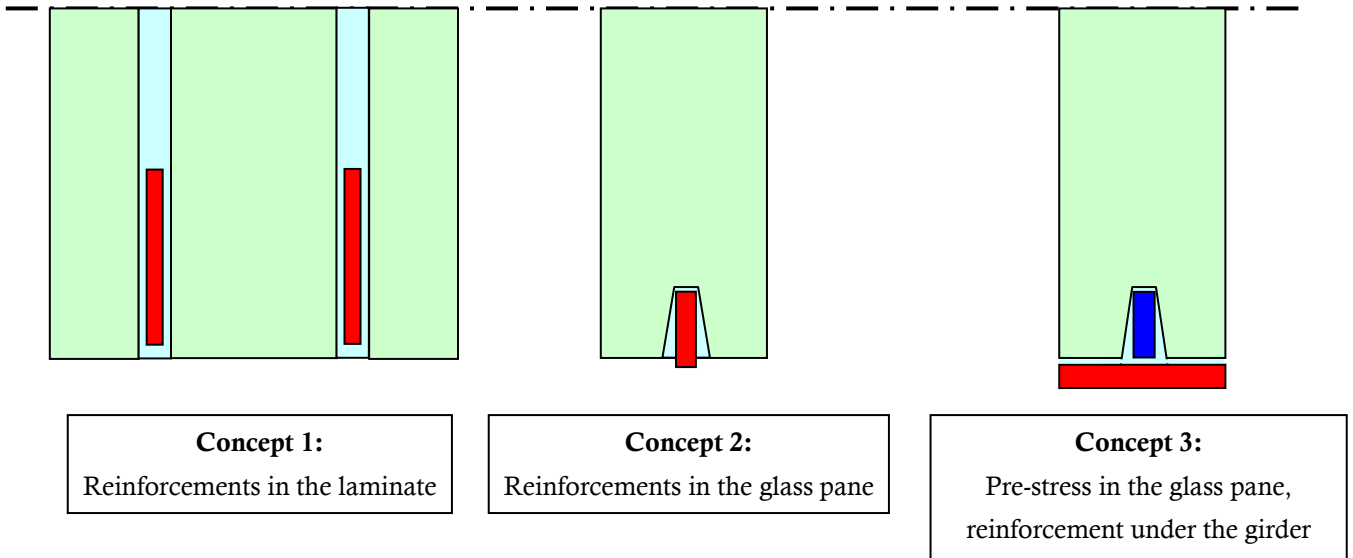


Figure 76, Simplified cross-sectional view of bottom of concept girders.

Light green: glass

Light blue: Adhesive / SGP foil

Red: reinforcing element

Blue: pre-stress element

4. Reinforcing concepts

4.1 Introduction

First a framework for the design is created by describing a set of requirements in chapter 4.2. With these requirements three different concepts for reinforcing principles are generated (presented in *Figure 76*). They are described in the following paragraphs:

4.3 Glass fiber reinforcements in the laminate

Two glass panes are laminated with two layers of 1,52mm thick SGP foil. Within these foil layers a pultruded glass fiber rod is melted.

4.4 Reinforcement in the glass pane

A groove is milled out in the bottom end grain of the glass pane. In this groove a reinforcing element (stainless steel, carbon fiber or glass fiber) is adhesively bonded.

4.5 Pre-stress in the glass pane, reinforcement under the girder

A groove is milled out in the bottom of the glass pane. In this groove a pre-stressed element is adhesively bonded. Conventional reinforcement is introduced in the girder, being stainless steel [12] or carbon fiber [14].

The concepts are checked by rough exploring calculations. By these rule-of-thumb calculations it is estimated if the concepts are realizable. They are evaluated and the best concept for use in this thesis is described in the conclusion.



Figure 78, Steel framed glass floor of CN Tower in Toronto at 342m above ground level.



Figure 77, Steel framed glass floor seen from above (left) and underneath (right). [www.productanddesign.com]

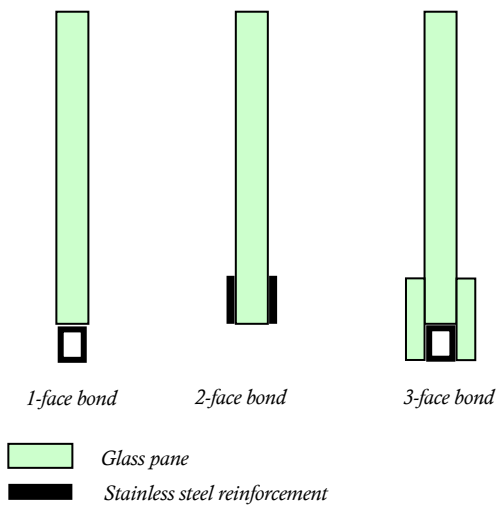


Figure 81, Concept girders. Based on [12]

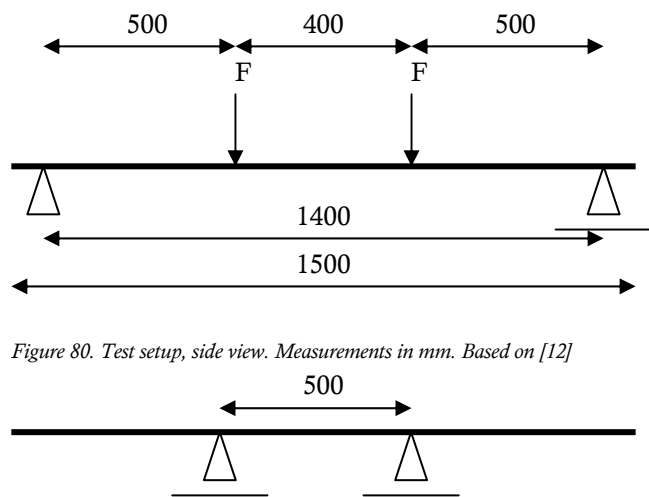


Figure 80. Test setup, side view. Measurements in mm. Based on [12]

Figure 79. Test setup, top view. Measurements in mm. Based on [12]

Table 9, Deformation capacity and remaining load bearing capacity for tested specimens as described in reference 3. [12]

Geometry	Deformation capacity [$u_{\text{ultimate}}/u_{\text{initial failure}}*100\%$]	Remaining load bearing capacity [$F_{\text{max}}/F_{\text{initial failure}}*100\%$]
1F	127 – 325 %	75 – 194%
2F	314 – 775%	85 – 164%
3F	340 – 510%	126 – 184%

4.2 Requirements

The possibilities for use of structural glass are endless. In this paragraph a framework is created for the intended applications for the girder that will be designed in this thesis.

The research will focus on the development of a new, more transparent reinforcing method for structural glass and the guarantee of its structural safety by practical research.

The intended application for the design is a small span girder in light use. For example a purlin in a glass facade or a support beam under a glass floor or roof. The girder should be able to span up to 3m. With such a girder the steel frames supporting the glass floors in *Figure 78* and *Figure 77* could be replaced by glass and a much more transparent and challenging structure could be obtained.

The most important requirement is a safe failure behavior of the glass beam: it should warn before failure. After initial glass failure the load should be able to be increased, the bending stiffness should degrade and the deflection of the beam should be substantial before the beam totally collapses.

The design will be related to the stainless steel reinforced glass girders as presented in *Figure 81* [12]. These girders have dimensions of length*width*height = 1500*10*115mm.

The deformation capacity and remaining load bearing capacity from these tests is taken as a reference in this thesis. The structural behavior of geometry 3F as described in *Table 9* is considered satisfactory. The desired mechanical behavior is extracted from this and presented in *Table 10*.

Another requirement is transparency. There is no sense in introducing a glass girder if it is hardly transparent

and even relatively small but clearly visible reinforcing elements are a disturbing factor.

Unfortunately it is hard to make an objective judgment on whether or not a design is transparent enough. The meeting of this demand is therefore left to individual opinion.

Table 10, Aimed deformation capacity and remaining load bearing capacity measured in % of initial failure.

Deformation capacity [$u_{\text{ultimate}}/u_{\text{initial failure}} * 100\%$]	400%
Remaining load bearing capacity [$F_{\text{max}}/F_{\text{initial failure}} * 100\%$]	130%

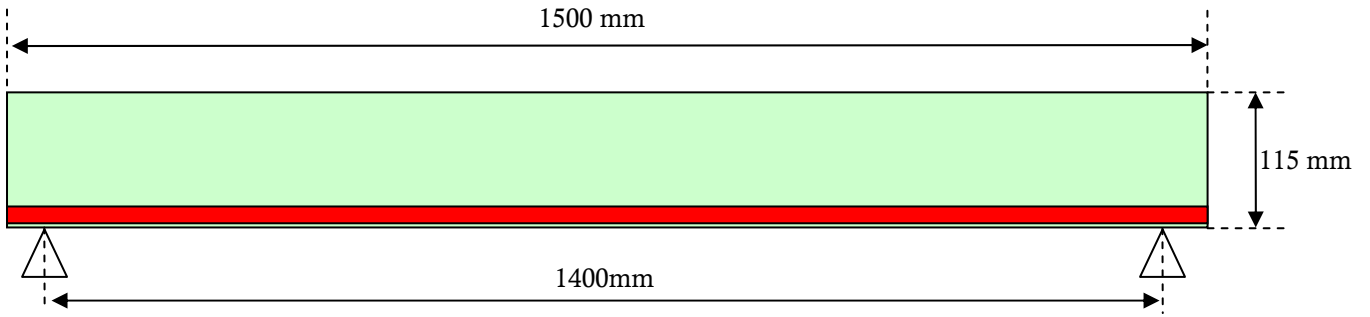


Figure 82, Schematic side view of concept design 1. Glass in light green, reinforcement in red.

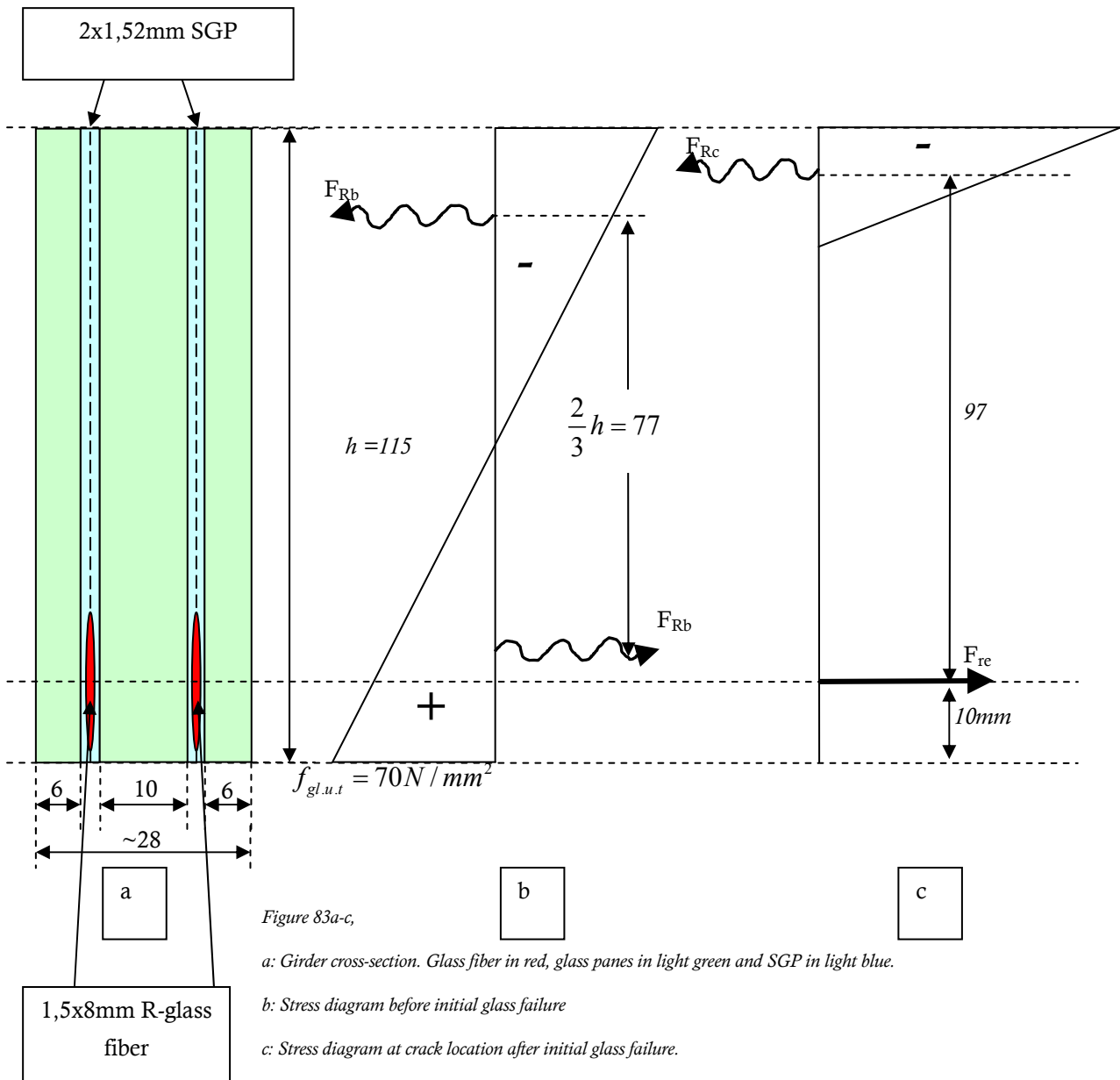


Figure 83a-c,

a: Girder cross-section. Glass fiber in red, glass panes in light green and SGP in light blue.

b: Stress diagram before initial glass failure

c: Stress diagram at crack location after initial glass failure.

4.3 Glass fiber reinforcements in the laminate

Description

The laminated beam is built up from one structural glass pane with a thickness of 10mm in the middle and two sacrificial glass panes of 6mm thick at both sides. The reinforcement is embedded in the laminate which is Sentry Glass Plus.

Sentry Glass Plus is usually used for laminating glass beams as it is stronger and stiffer than PVB. This concept uses the adhesive qualities of SGP foil to bond the glass with the reinforcing element.

A thin rectangular strip, preferably transparent glass fiber, is placed between two thick layers of SG foil in the first stage of the laminating process. In the autoclave the SGP foil melts around the reinforcement ensuring a good bonding with both glass and reinforcement.

Numerical support

Minimum reinforcement

At the moment of initial glass failure, the tensile bending stress in the glass pane is transmitted into tensile force in the reinforcement, which may not exceed its tensile strength. For this calculation the structural plus both sacrificial elements are included.

First the bending moment at initial glass failure (see *Figure 83b*) is calculated:

$$M_{ci} = F_r * \frac{2}{3} h$$

$$F_r = \frac{1}{2} f_{br} * \frac{1}{2} h * d = \frac{1}{4} * 70^{\#} * 115 * 22 = 44.275 N$$

$$M_{ci} = 44.275 N * 76,7 mm = 3.394.416 Nmm$$

$$M_{ci} = 3,40 kNm$$

#: 70N/mm² is based on the 5% upper value for bending strength according to [1]

This equals the moment generated by the tensile force in the reinforcement and the compressive zone in the glass (see *Figure 83c*). Note that cracks run up to 80% of the height of the girder [12] so the resulting force from the compressive zone is positioned at 7,7mm from the top.

$$F_{re} = \frac{M_{ci}}{d} = \frac{3,40 * 10^6 Nmm}{97 mm} = 35.052 N$$

$$F_{re} = 35 kN$$

For this beam a pultruded rod of 50 % R-glass will be taken, with a theoretical tensile strength of 0,5*3600=1800N/mm².

$$A_{re} = \frac{35.052 N}{1.800 N / mm^2} = 19,5 mm^2$$

The two rods have to have a minimum surface of 20 mm², or 10 mm² each. Two rods of 1,5x8 mm will be taken which will result in 24 mm² of pultruded R-glass fiber, 12 mm² of R-glass fiber with an ultimate tensile strength of 43,2 kN.

Maximum reinforcement

Control of maximum reinforcement (brittle compressive failure of top of glass beam). Note that only the structural inner glass pane is included in this calculation.

Stress diagram is similar to Figure 83c.

$$\sigma_{gl,max} = 500 \text{ N/mm}^2 \#$$

$$A_{gl} = 0,2 * h * d = 0,2 * 115 * 10 = 230 \text{ mm}^2$$

$$F_{R,gl,max} = \frac{\sigma_{gl,max}}{2} * 0,2h * d_{gl}$$

$$F_{R,gl,max} = 250 * 0,2 * 115 * 10 = 57.500 \text{ N}$$

$$F_{re,max} = 24 \text{ mm}^2 * 1800 \text{ N/mm}^2 = 43.200 \text{ N}$$

$$F_{R,gl,max} = 57,5 \text{ kN} > F_{re,max} = 43,2 \text{ kN}$$

$$M_{cu} = 43,2 \text{ kN} * 0,097 \text{ m} = 4,2 \text{ kNm}$$

#: Conservative estimation to [8, p.20]

→ 24 mm² is OK.

Discussion

Strong points:

Transparent design. Refractive index of glass, SGP foil, Epoxy pultrusion plasma and glass fiber all between 1,48 and 1,6. It will have to be seen how good the glass-fiber is visible in the girder in reality.

Reinforcing element is well protected in the girder. Favorable with fire-safety, vandalism, etc.

Easy to inspect. Because of transparent design, the state of the reinforcements can be inspected.

Free in reinforcement positioning. Also shear force reinforcements (vertical) or other directions or curved reinforcements are possible.

Up- and down scaling possible. This design involves a small span girder of three glass panes, but the

possibilities are endless; downscaling to for instance two glass panes of 4mm, or up scaling to several glass panes of up to 25mm thick is possible.

Weak points:

Manufacturing errors. Laminating personnel is not used to precise placement of reinforcing elements.

Delamination. Due to manufacturing errors, microscopic air bubbles can be included in the laminate at the reinforcing element. Due to constant heating and cooling, thus expanding and shrinking of the air, this may lead to delaminating after several years.

Unknown adhesive and shear strength qualities of SGP foil. SGP is designed for transferring shear force over a large surface under low stress. This reinforcing method would require high shear stress capacities. The suitability for this purpose has to be examined.

Warning by solar radiation. The shear stress capacity of SGP is poor at temperatures above 50°C. This is a problem for structures exposed to direct sunlight because the temperature can increase to around 60°C. This needs special attention.

At room temperature the shear capacity is quite satisfactory, but due to its visco-elasticity this degrades fast at high temperatures. Although the latest developments in SGP production have improved this considerably and the expected progress in the near future is favorable, it remains a point of great attention.

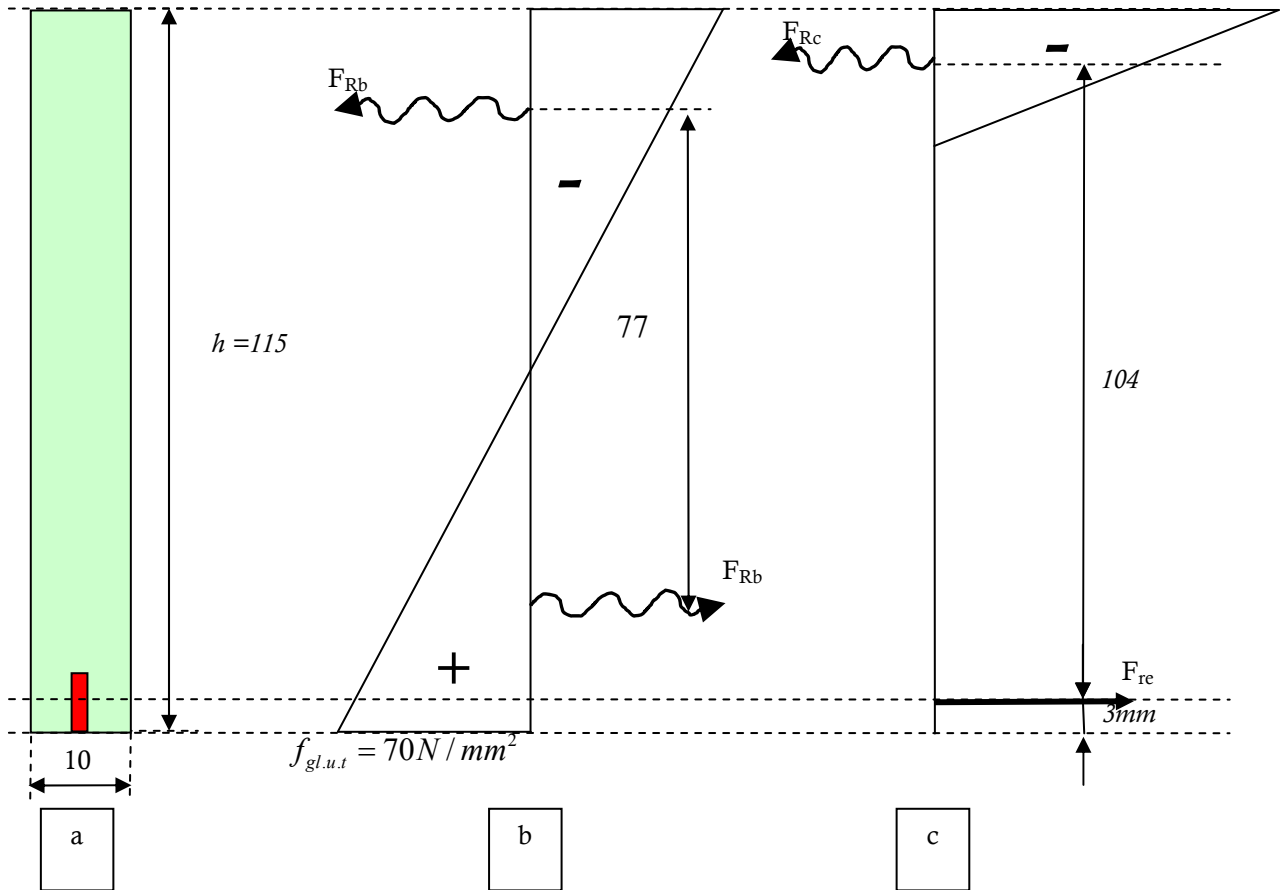


Figure 84 a-c,

a: Girder cross-section. Glass fiber in red, glass panes in light green.

b: Stress diagram just before initial glass failure

c: Stress diagram at crack location after initial glass failure.

4.4 Reinforcement in the glass pane

Description

This concept consists of a single glass pane with a thickness of 10mm. The bottom is finished with the SGG Plug-in groove. A reinforcing element is positioned in this groove and bonded to the glass by an adhesive (*Figure 84a*).

In this design there is a maximum amount of reinforcement, since the groove has a maximum surface area of $6 \times 2 = 12 \text{ mm}^2$. This limits the tensile strength of the reinforcement and therefore the height of the girder. For a small span girder as intended in this thesis though, it might be suitable.

Numerical support

Minimum reinforcement

First the bending moment at initial glass failure (see *Figure 84b*) is calculated:

$$M_{ci} = F_r * \frac{2}{3} h$$

$$F_r = \frac{1}{2} f_{br} * \frac{1}{2} h * d = \frac{1}{4} * 70 * 115 * 10 = 20.125 \text{ N T}$$

$$M_{ci} = 20.125 \text{ N} * 76,7 \text{ mm} = 1.542.917 \text{ Nmm}$$

$$M_{ci} = 1,54 \text{ kNm}$$

this equals the moment delivered by the tensile force in the reinforcement and the compressive zone in the glass (see *Figure 84c*). Supposing a crack depth of 80% of the height of the girder, the resulting force from the compressive zone is positioned at 7,7mm from the top.

$$F_{re} = \frac{M_{ci}}{d} = \frac{1,54 * 10^6 \text{ Nmm}}{104 \text{ mm}} = 14.836 \text{ N}$$

$$F_{re} = 14,8 \text{ kN}$$

Two materials are considered:

R-glass fiber, $\sigma_u = 1800 \text{ N/mm}^2$.

$$A_{re} = \frac{14836 \text{ N}}{1800 \text{ N/mm}^2} = 8,24 \text{ mm}^2$$

$A_{\min} = 8,24 \text{ mm}^2 \rightarrow 1,8 \times 6 \text{ mm} = 10,8 \text{ mm}^2$ leaves 0,1mm space for adhesive on both sides.

$$A = 10,8 \text{ mm}^2, N_u = 19,44 \text{ kN.}$$

Carbon fiber, $\sigma_u = 1950 \text{ N/mm}^2$.

$$A_{re} = \frac{14836 \text{ N}}{1950 \text{ N/mm}^2} = 7,61 \text{ mm}^2$$

$A_{\min} = 7,61 \text{ mm}^2 \rightarrow 1,8 \times 6 \text{ mm}$ leaves 0,1mm room for adhesive on both sides.

$$A = 10,8 \text{ mm}^2, N_u = 21,06 \text{ kN.}$$

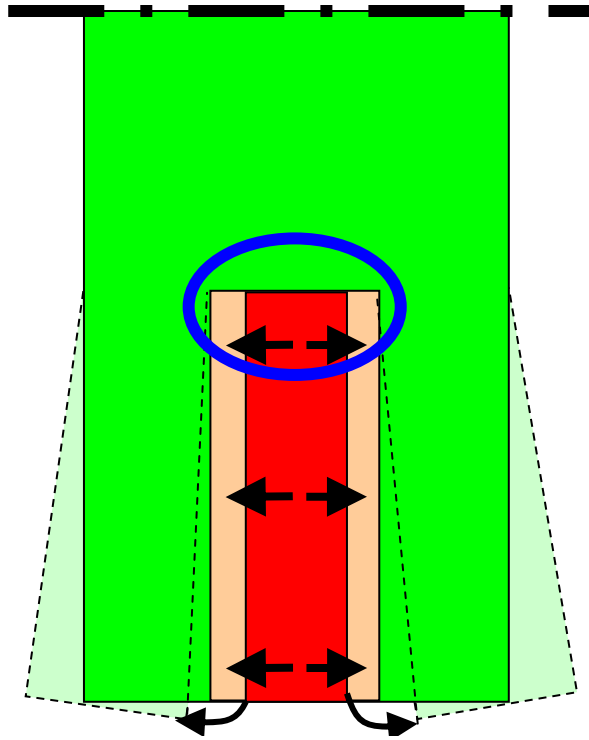


Figure 85, Schematical close-up of bottom of girder with reinforcement.

Green: Glass pane

Light green: glass pane after thermal expansion

Red: Reinforcement

Light red: reinforcement after thermal expansion

Maximum reinforcement

Control of maximum reinforcement (brittle compressive failure of top of glass beam):

50% pultruded R-glass fiber

Stress diagram is similar to *Figure 84c*.

$$\sigma_{gl,max} = 500 N / mm^2$$

$$A_{gl} = 0,2 * h * d = 0,2 * 115 * 10 = 230 N / mm^2$$

$$F_{R,gl,max} = \frac{\sigma_{gl,max}}{2} * 0,2h * d_{gl}$$

$$F_{R,gl,max} = 250 * 0,2 * 115 * 10 = 57.500 N$$

$$F_{R,gl,max} = 57,5 kN > F_{re,max} = 19,44 kN$$

$$M_{cu} = 19,440 kN * 0,104 m = 2,02 kNm$$

→ 10,8 mm² is OK.

50% pultruded Carbon fiber

Stress diagram is similar to *Figure 84c*.

$$F_{R,gl,max} = 57,5 kN > F_{re,max} = 21,06 kN$$

$$M_{cu} = 21,06 kN * 0,104 m = 2,19 kNm$$

→ 10,8 mm² is OK.

Discussion

Strong points:

Reinforcement well protected in the glass pane. The reinforcement is embedded at 3 sides by the glass pane.

Controlled product quality. Milling of groove is done by an industrial machine which ensures a constant dimension and quality of the groove. Critical adhesion manufacturing can be done by experts.

Possible introduction of standardized ‘prefab’ reinforced glass pane with no external reinforcing elements. Most structural engineers are reluctant to

work with structural glass because of its lack of ensured mechanical behavior.

This concept could provide architects and engineers with a small span building element that can be applied without further thorough calculations. Comparable to for instance a steel HE140A profile of which all mechanical properties are known.

Weak points / points of attention:

Limited size of girder. The SGG plug-in groove has definite dimensions that limit the amount of reinforcement that can be introduced in the girder. To ensure the minimum amount of reinforcement in the girder this directly limits the size of the girder in total.

Possible air encapsulations in adhesive when not manufactured correctly. Adhesion process needs to be done carefully

Milling of the groove may damage the glass pane decreasing its tensile bending strength. This is a theoretical assumption that, although contradicted by the manufacturer, has to be verified by testing.

Reinforcements are bonded to the roughest, weakest part of the glass pane. This could influence the strength of the joint.

Unequal thermal extension coefficient of glass, adhesive and reinforcement. See *Figure 85*. If large temperature fluctuations occur, the reinforcement expands more, or shrinks less than the glass pane. This causes tensile stress in the bottom of the groove (encircled in blue) which may cause the glass to fracture. This effect is enlarged by the fact that the surface of the glass is rough in the groove thus larger stress peaks occur.

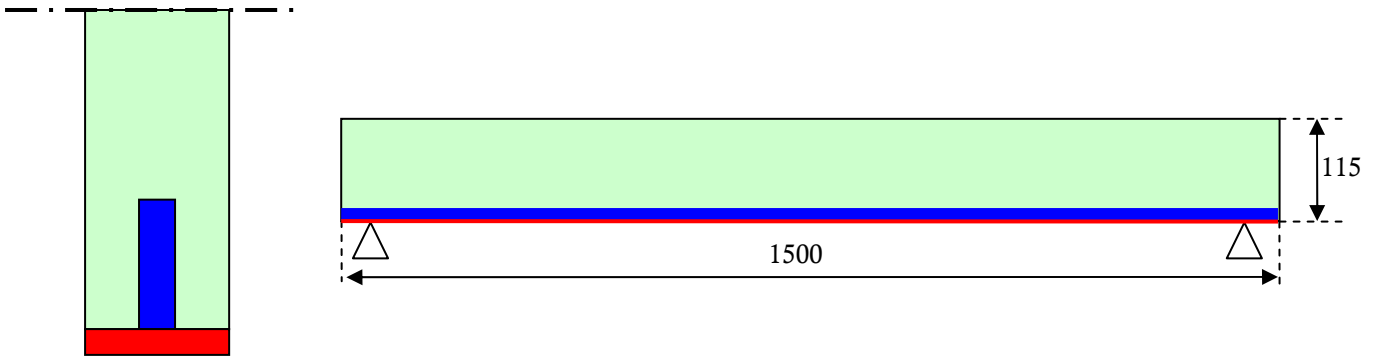


Figure 86, Left: Close-up of cross-section of bottom of girder. Right: side view. Dimensions in mm.

Glass: light-green.

Pre-stress element: blue.

Reinforcement: red.

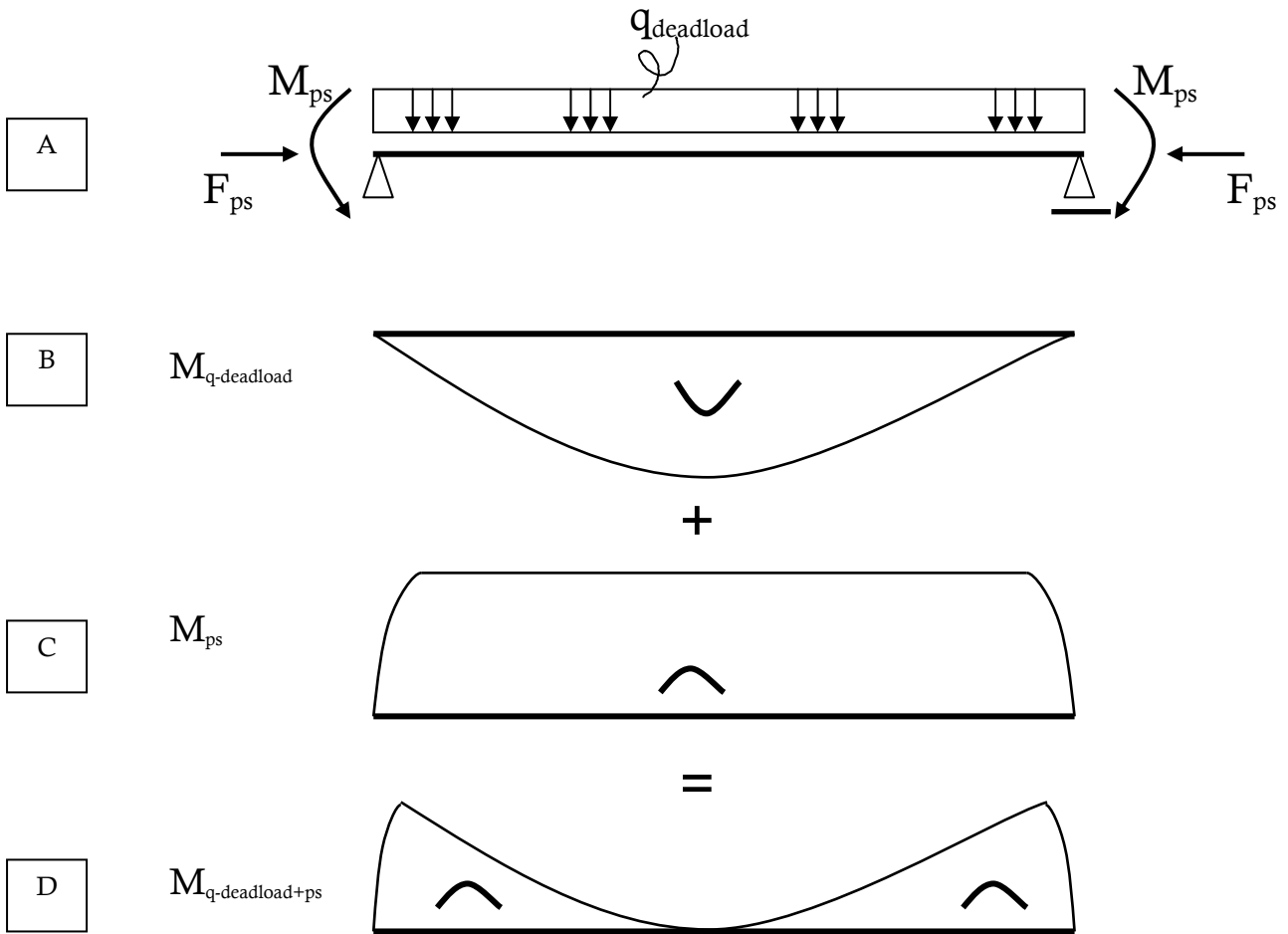


Figure 87,

A: Schematic representation of working forces on pre-stressed beam in rest.

B: Moment line due to dead load.

C: Moment line due to pre-stress load.

D: Moment lines combined.

4.5 Pre-stress in the glass pane, reinforcement under the girder

Description

In glass design the dead load on a structure is considerable. The bending moment due to the dead load can be neutralized by an upward bending moment created by a pre-stressed element in the bottom of the girder:

$$M_{deadload} + M_{Prestress} \approx 0$$

The sum of pre-stress load and dead load result in a permanent compression of the glass.

This concept uses the same SGG plug-in groove as the previous. The groove is not used for reinforcement, but for a pre-stressed element that is bonded by an adhesive. A carbon fiber reinforcing element is placed under the girder (see *Figure 86*). This principle was introduced in 'A New Roof for the XIIIth Century' [14] and proved satisfactory.

Numerical support

See *Figure 88*. Just after pre-stressing, without dead-load, the stress in the beam may not exceed the ultimate compressive and tensile strength of the beam (50N/mm²).

$$W_b = \frac{b * h^2}{6} = \frac{10 * 115^2}{6} = 22.041,7 mm^3$$

$$\sigma = \frac{F_{ps}}{h * d} + \frac{F_{ps} * e_{ps}}{W_b} \leq 50 N / mm^2$$

$$e_{ps} = \frac{h}{2} - 3 = 54,5 mm$$

$$50 = \frac{F_{ps}}{1.150} + \frac{54,5 * F_{ps}}{22.041,7}$$

$$F_{ps} = 14.960 N$$

The maximum surface of the pre-stress element is 10 mm², so minimum strength of reinforcement material:

$$F_{ps_max} = 14.960 N$$

$$A_{ps} \approx 10 mm^2$$

$$\sigma_{ps} = \frac{14.960 N}{10 mm^2} = 1.496 N / mm^2$$

Possible materials:

- Pultruded carbon fiber HM (Ultimate tensile strength 2000 N/mm²)
- Pultruded R-glass (ultimate tensile strength 1800 N/mm²)
- High-strength steel wire (piano wire; 2200N/mm²)

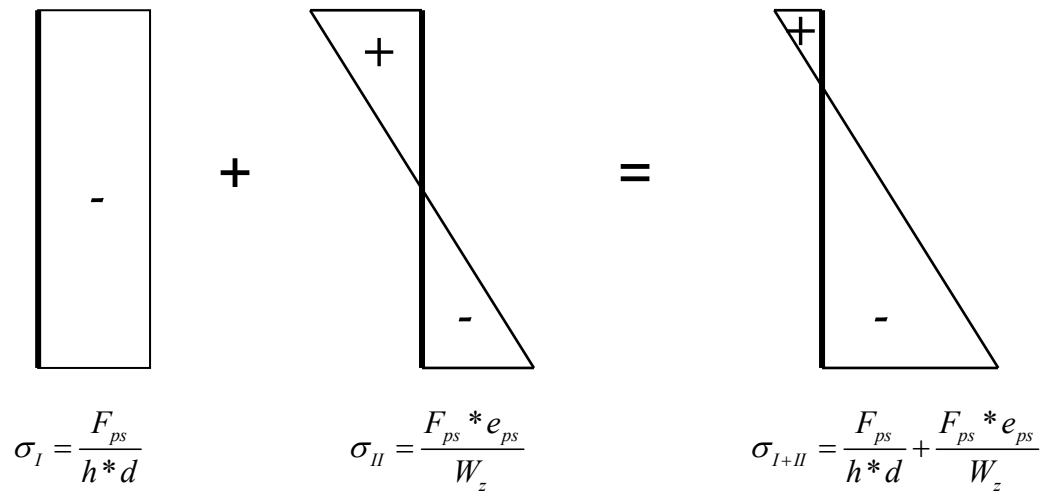


Figure 88, Stress diagram of beam cross-section.

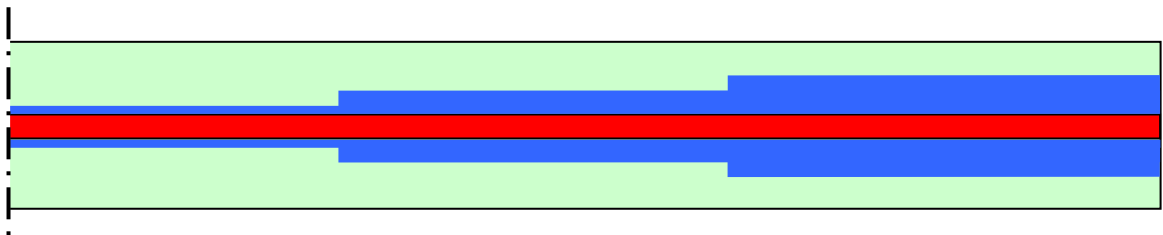


Figure 89, Adhesive joint principle of pre-stress strand (not to scale). Light green: glass, red: pre stress strand, blue: Adhesive layer.

The pre-stress forces will be adhesively bonded to the glass pane. In a normal adhesive connection, the shear force is transferred in the first 5mm of the connection. If that is done here, the ultimate shear stress of the adhesive is exceeded:

- Force to be transferred: $F = 15000N$

- Surface area per mm where the adhesive can bond:

$$A = 5 + 2 + 5 = 12mm^2 / mm$$

- Maximum shear stress allowed in adhesive (estimated): $\tau_{max} = 6N / mm^2$ (to suppress creep)

- Shear force that can be transferred per mm bond:

$$12mm^2 / mm * 6N / mm^2 = 72N / mm$$

- Length over which the adhesive is loaded:

$$15000 / 72 = 208,333mm$$

To prevent a stress peak in the end of the pre-stress strand, the adhesive layer will have to be thickened locally.

Conventional reinforcement has to be able to handle tensile forces after the pre-stressing strand and the glass fail and provide a safe failure behavior.

For the reinforcing element a stainless steel or carbon fiber strip can be used.

Discussion

Strong points:

Higher bending strength with less construction height.

Continuous compressive stress in glass surface which has positive effect on life-span of the glass. Glass loaded under compression is less susceptible to

penetration of water and chemicals into the micro cracks. This enhances the lifespan of the beam.

Micro-cracks introduced by milling the groove are loaded under compression. The weak point of the groove is neutralized by this.

Weak Points / points of attention:

Buckling. The pre-stressed element introduces a large compressive force in the bottom of the beam. The buckling behavior will have to be considered.

Creep. Introduction of pre-stress by adhesive bonding will have to be guaranteed for decennia. Creep behavior of adhesive bond will have to be considered. If the adhesive is loaded well under the 'knee-point' the creep behavior is predictable, but this has to be guaranteed.

Shear stress level in the glass pane at upper section of pre-stress strand might be governing. This needs further attention.

Table 11, Comparison of concept designs.

	Strong	Weak
1. Reinforcement in laminates	Transparent Design	Manufacturing errors
	Reinforcement protected	Delamination
	Free positioning	Unknown properties SGP
	Up- and downscaling	Fire safety
2. Reinforcement in groove	Reinforcement protected	Limited size Manufacturing errors
	Introduction of 'prefab' reinforced glass pane	Weakening glass by milling groove
3. Pre-stress in groove, Reinforcement in laminates	Higher bending strength with less construction height.	Buckling Possible creep
	Continuous compression in glass	Shear stress in glass pane governing?
	Groove loaded under compression	

4.6 Conclusions and recommendations

Concept 2 seems the most favorable reinforcing method for further investigation in this thesis.

Concept 1 has good potential. Especially the fact that the reinforcements of any size can be placed in any direction makes it possible to introduce reinforcements for shear force as well as bending moment.

Problem with this concept is that Sentry Glass Plus is a thermoplastic material of which the mechanical properties degrade fast above 40°C. This temperature could very well be reached when the beam is exposed to sunlight or during fire conditions.

Concept 3 also has good potential. However there are many unknown factors concerning the adhesive bonding of reinforcements to glass. To take it even one step further to adhesively bonding a pre-stressed element may be a bit too far-fetched for this thesis.

5. Tests

5.1 Introduction

More detailed information is needed about the structural properties of the intended materials to elaborate the chosen preliminary design. This information is not available from literature and has to be determined by practical research. A summarized description of these tests is presented in this chapter. The full test reports are enclosed in the appendices corresponding to the paragraph number.

A lot of possible reinforcement materials have been reviewed during the literature study. In paragraph 5.2 they are compared and weighed on different important aspects like strength, stiffness, transparency and, last but not least, availability in the desired measurements. The range of materials is brought back to three (steel, carbon fiber and glass fiber) which are tested for strength and stiffness.

Paragraph 5.3 contains an exploring test into the effects of adhesive layer thickness on the strength of the connection.

An important aspect of a reinforced girder is the maximum tensile force that the reinforcement can bear. This does not only rely on the tensile strength of the reinforcing element itself, but also on the glass pane and the adhesive connection.

With the results of the first three paragraphs of this chapter several alternatives for reinforcement configurations are generated. Tests to determine the maximum tensile force that the reinforcement can take are described in paragraph 5.4.

To gain experience in practical research a preliminary test series of three reinforced glass girders is done. This is described in Paragraph 5.5.

This chapter is ended by conclusions about the tests and recommendations for the final design of the girder.

Table 12, Review of materials

	Available in desired size?	Satisfactory structural properties?				Applicable?
		E	σ_{\max}	Transparency	Creep	
Structural steel	No	Yes	Yes	No	Yes	No
Stainless steel	Yes	Yes	Maybe	No	Yes	Yes
Piano wire	No	Yes	Yes	No	Yes	No
Carbon fiber	Yes	Yes	Yes	No	Yes	Yes
Glass fiber	Yes	Maybe	Maybe	Maybe	Yes	Maybe
Nylon	Yes	No	No	No	No	No
Zylon	No	Yes	Yes	No	Yes	No
Dyneema, Spectra	Yes	Yes	Yes	No	No	No
Kevlar, Vectran, Twaron	No	Yes	Yes	No	Yes	No

5.2 Material tests

Material review

The materials that are discussed in the literature study are reviewed for their suitability in this research (see *Table 12*).

An important aspect turned out to be availability. If it cannot be obtained on time and in budget it cannot be used. Although some materials like zylon, piano wire and Kevlar could be interesting for application as reinforcement they will not be included in this research.

The only material that can theoretically be made transparent is glass fiber. Unfortunately this is not yet produced or on the market, therefore the transparency of the materials is not taken into consideration.

The following materials are used in this thesis:

1. Stainless steel
2. Carbon Fiber (pultruded)
3. Glass Fiber (pultruded)

The structural properties, proclaimed by the manufacturer, of the obtained carbon and glass fiber are not proven. The materials have to be tested to determine this.

The results of these tests are presented in paragraph 5.3.

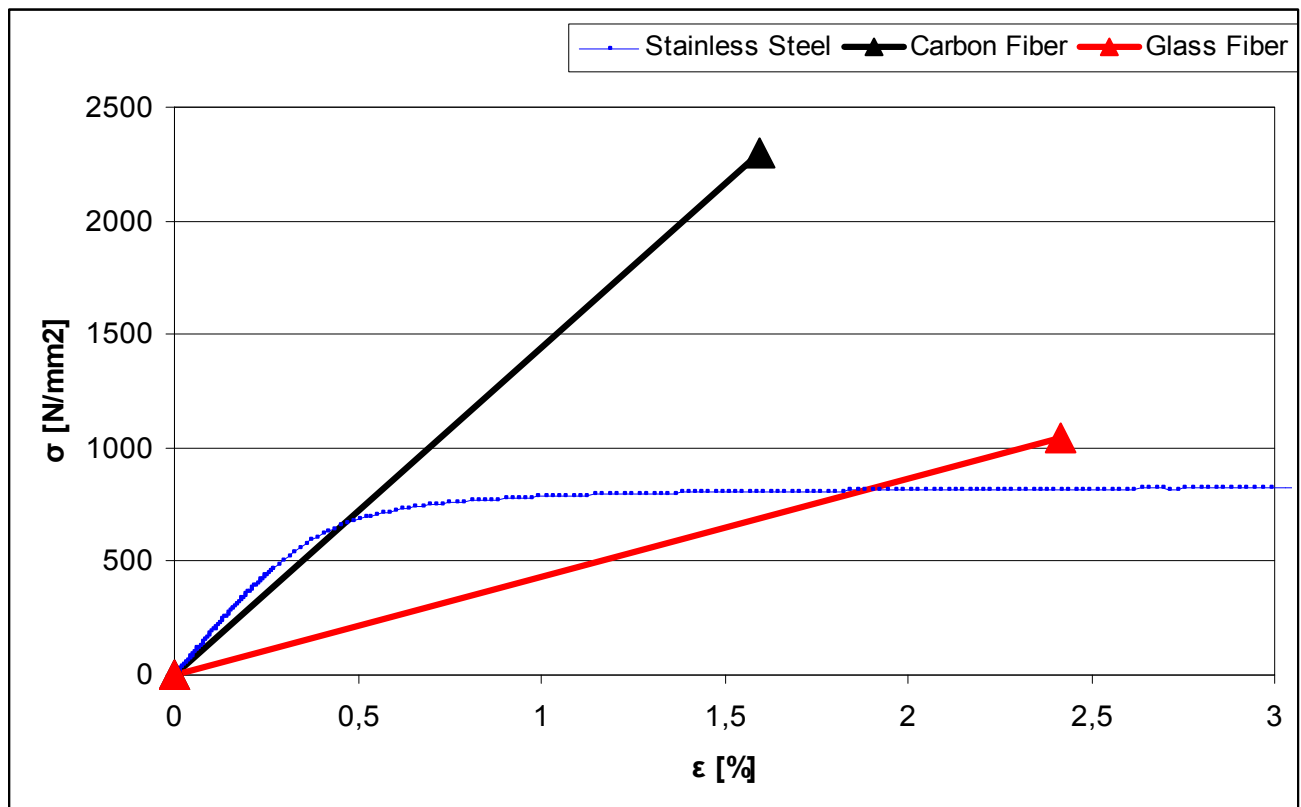


Figure 90, σ - ϵ curves of stainless steel, carbon fiber and glass fiber

Table 13, Structural properties of tested materials

Material	σ_{\max} [N/mm ²]	Young's modulus [GPa]
Carbon fiber	2300	145
Glass Fiber	1050	45
Steel	700	180

Structural properties of selected materials

Abstract

A summary of the results is presented in *Table 14*, σ - ϵ curves are in *Figure 90*

Method

The specimens are tested in a displacement controlled tensile test. A photograph of the setup is presented in *Figure 91*.

From the resulting data the Young's modulus, ultimate tensile stress, elongation at break, is derived.

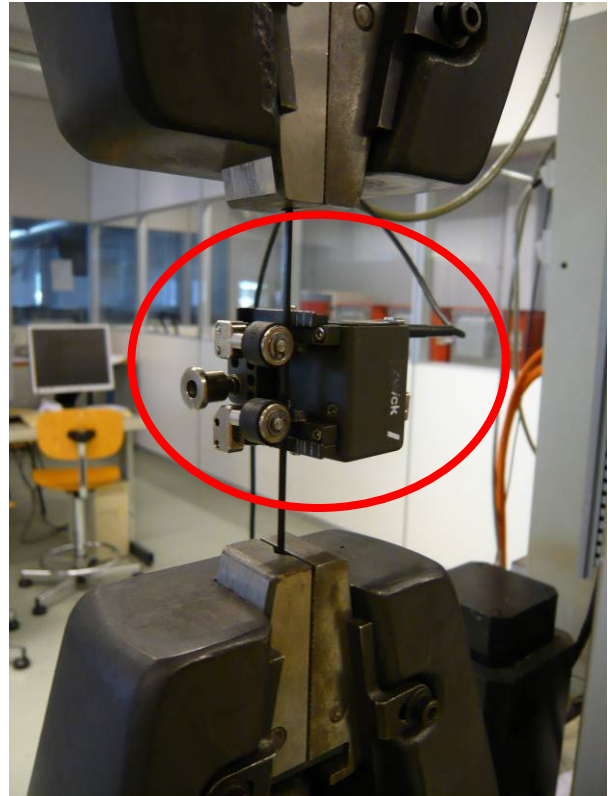


Figure 91, Photo of test set-up with round carbon fiber specimen. The device in the middle of the picture (circled in red) is the Zwick extensometer

Table 15, Summary of test results stainless steel

Specimen #	Shape	Cross-section [mm ²]	Clamp to clamp distance [mm]	Strain at break [%]	Tensile strength [N/mm ²]
4	Ø2mm	3,14	91,0	44	884
5	Ø2mm	3,14	90,5	23	869
6	Ø2mm	3,14	90,5	30	871
Average				32	875

Table 17, Summary of test results carbon fiber

Specimen #	Dimension	Cross-section	σ-max
	[mm ²]	[mm ²]	[N/mm ²]
1	1,6 x 8 mm	12,80	2347
2	2,4 x 8 mm	14,40	2237
3	1 x Ø2mm	3,14	2172
4	2 x Ø2mm	6,28	2322
5	3 x Ø2mm	9,42	2332
Average			2282

Table 16, Summary of test results glass fiber

Specimen #	Dimension [mm]	Cross-section [mm ²]	Total failure?	σ max [N/mm ²]
1	1 x Ø2mm	3,14	Yes	1208
2	1 x Ø2mm	3,14	No	841
3	1 x Ø2mm	3,14	No	919
4	3 x Ø2mm	9,42	Yes	984
5	3 x Ø2mm	9,42	Yes	923
Average 1,4&5:				1038

Table 14, Summary of test results and deviations

Material			Hypothesis	Measured	Deviation
Steel	σ _{max}	[N/mm ²]	515	875	+70%
	E	[GPa]	193	180	-7%
Carbon fiber	σ _{max}	[N/mm ²]	2488	2282	-8%
	E	[GPa]	150	144	-4%
Glass Fiber	σ _{max}	[N/mm ²]	2300	1038	-55%
	E	[GPa]	53	43	-19%

Results

The results of the tensile tests on all specimens are presented in *Table 15*, *Table 17* and *Table 16*.

Conclusions and recommendations

From the three tested materials, carbon fiber is the most suitable for the intended use in this thesis. It has the highest tensile strength and is relatively stiff. Carbon fiber has an elastic behavior up to total failure.

Negative property is its lack of transparency.

Glass fiber also has an elastic behavior up to total failure.

This type of glass fiber is not suitable for use as reinforcement in a structural glass girder. It is not transparent, less stiff than carbon fiber and less strong.

The used glass fiber did not meet the expectations. Although the producer proclaimed to have delivered an R-glass fiber staff, it is more plausible that this profile consisted of E-glass fiber rovings.

Further search for a transparent, strong and stiff glass fiber profile is recommended.

The used stainless steel specimens are not suitable for use in the intended glass girder. The tensile stress to which it can be loaded is low compared to carbon fiber and glass fiber and modulus of elasticity is not much higher than that of carbon fiber.



Figure 92, 13 tested specimens after the tests. Specimens consist of $\varnothing 2\text{mm}$ bars adhesively bonded in aluminum blocks with different adhesive thicknesses.

From left to right: 1 carbon fiber, 5 glass fiber, 1 stainless steel, 1 glass fiber, 2 carbon fiber, 3 glass fiber.

5.3 Aluminum pull-out tests

Theory & Introduction

The tensile force in the reinforcement is transferred to the glass by an adhesive. This adhesive is therefore loaded primarily by shear stress.

In a typical ‘single lap joint’ the shear stress is not constant over the length of the connection because the substrates (glass and reinforcement) are not infinitely stiff. Most of the shear force is transferred in the first part of the connection, resulting in a ‘shear stress peak’ in the ends of the joint, as visible in *Figure 93a*.

In case of a completely elastic adhesive like in *Figure 93b*:

If this shear stress peak exceeds the maximum shear stress capacity of the adhesive, the adhesive connection will fail at the stress peak location, resulting in a shift of the stress peak along the length of the connection, until a total failure of the joint occurs.

If the adhesive has a perfect elastic-plastic behavior like in *Figure 93c*, the stress peak will not exceed the strength of the adhesive. The peak will widen as shear force on the joint increases until the maximum capacity of the joint is reached and the adhesive fails.

The strength of each adhesive is different. This capacity is (amongst other things) dependent on the type of adhesive, thickness of the adhesive layer, substrate materials, roughness of the surface and stiffness of the substrates.

The exploring tests described in this chapter are done to gain a rough insight in the behavior of selected adhesive systems to differences in the thickness of the layer and stiffness of the used substrates.

Goal is to find out if there is a great difference in shear stress capacity between the used adhesives and if the variables have a great influence on the strength of the connection. A secondary goal is to develop routine in applying the adhesive systems and experiencing if they are useful in practice.

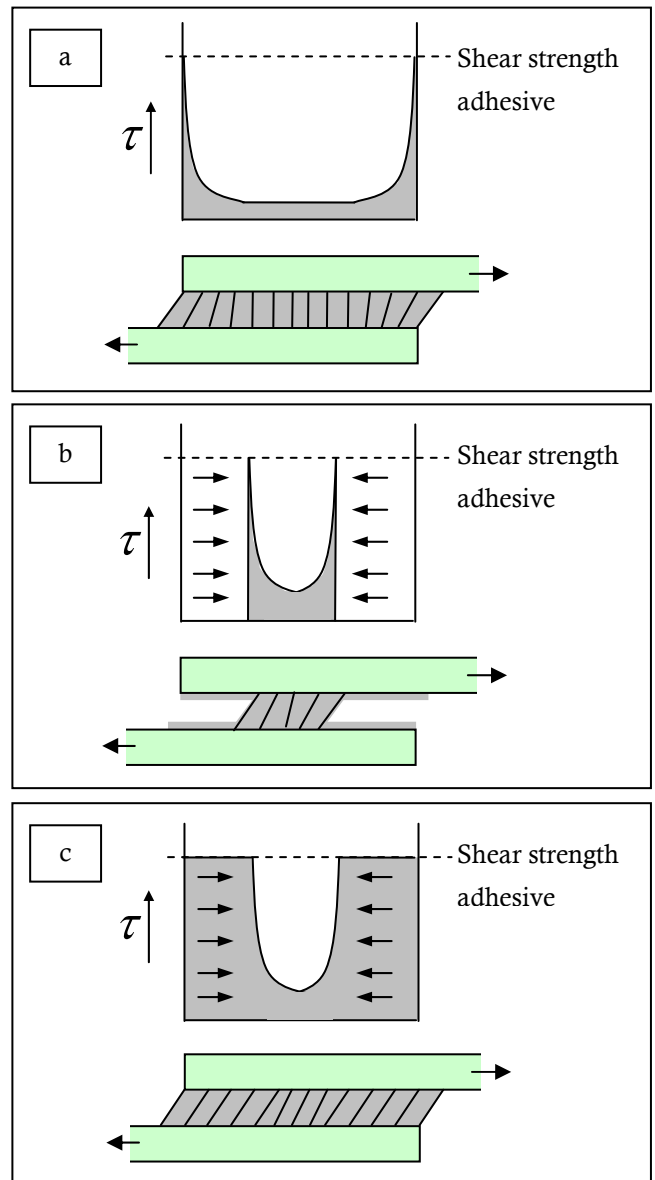


Figure 93, Shear stress concentrations in single lap joints. Adhesive in grey, substrates in green.

A: Adhesive deformed up to shear strength.

B: Elastic adhesive, partly ruptured.

C: Elastic-plastic adhesive, almost loaded up to maximum joint capacity.

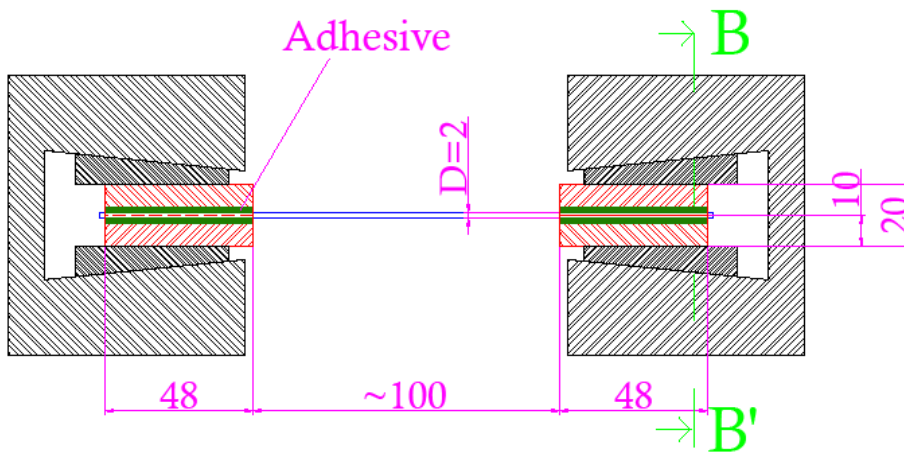
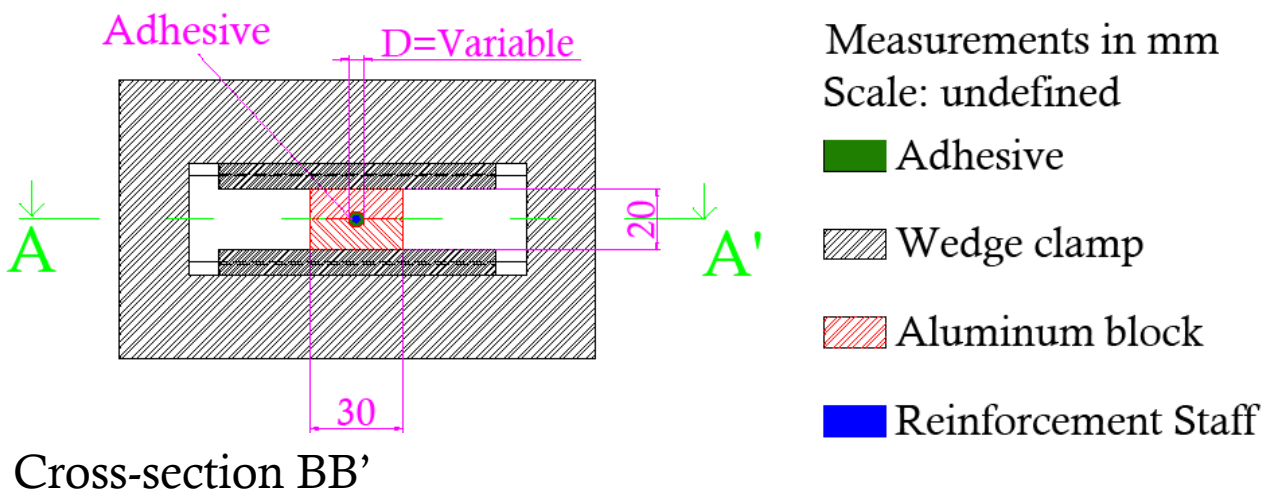


Figure 94, Test setup

Method

It is expected that the tensile force on the aluminum blocks will be transferred to the reinforcement bar in the first approximately 5mm of the connection. A factor 10 (~50mm) seems reasonable for an exploring test.

See *Figure 95*. A round bar with a thickness of 2mm is adhesively bonded over 48mm in the center of a cylinder-shaped hole in an aluminum block. Adhesive layer thickness is varied by the variation of the diameter of the hole.

Three adhesive systems are tested:

1. Huntsman Araldite 2013
2. DELO Rapid 03 Thix
3. Huntsman Araldite 2020

The specimens are tested in a displacement controlled tensile test setup similarly to the one described in the former paragraph.

The aluminum blocks are clamped in the wedge clamps, the Zwick extensometer is attached to the middle of the staff. The clamp displacement, tensile force and strain of the bar are measured.

Table 18, Tested specimens

#	Staff material	Adhesive	Diameter hole		Adhesive thickness	
1	Carbon fiber	R 03 Th	2,0	[mm]	< 0,1	[mm]
2	Carbon fiber	R 03 Th	3,0	[mm]	0,5	[mm]
3	Carbon fiber	R 03 Th	5,0	[mm]	1,5	[mm]
4	Glass fiber	R 03 Th	2,0	[mm]	< 0,1	[mm]
5	Glass fiber	R 03 Th	3,0	[mm]	0,5	[mm]
6	Glass fiber	R 03 Th	5,0	[mm]	1,5	[mm]
7	Glass fiber	2013	2,0	[mm]	< 0,1	[mm]
8	Glass fiber	2013	3,0	[mm]	0,5	[mm]
9	Glass fiber	2013	5,0	[mm]	1,5	[mm]
10	Glass fiber	2020	2,0	[mm]	< 0,1	[mm]
11	Glass fiber	2020	5,0	[mm]	1,5	[mm]

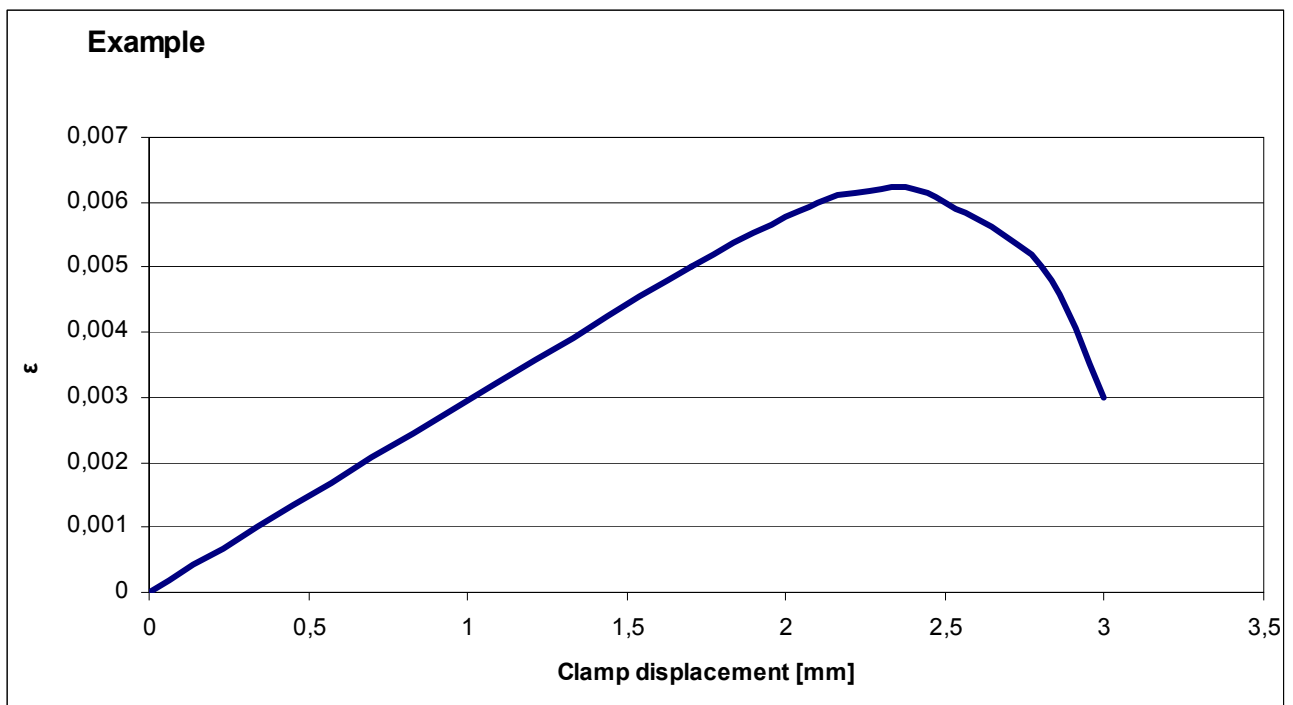


Figure 96, Example of stress-strain curve

The theoretical extension of the staff can be calculated from the E-modulus of the staff material (gained in the previous tests) and the initial distance between the aluminum blocks. The difference between this and the clamp displacement is caused by deformation (failure) of the adhesive connection between aluminum and staff.

If the strain-clamp displacement diagram is presented (see example *Figure 96*), it should give a linear curve up to the point where the adhesive reaches its maximum shear stress. At that point the curve should bend off to level and eventually drop down when the adhesive totally fails.

With a stiff adhesive the curve will bend off less and drop down abruptly when the maximum shear stress is reached. With a ductile adhesive the curve will bend off more.

An overview of the specimens can be found in *Table 18*.

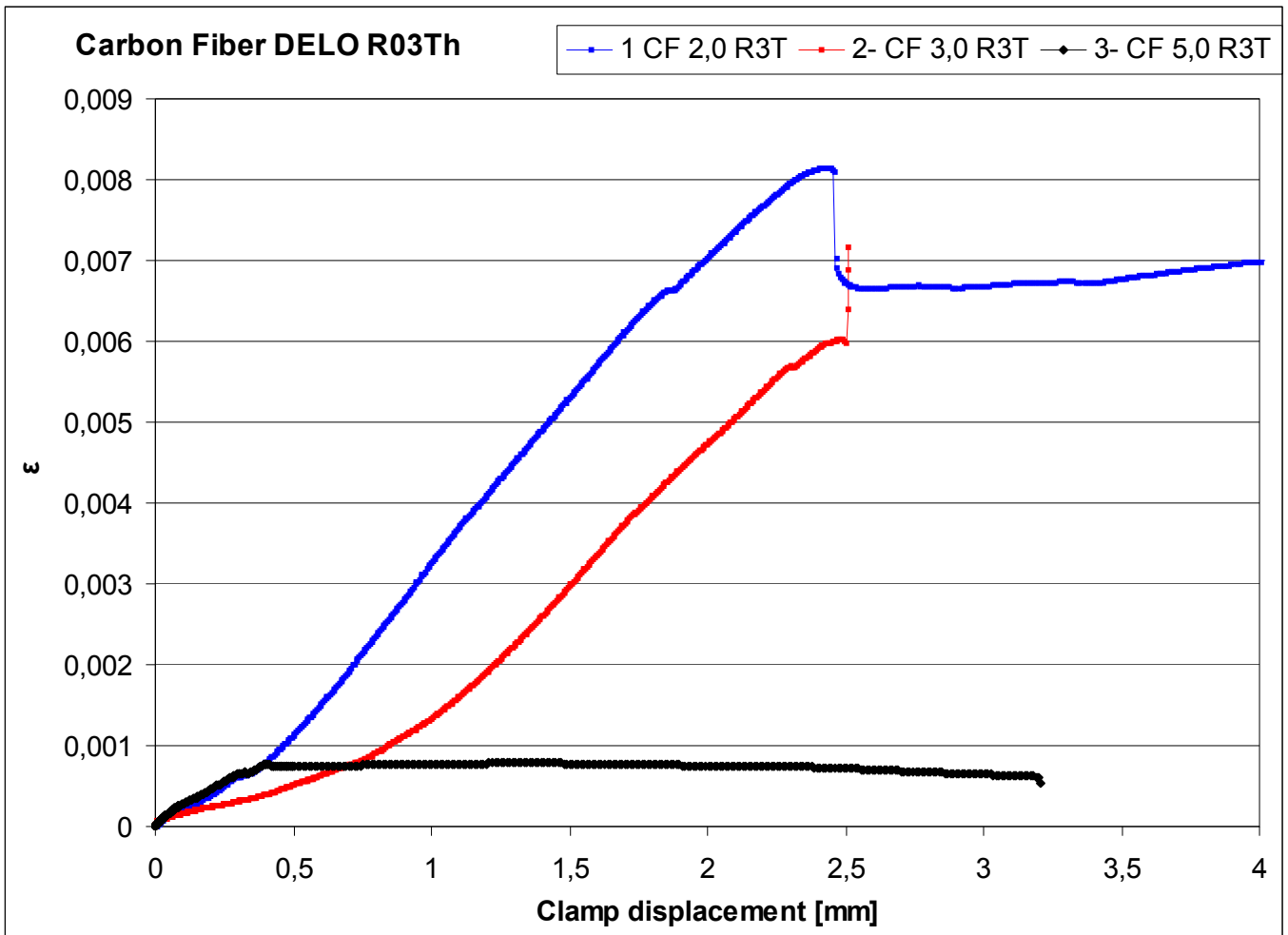


Figure 97, Strain-displacement curve of carbon fiber staff in combination with DELO Rapid 03 Thix

Table 19, Results specimens 1 to 3

#	Staff material	Adhesive	Diameter hole		Adhesive thickness		F _{max}		Failure mode	
									Adhesive	Staff
1	Carbon fiber	R 03 Th	2,0	[mm]	< 0,1	[mm]	3395	[N]	X	
2	Carbon fiber	R 03 Th	3,0	[mm]	0,5	[mm]	2496	[N]	X	
3	Carbon fiber	R 03 Th	5,0	[mm]	1,5	[mm]	333	[N]	X	

Carbon fiber

Hypothesis

Hypothesis is that the maximum tensile strength of the carbon fiber will not be reached.

The carbon fiber bar will break at a tensile force of:

$$F_{\max} = \sigma_{\max} * \pi r^2$$

$$F_{\max} = 2300 * \pi \approx 7200\text{N}$$

Results

The results are presented in *Table 19*.

None of the specimens failed due to breaking of the carbon fiber strip

The highest force was gained with the thinnest adhesive layer.

Specimen 3 failed at a tensile force of 333N. This is much less than expected.

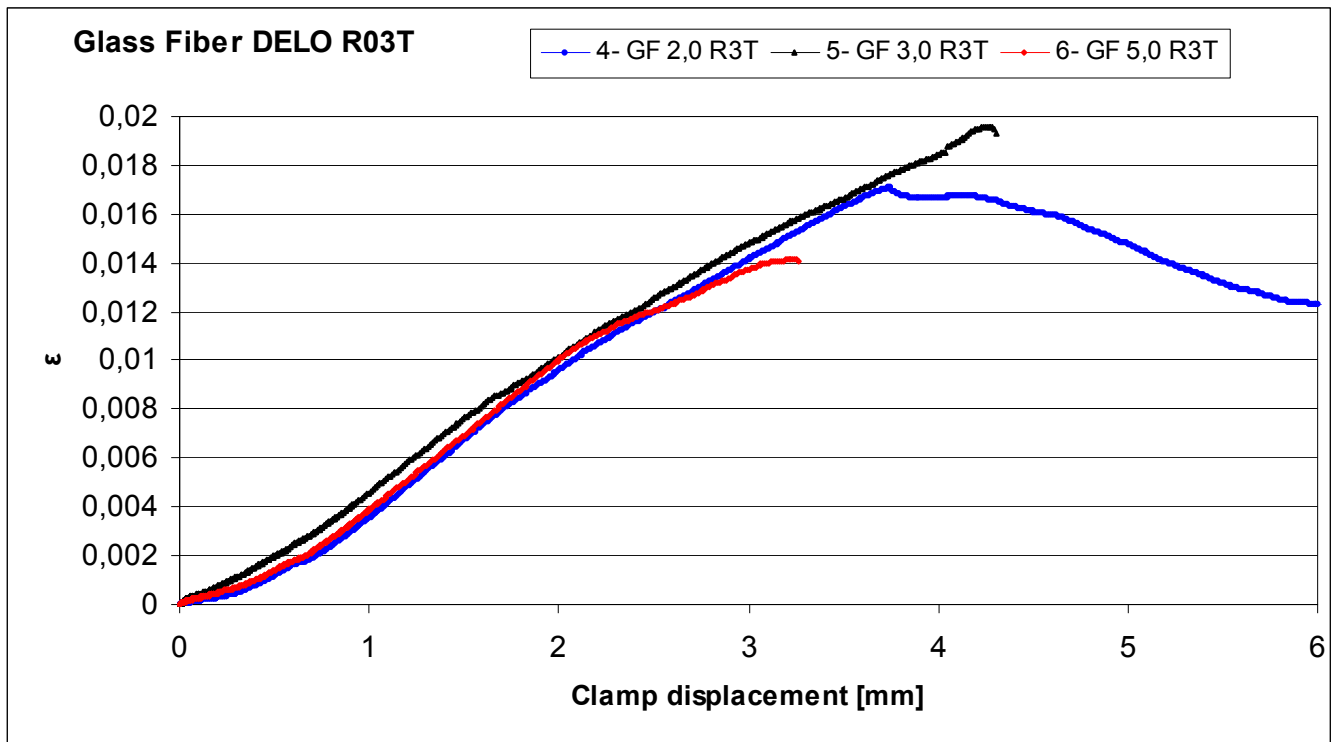


Figure 98, Strain-displacement curves for specimens 4 to 6

Table 20, Results specimens 4 to 6

#	Staff material	Adhesive	Diameter hole		Adhesive thickness		F _{max}		Failure mode	
									Adhesive	Staff
4	Glass fiber	R 03 Th	2,0	[mm]	< 0,1	[mm]	2336	[N]	X	
5	Glass fiber	R 03 Th	3,0	[mm]	0,5	[mm]	2668	[N]	X	
6	Glass fiber	R 03 Th	5,0	[mm]	1,5	[mm]	2035	[N]	X	

Glass fiber

Hypothesis

Hypothesis is that the maximum tensile strength of the glass fiber might be reached and the glass fiber could break before the adhesive fails.

The glass fiber staff will break at a tensile force of approximately:

$$F_{\max} = \sigma_{\max} * \pi r^2$$

$$F_{\max} = 1050 * \pi \approx 3300\text{N}$$

Results

The glass fiber staff has not broken for specimens 4 to 6.

The highest tensile force was reached with an adhesive thickness of 0,5 mm.

Specimen 4 started slipping in the aluminum block after the maximum tensile force was reached.

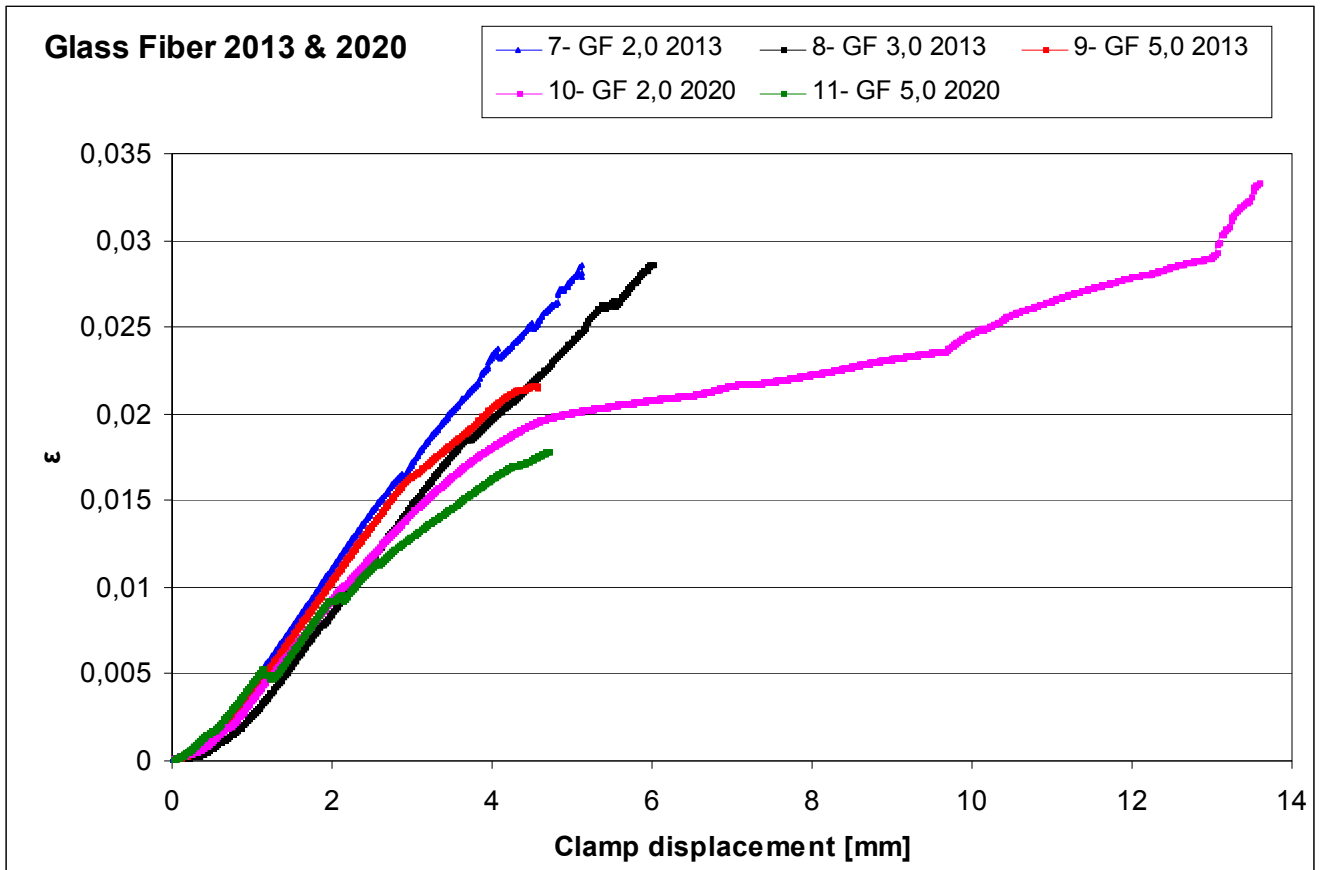


Figure 99, Strain-displacement curves for specimens 7 to 11

Table 21, Test results for specimens 7 to 11

#	Staff material	Adhesive	Diameter hole	[mm]	Adhesive thickness	[mm]	Fmax	[N]	Failure mode	
									Adhesive	Staff
7	Glass fiber	2013	2,0	[mm]	< 0,1	[mm]	3073	[N]		X
8	Glass fiber	2013	3,0	[mm]	0,5	[mm]	3474	[N]	X	X
9	Glass fiber	2013	5,0	[mm]	1,5	[mm]	3012	[N]	X	
10	Glass fiber	2020	2,0	[mm]	< 0,1	[mm]	3796	[N]	X	X
11	Glass fiber	2020	5,0	[mm]	1,5	[mm]	2887	[N]	X	

Specimen 10 failed at a force of approximately 2700 N. The rest of the curve is caused by slipping in the block. This continued for about 10mm. Eventually the force increased again because the specimen was thicker at the end and the friction increased.

The highest tensile force was reached with a layer thickness of 0,5mm.

The curves of specimens 9, 10 and 11 bend off, unlike specimens 7 and 8.

Table 22, Test results for specimens 1 to 11

#	Staff material	Adhesive	D-hole	[mm]	Adhesive thickness	[mm]	Fmax	[kN]	Failure mode	
									Adhesive	Staff
1	Carbon fiber	R 03 Th	2,0	[mm]	< 0,1	[mm]	3395	[kN]	X	
2	Carbon fiber	R 03 Th	3,0	[mm]	0,5	[mm]	2496	[kN]	X	
3	Carbon fiber	R 03 Th	5,0	[mm]	1,5	[mm]	333	[kN]	X	
4	Glass fiber	R 03 Th	2,0	[mm]	< 0,1	[mm]	2336	[kN]	X	
5	Glass fiber	R 03 Th	3,0	[mm]	0,5	[mm]	2668	[kN]	X	
6	Glass fiber	R 03 Th	5,0	[mm]	1,5	[mm]	2035	[kN]	X	
7	Glass fiber	2013	2,0	[mm]	< 0,1	[mm]	3073	[kN]		X
8	Glass fiber	2013	3,0	[mm]	0,5	[mm]	3474	[kN]	X	X
9	Glass fiber	2013	5,0	[mm]	1,5	[mm]	3012	[kN]	X	
10	Glass fiber	2020	2,0	[mm]	< 0,1	[mm]	3796	[kN]	X	X
11	Glass fiber	2020	5,0	[mm]	1,5	[mm]	2887	[kN]	X	

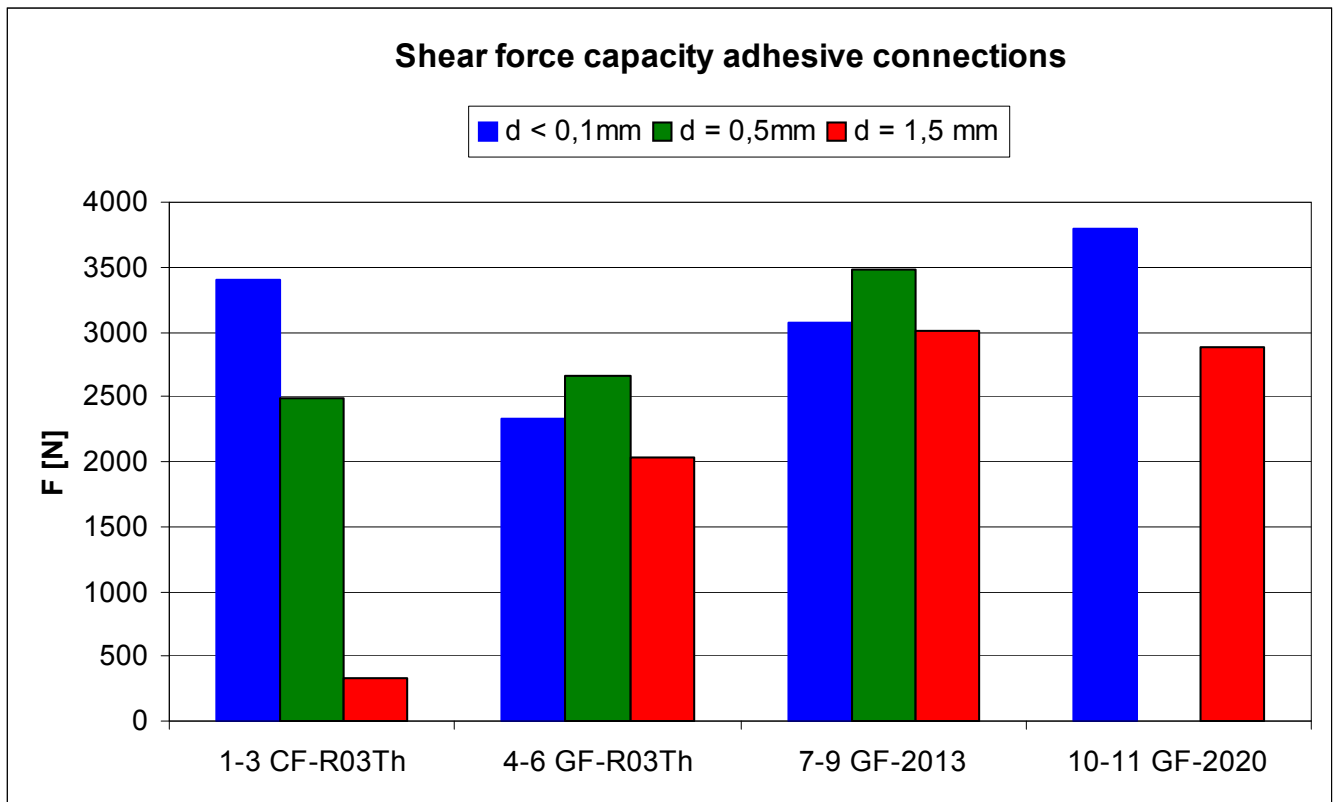


Figure 100, Maximum tensile forces for specimens 1 to 11, from left to right. The colors mark the adhesive layer thicknesses.

Discussion

General remark that has to be made is that the amount of tested specimens is not enough to draw solid conclusions. The tests are done for roughly exploring these adhesive systems and to interpret a trend in the results. Further research has to be conducted after these tests.

The results for specimen 3 are remarkably bad. Half of the length of the adhesive connection failed due to adhesive failure to the carbon, the other half due to adhesive failure to the aluminum.

The outcome of this test will not be taken seriously into consideration.

Comparing specimens 4 to 6 with 7 to 9, one could get the impression that Araldite 2013 is stronger than DELO Rapid 03 thix. Araldite 2020 also delivered better results than DELO Rapid 03 Thix.

Comparing specimens 1 and 4 implies that a stiffer staff (carbon fiber) has better results with a thin adhesive layer. This endorses the hypothesis that the shear stress peak in the adhesive layer spreads out as the substrate becomes stiffer.

Comparing specimens 4 to 6 and 7 to 9 implies that a less stiff staff (glass fiber) has better results with a slightly thicker adhesive layer. This implies that the optimum adhesive layer thickness for these specimens lies somewhere between 0,1 and 1,5mm.

Conclusions and recommendations

Araldite 2020 reached the highest shear strength.

Araldite 2013 reached the highest shear strength with a thick adhesive layer.

DELO Rapid 03 Thix is a very fast curing adhesive. For the intended use in a girder the processing time is too short. Apart from that, the structural properties are not as good as those of other transparent adhesives, like for instance Araldite 2020.

The best overall results with Glass fiber in combination with Rapid 03 Thix were gained with an adhesive layer thickness of 0,5mm. This gives the idea that there is an optimum in the thickness of the adhesive layer which is somewhere between 0,1mm and 1,5mm.

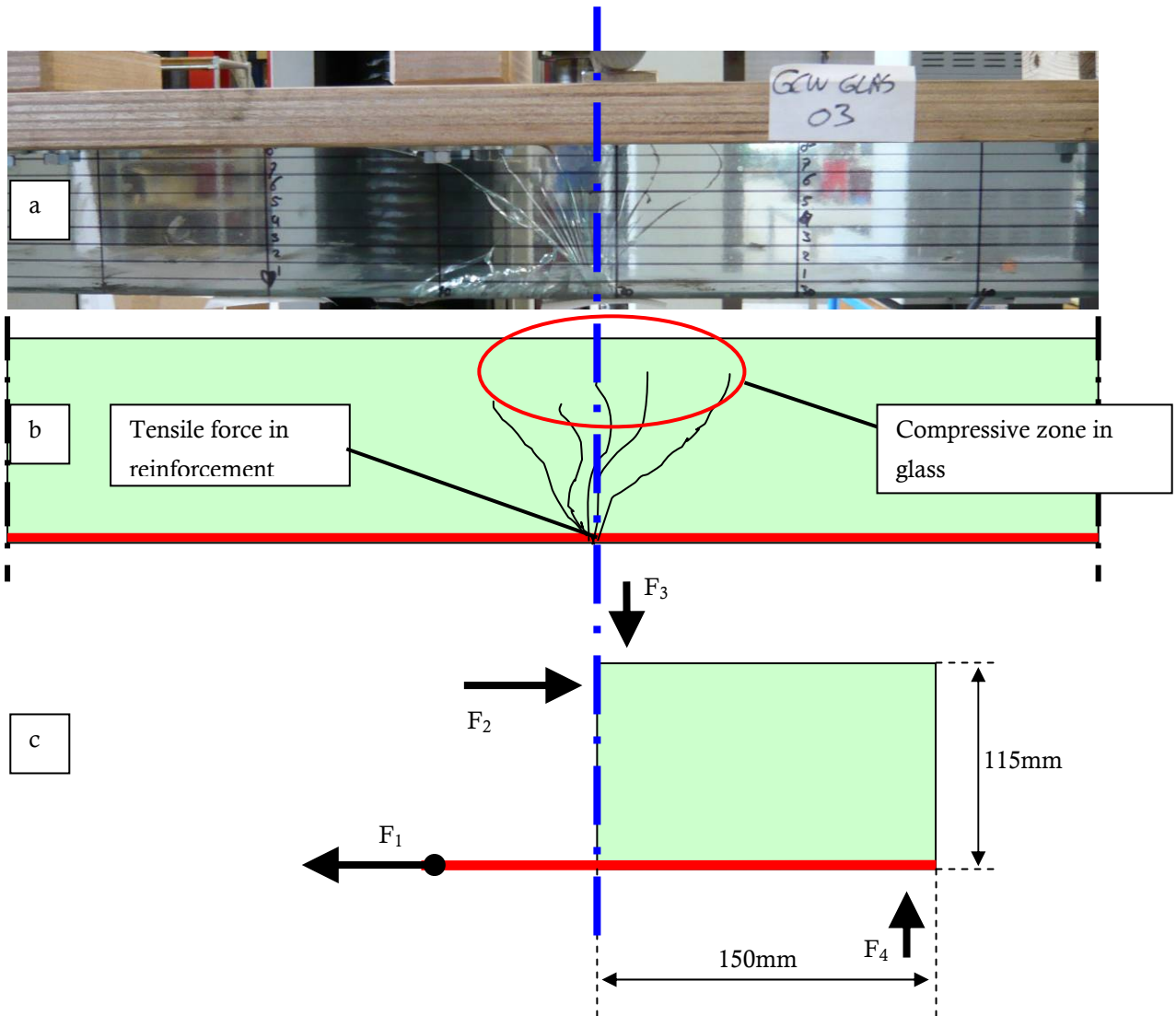


Figure 101 a to c, Middle part of specimen 3 from the preliminary beam tests after initial glass failure and derived specimen geometry for glass pull-out tests. Light green: glass pane, red: reinforcement.

a: Photograph.

b: Schematical representation of girder.

c: Schematical representation of specimen with dimensions and applied forces.

5.4 Glass pull-out tests

Introduction

It is concluded from the research described in paragraph 5.1 that carbon fiber is the best material to use for reinforcement in the intended glass girder.

Paragraph 5.2 implied that, with some adjustments, it is possible to use the SGG clip-in groove for reinforcing the girder.

The results from paragraph 5.3 show that there is an optimum adhesive layer thickness somewhere between 'very thin' and 1,5mm. This means that the best reinforcement configuration in the girder will not be a maximum amount of carbon fiber in the groove, filling it completely and leaving little space for an adhesive layer, but there has to be enough reinforcement to take on the tensile force that is released when the glass breaks.

The goal of the practical research described in this chapter is to find out which adhesive system in combination with which configuration of carbon fiber strips results in the best reinforcing principle in the SGG Clip-Inn groove.

Variables in this configuration are:

- A) Adhesive system
- B) Carbon fiber profile
- C) Adhesive layer thickness

Note that the options B and C are dependent on one another because the shape of the groove is constant: more carbon fiber means less adhesive and vice versa.

Another interesting factor is the length over which the force is transferred. This length varies for different adhesive systems and layer thicknesses.

To gain the required data several tests are performed with specimens that approach the situation of the fractured girder where the reinforcement is loaded by a

tensile force (F_1) and the glass pane by the compressive zone (F_2) as presented in *Figure 101*.

The tests are done in several sequences. After each sequence the results were evaluated and the setup was adjusted where it seemed necessary. Note that because the setup changed for every test sequence, comparison between the results of the test has to be done cautiously.

Sequence 1 consists mainly of adjustments to the setup after each specimen. Therefore the tests give bad comparable results. The last tests however, deliver satisfactory results.

The setup is adjusted for sequence 2 after which satisfactory results for the sake of maximum tensile force were gained. However, the interpretation of the force/displacement curves and therefore the failure mechanism, remained hard.

Four more measuring devices are installed for sequence 3 and this finally gave the desired data.

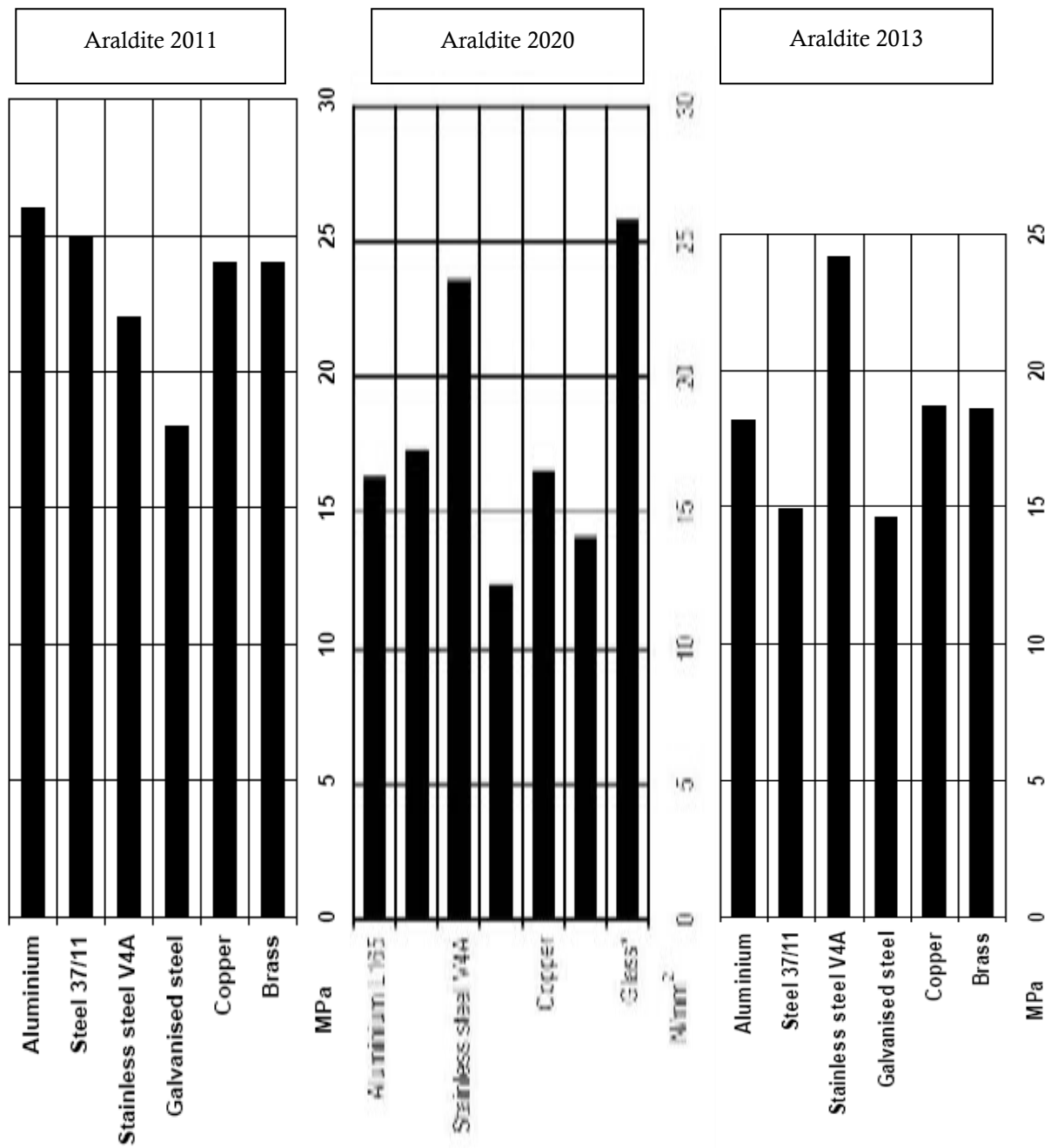


Figure 102

Average lap shear strength of typical single lap joints according to ISO 4587 for Araldite 2011, 2020 and 2013.

Cured for 16 hours at 40°C and tested at 23°C

Pretreatment: Sand Blasting

*Compression lap shear strength

Theory

Adhesive systems

Three adhesive systems are tested in the previous paragraph: Araldite 2013, Araldite 2020 and DELO Rapid 03 Thix.

It was concluded that Huntsman Araldite 2013 and 2020 will be tested further and Rapid 03 Thix did not suffice.

The two remaining adhesives are extended with another promising adhesive: Araldite 2011.

The shear strengths of the adhesives depend greatly on

the material of the substrates. This is visible in *Figure 102*. A summary of specifications of all three adhesives is found in *Table 23*.


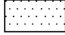

Araldite 2020 is developed specially for use with glass substrates. It has the same breaking index, very good transparency and promising strength. However, this adhesive is suitable for use in layer thicknesses of 0,05 to 0,1 mm.

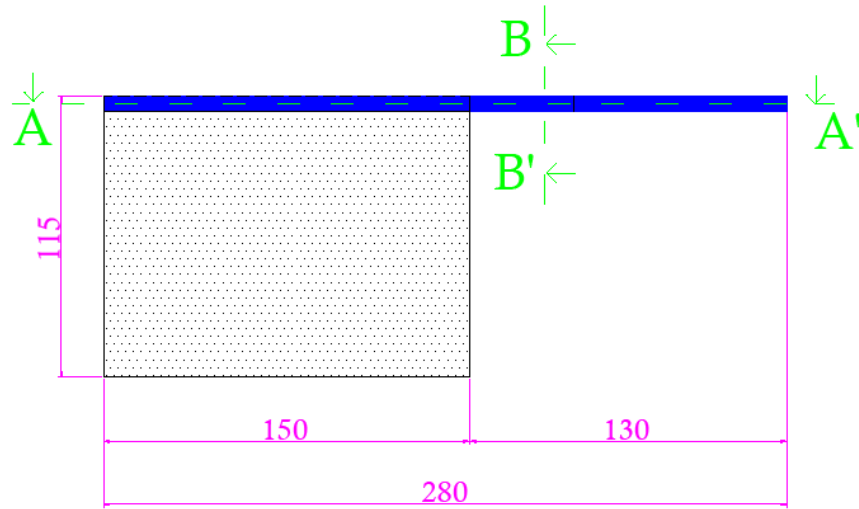
Note that there is no data available for these adhesives concerning characteristics like ductility, elongation at break etc. This will have to be concluded from the tests. Also the adhesion of glass with Araldite 2011 and 2013 is to be seen as well as the adhesion to the carbon fiber reinforcement.

Table 23, Summarized adhesive specifications in comparison to each other

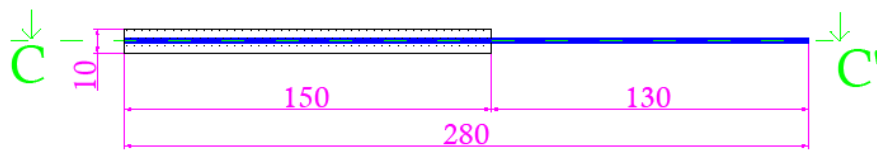
	Araldite 2011	Araldite 2013	Araldite 2020
Short description	Two component epoxy paste adhesive. Multi purpose, low shrinkage, bonds a wide variety of materials, good resistance to dynamic loading.	Two component epoxy paste adhesive. Low shrinkage, bonds a wide variety of materials, good environmental and chemical resistance.	Two component clear epoxy adhesive system especially suitable for glass and ceramics bonding. Refractive index similar to that of glass.
Typical lap shear strength at 23°C (sand blasted aluminium) (N/mm ²)	27,0	18,0	17,0
Typical lap shear strength at 23°C (Glass) (N/mm ²)	N/A	N/A	25,7
Flexibility/toughness	Rigid	Rigid	Rigid
Mix ratio (pbw)	100:100	100:100	100:30
Work Life at 23°C (mins)	120	65	45
Appearance of resin / hardener (mixed)	Yellow / translucent	Grey / beige	Water white
Recommended cure Schedule (°C)	12 hr @ 23°C or 50 min @ 70°C or 10 min @ 100°C	10 hr @ 23°C or 6 min @ 100°C	16 hr @ 40°C of >7 days @ 23°C
Recommended layer thickness (mm)	0,05 – 0,1	0,05 – 0,1	0,05 – 0,1
Suitability for thicker adhesive layer	N/A	Yes, up to 5 mm	No

Measurements in mm
Scale: undefined

-  Adhesive
-  Glass
-  Reinforcement



Cross section CC'



Cross section AA'

Figure 105, Specimen dimensions

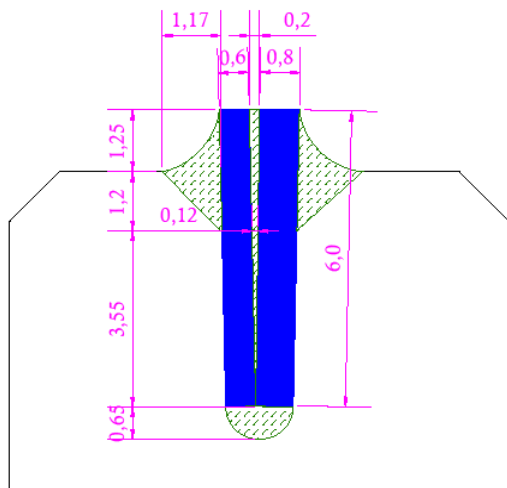


Figure 104, Close-up of Plug-in groove in cross-section BB'

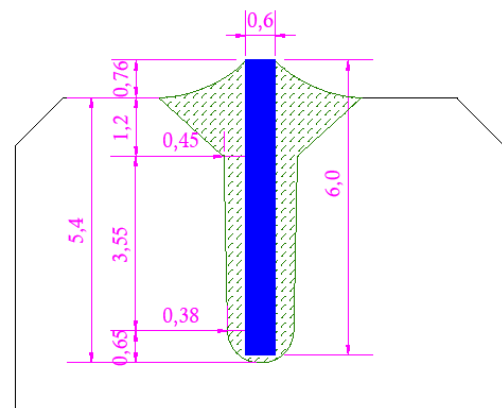


Figure 103, configuration of carbon strip in groove

Method

Displacement controlled tensile tests are done where the glass pane is fixed and the reinforcement is pulled out.

Specimens

The specimens are constructed as 150mm length of the girder with the reinforcement stretching out, like presented in *Figure 105*.

The reinforcement is adhesively bonded in the SGG Plug-in groove. There are two different reinforcement geometries tested (*Figure 104* and *Figure 103*):

Geometry 1: Thick reinforcement, thin adhesive.

Geometry 2: Thin reinforcement, thick adhesive.

With these geometries the 3 different adhesive systems are tested over 4 different lengths; 150mm, 75mm, 40mm and 20mm.

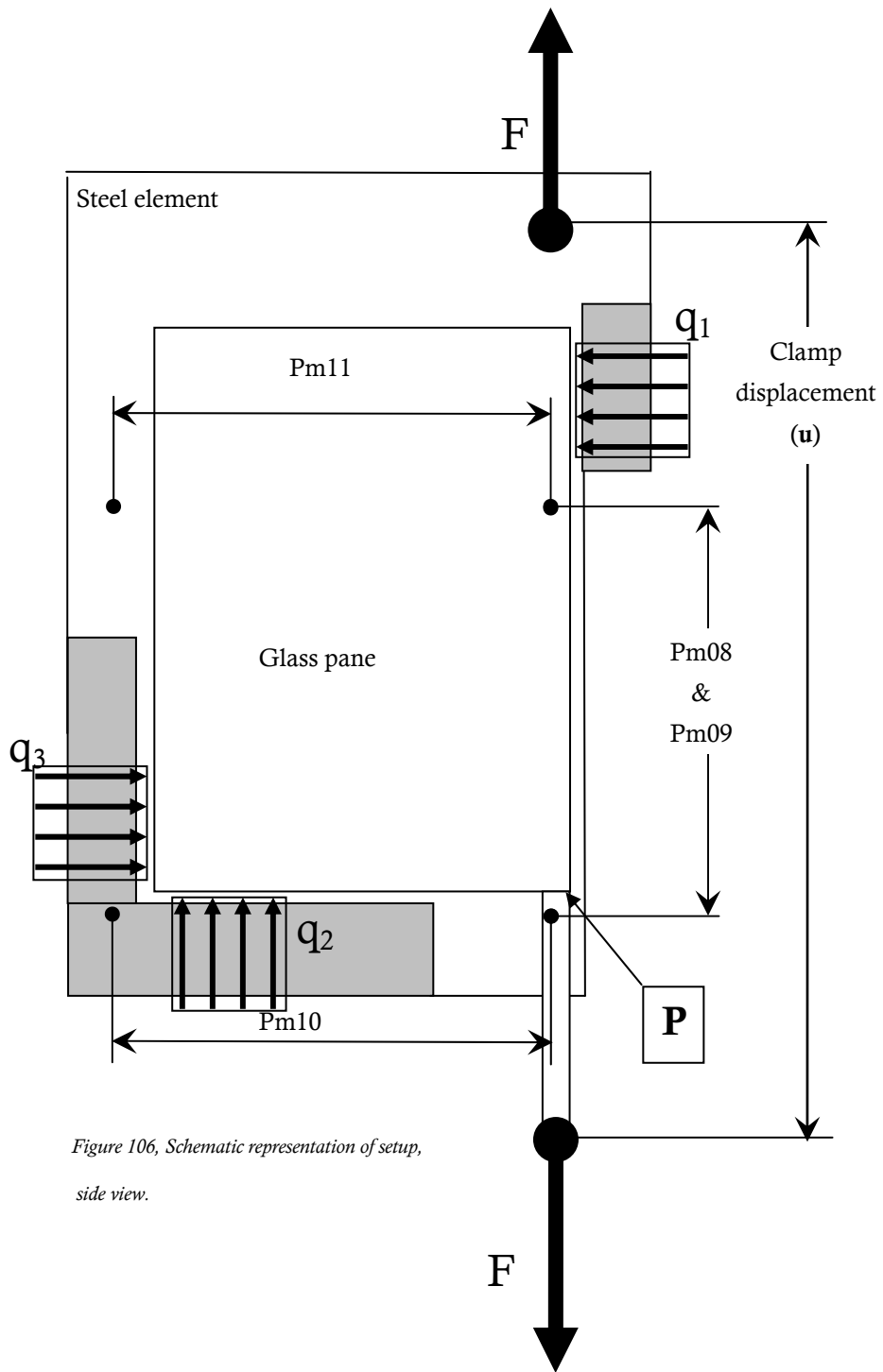


Figure 106, Schematic representation of setup, side view.

Setup

Specimens are tested in a displacement controlled tensile test up to total failure.

The specimen is mounted in a steel support element that is clamped in the upper wedge clamp of the setup. The reinforcement is clamped in the lower wedge clamp. During the test the applied load and clamp displacement are measured.

Point P marks the edge of the glass pane where the adhesive connection between the carbon fiber reinforcement and the glass pane begins. The displacement of this point against the glass pane is measured by sensors Pm08 and Pm09.

Horizontal position of the specimen is monitored by sensors Pm10 and Pm11.

The tensile force applied to the reinforcement is equal to the force delivered by q_2 ($\Sigma F_z=0$). The moment that is created by F and q_2 is equalled by the moment created by q_1 and q_3 ($\Sigma M=0$).



Figure 107, Photograph of test setup.

Table 24, Overview of test results

Specimen			Configuration		Length [mm]	Adhesive	Block material	F _{max} [kN]	Average [kN]	Deviation [kN]
			0,6x6	0,8x6						
A	1	2011_01	x	x	150	2011	perspex	5.27	7.20	1.59
	2	2011_02	x	x	150	2011	perspex	8.70		
	3	2011_03	x	x	150	2011	perspex	5.27		
	4	2011_04	x	x	150	2011	Wood	5.70		
	5	2011_05	x	x	150	2011	Wood	7.50		
	6	2011_36	x	x	150	2011	Wood	7.35		
	7	2011_32	x	x	150	2011	perspex	9.44		
	8	2011_33	x	x	150	2011	perspex	6.68		
	9	2011_34	x	x	150	2011	perspex	8.89		
B	1	2011_07	x		150	2011	Wood	7.90	7.22	0.85
	2	2011_08	x		150	2011	Wood	5.40		
	3	2011_09	x		150	2011	Wood	7.90		
	4	2011_21	x		150	2011	Wood	7.30		
	5	2011_22	x		150	2011	Wood	6.75		
	6	2011_40	x		150	2011	perspex	7.35		
	7	2011_41	x		150	2011	perspex	6.65		
	8	2011_42	x		150	2011	perspex	8.12		
	9	2011_43	x		150	2011	perspex	7.63		
C	1	2011_35	Various		150	2011	perspex	4.27	4.27	-
D	1	2011_10	x	x	75	2011	Wood	5.85	5.33	0.89
	2	2011_11	x	x	75	2011	Wood	4.30		
	3	2011_12	x	x	75	2011	Wood	5.85		
E	1	2011_23	x		75	2011	perspex	5.47	5.53	0.08
	2	2011_24	x		75	2011	Wood	5.59		
F	1	2011_14	x	x	40	2011	Wood	6.14	5.71	0.62
	2	2011_15	x	x	40	2011	Wood	5.27		
G	1	2011_26	x		40	2011	Perspex	4.17	4.24	0.28
	2	2011_27	x		40	2011	Perspex	4.00		
	3	2011_28	x		40	2011	Wood	4.54		

Results

The different geometries are given a letter A to L. A summarized overview of the results of can be found in *Table 24*. Elaborate results of the individual specimens can be found in the appendices.

Table 25, Overview of test results

Specimen			Configuration		Length [mm]	Adhesive	Block material	F _{max} [kN]	Average [kN]	Deviation [kN]
			0,6x6	0,8x6						
H	1	2011_16	x	x	20	2011	Wood	3.22	3.61	0.61
	2	2011_17	x	x	20	2011	Wood	3.51		
	3	2011_18	x	x	20	2011	Wood	3.22		
	4	2011_37	x	x	20	2011	perspex	4.50		
I	1	2011_29	x		20	2011	perspex	4.39	4.07	0.29
	2	2011_30	x		20	2011	perspex	3.99		
	3	2011_31	x		20	2011	perspex	3.83		
J	1	2013_01	x	x	150	2013	Wood	5.85	6.18	0.39
	2	2013_02	x	x	150	2013	Wood	6.14		
	3	2013_03	x	x	150	2013	Wood	6.44		
	4	2013_04	x	x	150	2013	Wood	6.44		
	5	2013_05	x	x	150	2013	Wood	6.44		
	6	2013_10	x	x	150	2013	Wood	5.47		
	7	2013_11	x	x	150	2013	perspex	6.51		
K	1	2020_01	x	x	150	2020	Wood	5.56	6.18	0.84
	2	2020_02	x	x	150	2020	Wood	5.85		
	3	2020_03	x	x	150	2020	Wood	7.14		
L	1	2020_10		x	150	2020	Wood	3.80	3.80	-

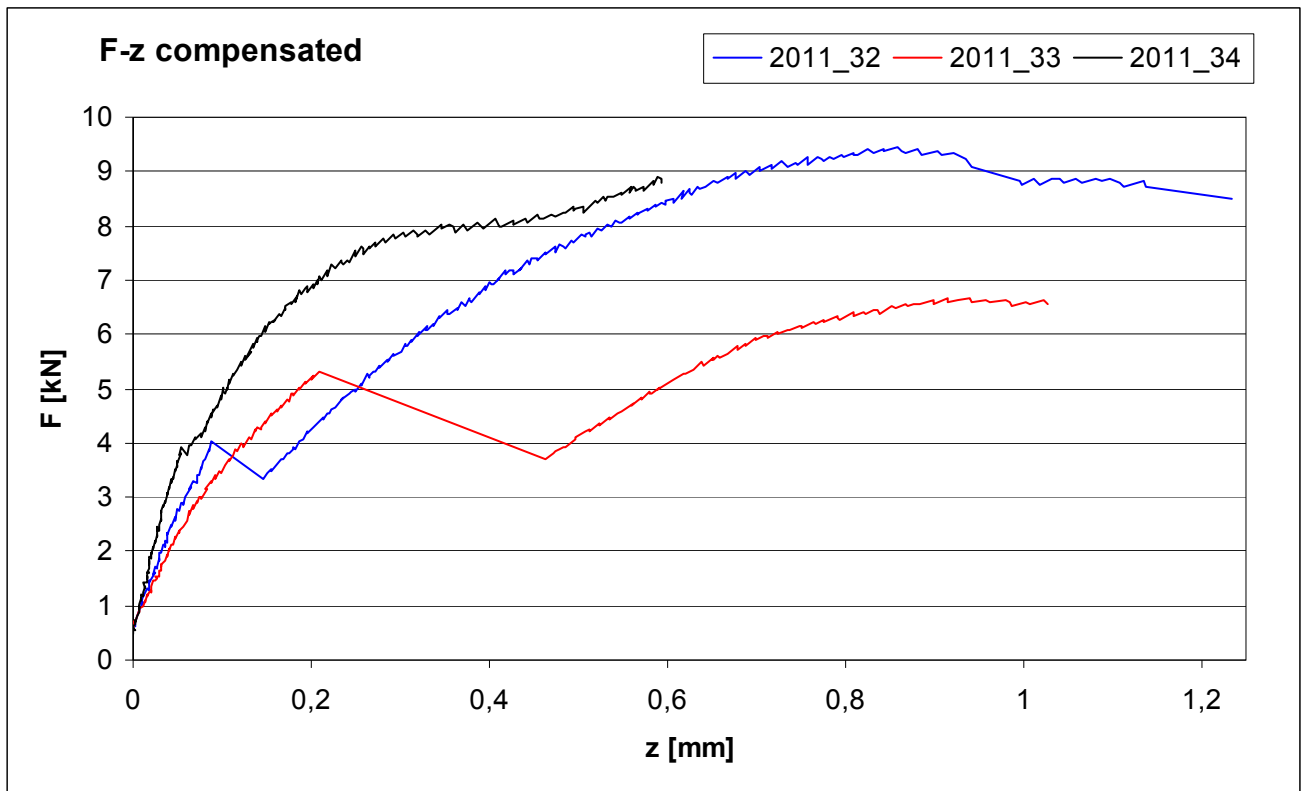


Figure 109, Force-displacement curves for point 'P' of specimens 2011_32 to 2011_34.

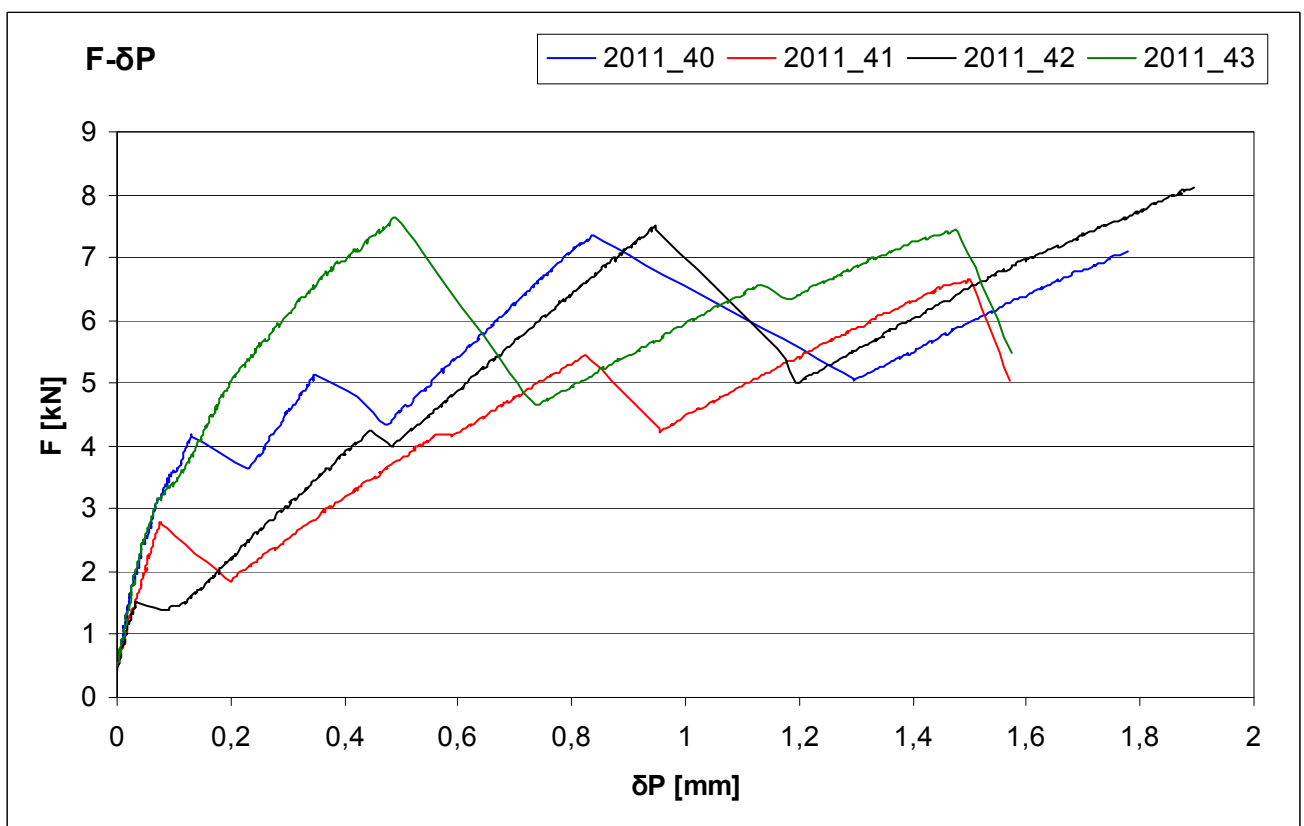


Figure 108, Force-displacement curves for point P for specimens 2011_40 to 2011_43.

Discussion

The setup was changed considerably between sequence 1, 2 and 3. Comparisons between the results have to be made with caution.

Configurations A, B, J and K are discussed individually. Then comparisons are made between the different lengths of the joints.

A: Araldite 2011, config. 1.

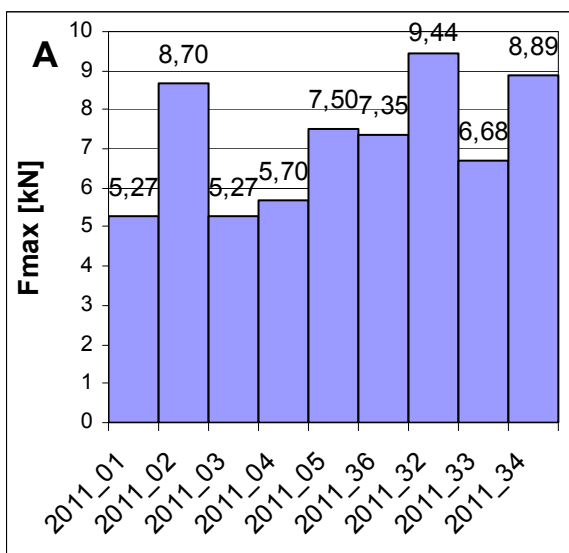


Figure 110, Ultimate strengths of specimens A

Although the highest tensile forces are gained with this configuration, the results are not reliable; the deviation is large. The specimens that were prepared with perspex blocks (32, 33 & 34) have a higher ultimate strength (average 8,34kN) than the other specimens that were not (average 6,63).

The large difference in strength between the specimens could be explained by the potential difference in adhesive thickness. If the two carbon strips are placed firmly against each other, the adhesive thickness in the top of the groove is 0,075mm, which is in the middle of the theoretical optimum of 0,05-0,1mm. If the strips are placed outwards, the adhesive layer is very thin.

By sight the carbon strips of most specimens were equally placed outwards; with a thin adhesive layer to the glass.

B: Araldite 2011, config. 2.

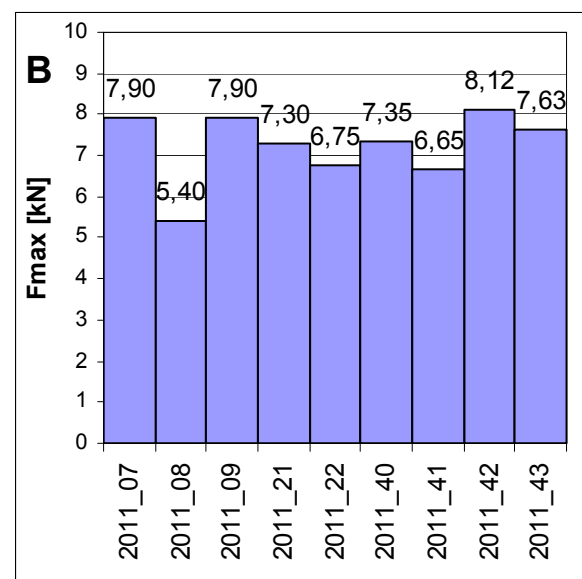


Figure 111, Ultimate strengths of specimens B

A high ultimate strength is combined with acceptable reliability. Especially the last specimens, 40 to 43, give very reliable results.

It does not seem to matter whether the strip is placed exactly straight in the middle of the specimen (#43), or very oblique (#40), or if there is a crack in the glass pane over 40mm (#41&42). *Figure 108* indicates that the ultimate force for all specimens will level out between 7 and 8 kN if the length of the specimen does not limit this.

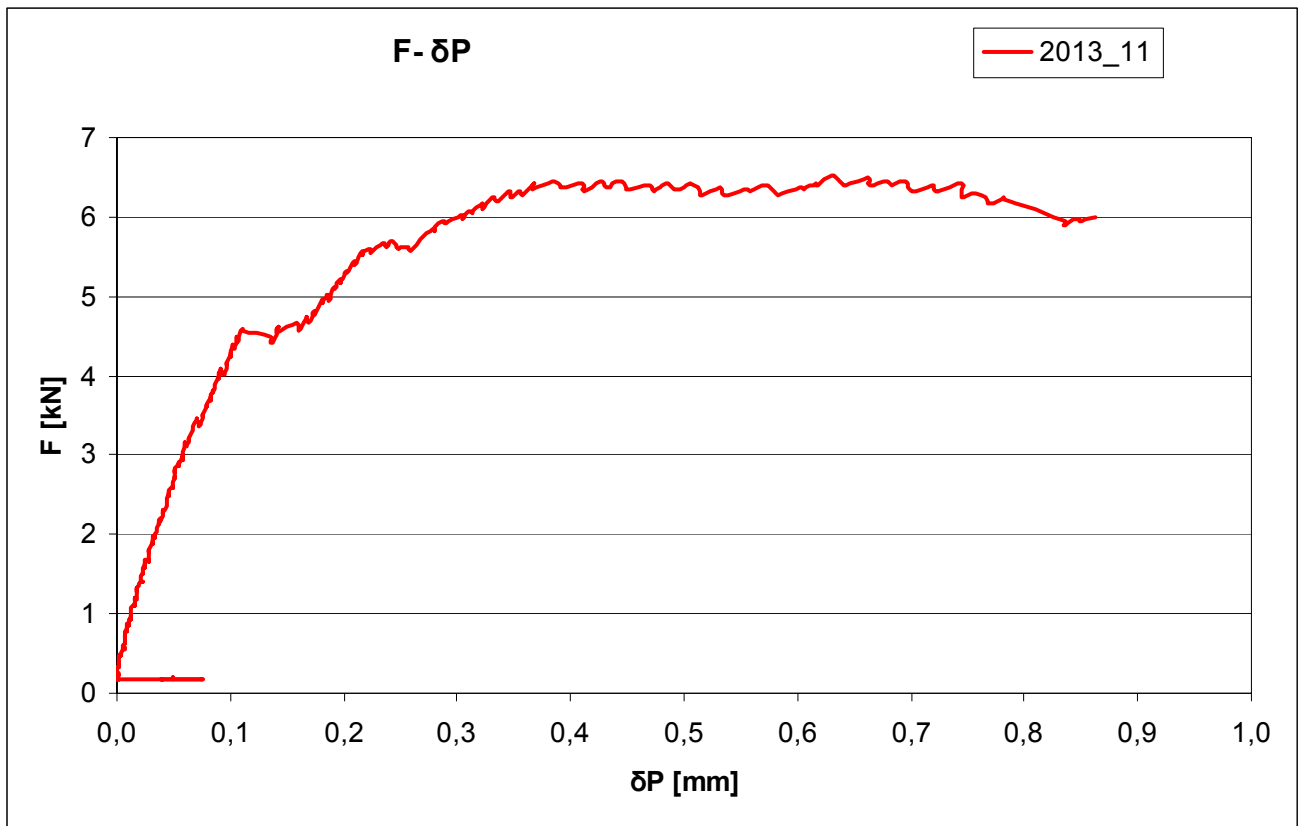


Figure 112, Force-displacement curve for point P of specimen 2013_11.

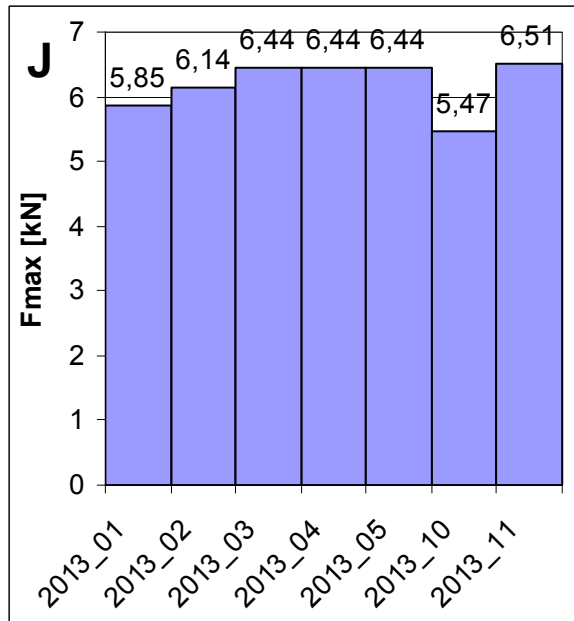
J: Araldite 2013, geom. 1.

Figure 113, Ultimate strengths of specimens J

The ultimate strength of Araldite 2013 seems to be lower than Araldite 2011, but much more reliable.

It is remarkable that all specimens fail due to glass failure, not to adhesive failure. The adhesive seems to be stronger than the glass.

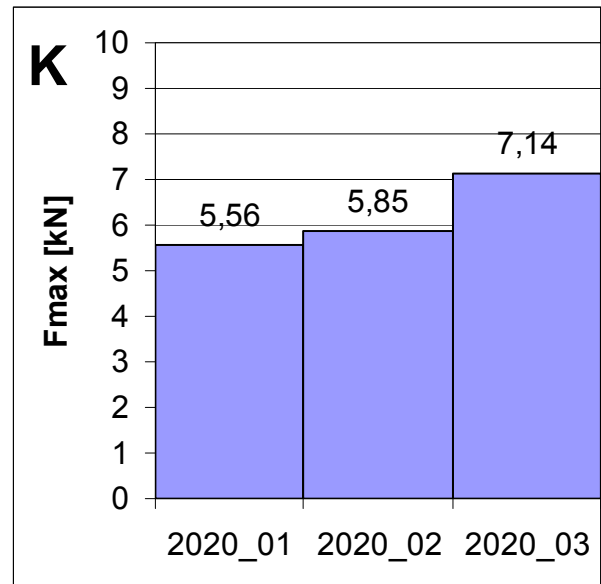
K: Araldite 2020, geom. 2.

Figure 114, Ultimate strengths of specimens K

The adhesive fails before the glass does. This is remarkable considering the theoretical shear strength which is higher than that of Araldite 2011 and 2013.

The structural capacity of Araldite 2020 is not high enough for use in the intended glass girder.

Thick strip, thin adhesive

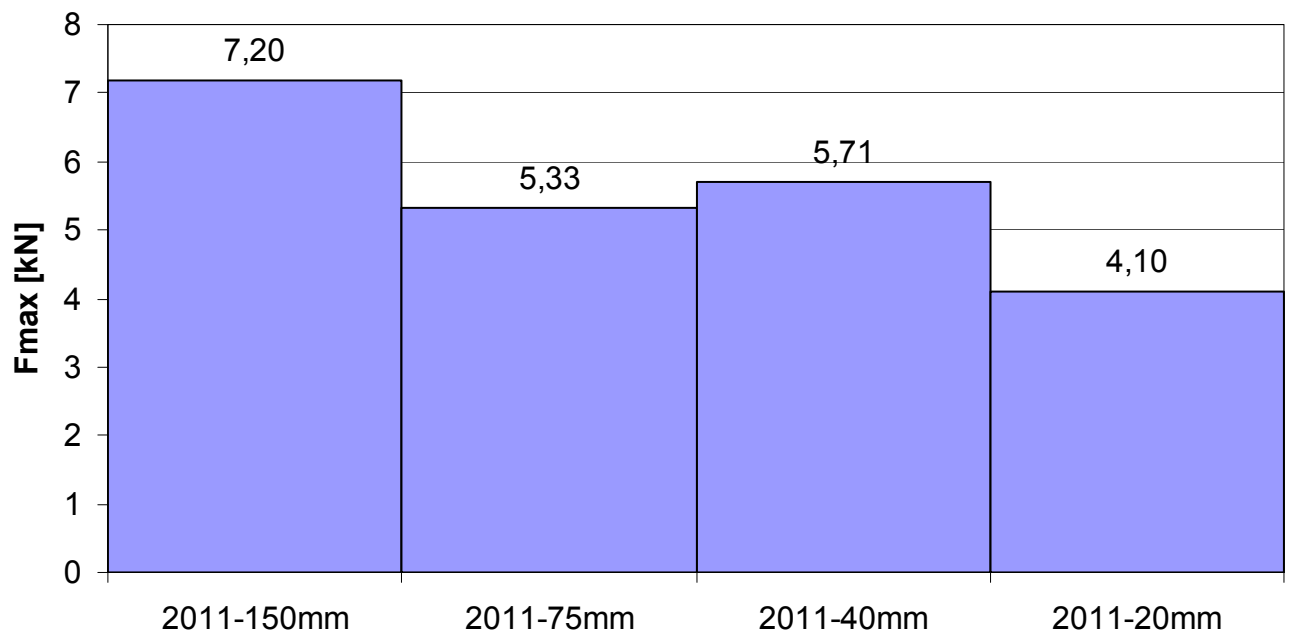


Figure 116, Ultimate strengths of specimens with different anchor lengths compared.

Thin strip, thick adhesive

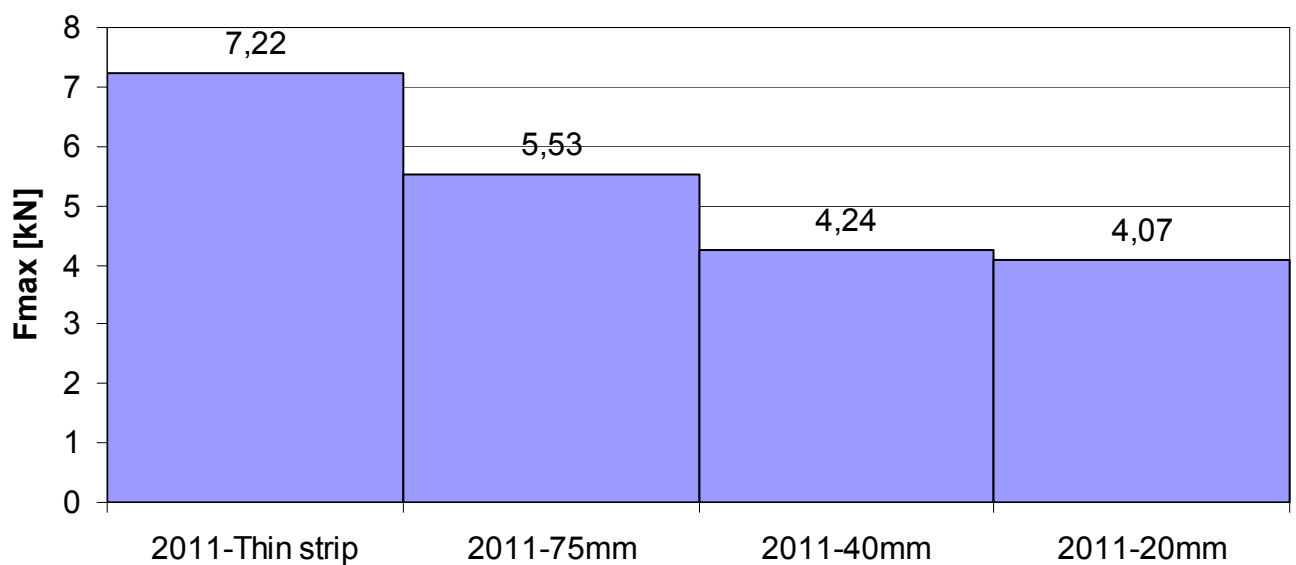


Figure 115, Ultimate strengths of specimens with different anchor lengths compared

Anchor length

The hypothesis was the following: A thin adhesive layer is strong and stiff and transfers the shear force over a small part of the joint at high stress. A thicker adhesive layer is less strong but more ductile and transfers the shear force over a larger part of the joint at low stress.

This is not endorsed by comparisons presented in *Figure 116* and *Figure 115*. The reason could be that the biggest difference in the shear stress peak is found in the first 20mm of the connection. This was not tested.

Overall

The first sign of failure of the adhesive connection for Araldite 2011 and 2020 is that the color of the adhesive turns into white. This is a sign of the arising of microscopic hair cracks in the texture of the adhesive known as “brittling” [31]. The same mechanism is observed in Araldite 2013 although there it is less obvious because the adhesive is not transparent. At the moment of brittling the adhesive is loaded to its maximum capacity. The strength of the adhesive degrades fast if the deformation then increases further. How much is not specified in the available literature.

Compare the failure behavior of specimens 2011_07 and 2011_09 to the failure behavior of 2011_08. The specimens are of similar configuration, but they have a difference of 32% in measured strength.

Strong specimens failed due to adhesive failure. Specimens with identical configuration but low strength failed due to progressive glass fracturing.

Specimens 2011_02, 2011_32 and 2011_34 reached the highest tensile force. They failed primarily due to

adhesive failure and eventually due to fracturing of the glass.

This implies that the strength of the glass is governing in the failure behavior of the specimens and the maximum shear strength of the adhesive has not been reached completely for each specimen.

Tests to obtain more information about the exact mechanism of the glass failure are recommended.

Conclusions

9,4kN is the highest force reached with a configuration of thick carbon fiber and thin adhesive. Therefore it is concluded that Araldite 2011 applied with a thin adhesive layer gains the highest shear strength, but it is not the most reliable.

7,2kN is the highest average force with a configuration of thin carbon fiber and thick adhesive. Araldite 2011 applied with a thicker adhesive layer gains high strength and is more reliable.

Araldite 2013 applied with a thin adhesive layer gains acceptable strength with high reliability.

Araldite 2020 applied with a thin adhesive layer gains moderate strength with poor reliability.

Most of the shear force is transferred in the first 20mm of the connection.

The strength of the glass pane has been governing in most of the tests. The shear strength of the adhesive connection has not been reached.

Recommendations

Two options are recommended to test as reinforcing method in a structural glass girder with the SGG Plug-in groove:

1. **Adhesive:** Huntsman Araldite 2011.

Geometry: 0,6x6mm carbon fiber in the middle of the groove.

2. **Adhesive:** Huntsman Araldite 2011.

Configuration: 0,6x6mm+0,8x6mm carbon fiber.

It is recommended to test 3 specimens of both options in a girder of 10mm wide and 70mm high.

The best functioning option can be tested for a higher girder of 90mm.

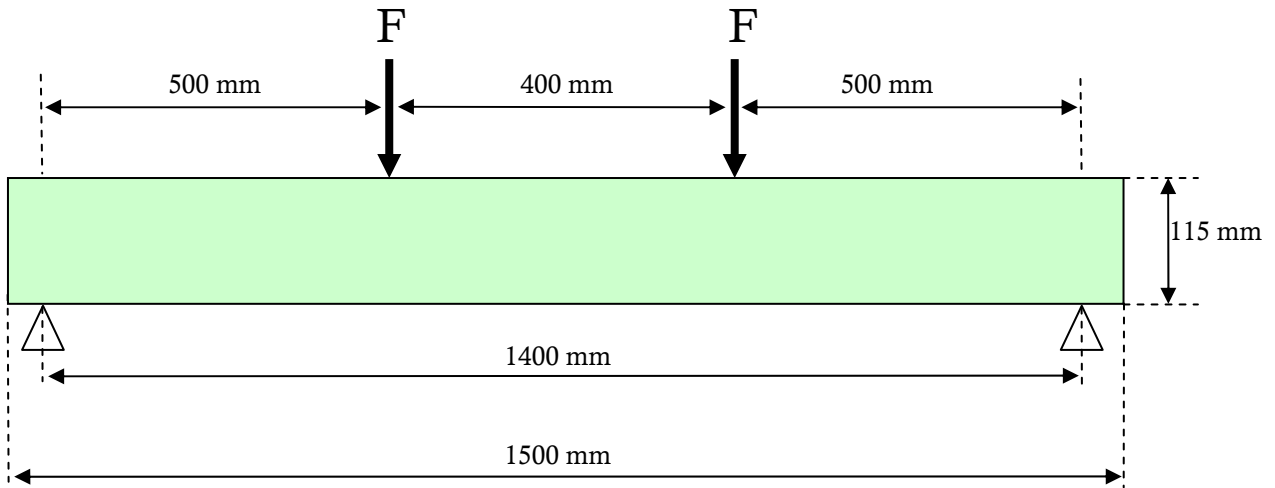


Figure 117, Schematical representation of test setup with dimensions. Girder in light green.

Table 26, Dimensions of specimen 1, 2 and 3

Specimen #	Adhesive	Reinforcement			Results	
		Measurement	Cross-section [mm ²]		σ_{max} [N/mm ²]	
1	DELO Rapid 03 Thix	2 Ø 2,0 mm	6,3		56,8	
2	DELO Rapid 03 Thix	2x 3x0,8 + 1x 6x0,8 mm	9,6		57,7	
3	Araldite 2013	2x 3x0,8 + 2x 3x0,13 mm	5,6		30,8	
Girder						
	Float glass	1500	12	115	mm	

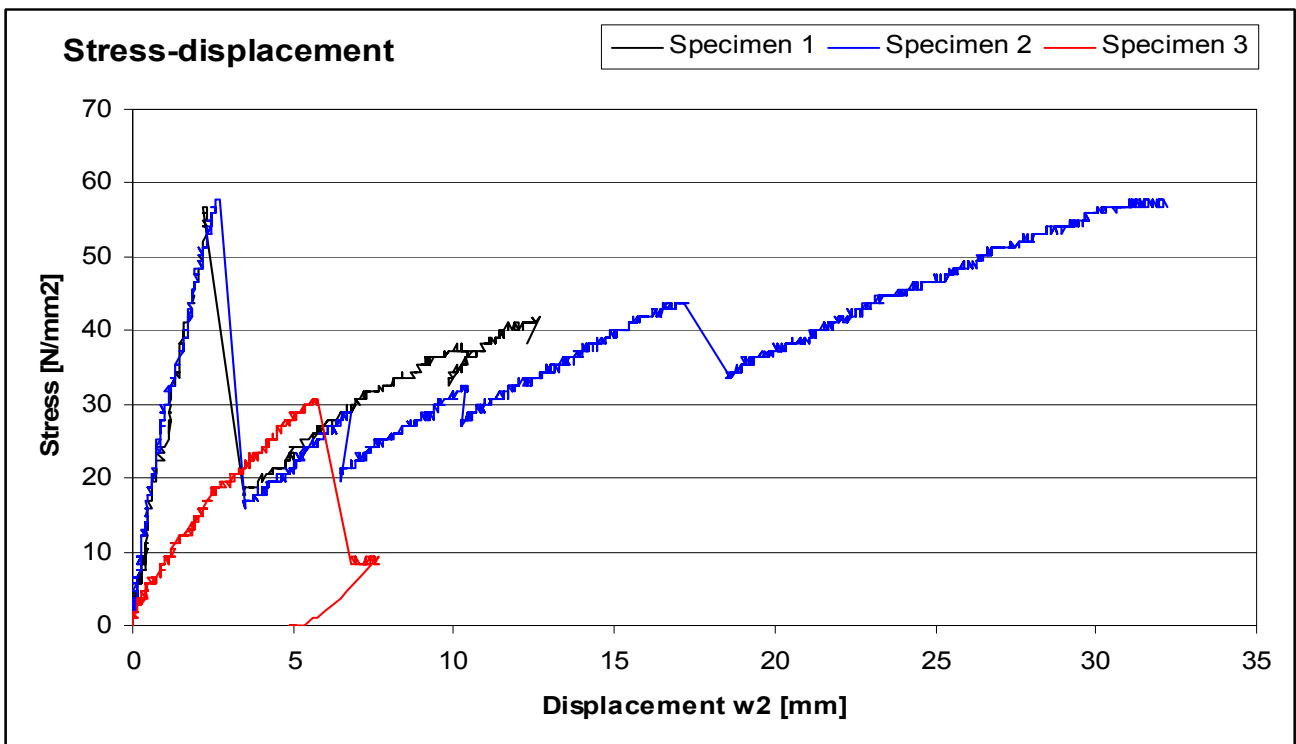


Figure 118, Stress-displacement curve for specimens 1, 2 and 3

5.5 Preliminary beam tests

Abstract

Three beam specimens are tested in a four point bending test up to total failure to validate the strength and failure behavior.

All specimens show linear elastic behavior up to initial failure, then a fallback in applied force and a reduction in bending stiffness occur. The first test was aborted due to sliding of the supports. The second test was successfully performed up to total failure. The third specimen was damaged prior to the test due to a mechanical failure of the test device. These results are discarded.

The adhesive bonding of reinforcing elements in the SGG Clip-in groove is possible, practical and with certain modification desirable. The test setup was slightly modified from its original configuration and functioning as desired. The practical tensile bending strength of the tested girders is comparable to that of girders with polished edges without the SGG clip-in groove as tested by Louter in 2005. Therefore it is likely that the cutting of the SGG Clip-in groove does not have a negative effect on the practical tensile bending strength of the glass. A great fallback in stiffness was observed after initial failure. This is probably the result of a lack of stiffness of the adhesive layer.

Introduction

Three glass girders as described in the recommendations from chapter 2 are tested in a displacement-controlled four-point bending test up to total failure.

The goal of these three exploring tests is to gain experience in laboratory testing and to find answers to the following questions:

- 1- Is bonding reinforcement to glass in the SGG clip-in groove possible, doable and desirable?
- 2- Does the test setup work in practice as it is designed in theory?
- 3- Does the cutting of the groove have a large negative effect on the practical tensile bending strength of the glass pane?

Method

The top of the girder is supported to prevent torsional buckling.

The middle part of the beam is pressed down by two hinged supports with a constant displacement and the force is measured. The vertical displacement of the center of the girder is measured.

From these data a force-displacement and stress-displacement diagram can be derived.

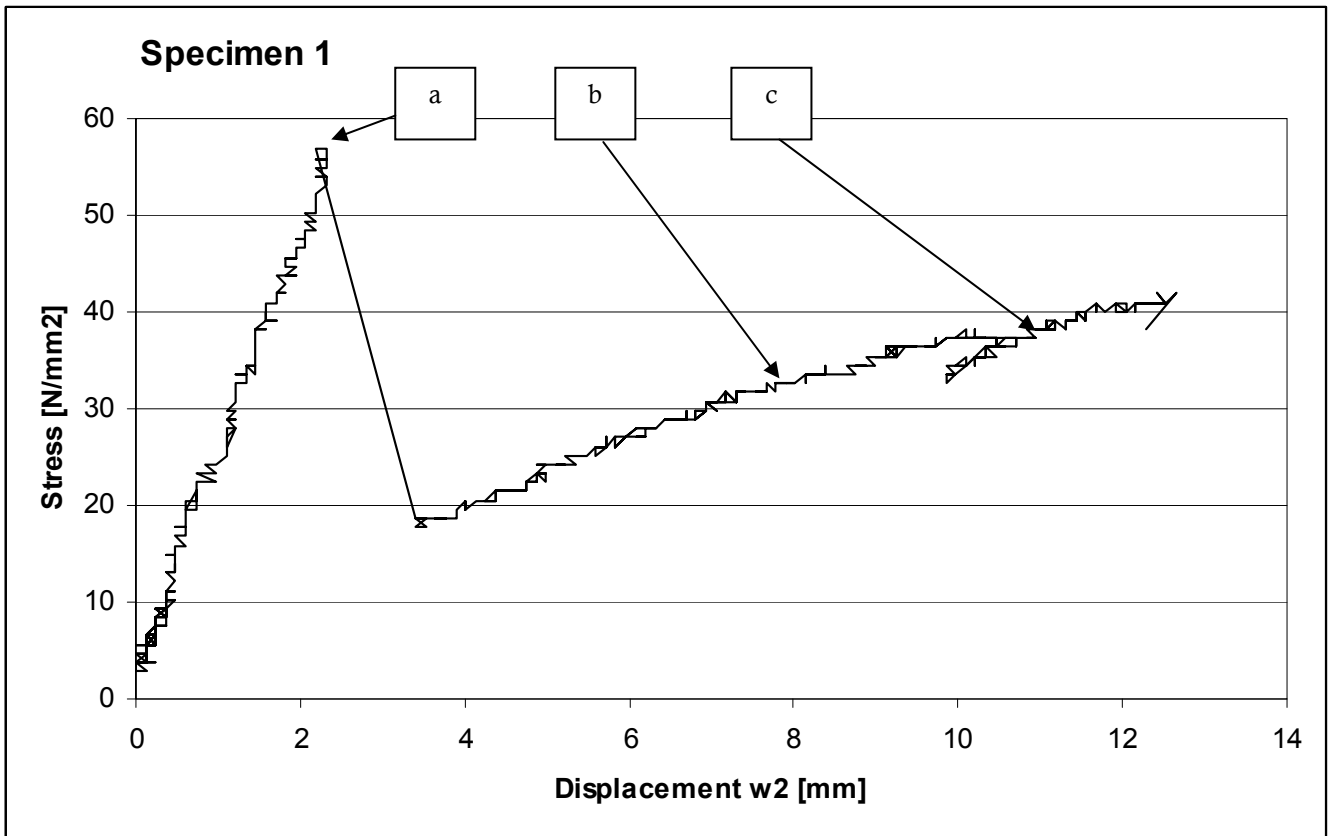


Figure 119, Stress-displacement curve for specimen 1. a, b and c refer to Figure 120.

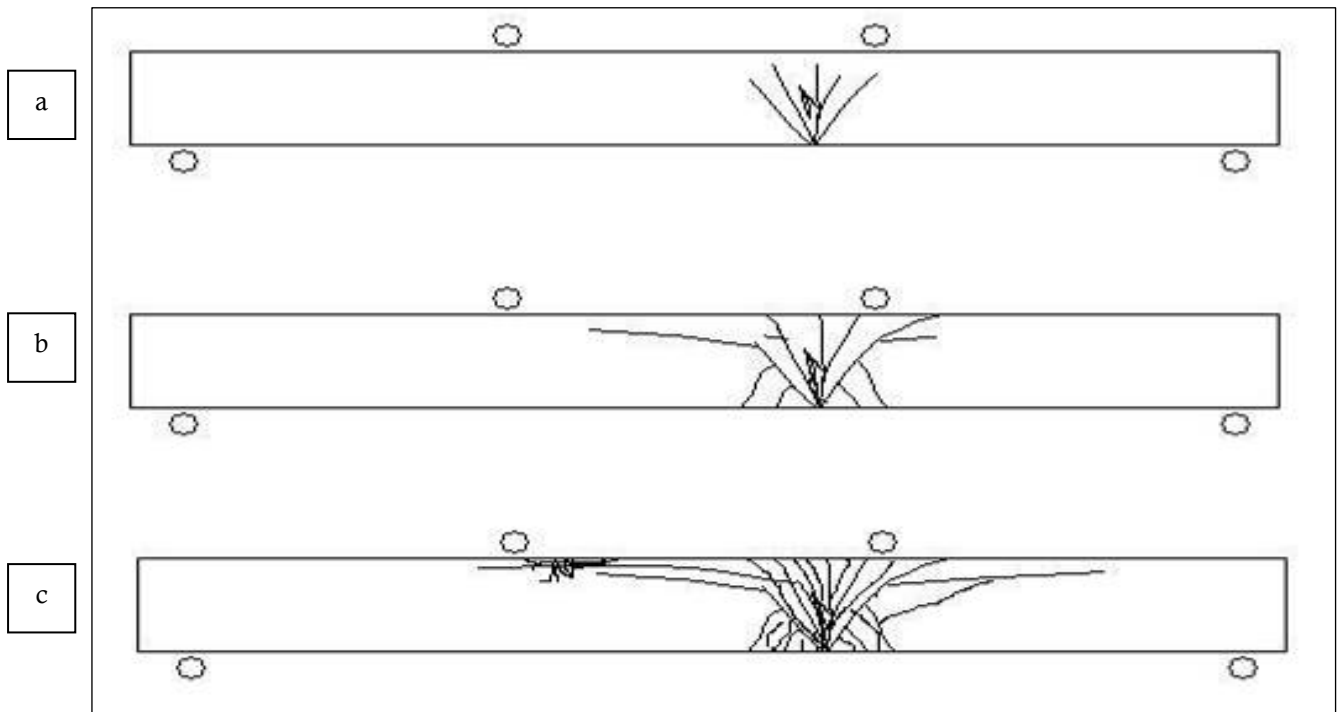


Figure 120 a/c, Schematic representation of crack growth at different stages of test 1.

Specimen 1

Dimensions

Reinforcement:

2x Ø2 mm Carbon Fiber (see *Figure 121*)

Total area of cross section reinforcement:

6,28 mm²

Adhesive:

DELO Rapid 03 Thix

Results

The beam showed a linear elastic behavior up to initial failure (point a). This occurred at a tensile bending stress of 56,8 N/mm² at the bottom of the beam.

A large fallback in force is noticed and a regression in stiffness after the crack has occurred.

Small glass fractures arised as force increased until the hinged support started sliding away from its position and the test was aborted.

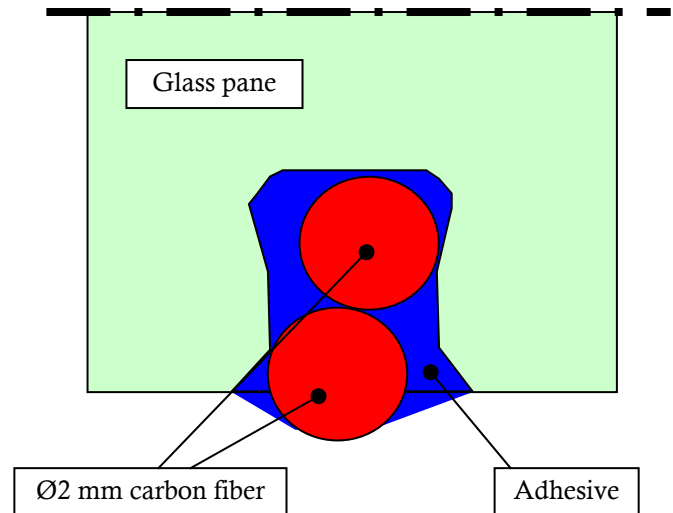


Figure 121, Close-up of bottom of girder cross-section with reinforcement geometry for specimen 1.

Light green: Glass pane.

Blue: Adhesive.

Red: Reinforcement

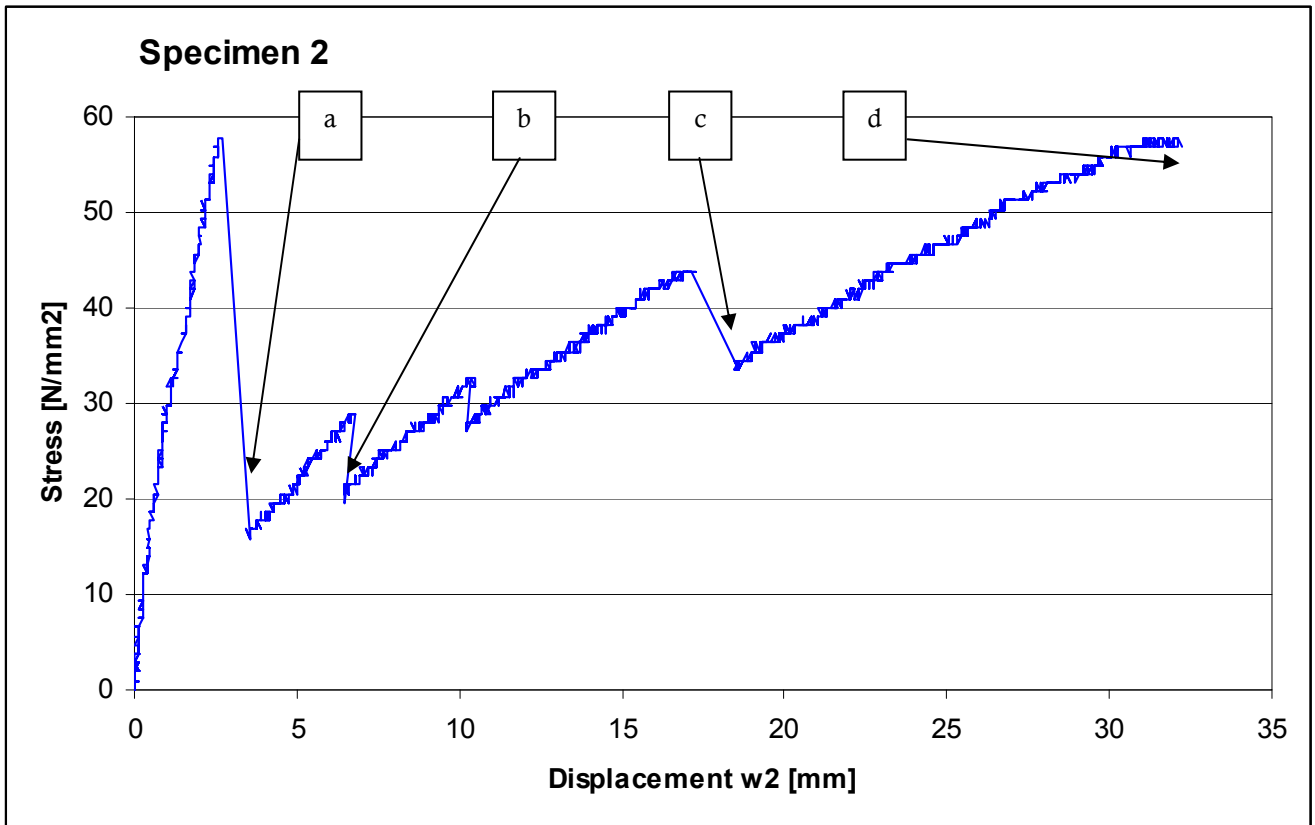


Figure 123, Stress-displacement curve for specimen 2. Letters refer to Figure 122.

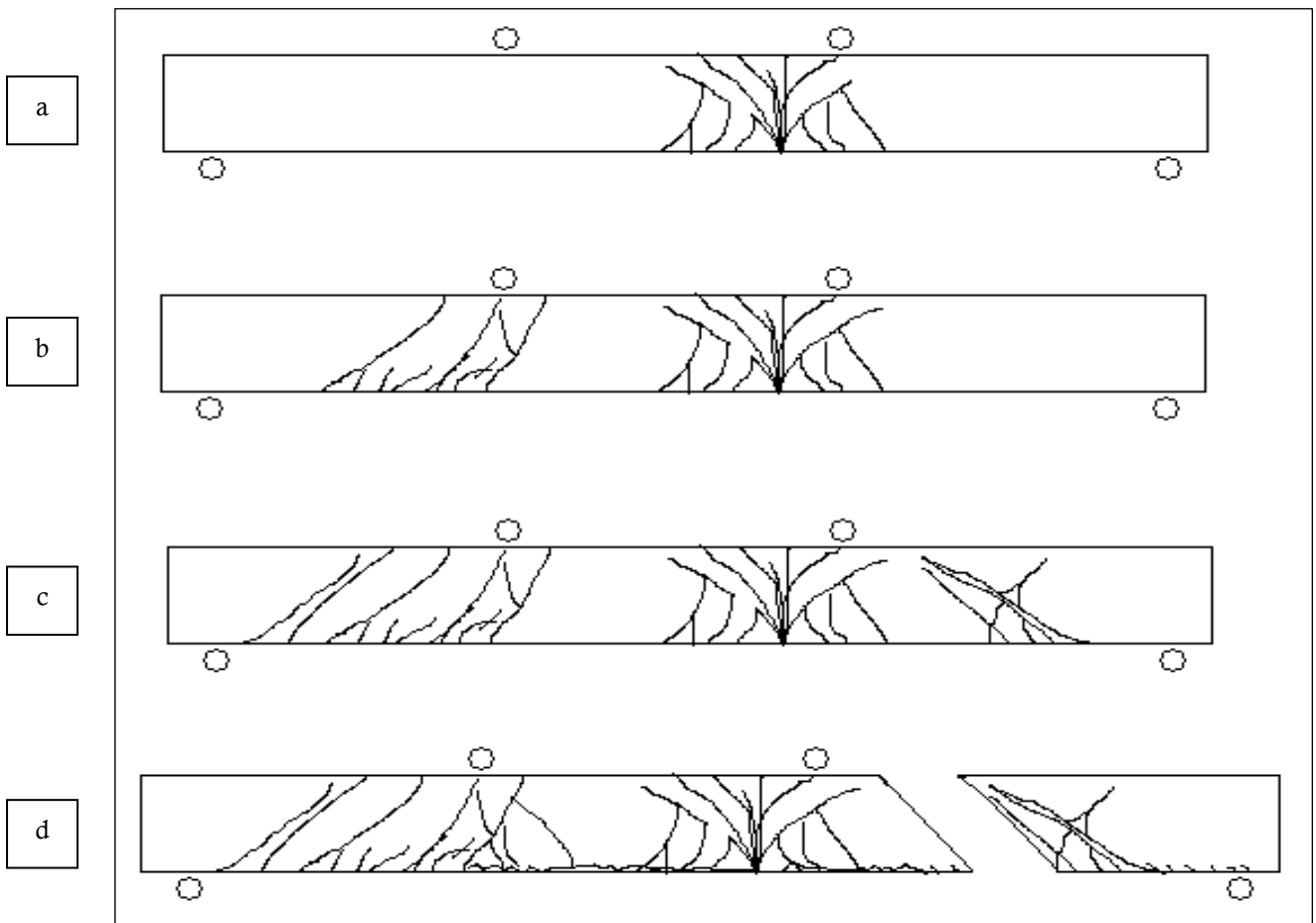


Figure 122, Schematic representation of crack pattern during several stages of test 2.

Specimen 2

Dimensions

Reinforcement:

2x 3x0,8 mm Carbon Fiber

1x 6x0,8 mm Carbon Fiber

Total area of reinforcement cross section:

9,6 mm²

Adhesive:

DELO Rapid 03 Thix

Curing time before testing:

29 hours

The upper support flange is slightly adjusted to prevent the sliding of the supports. See *Figure 125*.

Results

The beam performs linear up to initial failure at point 'a'. Then a large fall-back in applied force and bending stiffness occurred. This is increased with every small crack that occurs at point 'b' and 'c' until total failure due to shear force at point 'd'.

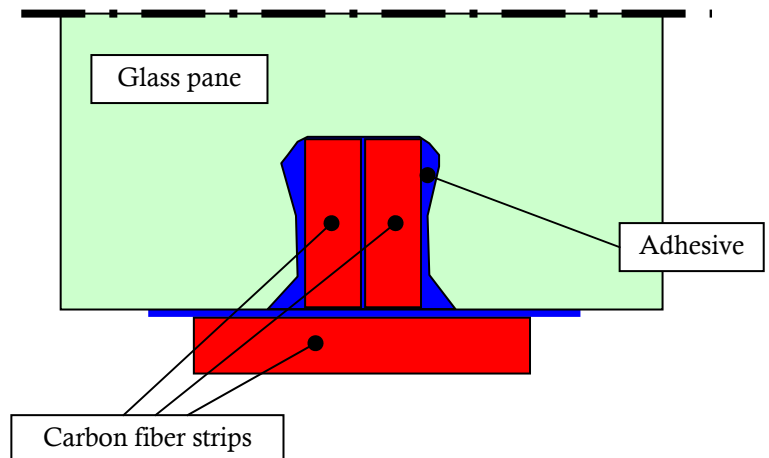


Figure 124, Close-up of bottom of girder cross-section with reinforcement geometry for specimen 2.

Light green: Glass pane.

Blue: Adhesive.

Red: Reinforcement



Figure 125, Altered upper support flange.

Specimen 3

Dimensions

Reinforcement:

2x 3x0,8 mm Carbon Fiber

2x 3x0,13 mm Carbon Fiber

Total area of reinforcement cross section:

5,58 mm²

Adhesive:

Huntsman Araldite 2013

Curing time before testing:

3 days

Results

The specimen was damaged due to a failure of the testing machine. One crack occurred at 150mm from the center of the beam at unknown force.

Further results are discarded.

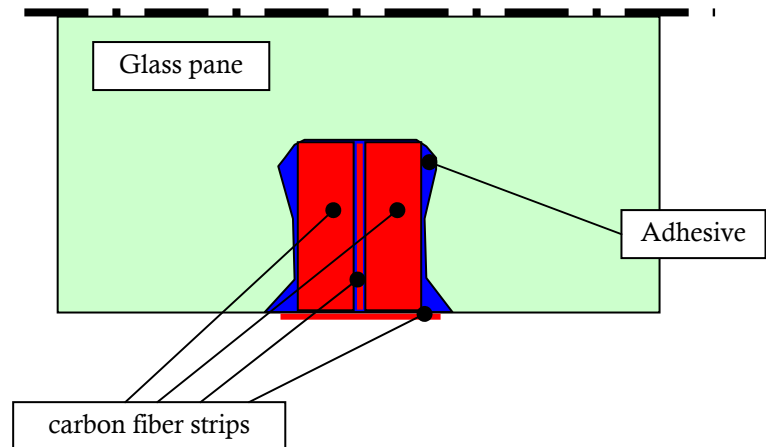


Figure 126, Close-up of bottom of girder cross-section with reinforcement geometry for specimen 2.

Light green: Glass pane.

Blue: Adhesive.

Red: Reinforcement

Discussion

Initial failure for specimen 1 and 2 occurred when the tensile bending stress in the bottom fiber of the girder has reached approximately 57 N/mm^2 . This is comparable to previous tests with glass girders of the same dimensions without a groove milled in the bottom [12]. This implies that the cutting of the SGG Clip-in groove does not have a large negative effect on the practical tensile bending strength of this glass girder. Perhaps it is even more predictable. This will have to be validated by further tests.

In all three specimens the first crack occurs approximately 150mm from the middle of the beam. This could either be a coincidence or it could be explained by a local stress peak that occurred in all three tests.

Possible explanation could be that a local stress peak arises due to the introduction of the compressive forces of the upper support:

Where these forces result in compressive stress in a certain direction, tensile stress arises perpendicular to that direction. These tensile stresses have to be summated with the tensile stress due to the bending moment. This results in local tensile stress peaks in the bottom of the beam.

This way the total tensile stress in the bottom of the beam is not constant, but a sum of the tensile stress due to the bending moment (which is constant over the middle part of the beam) and a local tensile stress peak due to the introduction of the support forces.

The magnitude of the stress peak was considered marginal compared to the bending stress. In previous tests with glass girders with polished edges, microscopic cracks in the surface of the bottom of the girder are of much more influence to the location of the first crack than the additional stress due to this stress peak. It

could be that the milling of the SGG Clip-in groove has caused a constant damaging of the girder. Due to this, the glass tends to break where the tensile stress in the bottom of the girder is the highest. Therefore the local stress peak has become influential in the failure of the beam.

Table 27, Recommended configurations for further tests

Specimens of 150x150x10 mm with rectangular, 2x6mm groove					
# specimens	Reinforcement:			Adhesive	
	Material	Shape and size of reinforcement:	Area [mm ²]	System	Layer thickness
3	Stainless steel	3-Ø2,0 mm	9,42	DELO Rapid 03 Thix	Variable
3	Stainless steel	3-Ø2,0 mm	9,42	Araldite 2013	Variable
3	Carbon Fiber rod	3-Ø2,0 mm	9,42	DELO Rapid 03 Thix	Variable
3	Carbon Fiber rod	3-Ø2,0 mm	9,42	Araldite 2013	Variable
3	Glass Fiber rod	3-Ø2,0 mm	9,42	DELO Rapid 03 Thix	Variable
3	Glass Fiber rod	3-Ø2,0 mm	9,42	Araldite 2013	Variable
3	Carbon Fiber rod	2x 6,0x0,8 mm	9,60	DELO Rapid 03 Thix	0,1-0,3 mm
3	Carbon Fiber rod	2x 6,0x0,8 mm	9,60	Araldite 2013	0,1-0,3 mm

Conclusions

Bonding the reinforcement in the groove

The bonding of reinforcing elements in a groove like the SGG Clip-in groove is possible. The shape of the standard SGG clip-in groove however is not advisable for this purpose. The shape makes it difficult to create a constant thin layer of adhesive which is advised for a controlled and high-strength bonding between the glass and the reinforcement.

The ideal shape would be rectangular.

The ruggedness of the surface is also an important factor. A rough surface is better for the adhesive bond since this increases the bonding area. A too rough surface probably results in loss of tensile bending strength of the glass beam.

Setup configuration

The setup in its final form is suitable for the intended testing procedure.

Influence on practical tensile bending strength of cutting of SGG Clip-in groove.

The measured tensile bending strength of the glass with the SGG Clip-in groove is around 55 N/mm^2 . This is comparable to that of a glass girder with polished edge and no groove.

From the results of these tests there is no reason to assume that the SGG clip-in groove has a negative effect on the tensile bending strength of the glass girder.

Recommendations

Further study has to be done into the local tensile stress peak under the supports, approximately 150- 200 mm from the center of the beam. An answer has to be found to the question whether it has been a coincidence that the girders cracked at the same place, or that there is another explanation

Further testing has to be done to investigate the strength and stiffness of the used adhesives in this application. The strength and stiffness of the adhesive layer as a function of the layer thickness, the sort of adhesive and the used reinforcing element have to be investigated.

The following is advised:

Basic pull-out tests of adhesively bonded reinforcement in groove. The sort of adhesive and the shape and material of the reinforcement must be varied.

The proposed configurations are given in **Table 27**.

6. Beam tests

6.1 Introduction

The tests described in chapter 3.4 give an insight in the maximum shear force that can be transferred from the glass to the reinforcement. This is an important factor for the determination of the size of the girder.

At the moment of initial failure the reinforcement takes over the tensile bending stress from the glass. The larger this load can become, the larger the moment of inertia of the girder cross-section and therefore the size of the girder can be.

The first paragraph of this chapter describes a review of the strongest geometries from chapter 3.4 and the consequences for girder shape and size. Interesting factors in this review are strength and stiffness of the connection. This has a large effect on the depth, width and height of the crack and therefore size and curvature of the compressed zone of the girder in the ultimate limit state.

Paragraph 4.1 is concluded by a proposal for two different reinforcement geometries:

Thin carbon fiber strip with a thick adhesive layer.

Thick carbon fiber strip with a thin adhesive layer.

Geometry 1 is characterized by a relatively less stiff connection between the reinforcement and the glass. In theory this would allow a large crack width, causing a large deflection of the girder and ductile behavior.

Geometry 2 is characterized by a stiffer connection. Theoretically this would mean a smaller crack width, a smaller deflection and thus a less ductile behavior. On the other hand the connection would be a bit stronger, allowing a higher bending moment before total collapse occurs.

This hypothesis is validated in paragraph 4.2 by testing 3 specimens of both geometries. The specimens are tested for their failure behavior in a girder with a

relatively small cross-section in a displacement controlled four point bending test.

The tests are done to obtain answers to several questions: Which geometry will ensure the best, most ductile failure behavior? Do the in paragraph 3.4 obtained maximum values, concerning introduction of tensile force in the reinforcement by the glass pane, correspond to values that can be concluded from these tests?

In the preliminary beam tests described in paragraph 3.3 collapse due to shear force was governing above collapse due to bending moment. Will this remain the governing failure mode for these smaller girders?

If collapse due to bending moment will become governing, will the girder collapse due to failure of the compressive zone in the glass, breakage of the reinforcement itself or failure of the connection of the reinforcement to the glass?

With answers to these questions, the most suitable geometry is chosen for use in a girder with a larger cross-section. This will also be tested for 3 specimens.

With the data from these tests an insight can be obtained about the governing factors in the structural behavior of the girder with which optimizations in the dimensioning can be made.

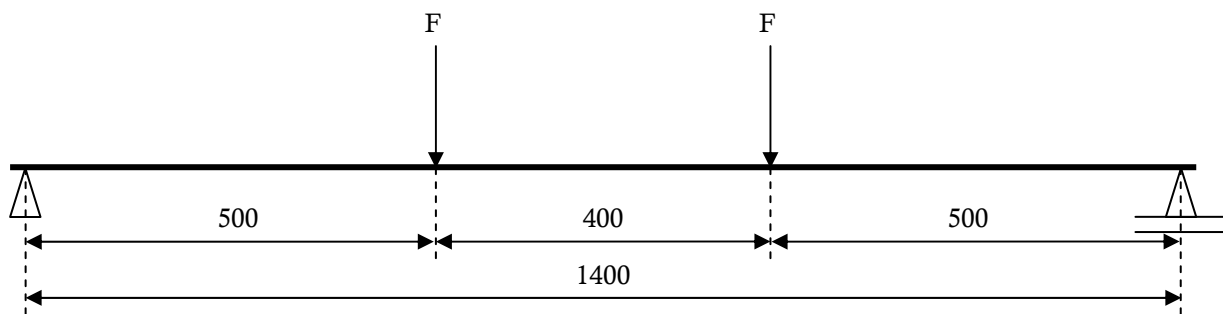


Figure 128, Mechanical scheme of test setup, side view.

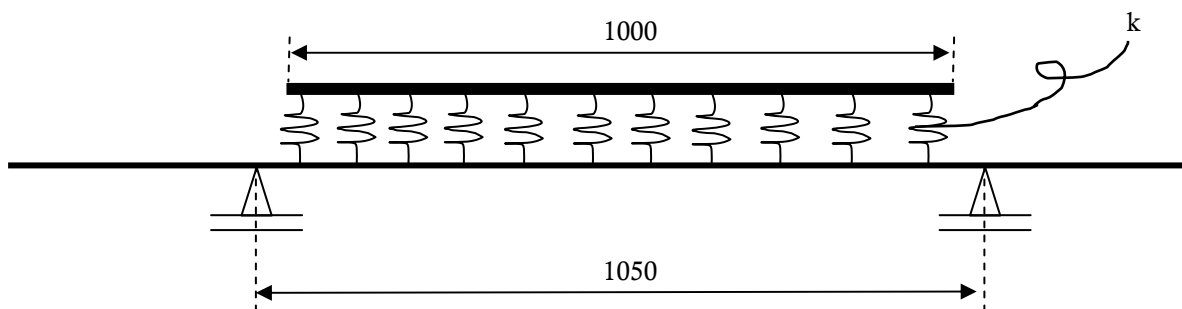


Figure 127, Mechanical scheme of test setup, top view.

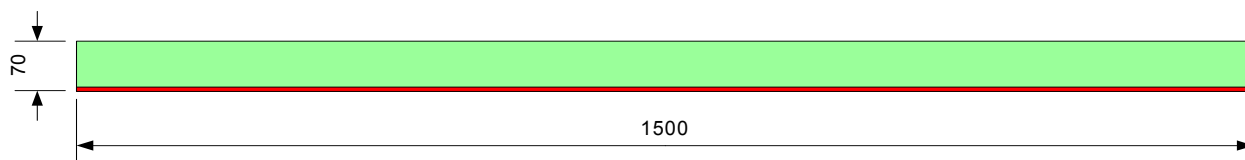


Figure 130, Girder, side view.

Glass in green, reinforcement in red.

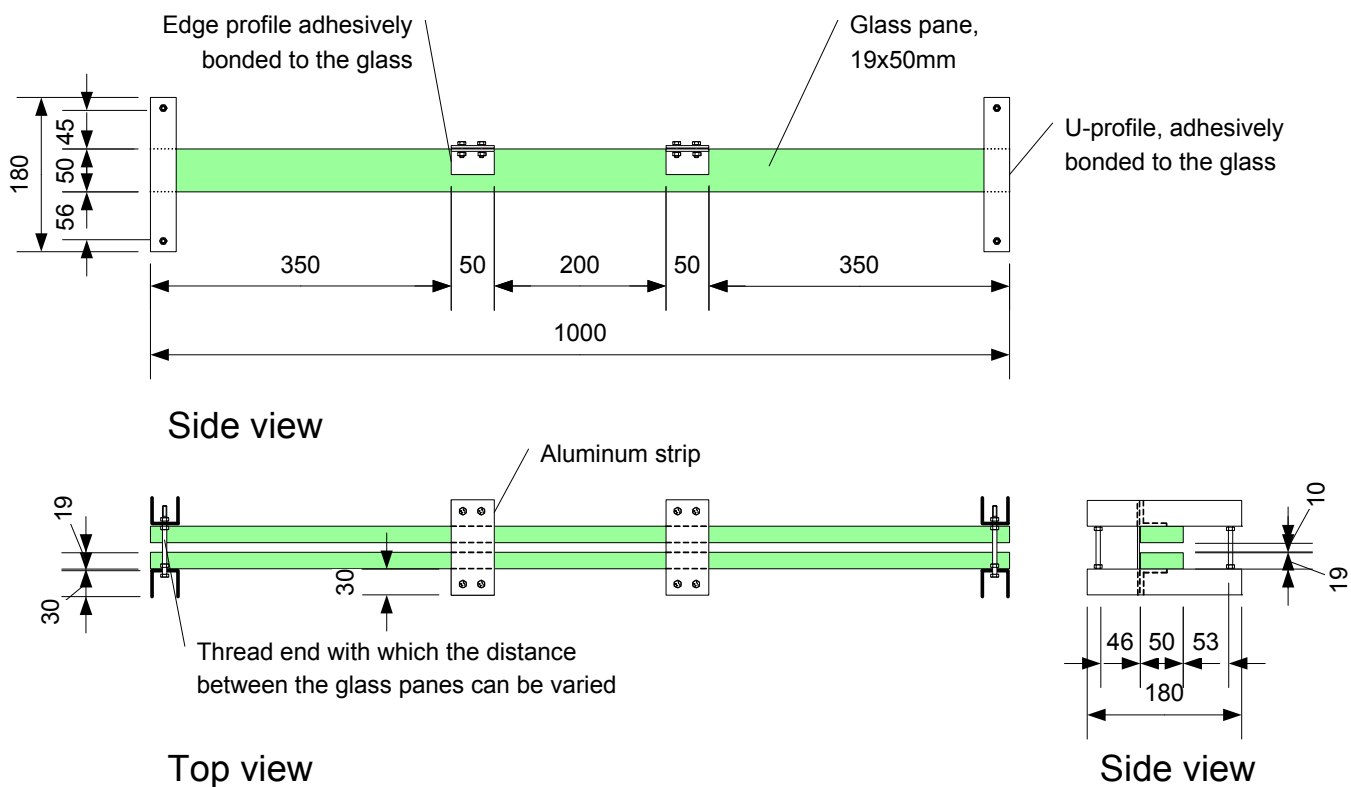


Figure 129, Mechanical drawing of lateral torsional buckling support.

6.2 Method

The test method is comparable to the preliminary beam tests: a displacement controlled four point bending test in which lateral torsional buckling is prevented.

The specimens consist of reinforced glass girders with a length of 1500mm, width of 10mm and a height of 70mm.

The span is 1400mm and the force is applied by two hinged roll supports 200mm from the center of the beam. The supports consist of steel cylinders with a diameter of 30mm. Aluminum plates with a thickness of 10mm and a length of 50mm are placed between the steel and the glass to spread the introduction of the support force.

The test speed is 1 mm/min up to initial failure (first glass fracturing). Then the speed is increased to 2 mm/min until ultimate failure occurs. The sensitivity of the load cell is 0,082 kN. The deflection of the girder is measured in the center of the beam at the top.

The top of the girder is supported against lateral torsional buckling over the middle 1000mm and horizontally supported 525 mm from the center.

See *Figure 129*. The lateral torsional buckling support consists of two glass panes along side the reinforced glass girder. The beams have a fixed distance towards

each other, restraining horizontal deflection square to the girder. The support is placed on the girder and can drop freely as the deflection of the beam increases. Even at progressed state of glass fracturing the friction between the support and the glass stayed minimal, as was tested by slightly sliding the support.



Figure 131, Test setup with camera position.



Figure 132, Girder in setup, isolated from the bench press.

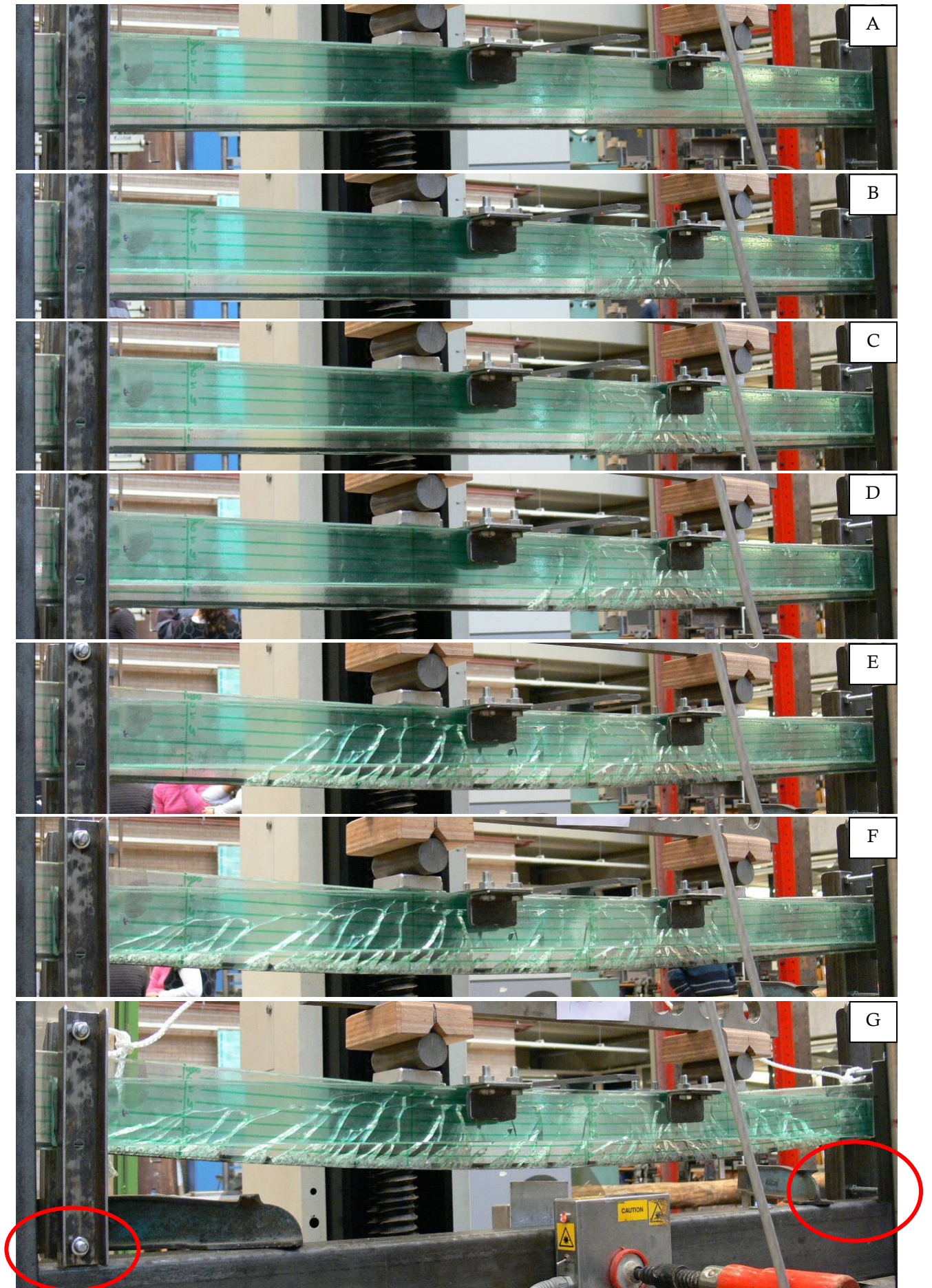


Figure 133 A to G, Specimen 70-01 at different moments during the test. Letters correspond to Figure 134.

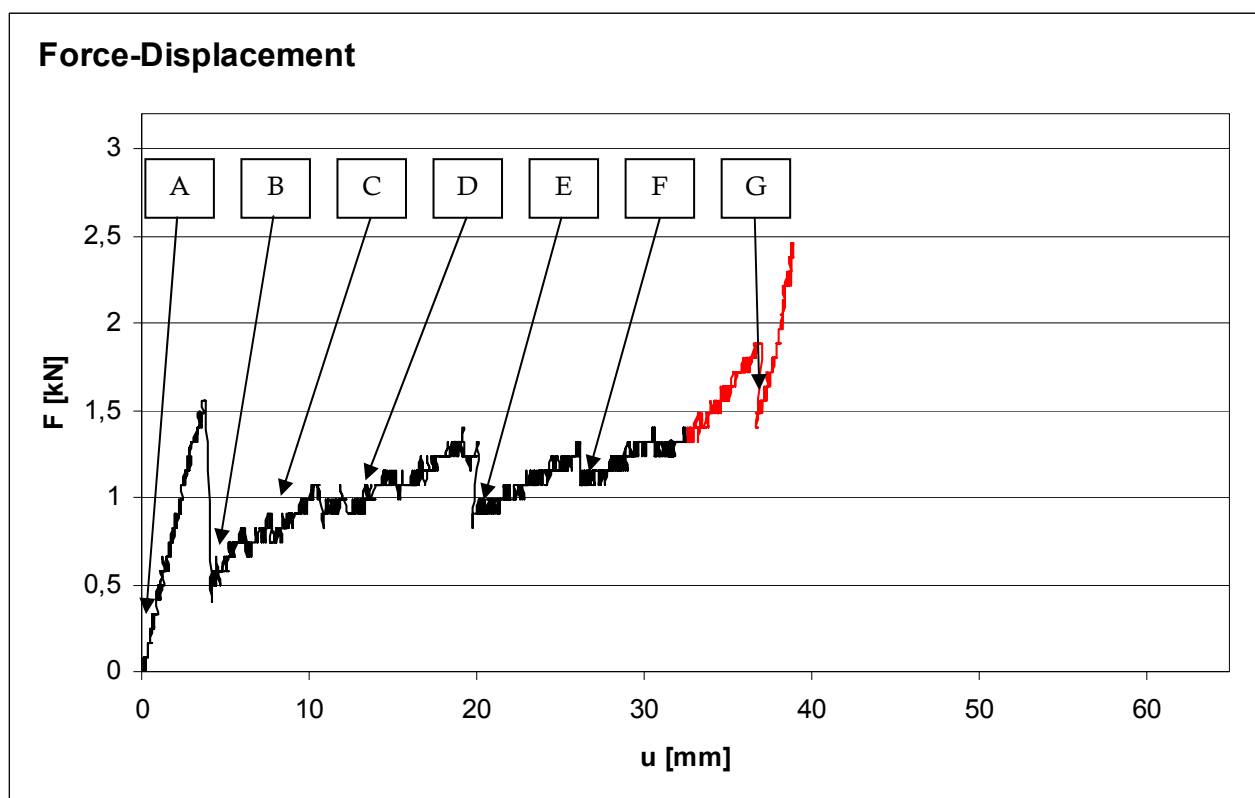


Figure 134, Force-displacement curve of specimen 70-01. In red the discarded part of the curve.

Specimen 70-01

The specimen showed a linear elastic deformation up to initial failure at 1,56 kN with a displacement of 3,8mm. Then a large drop-back in force to 0,5 kN set in as the first crack with a depth of approximately 60mm occurred.

This more or less vertical crack started progressing horizontally at a depth of 60mm for over a length of 100 mm, which is visible in *Figure 133c*. Then several more vertical cracks occurred in the middle part of the beam *Figure 133d*. As the cracks occurred more to the end of the beam the more diagonal they became. At the top of the beam an uncracked zone with a height of approximately 10mm existed.

At a deflection of 34 mm the support for lateral torsional buckling touched the setup and started resting on it and carrying load, as it is visible in *Figure 133g* (encircled in red). The sudden increase in stiffness in the curve in *Figure 134* is explained by this. This part of the test is discarded and given in red.

The test was aborted and the support adjusted for the test of specimen 70-02.

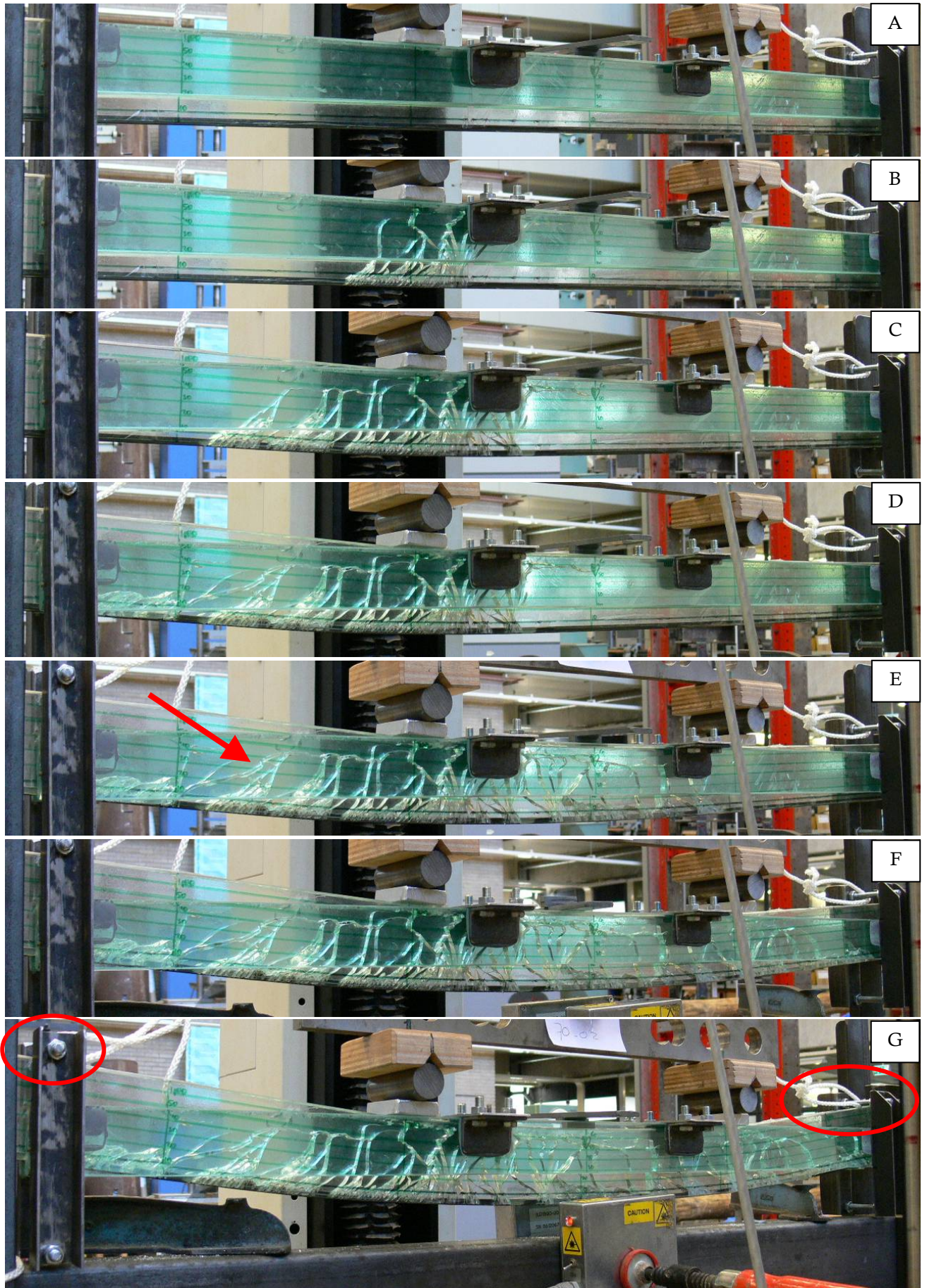


Figure 135 A to G, Specimen 70-02 at different moments during the test.

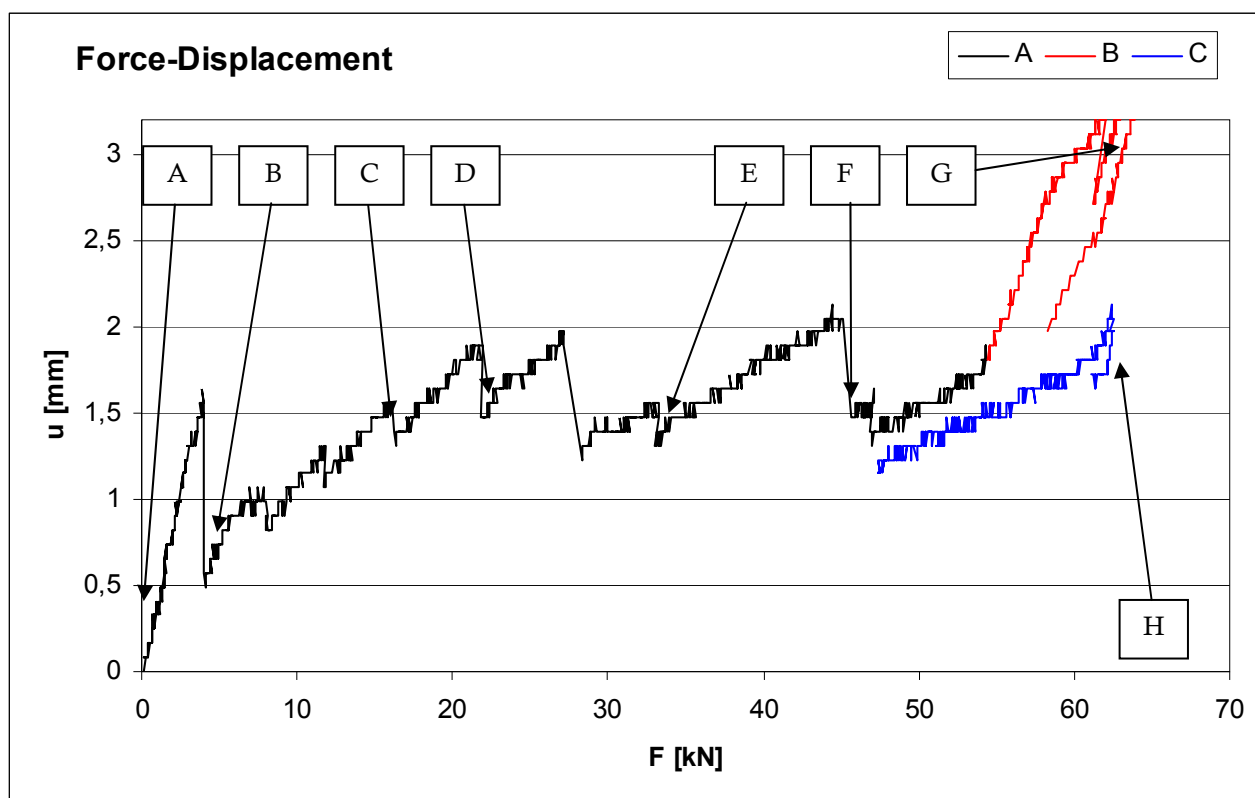


Figure 136, Force-Displacement curve for specimen 70-02.

Specimen 70-02

Linear elastic behavior occurred up to initial failure at 1,56 kN and 4,0 mm deflection. Ultimate failure did not occur due to setup difficulties. The highest force reached by the specimen was 2,13 kN.

The first crack arose under point B with a depth of 62mm. Then several cracks at the left part of the girder, until 500mm out the center of the girder (*Figure 135D*). More cracks in the center part of the beam occurred. At 33mm deflection (moment 'E') the crack width denoted by the red arrow in *Figure 135 E* is approximately 4 mm wide.

At 55 mm deflection the tread wire of the support rested on the beam and the support started bearing force. From this moment on (curve 'B' in *Figure 136*) the test is discarded. The support was adjusted and continued for a second run (curve 'C' in *Figure 136*) until the support rested on the setup again at 63 mm deflection and the test was terminated.

At 63 mm deflection the length over the glass is not fractured at the right side of the girder is approximately 60mm, as it is visible in *Figure 137*. The length over which the adhesive connection between glass and reinforcement is still intact, is approximately 40 mm.

The left side of the girder is fractured less than the right side.

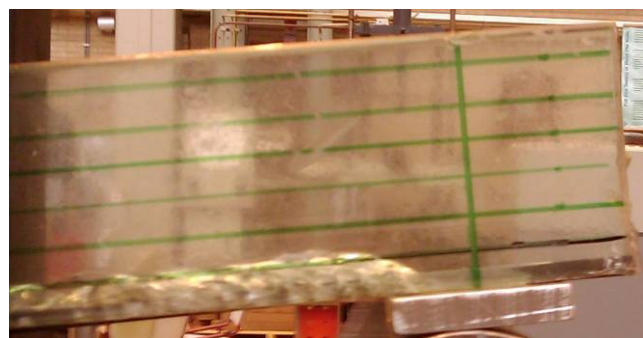


Figure 137, Close-up of left end of girder at moment 'H'.



Figure 138 A to G, Specimen 70-03 at different moments during the test.

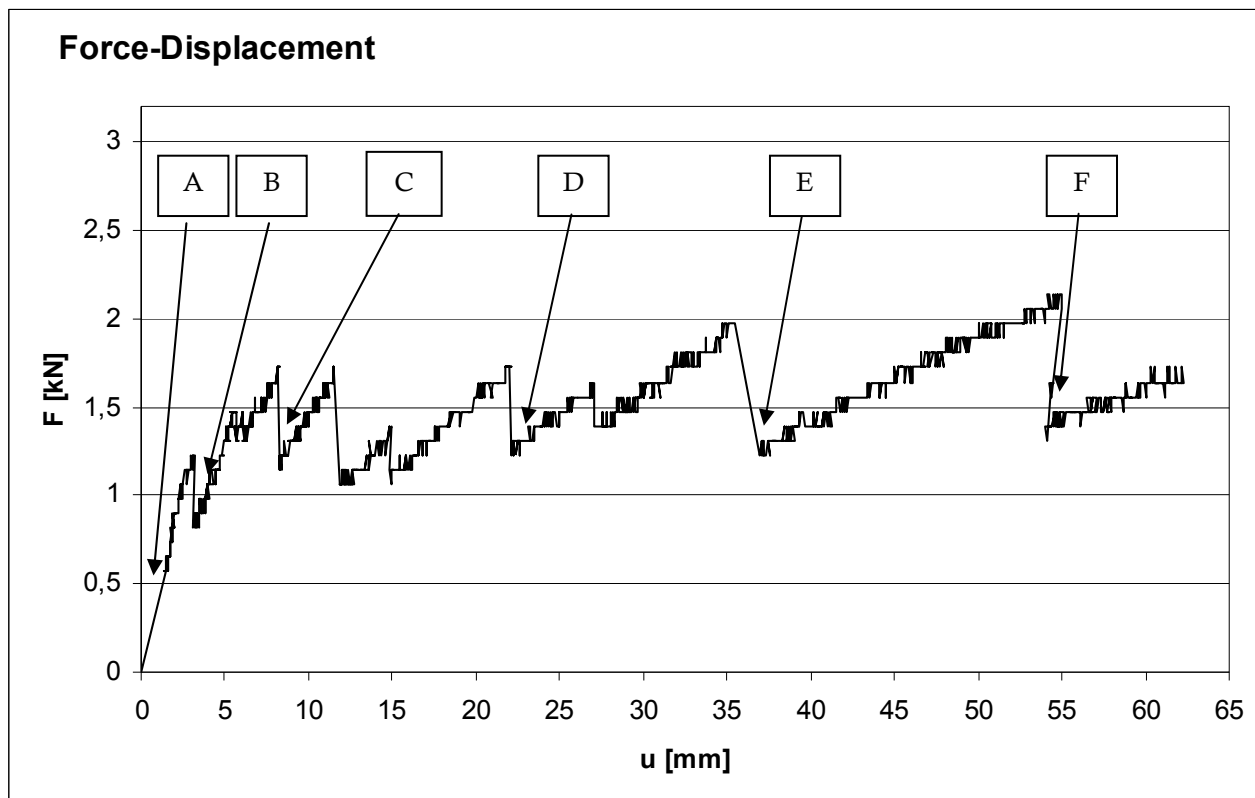


Figure 139, Force-Displacement curve for specimen 70-03.

Specimen 70-03

The girder showed linear deformation up to initial failure at 1,23 kN and 3,16mm. The first crack occurred at 300 mm right of the center of the beam with a depth of 62mm. The second crack occurred 150 mm left of the center, then multiple cracks in comparable pattern with specimen 70-01.

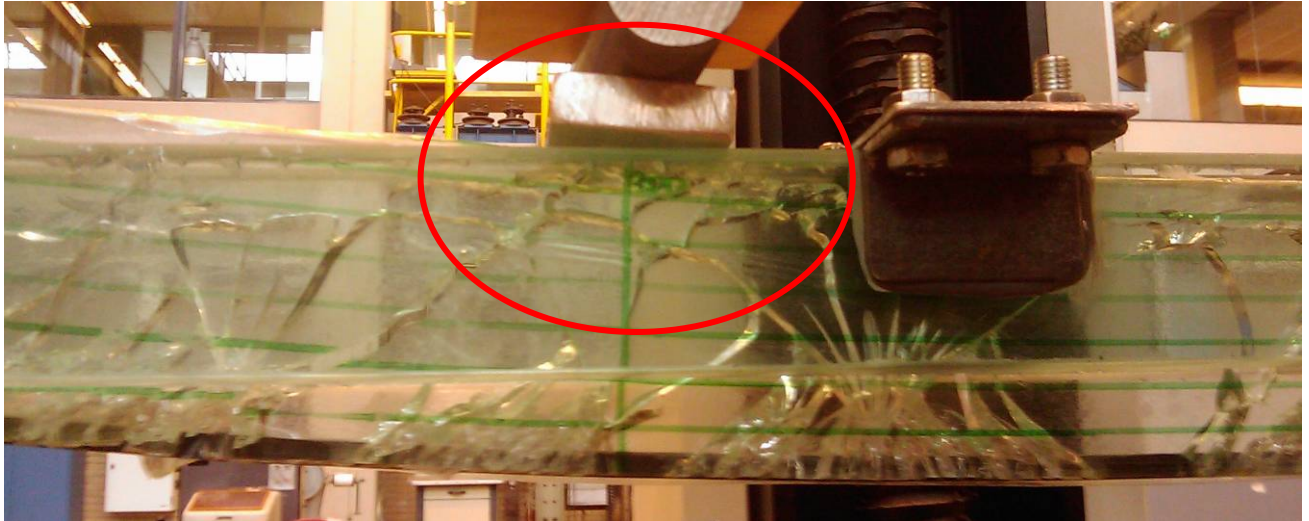


Figure 141, Close-up of specimen 70-03 200mm left of the center of the girder. The cracks run up far in to the top of the girder under the support (encircled in red).



Figure 140, Specimen 70-03 after the test with the broken reinforcement (encircled above). The end of the reinforcement is denoted by the arrow in the bottom picture.

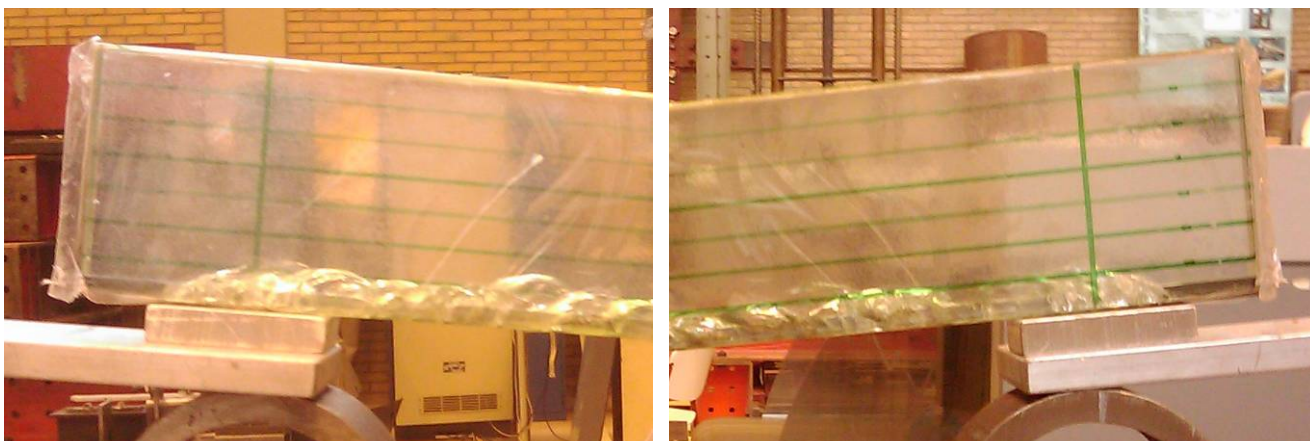


Figure 142, Close-up of both ends of specimen 70-03 just before ultimate failure.

The bottom of the glass kept fracturing progressively until the intact connection between the glass and the reinforcement was approximately 35mm (*Figure 142*).

Just before ultimate failure the top 10mm of the glass pane remained unfractured, except directly under the support. This is visible in *Figure 141*.

Ultimate failure occurred at 1,64 kN at a deflection of 63mm. *Figure 140* shows a close-up of the specimen after the test. Two things happened at once at ultimate failure: the reinforcement broke and it burst out of the glass.

The highest force reached was 2,13kN at a deflection of 55 mm.



Figure 143 A to F, Specimen 70-04 at different moments during the test.

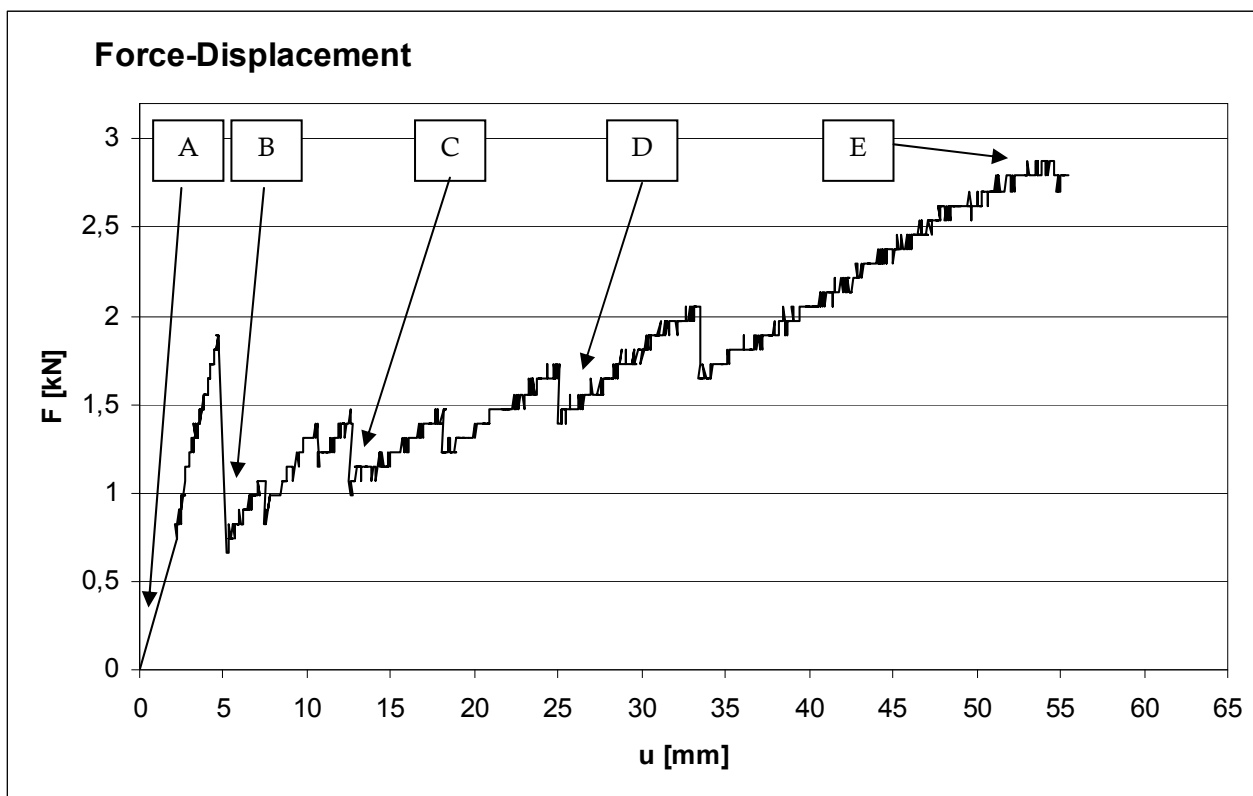


Figure 144, Force-Displacement curve for specimen 70-04.

Specimen 70-04

The specimen performed linear up to initial failure at 1,89 kN and 4mm deflection. This consisted of many large cracks in the middle 300mm of the beam, with higher density than specimens 70-01 to 70-03 showed. A large fall-back in force to 0,65kN and a lower bending stiffness were noticed after the first crack. Then several more cracks occurred of comparable nature as the first: 150-300mm in width, consisting of many cracks close to each other. The direction of the cracks is comparable to other specimens. After each crack the bending stiffness decreases slightly.

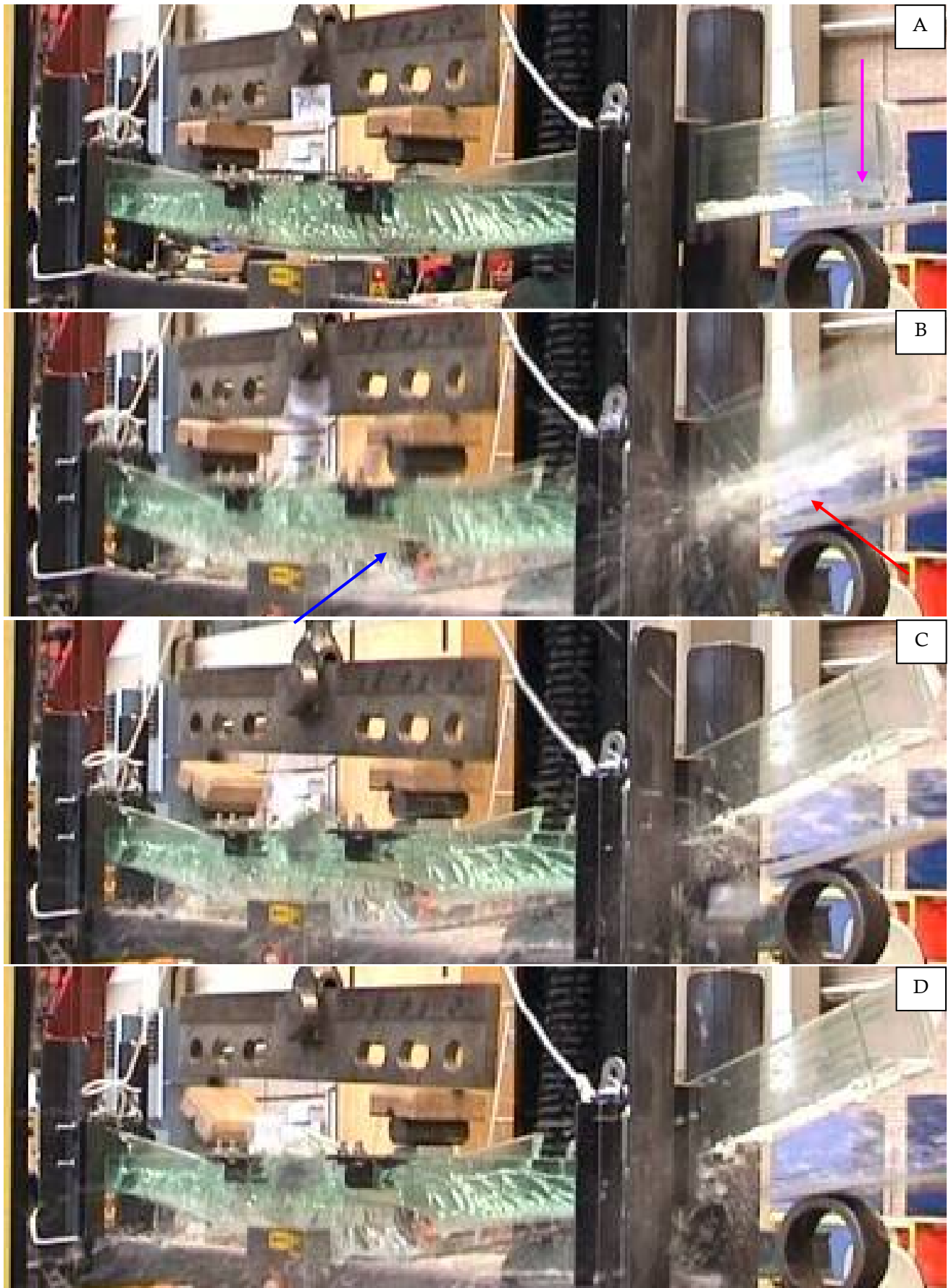


Figure 145 A to D, Ultimate failure of specimen 70-04. The photographs are stills from the video camera, each 0,16 second after each other.

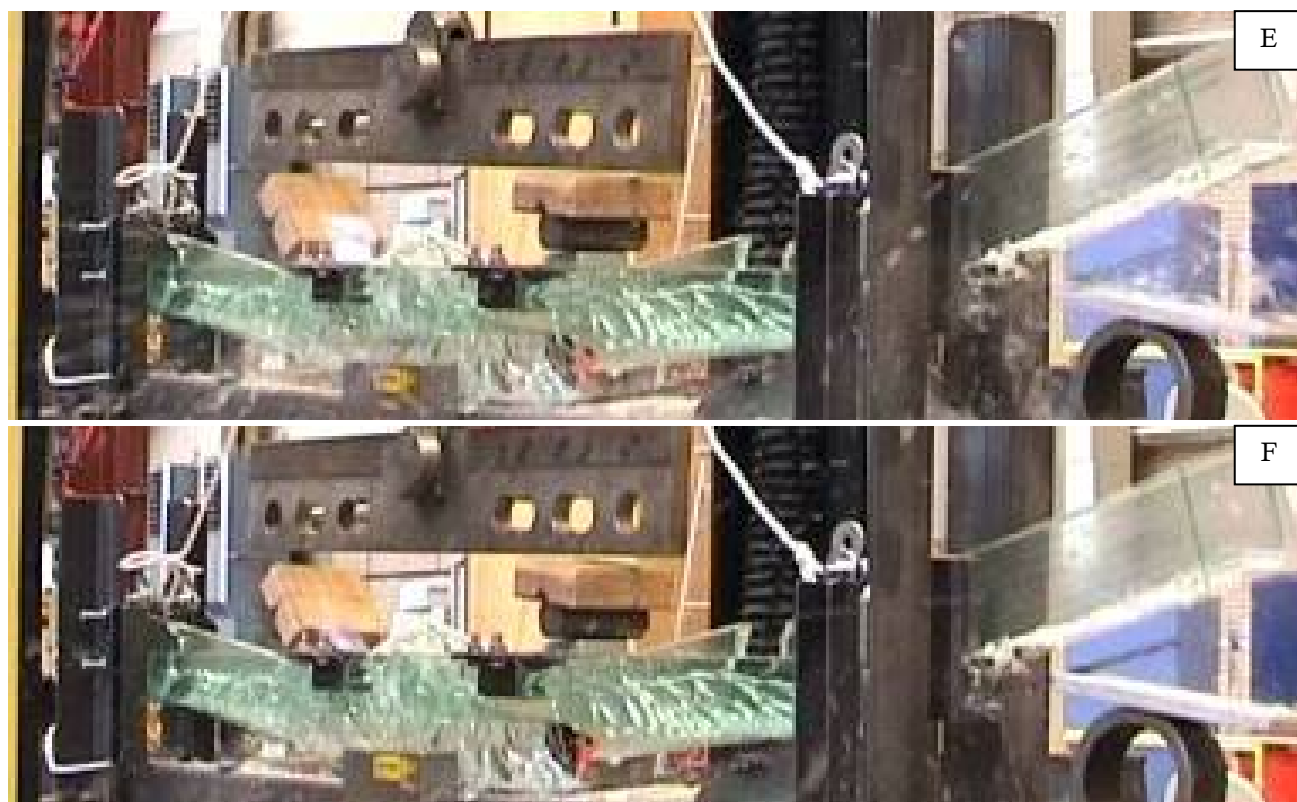


Figure 146 E and F, Continuation of Figure 145.

Figure 145 and Figure 146 show the collapse of specimen 70-04 at 6 different moments, each 0,16 seconds after the other.

The pink arrow at photo A shows that the length of the intact adhesive connection between reinforcement and glass at the end of the beam is about 20mm with approximately 40mm brittle.

At photo B it is visible that the bottom of the girder, where the reinforcement is bonded to the glass, explodes quite drastically and the reinforcement is detached from the glass the first moment (red arrow). The middle part of the girder is separated in several pieces with one crack dominating, denoted by the blue arrow.

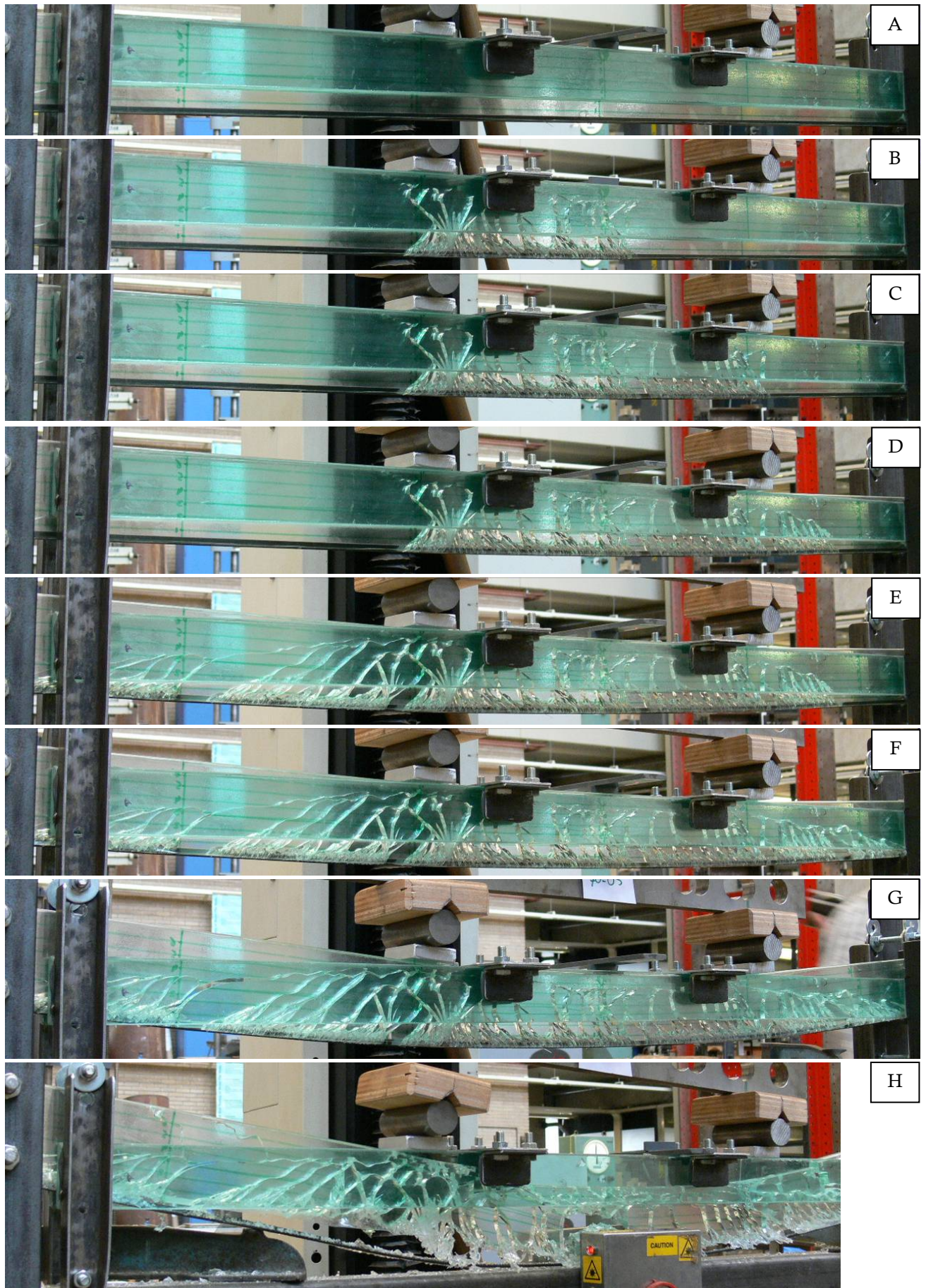


Figure 147 A to H, Specimen 70-05 at different moments during the test.

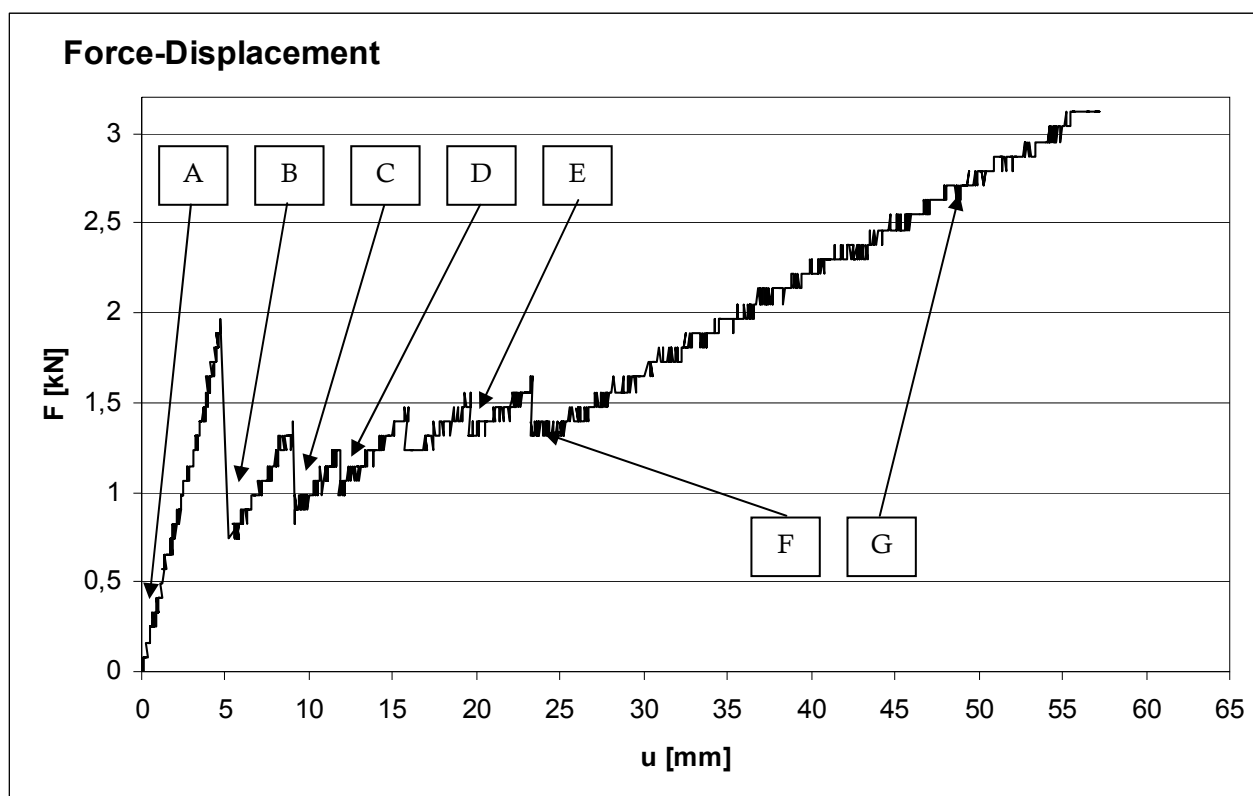


Figure 148, Force-displacement curve for specimen 70-05.

Specimen 70-05

The specimen performed linear up to initial failure at 1,96kN and 4,7mm deflection. This consisted of multiple large cracks over 300mm with a depth of 60mm and a large fallback in force and bending stiffness was observed.

More cracks occurred with widths of approximately 150-300mm consisting of multiple fractures. After moment 'F' no more large cracks occurred, but slow progressive failure of the adhesive connection between reinforcement and glass occurred at both ends of the specimen. At moment 'G' the intact connection length was approximately 45mm, with 20mm brittle adhesive connection.

Loud cracking was observed from moment 'g' up to total failure. The last 2 minutes of the test (4mm deflection) it was clear that the specimen could collapse any moment.

Ultimate failure occurred when the reinforcement burst out of the glass pane at the right side of the girder, comparable to specimen 70-04.



Figure 149, left end of specimen 70-05 at moment G. This is comparable to the right end.



Figure 150 A to H, Specimen 70-06 at different moment during the test.

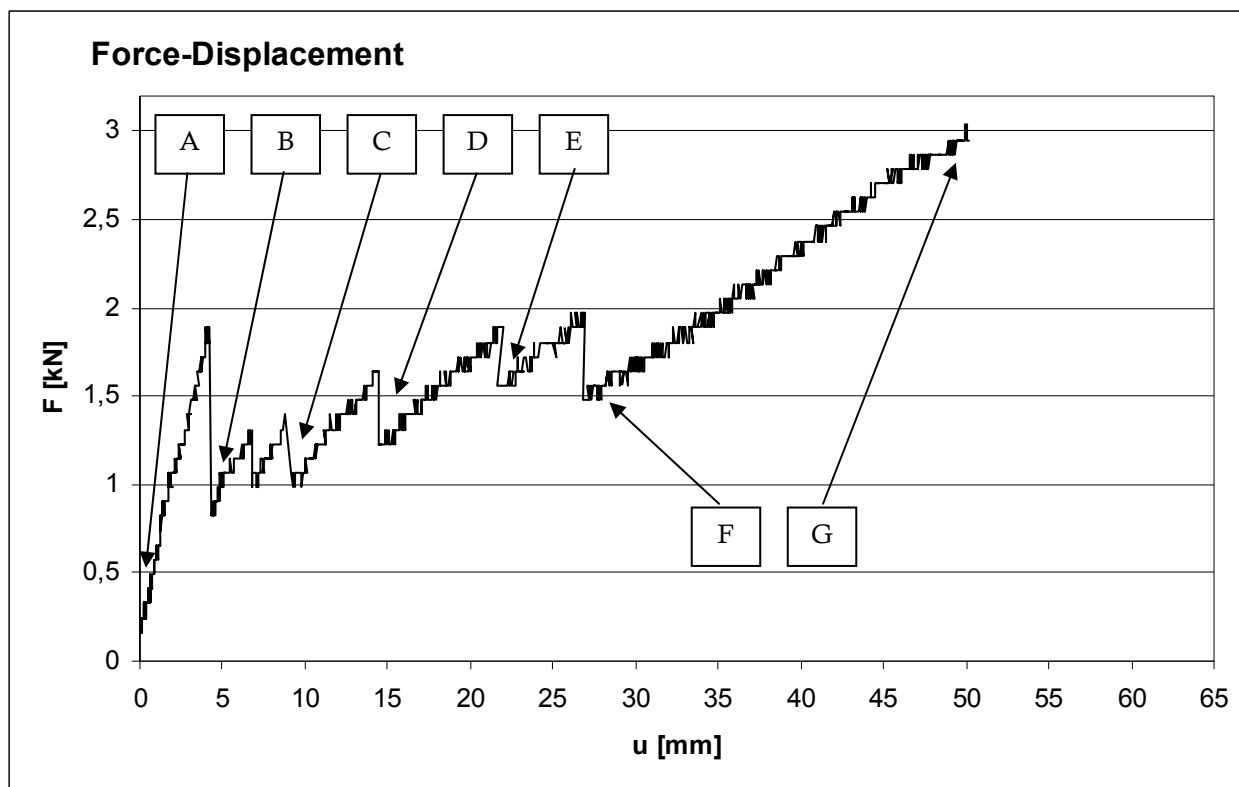


Figure 151, Force-Displacement curve for specimen 70-06.

Specimen 70-06

The behavior and fracture pattern of specimen 70-06 is comparable to specimens 70-04 and 70-05.

Initial failure occurred at 1,89kN and 4,27mm deflection. Ultimate failure occurred at a force of 3,05kN and 50mm deflection, after loud cracking in the last 4mm deflection.



Figure 152, Specimen 90-01 at different moments during the test.

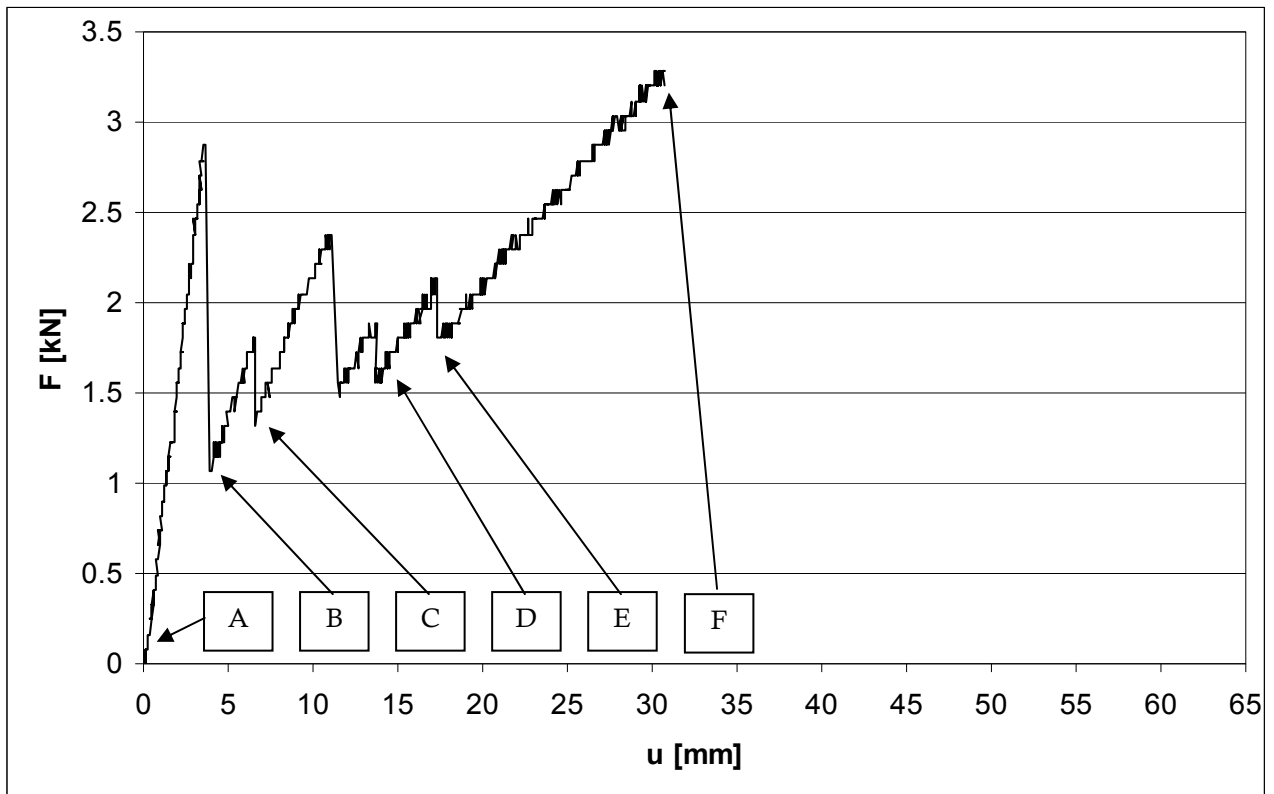


Figure 153, Force-displacement curve of specimen 90-01.

Specimen 90-01

The specimen performed linear up to initial failure at 2,87kN and 3,65mm deflection. The first crack consisted of several large cracks close to each other from 100mm to 300mm right of the center of the beam (photo B). The largest cracks had a depth of 80mm. One of them running vertically and bending of to horizontal direction 10mm under the top of the beam. Other cracks also ended horizontally 10mm under the top.

The next crack occurred right of this, then a large one with a width of 300mm running from 200mm left to 100mm right of the center, visible on photo D. More cracks evolved closer to the ends of the girder, progressing more rapidly to the left than to the right.

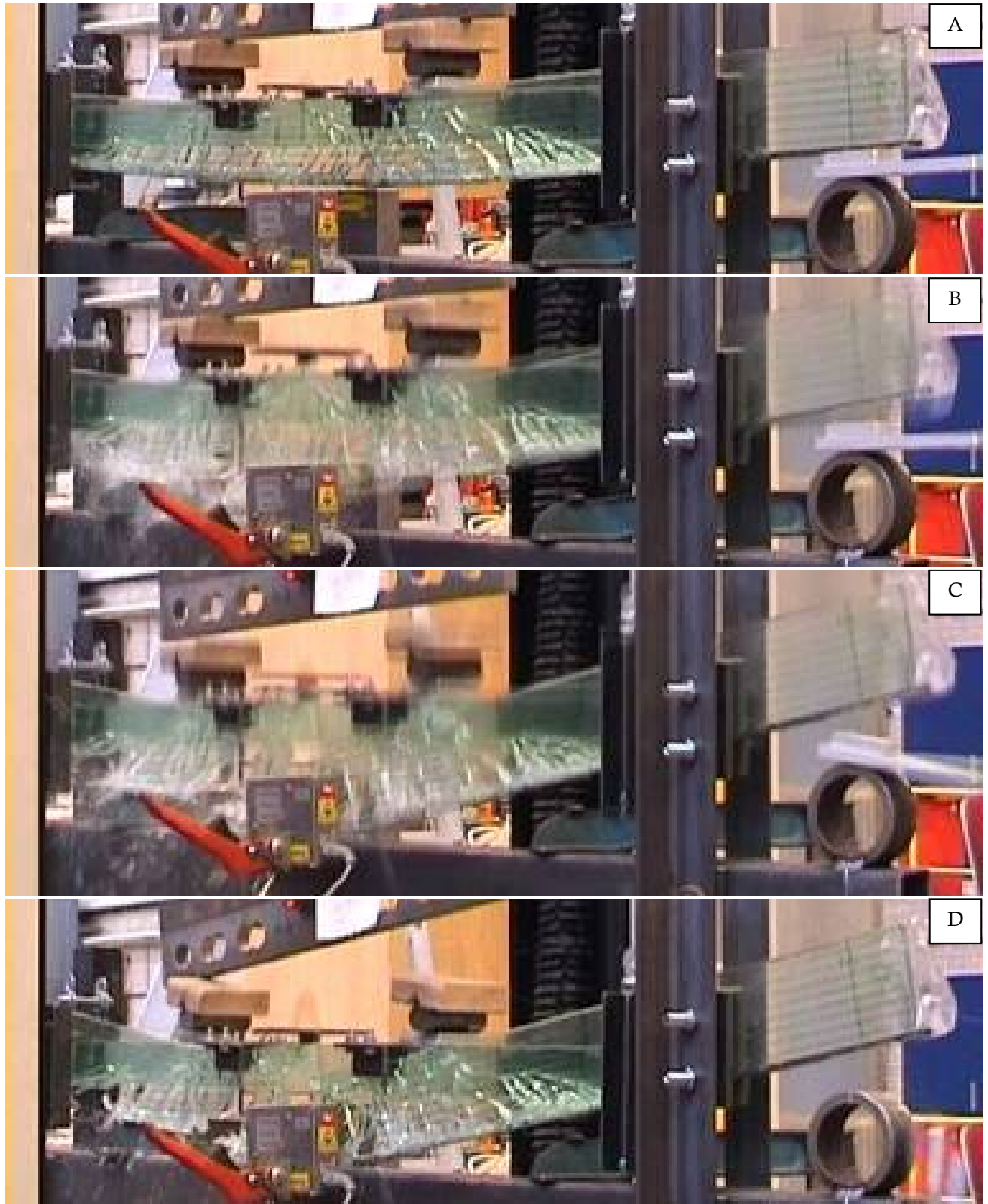


Figure 154, Specimen 90-01 at different moment during collapse. Pictures are 0,04s after each other



Figure 155, Left and right end of specimen 90-01 after collapse.

Ultimate failure occurred at 3,28kN and 30,7mm. **Figure 154** shows the collapse of the specimen at 4 different moment close after each other.

See **Figure 155**. The reinforcement has burst out of the girder at the left end, while the connection at the right end was still intact over 300mm. Right before the collapse the connection between the reinforcement and the glass at the left end of the girder was also still intact over at least 200mm.



Figure 156, Specimen 90-02 at different moment during the test.

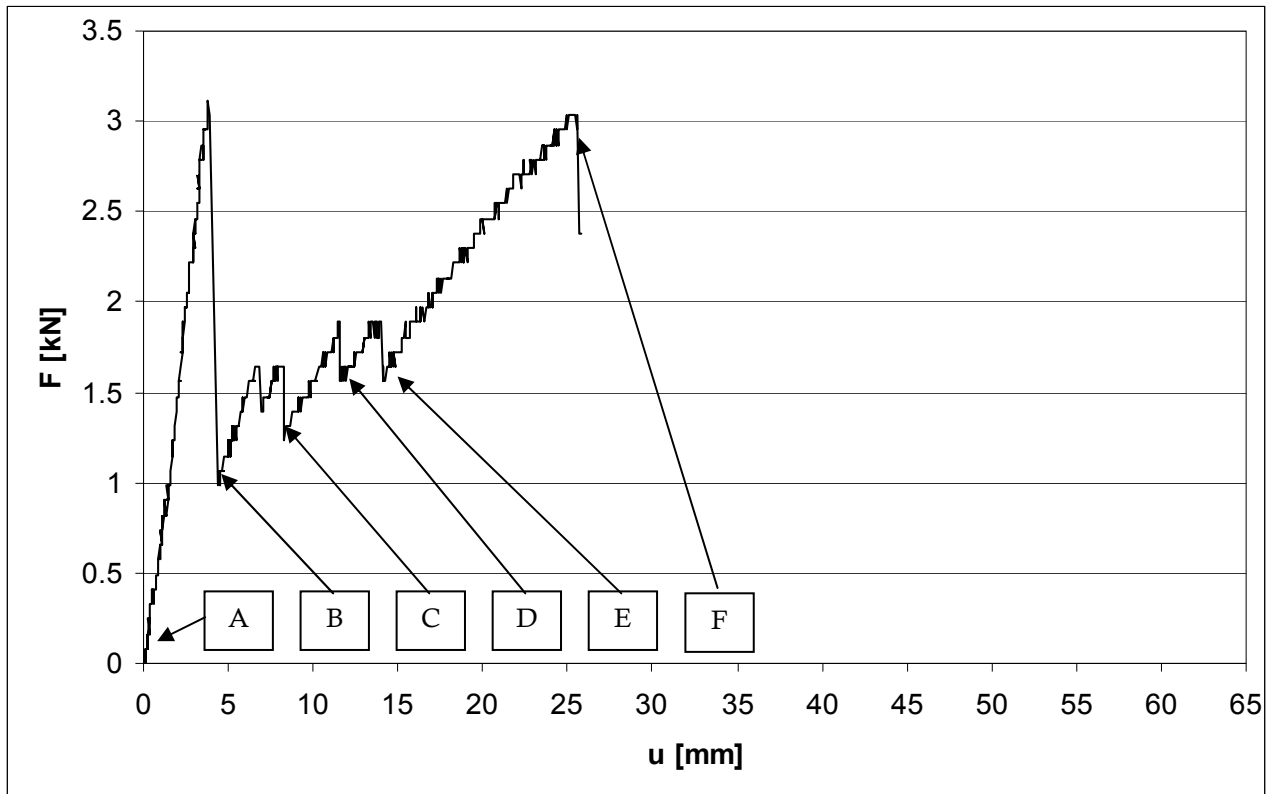


Figure 157, Force-displacement curve for specimen 90-02

Specimen 90-02

The specimen performed linear behavior up to initial failure at 3,1kN and 3,89mm deflection. The first crack consisted of several large cracks close to each other from 150mm left to 50mm right of the center of the beam (photo B). The largest crack, right of the center of the beam, had a depth of approximately 85mm, 5mm under the top. This is denoted by the red arrow.

Each fallback of the curve in *Figure 157* marks several cracks evolving together. Other cracking is observed in progressive small cracks occurring near the reinforcement, comparable to what is seen with the glass pull-out tests.

Just before ultimate failure the cracks run symmetrically to about 200mm from the center. Brittling of the adhesive is observed over 50mm, as visible in photo F.

Ultimate failure occurs at 3,0kN and a deflection of 25,5mm. The most left fissure collapses under shear force and the reinforcement bursts out of the glass.



Figure 158, close-up of left end of specimen 90-02 after the test.



Figure 159, Specimen 90-03 at different moments during the test.

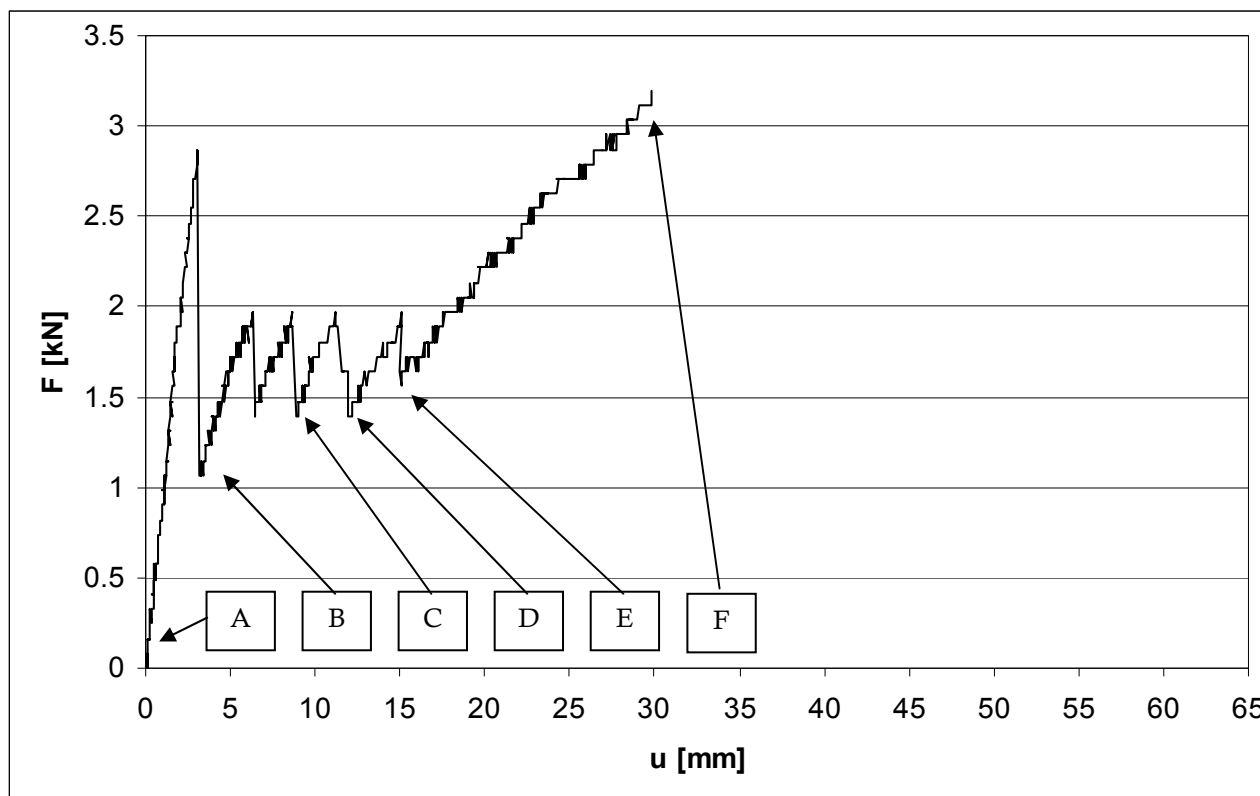


Figure 160, Force-displacement curve for specimen 90-03

Specimen 90-03

The specimen performed linear behavior up to initial failure at 2,87kN and 3,1mm deflection. The first crack consisted of several large cracks close to each other from 150mm to 300mm right of the center of the beam (photo B). The largest crack had a depth of approximately 80mm, bending off and running approximately 150 in horizontal direction 10mm under the top of the beam. The end is denoted by the red arrow, approximately 10mm left of the center of the beam.

Gradually more cracks evolved over approximately 150mm lengths, in comparable pattern to specimens 90-01 and 90-02.

Ultimate failure occurred at 3,2kN and a deflection 29,8mm by shear force at the left side of the beam. Just before ultimate failure the connection between reinforcement and glass was symmetrical on both sides and intact for over approximately 200mm.

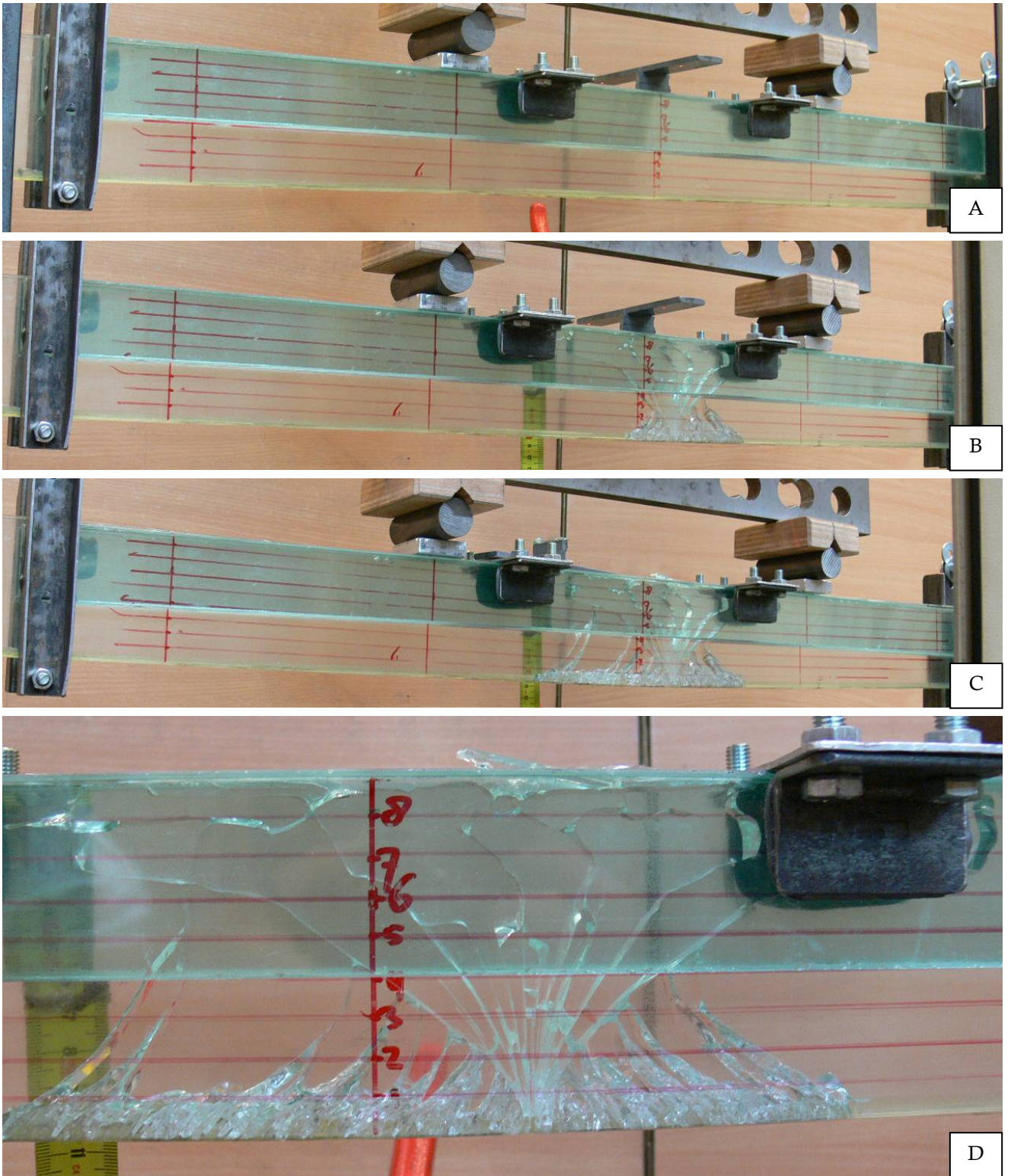


Figure 161, Specimen 90-04 at different moment during (a, b and c) and a close-up of the crack pattern after (d) the test.

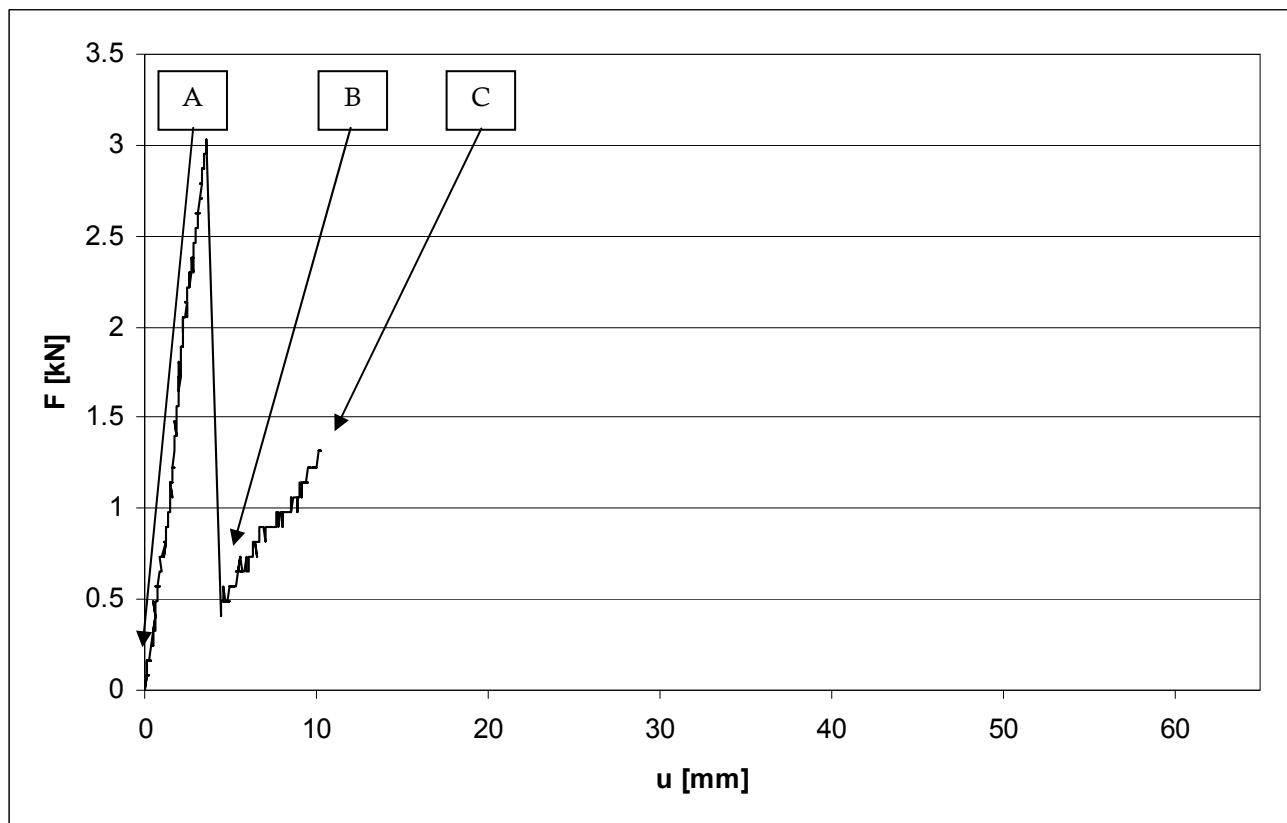


Figure 162, Force-displacement curve of specimen 90-04.

Specimen 90-04

Specimens 90-04 and 90-05 are mounted with a glass fiber reinforcement. The geometry is comparable to geometry 1, but with a slightly thicker reinforcement of 0,8mm which results in an adhesive layer thickness of approximately 0,3mm.

The girder performed linear elastic behavior up to initial failure at 3,0 kN. The cracks ran up to 3 mm under the top of the girder, deep into the compressive zone of the glass. The force dropped back to under 0,5kN and the bending stiffness decreased severely.

At a deflection of 10mm and a force of 1,3kN ultimate failure occurred at a new crack and failure of the compressive zone in the glass. The residual load bearing capacity of this specimen was 43%.

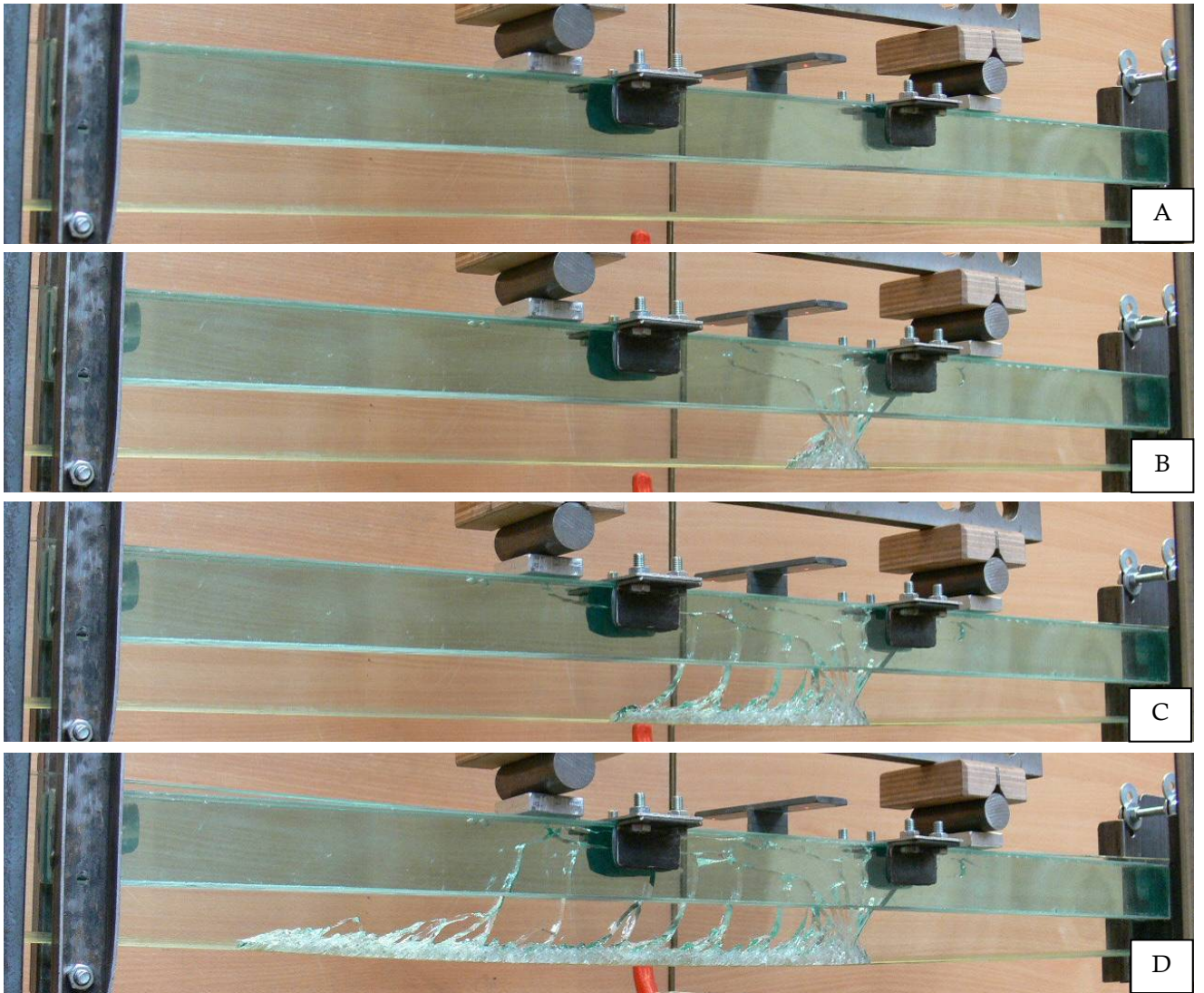


Figure 163, Specimen 90-05 at different moments during the test.

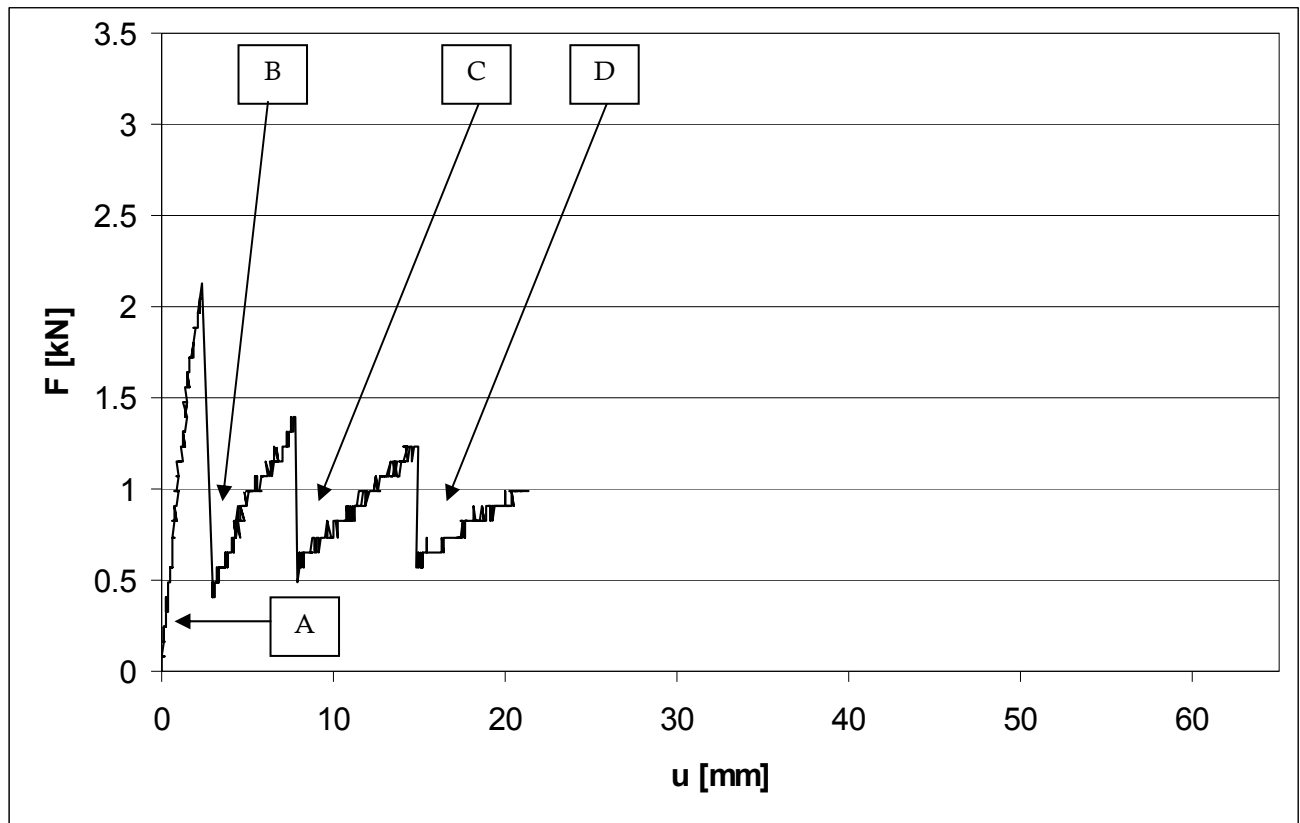


Figure 164, Force-displacement curve of specimen 90-05.

Specimen 90-05

Linear elastic deformation was observed until initial failure at 2,1kN and a deflection of 3mm, at much lower bending stress than the other 90mm specimens. The first cracks run up deep into the compressive zone of the glass.

A great fall-back of force to 0,4kN occurred, which repeated for two more cracks at 8 and 15mm deflection. Ultimate failure happened at 20mm deflection at a force of 1,0kN.

The residual load bearing capacity was not enough to reach the bending moment at initial failure, only 65% of M_i was reached.

Table 29, Dimensions specimens 70-01 to 70-03

Glass pane		Reinforcement		Girder	
l	1.500 mm	l	1.500 mm	l	1.500 mm
b	10 mm	h	6 mm	h	71 mm
h	70 mm	b	0,6 mm	b	10 mm
E	$70 \cdot 10^3 \text{ N/mm}^2$	E	$145 \cdot 10^3 \text{ N/mm}^2$	EI	$20.000 \cdot 10^6$
I	$278 \cdot 10^3 \text{ mm}^4$	I	3.931 mm^4		
EI	$19.431 \cdot 10^6$	EI	$570 \cdot 10^6$		

Table 29, Relevant bending moments, forces and stresses

70-01			70-02			70-03		
F_i	1558 [#]	[N]	F_i	1558 [#]	[N]	F_i	1231 [#]	[N]
M_i	$0,390 \cdot 10^3$	[Nmm]	M_i	$0,390 \cdot 10^6$	[Nmm]	M_i	$0,308 \cdot 10^6$	[Nmm]
$\sigma_{i.gl.}$	47,7	[N/mm ²]	$\sigma_{i.gl.}$	47,7	[N/mm ²]	$\sigma_{i.gl.}$	30,1	[N/mm ²]
$\sigma_{i.re.}$	98,8	[N/mm ²]	$\sigma_{i.re.}$	98,8	[N/mm ²]	$\sigma_{i.re.}$	57,2	[N/mm ²]
			F_{max}	2,13 [#]	[N]	F_{max}	2,13 [#]	[N]
			M_{max}	$0,533 \cdot 10^6$	[Nmm]	M_{max}	$0,533 \cdot 10^6$	[Nmm]
			$F_{max.re.}$	8267	[N]	$F_{max.re.}$	8267	[N]
			$\sigma_{max.re.}$	2296	[N/mm ²]	$\sigma_{max.re.}$	2296	[N/mm ²]

Sensitivity load cell = 82N

Table 31, Dimensions specimens 70-04 to 70-06

Glass pane		Reinforcement		Girder	
l	1.500 mm	l	1.500 mm	l	1.500 mm
b	10 mm	h	6 mm	h	71 mm
h	70 mm	b	1,4 mm	b	10 mm
E	$70 \cdot 10^3 \text{ N/mm}^2$	E	$145 \cdot 10^3 \text{ N/mm}^2$		
I	$278 \cdot 10^3 \text{ mm}^4$	I	9172 mm^4		
EI	$19.431 \cdot 10^6$	EI	$1330 \cdot 10^6$	EI	$20.760 \cdot 10^6$

Table 31, Relevant bending moments, forces and stresses

70-04			70-05			70-06		
F_i	1887 [#]	[N]	F_i	1887 [#]	[N]	F_i	1887 [#]	[N]
M_i	$0,472 \cdot 10^6$	[Nmm]	M_i	$0,472 \cdot 10^6$	[Nmm]	M_i	$0,472 \cdot 10^6$	[Nmm]
$\sigma_{i.gl.}$	55,7	[N/mm ²]	$\sigma_{i.gl.}$	55,7	[N/mm ²]	$\sigma_{i.gl.}$	55,7	[N/mm ²]
$\sigma_{i.re.}$	269	[N/mm ²]	$\sigma_{i.re.}$	269	[N/mm ²]	$\sigma_{i.re.}$	269	[N/mm ²]
F_{max}	2871 [#]	[N]	F_{max}	3120 [#]	[N]	F_{max}	3036 [#]	[N]
M_{max}	$0,718 \cdot 10^6$	[Nmm]	M_{max}	$0,779 \cdot 10^6$	[Nmm]	M_{max}	$0,759 \cdot 10^6$	[Nmm]
$F_{max.re.}$	11.129	[N]	$F_{max.re.}$	12.082	[N]	$F_{max.re.}$	11.764	[N]
$\sigma_{max.re.}$	1325	[N/mm ²]	$\sigma_{max.re.}$	1438	[N/mm ²]	$\sigma_{max.re.}$	1401	[N/mm ²]

Sensitivity load cell = 82N

Results summary

Table 31 to Table 33 present the results from the tests. Relevant bending moments, forces and stresses are derived from these values. Calculations are found in the appendix, chapter 4.

Note that the sensitivity of the bench press was 82N. Therefore some values are given more precise than the allowed significance.

Table 33, Dimensions specimens 90-01 to 90-03

Glass pane		Reinforcement		Girder	
l	1.500 mm	l	1.500 mm	l	1.500 mm
h	90 mm	h	6 mm	h	91 mm
B	10 mm	b	1,4 mm	b	10 mm
E	$70 \cdot 10^3 \text{ N/mm}^2$	E	$145 \cdot 10^3 \text{ N/mm}^2$	EI	$43,8 \cdot 10^9$
I	$594 \cdot 10^3 \text{ mm}^4$	I	15.557 mm^4		
EI	$41,6 \cdot 10^9$	EI	$2,256 \cdot 10^9$		

=

Table 33, Relevant bending moments, forces and stresses

90-01			90-02			90-03		
F_i	2.871 [#]	[N]	F_i	3117 [#]	[N]	F_i	2.871 [#]	[N]
M_i	$718 \cdot 10^3$	[Nmm]	M_i	$779 \cdot 10^3$	[Nmm]	M_i	$718 \cdot 10^3$	[Nmm]
$\sigma_{i.gl.}$	51,6	[N/mm ²]	$\sigma_{i.gl.}$	56,0	[N/mm ²]	$\sigma_{i.gl.}$	51,6	[N/mm ²]
$\sigma_{i.re.}$	102	[N/mm ²]	$\sigma_{i.re.}$	111	[N/mm ²]	$\sigma_{i.re.}$	102	[N/mm ²]
F_{max}	3.281 [#]	[N]	F_{max}	3.035 [#]	[N]	F_{max}	3.199 [#]	[N]
M_{max}	$820 \cdot 10^3$	[Nmm]	M_{max}	$759 \cdot 10^3$	[Nmm]	M_{max}	$800 \cdot 10^3$	[Nmm]
$F_{max.re.}$	9.707	[N]	$F_{max.re.}$	8.979	[N]	$F_{max.re.}$	9.464	[N]
$\sigma_{max.re.}$	1.156	[N/mm ²]	$\sigma_{max.re.}$	1.069	[N/mm ²]	$\sigma_{max.re.}$	1.127	[N/mm ²]

Sensitivity load cell = 82N

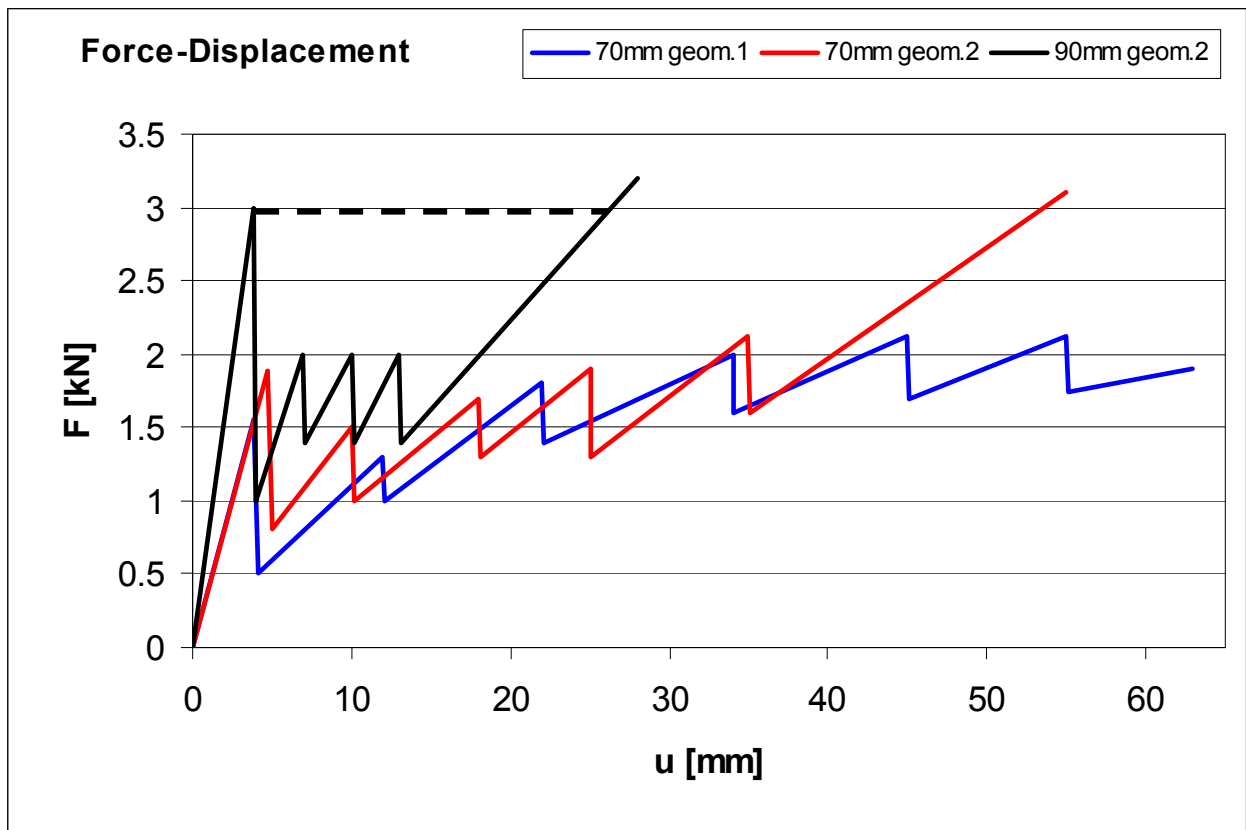


Figure 165, Typical force-displacement curves for different specimen types.

Table 34, Failure values and safety margins

Specimen	Force			Deflection		
	F_i [kN]	F_{max} [kN]	Safety margin ($F_u/F_i \cdot 100\%$)	u_i [mm]	u_u [mm]	Safety margin ($u_u/u_i \cdot 100\%$)
70-01	1,56 kN	-	-	3,83 mm	-	-
70-02	1,56 kN	2,13 kN	137 %	3,95 mm	61,5 mm	1550 %
70-03	1,23 kN	2,13 kN	173 %	3,16 mm	62,2 mm	1970 %
70-04	1,89 kN	2,87 kN	152 %	4,74 mm	55,5 mm	1170 %
70-05	1,89 kN	3,11 kN	165 %	4,74 mm	57,2 mm	1200 %
70-06	1,89 kN	3,04 kN	160 %	4,26 mm	50,2 mm	1180 %
90-01	2,87 kN	3,20 kN	111 %	3,65 mm	30,8 mm	840 %
90-02	3,11 kN	3,03 kN	97 %	3,89 mm	25,5 mm	650 %
90-03	2,87 kN	3,20 kN	111 %	3,1 mm	29,8 mm	960 %

6.4 Discussion

Method & preparation

The specimens deformed much more than expected. Initially the setup was not designed for this, resulting in the premature abortion of tests 70-01 and 70-02. However, up to that moment the specimens presented comparable behavior to 70-03. Judged by the behavior of the other specimens it is fair to expect that 70-01 and 70-02 would have performed in similar way to specimen 70-03, with approximately the same maximum deflection and bending moment.

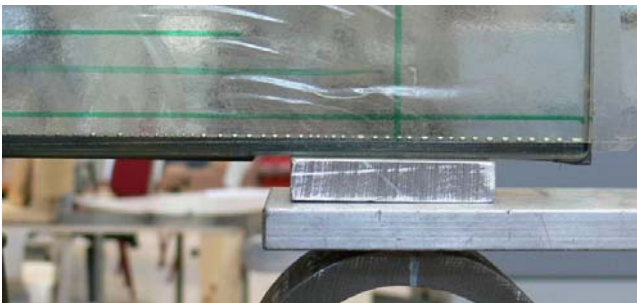


Figure 166, Close-up of air encapsulations in adhesive connection at right end of specimen 70-05.

Notice the air encapsulations in the end of the adhesive connection in specimen 70-05 (*Figure 166*). This specimen reached a higher force than 70-04 and 70-06 that did not have air encapsulated in the adhesive. It seems that production imperfections do not have a large negative effect on the strength of the beam. This was already concluded for the glass pull-out tests in chapter 3.4 and reconfirmed here. The long-term effects of encapsulated air are unknown.

For Specimens 70-03 to 70-06 the reinforcement burst out of the glass at the hinged support. Specimen 90-01 to 90-03 failed at the rolled support.

The two upper supports consist of solid steel cylinders which are presumed to function as hinged rolls. In

practice this rolling might be partly constrained by friction. If the end support does not allow horizontal displacement this part of the girder will be loaded by tension when sag increases. This results in a higher shear stress in the connection of the reinforcement to the glass at the hinged compared to the rolled support.

This assumption is endorsed by the fact that failure of the adhesive connection remained more or less symmetrical up to certain deflection and started progressing more at the hinged support above approximately 40mm deflection.

The 90mm specimens did not suffer from this effect since the deflection was much less and they failed due to bending moment. The fact that all three failed at the rolled support could have been a coincidence and is not studied further.

The four point bending tests are performed with a displacement controlled setup. This means that the applied force varies with the constant increase of displacement. After initial failure, the applied force falls back at least 50% after which it gradually increases until it reaches (more than) its initial failure level at very large deformations.

If applied in a glass floor for example, the applied force will remain constant since the applied load sags along with the girder as it deforms. This will cause a sudden and large deformation after initial failure. The force-displacement curve in this situation would be represented by the black dotted line in *Figure 165*.

The failure behavior in this situation is better approached by a force controlled test setup than by the displacement controlled that is used in this research. Therefore additional force controlled bending tests are recommended to validate the failure behavior in the ultimate limit state.

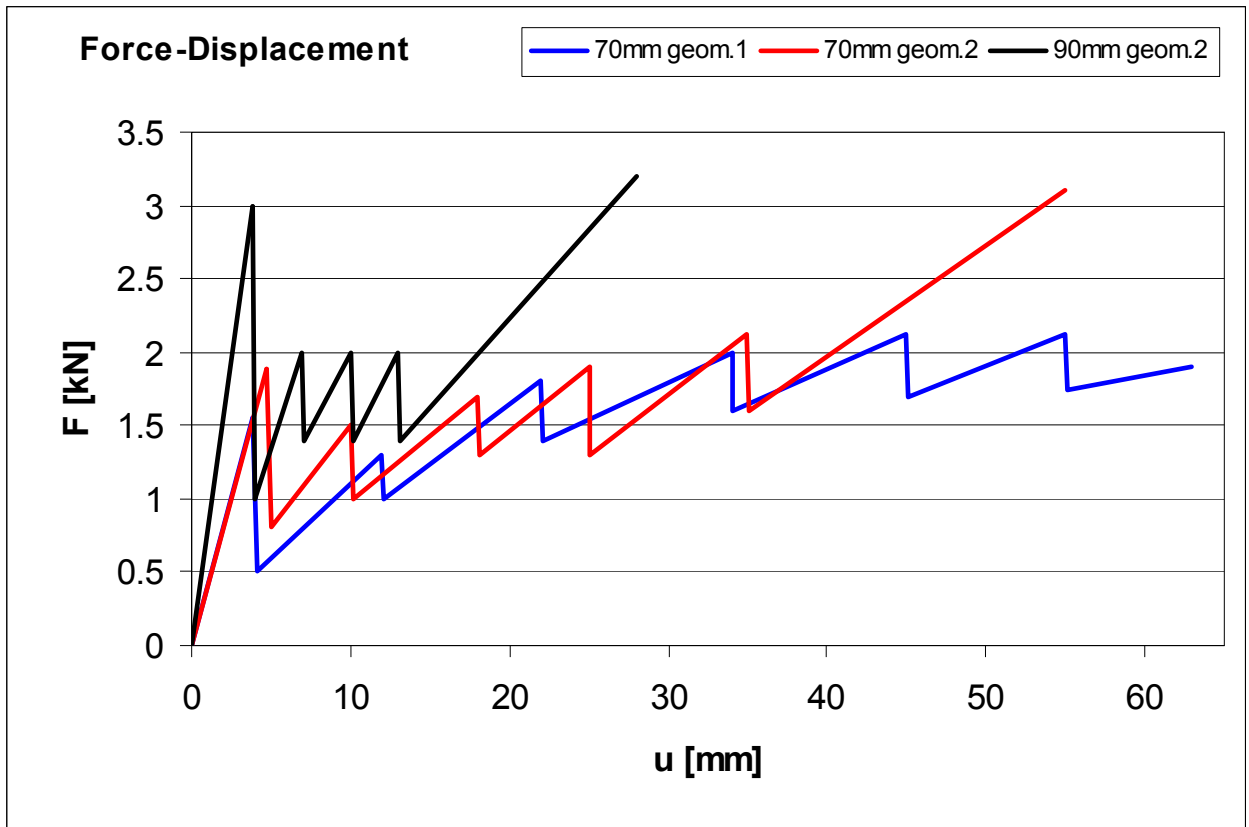


Figure 167, Typical force-displacement curves for different specimen types.

Failure behavior

All specimens show remarkable resilience in case of load bearing capacity in the ultimate limit state. A totally shattered beam seems to be able to resist the highest loading.

The aimed safety margins concerning deformation capacity is well reached for all specimens. The goal for residual load bearing capacity is reached for the 70mm specimens, not for the 90mm specimens.

Failure of neither the compressive zone in the top of the glass nor the reinforcement itself was observed. The governing factor for ultimate failure of all specimens was the strength of the connection of the reinforcement.

The 70mm specimens collapsed mainly because of bending moment. The reinforcement connection to the glass pane failed progressively, similar to the glass pull-out tests described in chapter 3.4. This is caused predominantly by tensile force in the reinforcement.

The 90mm specimens collapsed mainly because the reinforcement was torn out of the groove in vertical direction, perpendicular to the direction of the reinforcement. This is caused by shear force.

Consider *Figure 167*. Every large fracture of the glass pane causes a fallback in force. Multiple fractures result in a more or less horizontal course of the force-displacement curve, which indicates a ductile failure pattern. When no more fractures occur, the curve rises linearly like is visible in the ends of the curves of geometry 2 in the 70mm and 90mm specimens. The ductility of the girder is therefore provided by the progressive fracturing of the glass pane.

Initial failure of specimen 70-03 happened at 1,23kN approximately 300mm right of the center of the girder where the bending moment is 20% lower than in the middle part of the beam. The tensile bending stress at the crack location was approximately 63% of the values to which 70-01 and 70-02 fractured. This is probably caused by a local degradation of the glass.

A remarkable difference exists in the initial failure moment of the 70mm specimens geometry 1 compared to geometry 2. If specimen 70-03 is discarded, the glass pane of geometry 1 failed at a tensile bending stress of approximately 48N/mm² and geometry 2 at 56N/mm²; a gap of 8N/mm², or 17% (see *Table 29* and *Table 31*).

Similar behavior is observed in the 90mm specimens; specimens 1, 2 and 3 are mounted with geometry 2 and initial failure occurs between 51N/mm² and 56N/mm² while specimen 90-04 failed at 40N/mm².

The small number of specimens does not suffice for a well-grounded conclusion that there is an anomaly, but suspicion arises that the stiffness of the reinforcement does have an influence on the failure behavior of the beam. If further tests are conducted extra attention on this point is advised.

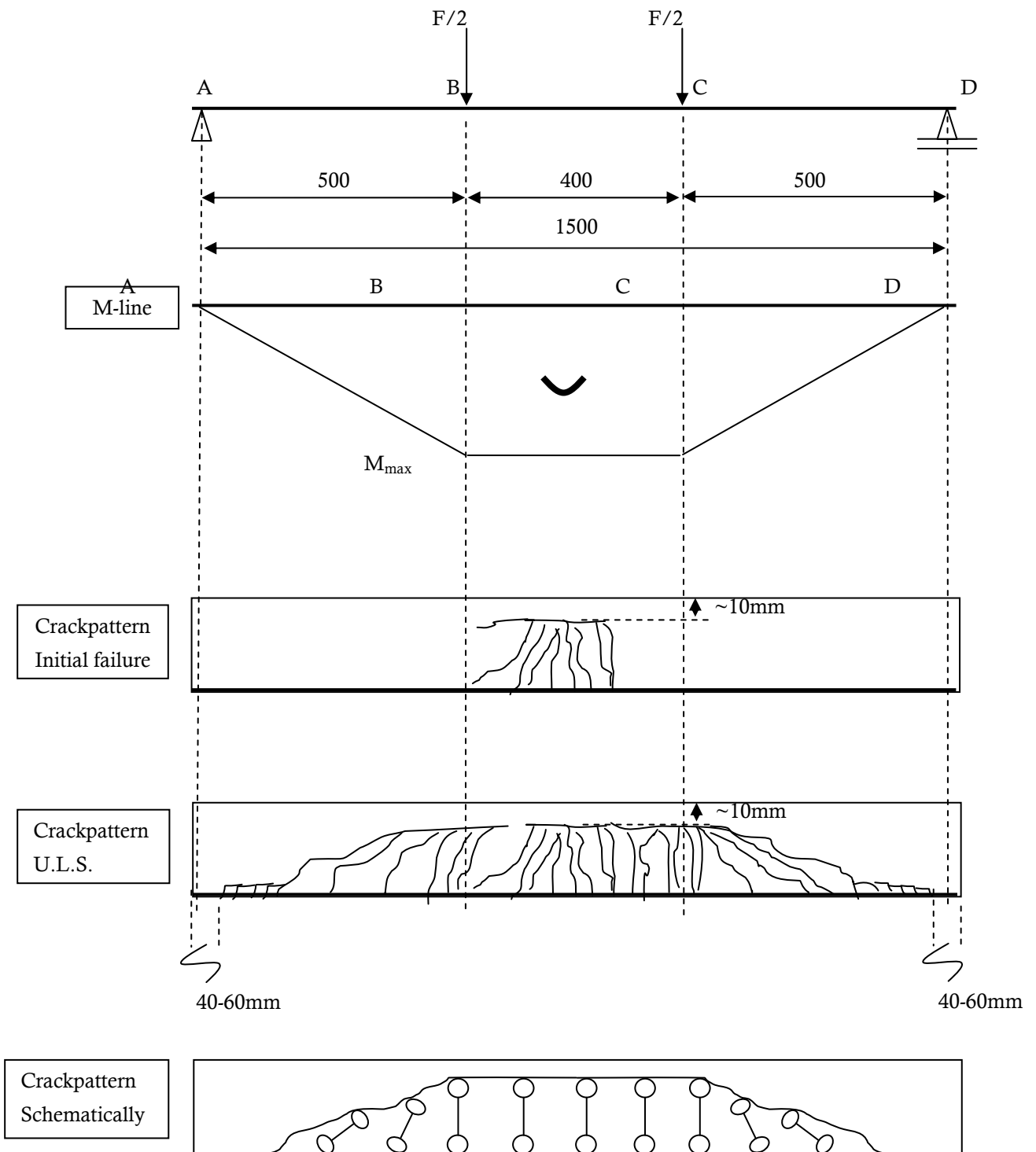


Figure 168, Predominant crack pattern for specimens 70-04/70-06. The glass fractures act as rocker bars in U.L.S.

Internal structural mechanism

See *Figure 168*. The predominant crack pattern shows resemblance to a pre-stressed concrete beam without bond, for example like in the ‘test of Ivanyi’ [7]. Typical for this pattern are so-called ‘Fork cracks’. These are vertical cracks up to the compressed zone where they bend off and continue in horizontal direction. The compressed zone gets more or less detached from the rest of the girder. This is caused by a large crack width.

Although the crack pattern is comparable to the test described above it is caused by a different mechanism.

$$N = E * A * \frac{\Delta l}{l} \rightarrow \Delta l = \frac{N * l}{E * A}$$

The image in the test of Ivanyi is caused by the fact that the extra tensile load that is distributed to the reinforcement at initial failure is introduced in the *whole length* of the reinforcement.

The reinforcement in the glass girders is bonded to the glass, resulting in a relatively small length over which the tensile force is introduced. This is compensated by the fact that the carbon reinforcement has a much smaller cross-section and a modulus of elasticity that is 25% smaller than that of steel.

Another important factor is the extremely low E-modulus of the adhesive, which allows large deformations of the bond, thus large crack width. Theoretically the ‘strain at break’ of the adhesive is the strain at which brittling occurs. With two-component epoxy adhesive this is approximately the same as the thickness of the adhesive layer. Note that the length of the connection over which the adhesive is brittle but still structurally functioning is not included in this.

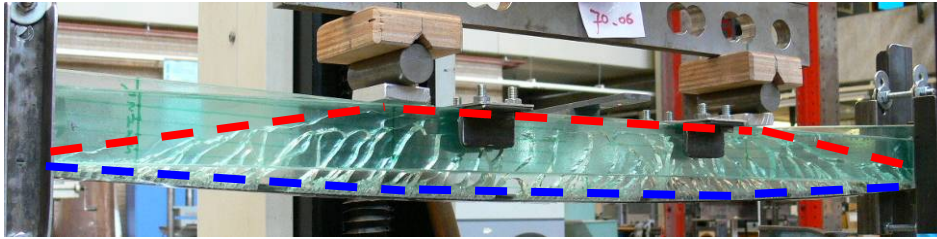
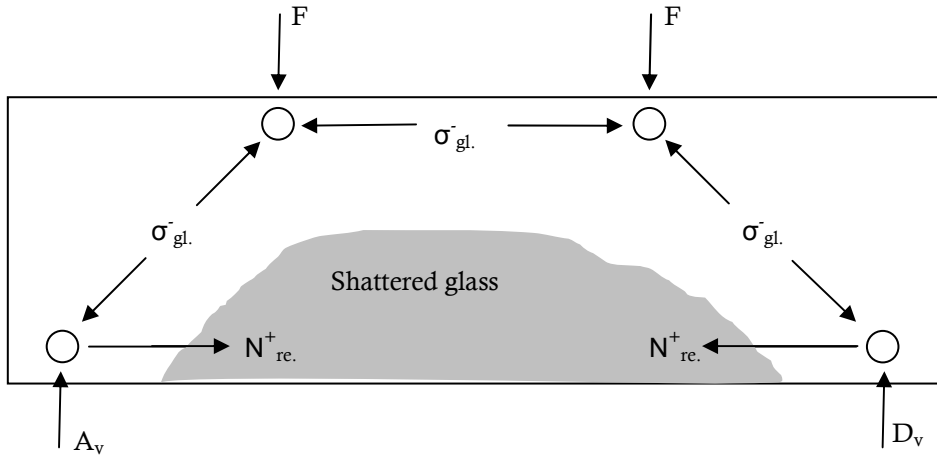
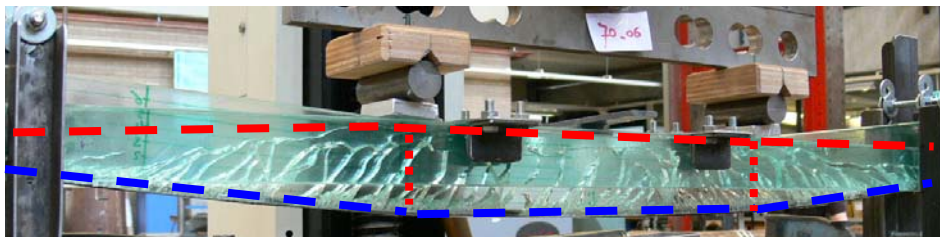
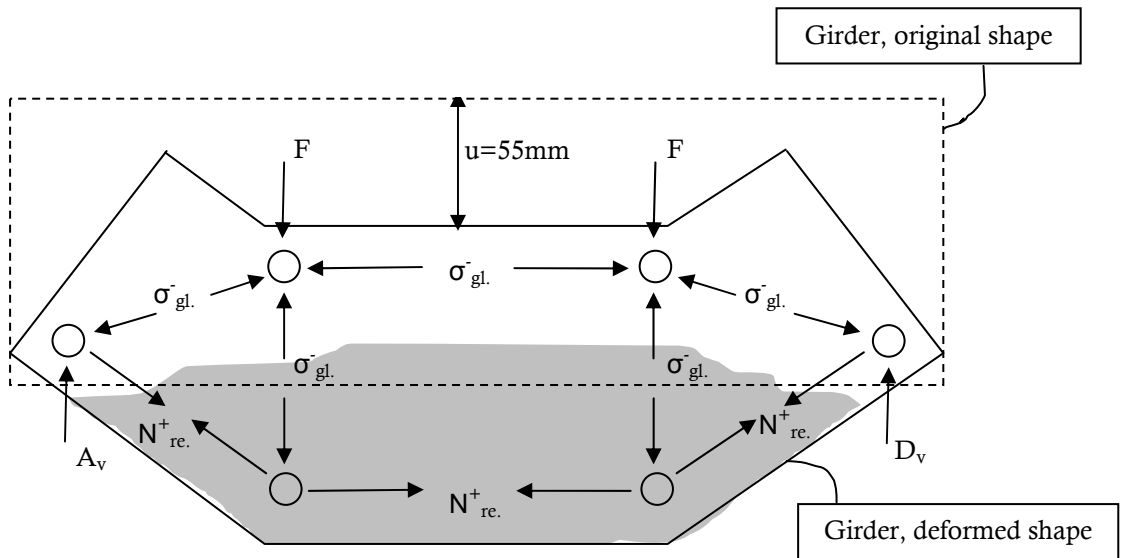


Figure 169 A (above) and B (below), simplified drawing of typical 70mm girder in slightly deformed (above) and ultimate limit state (below) with 'strut and tie' diagram of internal force distribution and photographs of girder during the test. The drawings are not to scale.

A: The girder is slightly deformed, but severely fractured; the glass takes most of the vertical load at the end supports.

B: The girder is deflected over 55mm; the compressive zone in the glass is nearly a straight line and the reinforcement takes most of the vertical load at the end supports.



This section applies to the 70mm girders.

In the U.L.S. the intact connection of the reinforcement to the glass is approximately 50mm in both ends of the beam. The deflection at the highest load was approximately 55 mm for specimens 70-03/06. Because of the large deformation a relocation of internal force distribution arises. A simplified representation is given in *Figure 169* as 'strut and tie' diagram, with the flow of force sketched in red (compression) and blue (tension) in the photographs.

When deflections are small, the vertical force from the support is totally compensated by compressive stress in the glass. This results in a compressed zone in the glass that has more or less the shape of an arc. When the sag of the girder increases to near its own height, the compressive zone deforms to nearly a straight line, being unable to compensate large vertical forces by the support.

The reinforcement, having the shape of a straight line at low deflections, has deformed to an arc and functions more or less like a cable with a considerable vertical component in the U.L.S. This means that the support force in the end of the girder is no longer predominantly taken by compression in the glass, but by tension in the reinforcement.

The amount of vertical force that is taken by the reinforcement can be determined by considering the deflection of the girder in the U.L.S., which in this case is presumed 55mm. From this it follows that the reinforcement takes over 85% of the vertical load from the glass pane.

Remarkable fact is that the maximum force that was reached in the glass pull-out tests was 9,4kN (specimen 2011_36). The tensile force in the reinforcement in

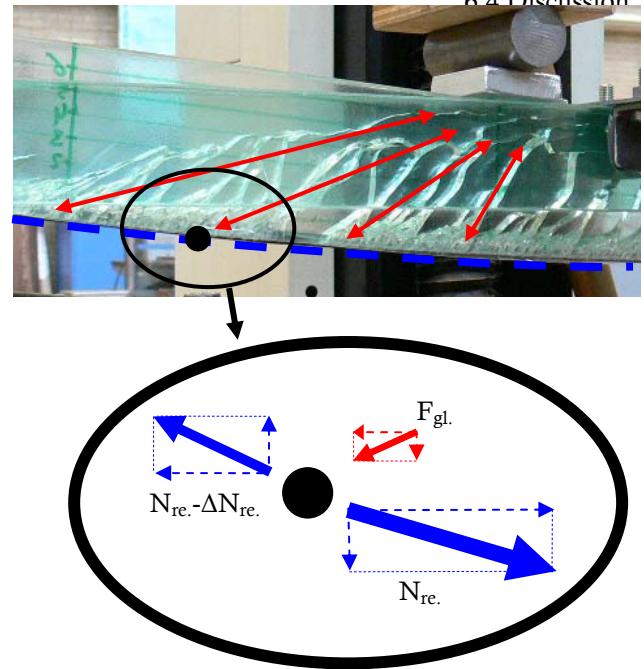


Figure 170. Close-up of girder with curved reinforcement in U.L.S. Compressive forces sketched in red, tensile forces in blue. The forces form an equilibrium: the force from the glass rocker bar equals ΔN in the reinforcement.

specimen 70-05 reached up to 12kN. This remarkable gap can be explained because the girders have been pretreated by a Silan primer, which theoretically improves the strength of the adhesive connection up to 20% [31].

Another possible contributing factor could be the following:

See *Figure 170*. The reinforcement in the U.L.S. is slightly curved over the whole length of the girder. This curvature indicates that the reinforcement delivers a distributed load in vertical direction into the glass fractures.

In the middle part of the girder this load is compensated by an equal but opposite divided load delivered by the curvature of the compressive zone.

Between A-B and C-D this load is introduced into the glass fractures that act as rocker bars (see *Figure 168*). The angle of the glass fractures and the fact that they are still attached to the glass, indicate that apart from the vertical component that creates the curvature of the reinforcement, a horizontal component is introduced in the reinforcement. This horizontal force reduces the tensile force in the reinforcement near the end supports.

The size and contribution of this force is unknown.

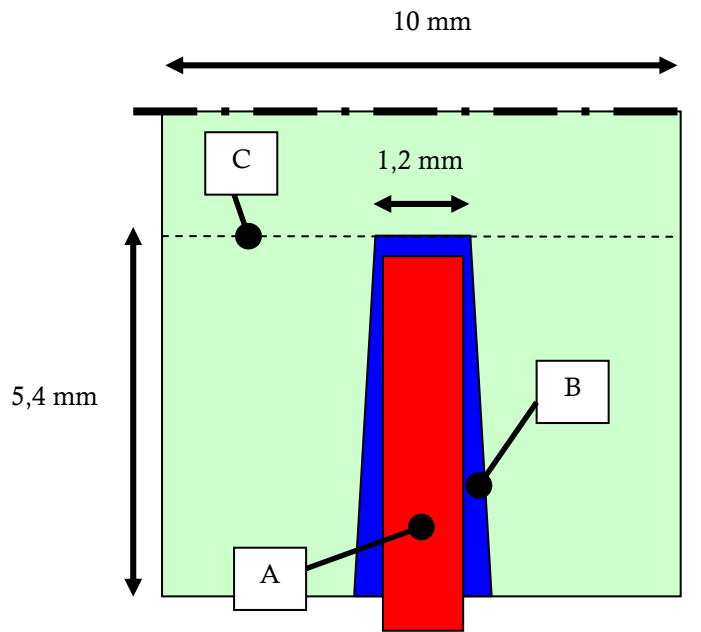


Figure 172, Close-up of cross-section of bottom of girder, not to scale. Possible failure mechanisms of the reinforcement connection, indicated by A, B and C:

A: Failure of reinforcement.

B: Failure of adhesive.

C: Fracturing of glass pane.

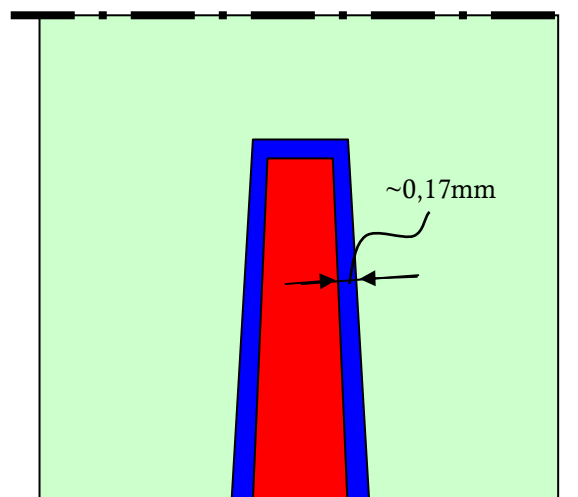


Figure 171, Recommended reinforcement geometry for further development. Adhesive thickness $\sim 0,17\text{mm}$.

Green: Glass pane.

Blue: Adhesive.

Red: Reinforcement

Reinforcement connection

The girders collapsed because the reinforcement failed. This can be caused by three mechanisms as is shown in *Figure 172*. The governing factor in the failure of the reinforcement connection is fracturing of the glass pane ('C'). Brittling of the adhesive connection is observed for some specimens. This indicates that the adhesive was loaded up to its maximum strength.

The tensile force of the reinforcement is introduced into the glass by shear stress in the adhesive. The plane of rupture indicated by the dotted line 'C' in *Figure 172* is governing for shear in the glass pane and has to be able to cope with the load introduced by the adhesive over the perimeter of the groove. This means that the width (10mm) of the glass pane is not able to cope with the force introduced by the adhesive over the perimeter of the groove (12mm). The theoretical strength of Araldite 2011 in combination with these substrates is 19N/mm^2 [10]. This indicates that the maximum shear stress capacity of the glass pane would locally be no more than 16N/mm^2 .

The tested geometry 1 has an average adhesive thickness of 0,45mm. Geometry 2 has a very thin adhesive thickness of less than 0,06mm. The strongest joint connection with a two-component epoxy adhesive as used in this thesis is gained with a thickness of 0,15mm to 0,20mm [10] [31].

Pultruded glass fiber and carbon fiber elements can be produced in almost any profile geometry. To gain the strongest connection a reinforcement bar has to be produced that fits in the SGG Plug-in groove with approximately 0,17mm space for adhesive layer *Figure 171*. Production inaccuracies like dislocation of the profile will have to be prevented.

The reinforcing elements and the glass are both linear elastic materials. Working together in the described geometry the girder shows a plastic deformation curve after initial failure. This is caused by the fact that the glass pane fractures progressively before ultimate failure, repeatedly causing a sudden increase in deflection and fallback in applied force.

If the glass pane would have been able to withstand the load and not have fractured progressively, this decrease in bending stiffness would have been much less and the horizontal part in the stress-deflection curve would not have arisen.

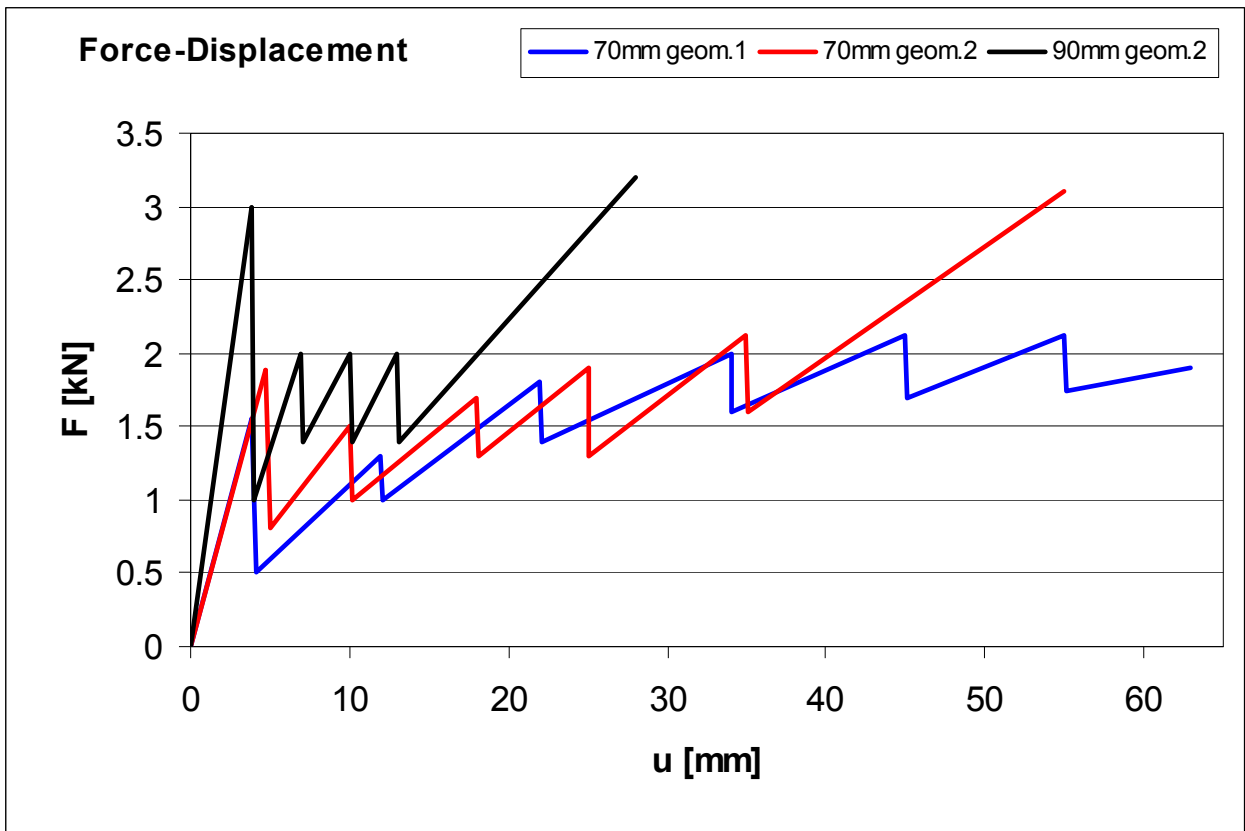


Figure 173, Typical force-displacement curves for different specimen types.

6.5 Conclusions and Recommendations

Conclusions

The tested reinforced glass girders, where the SGG plug-in groove is used for adhesively bonding carbon fiber reinforcement, show a ductile failure behavior with good residual load bearing capacity and remarkable resilience to fractures and large deflections.

In the girders with a height of 70mm geometry 1 ensures the most ductile behavior. A large ultimate deflection of 63mm is gained with sufficient load bearing capacity. The maximum tensile force that can be introduced in the reinforcement in geometry 1 is approximately 8kN which is not enough to reach the requirements for minimum reinforcement capacity for a 90mm girder.

Geometry 2 in a 70 mm girder allows the highest residual load bearing capacity of 3,0kN with slightly smaller deformations (55mm). The maximum tensile force that can be introduced in the reinforcement in geometry 2 is approximately 12kN.

The girders with a height of 90mm fail because of shear force (3kN) at a deflection of approximately 30mm. The residual load bearing capacity of this reinforcing method in the described four point bending tests is governed by the shear force.

The local shear stress capacity of the glass is governing over the shear strength of the adhesive connection of the carbon fiber to the groove and the tensile strength of the reinforcement.

The progressive failure of the glass provides the plastic deformation capacity of the girder.

Recommendations

The tests are performed with a displacement controlled four point bending test. The intended structural application would be better approached by a force controlled bending test. Additional force controlled bending tests are advised in this situation.

The strength of the glass is governing in the failure of the girders in the described tests. To obtain better information about the strength of the adhesive connection of the reinforcement to the SGG Plug-in groove further investigation is recommended with a thicker glass pane where the stress in the glass will not be governing.

Further investigation is recommended into the presumption that the stiffness of the reinforcement in the Plug-in groove has an affect on the tensile bending strength of the glass pane.

Further investigation is recommended into the effects of thermal fluctuations on the deformation differences between glass and reinforcement and the resulting stress levels in the element.

Large load fluctuations after initial failure seem to have a devastating effect on the compressive zone of the glass and therefore on the residual load bearing capacity of the girder. Further investigation is recommended into the effects of load fluctuations in the ultimate limit state.

7. Discussion

The developed reinforcing principle

Review

The research, described in the previous chapters, concerns adhesively bonded carbon fiber or glass fiber reinforcement in the SGG Plug-in groove with two-component epoxy adhesive.

The size of the SGG Plug-in groove is limited by the maximum possible size of the disks in the milling machine. This limits the amount of reinforcement and therefore the size of the girder and also the freedom in adhesive layer thickness. Another limiting factor is the direction of the reinforcement which cannot be altered in this configuration. Vertical or diagonal reinforcements for failure due to shear force for example are therefore impossible.

The reinforcing elements are linear elastic high-strength materials ($\sigma_{\max} > 2000 \text{ N/mm}^2$) bonded to the glass by a strong adhesive (lap shear strength $> 20 \text{ N/mm}^2$) and a relatively thin adhesive layer ($< 0,5 \text{ mm}$). This results in a stiff joint and therefore high shear stress concentration near crack locations. The tests described in chapter 6 showed that this stress concentration was governing in the failure of the joint, resulting in progressive glass and/or local adhesive failure.

The principle of bonding the reinforcement to the glass with a thin layer of a very strong and stiff adhesive might not be the most favorable in glass design since it results in large stress concentrations at crack locations, where the glass is most vulnerable.

Further developments

The setup of the bending tests, with the continuous lateral torsional buckling support, could prevent the glass splinters from displacing in the ultimate limit state. If the element is applied as single glass pane this would not be prevented which might cause the beam to lose its consistency.

It is recommended to laminate multiple glass panes into a composed girder, for example as presented in *Figure 174*. The individual splinters will then be held in place by the laminate.

Additional advantage of laminating multiple panes would be that part of the fracture energy at initial failure of one element is transferred to the other glass panes thru the SGP foil. This would reduce the crack depth and increase the residual load bearing capacity of the individual elements and the composed girder as a whole.

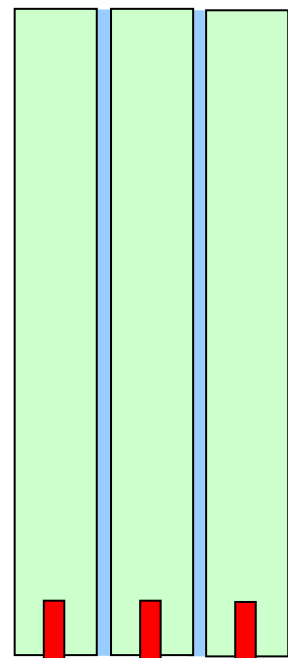


Figure 174, Cross-section of proposed girder, laminated with three elements.

Light green: glass

Red: Reinforcement

Blue: SGP foil

Other reinforcing principles

Reinforcements in the laminate

If the connection of the reinforcing element to the glass is made with a less strong and less stiff adhesive system with a much thicker adhesive layer, the force distribution in the joint near a crack location would be spread out over a larger distance. This would introduce the tensile force into the glass at lower stress over a larger surface, reducing the stress peak which caused the joint to fail.

A disadvantage of this method would be that it results in a less stiff connection and therefore larger crack width and height, and a smaller compressive zone. Failure of the compressive zone has been governing for specimens 90-04 and 90-05 because the cracks at initial failure were too large.

Reinforcing concept 1 from chapter 4.3 is a method in which this principle could be applied. By varying the thickness of the SGP foils an optimum could be found in various reinforcement stiffnesses and strengths, foil thickness and glass pane thicknesses. Other possible advantage of this method would be the freedom in positioning and direction of the reinforcement, for instance for shear force (vertical or diagonal).

Pre-stress in the SGG Plug-in groove

The tests in chapter 5 and 6 have shown that the adhesive connection of a glass – or carbon fiber reinforcement in the plug-in groove can cope with considerable forces of up to at least 12 kN. The strength of the glass is governing for this joint. This might very well be caused by stress peaks at imperfections in the surface of the groove. If a pre-stressed element would be adhesively bonded in the SGG Plug-in groove, the microscopic cracks at the surface would be loaded under compression and tensile stress peaks will no longer occur.

With the acquired information about the strength of the adhesive connection a design for a glass girder with a pre-stressed element in the plug-in groove could be developed.

8. Conclusions

This report concerned the development of an alternative method for reinforcing a structural glass girder where optimal structural behavior is combined with maximum transparency. The problem was tackled by investigating possibilities, generating several concepts of which one was worked out into an applicable method. The worked out concept was subjected to practical tests to ensure the safety of its failure behavior.

This resulted in a structural glass girder where carbon fiber or glass fiber reinforcement is bonded by two-component epoxy adhesive in the SGG Plug-in groove.

1. The developed girder with carbon fiber reinforcement shows ductile failure behavior with sufficient residual deformation and load bearing capacity. However the black reinforcement is clearly visible in the bottom of the girder.

A similar girder reinforced with specially developed transparent glass fiber meets the demand for transparency much better. However in the conceived geometry it does not show a safe ductile failure behavior.

Therefore it can be concluded that the goal of this master thesis - to develop a reinforced structural glass girder with safe failure behavior where reinforcing elements are invisible or at least hardly noticeable - has been partly reached.

2. The developed reinforcing method, where carbon fiber is adhesively bonded in the SGG Plug-in groove, is a potentially good possibility for creating a small span structural glass girder with safe failure behavior.

However, the size of the developed girder is limited by the size of the SGG Plug-in groove. If up-scaling

of the developed girder is desired, the milling machine has to be altered for a larger groove dimension. Another possibility for creating a girder with larger load bearing capacity is to laminate multiple smaller reinforced glass panes.

3. In the adhesive joint of the carbon fiber to the SGG Plug-in groove in the glass pane, the strength of the glass is governing over the strength of the adhesive.
4. In the developed geometry the two linear elastic materials glass and carbon fiber combine to an element with elastic-plastic failure behavior.

9. Recommendations

1. Two component epoxy adhesive applied in a thin layer ensures a strong and stiff connection. This has proven to result in stress concentrations that exceed the strength of the glass.

It is recommended to develop a reinforcing principle where the stress concentrations are lower and the transfer of forces is distributed over a larger surface. Bonding reinforcement to the SGP laminate foil could be a possibility.

2. The tests are performed with a displacement controlled four point bending test setup. The intended structural application would be better approached by a force controlled bending test. Additional force controlled bending tests are advised to validate the failure behavior.

3. Future development of this reinforcing principle could focus on laminating multiple reinforced glass panes as described on page 172, which would probably reduce the initial crack depth and therefore increase the residual load bearing capacity of the individual glass panes as well as the laminated girder as a whole.

Other improvement could be to produce a reinforcing element that allows a constant adhesive layer thickness between the glass and the reinforcement of 0,15mm to 0,20mm.

11. References

Books, reports and articles

- [1] Schittich, Staib, Balkow, Schuler, Sobek, 1999. *Glass Construction Manual*, Birkhauser Publishers.
- [2] R. Nijse, 2003. *Glass in structures*, Birkhauser Publishers.
- [3] J. Luttmer, 2005. *Lightness in constructions*, Master thesis. Delft University of Technology.
- [4] J. van Heusden, 2005. *Constructief glazen element*, Master thesis. Delft University of Technology.
- [5] DELO, 2007. *BOND it*, DELO.
- [6] A.J. Kinloch, Chapman, Hall, 1936. *Adhesion and Adhesives, science and technology*. Department of Mechanical Engineering, Imperial College of science and technology, University of London.
- [7] Prof. dr. ir. J.C. Walraven, ir. J.C. Galjaard, 1997. *Voorgespannen beton*, ENCI Media, ISBN 90-71806-47-2.
- [8] ETH Zurich, 2000. *Glastrager*, vdf Hochschulverlag AG Zurich.
- [9] Prof. ir. L.A.G. Wagemans, ir. F.A.M. Soons, B.P.M. van Raaij, 2002. *Info Map Constructieeler*, Sectie Algemene Constructieeler, Delft.
- [10] Huntsman Corporation, 2007. *Users guide to adhesives, Surface preparation and pretreatments, Technical data sheet Araldite 2011*, Huntsman.
- [11] Angelo Simone, 2008. *Analysis of slender structures*, Lecture notes to the course CT3110, Delft University of Technology.
- [12] P.C. Louter, 2005. *Adhesively bonded reinforced glass beams*, HERON
- [13] P.C. Louter & F. Veer, 2006. *Redundancy of reinforced glass beams; temperature, moisture and time dependent behaviour of the adhesive bond*, <http://www.glassfiles.com>
- [14] M. Palumbo, D. Palumbo, M.T. Mazzucchelli, G. Plizzarri, 2007. *3 case studies, how to use glass as load bearing element*, Universita de Brescia, www.gpd.fi.
- [15] P.J.S. Cruz and J.M. Pequeno, 2008. *Timber Glass Composite Beams: Experimental Studies & Architectural Applications*, Challenging Glass Conference, Conference on Architectural and Structural Applications of Glass, Faculty of Architecture, TU Delft, May 22-23
- [16] W. Althof, 1982. *Creep Recovery and Relaxation of Shear-loaded Adhesive Bondlines*, Journal of Reinforced Plastics and Composites.
- [17] S. Feirabend, *Reinforced Laminated Glass*, Institute of Lightweight Structures and Conceptual Design (ILEK), University of Stuttgart.
- [18] J.C.J. Hofstede, 2007. *Advanced Adhesive Bonding Technology*, Final Project Report. Delft Hechtingsinstituut.
- [19] B. Freytag, 2004. *Glass-Concrete Composite Technology*, Structural Engineer International, Journal of IABSE, Volume 14.
- [20] F.Veer, 2003. <http://www.zappi.bk.tudelft.nl>
- [21] Kreher, 2004. *Tragverhalten und Bemessung von Holz-Glas-Verbundträgern unter Berücksichtigung der Eigenspannungen im Glas*. Thèse EPFL, no 2999 (2004). Dir.: Julius K. Natterer.
- [22] B. Freytag, 2002. *Glass-Concrete-Composite method of construction*. Technische Universität Graz
- [23] J. Hamm, 2000. *Tragverhalten von Holz und Holzwerkstoffen im statischen Verbund mit Glas*, PhD Thesis Nr. 2065, IBOIS/EPFL2000

- [24] <http://www.palafitte.ch>
- [25] F. Wellershoff, Sedlacek G., 2003. *Structural Use of Glass in Hybrid Elements, Steel-Glass-Beams, Glass-GFRP-Plates*. In J Vitkala (Ed.), *Glass processing days* (pp. 268-270). Tampere: GPD2003
- [26] A. Flinterhoff, 2003. *Load carrying behaviour of hybrid steel-glass beams in bending*. Master Thesis. University of Dortmund. Institute of Steel Construction.
- [27] B. Grotepaß, 2006. *Application of hybrid steel-glass beams in modern architecture*. Master Thesis, University of Dortmund, Institute of Steel Construction.

WebPages

- [28] <http://www.wikipedia.org>
- [29] <http://www.vetrotextiles.com>
- [30] <http://www.glassfiles.com>

Interviews

- [31] John van Klaren, 2009. Adhesive systems specialist at VIBA B.V.